NORTHROP

NASA CR-66918

FREE FLIGHT INVESTIGATION OF LARGE ALL-FLEXIBLE PARAWINGS AND PERFORMANCE COMPARISON WITH SMALL PARAWINGS - FINAL REPORT

By

J. H. Moeller, E. M. Linhart, W. M. Gran and L. T. Parson

Prepared under Contract No. NAS 1-7467 by

NORTHROP CORPORATION, VENTURA DIVISION
Newbury Park, California 91320

for

NATIONAL AERONAUTICS AND SPACE ADMINISTRATION

March 1970

NORTHROP

NASA CR-66918

FREE FLIGHT INVESTIGATION OF LARGE ALL-FLEXIBLE PARAWINGS AND PERFORMANCE COMPARISON WITH SMALL PARAWINGS - FINAL REPORT

Prepared by:

J. H. Moeller, E. M. Linhart, W. M. Gran and L. T. Parson

March 1970

Approved:

R. P. Wondka
Recovery Systems
Chief Project Engineer

NORTHROP CORPORATION, VENTURA DIVISION
1515 Rancho Conejo Boulevard
Newbury Park, California 91320

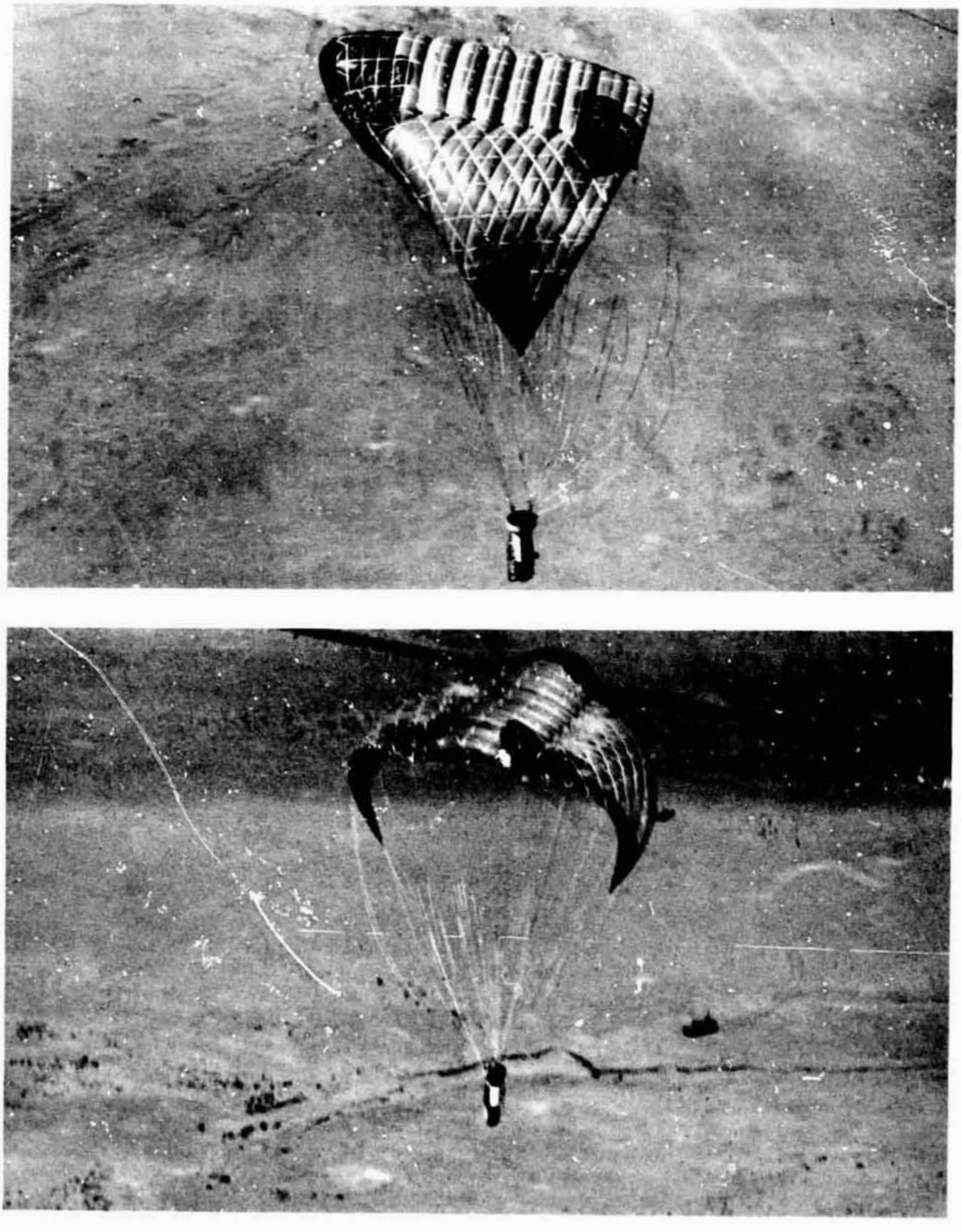

4000 sq ft twin keel parawing on bomb-type test vehicle

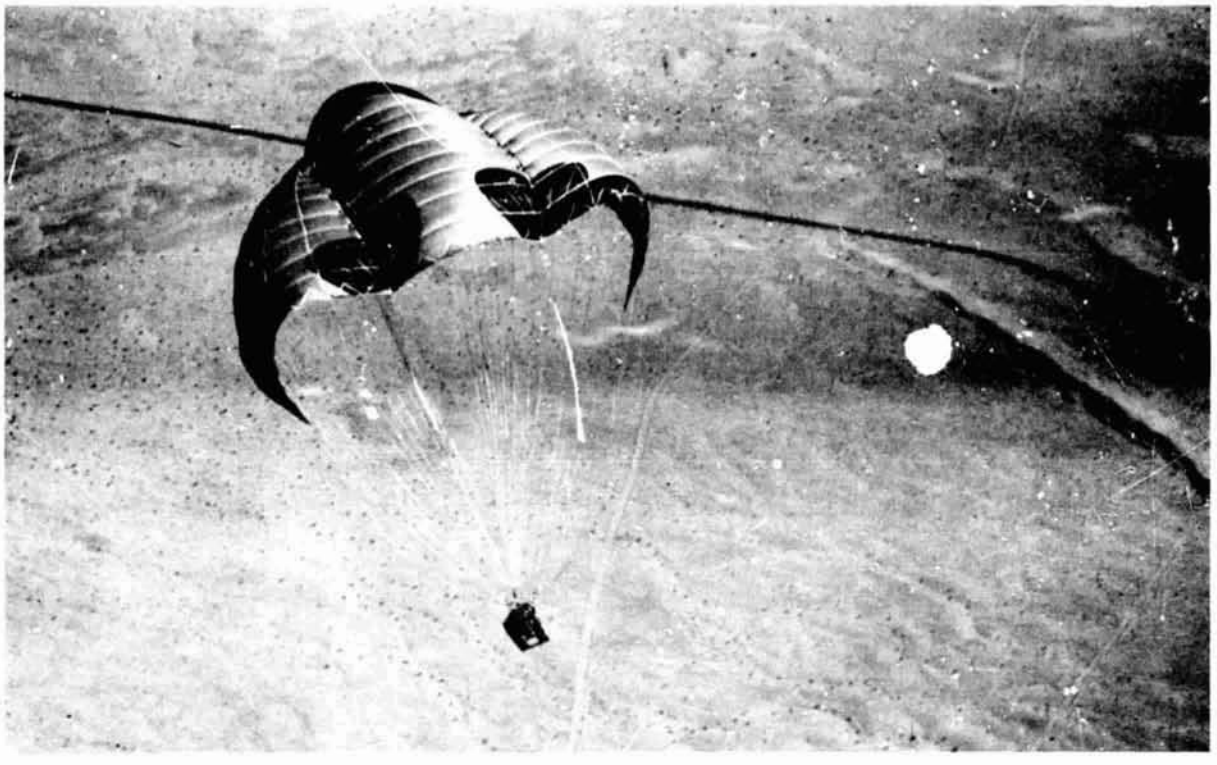

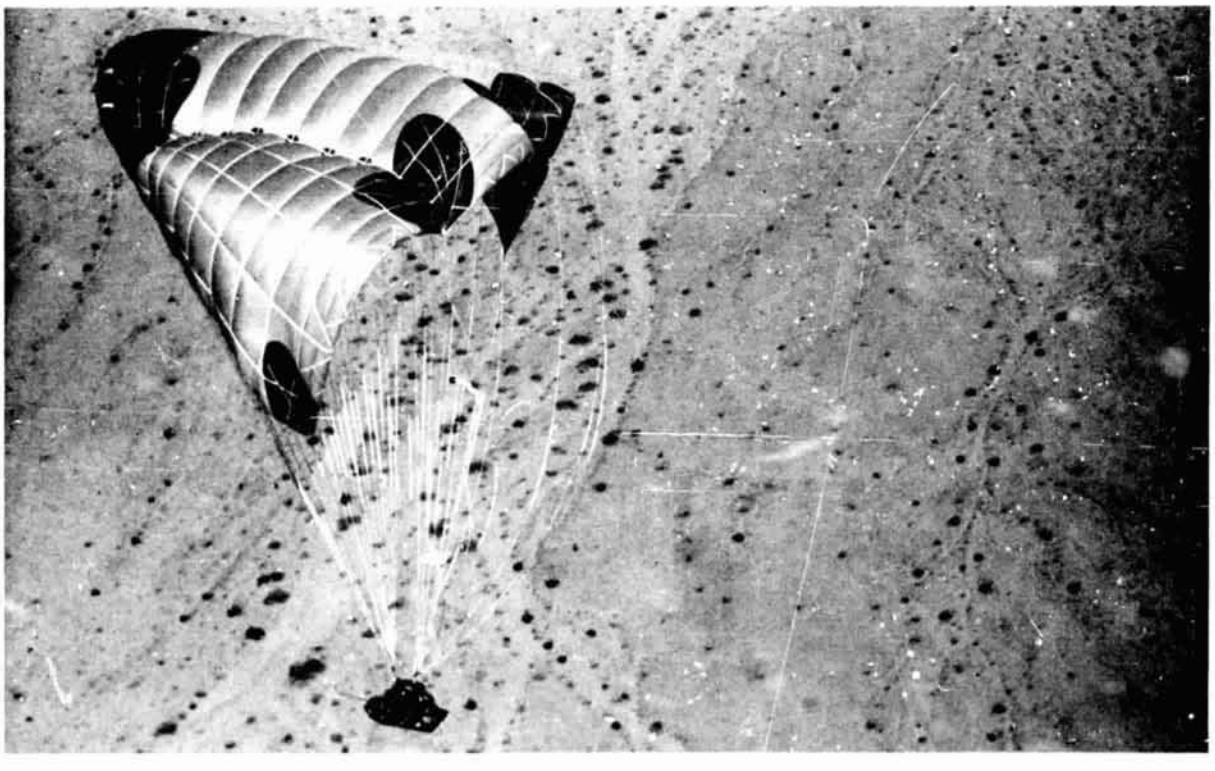

4000 sq ft twin keel parawing on controllable, sled-type test vehicle

CONTENTS

TABLES

FIGURES

Page

Page

FREE FLIGHT INVESTIGATION OF LARGE ALL-FLEXIBLE PARAWINGS AND PERFORMANCE COMPARISON WITH SMALL PARAWINGS FINAL REPORT

By J.H. Moeller, E.M. Linhart, W.M. Gran and L.T. Parson
Northrop Corporation, Ventura Division

SUMMARY

This report presents the results and analysis of the results of a series of twenty aerial drop tests conducted with 4000 sq ft planform area (intermediate-scale) all-flexible parawings. Both single keel and twin keel parawing models were tested; however, twin keel parawings were flown in eighteen of the twenty tests. The report also compares the results of the intermediate-scale parawing tests with the results of tests previously conducted with 400 sq ft planform area (small-scale) all-flexible parawings.

The aerial drop tests with the intermediate-scale parawings demonstrated the feasibility of their deployment within the prescribed deployment envelope. However, the tests showed that the larger parawings, in the configurations tested, were susceptible to localized, canopy cloth damage in the early stages of deployment, particularly at the higher initial dynamic pressures.

The tests confirmed the need for a five-stage deployment process to maintain deployment decelerations at or near the 3 G level. Comparison of deployment deceleration test data from scaled 400 sq ft parawing tests with test data from 4000 sq ft parawing tests indicated that the scaling method used in this program was not wholly valid.

For the parawing in gliding flight, the tests showed the larger parawings to be stable, controllable, and responsive to turn commands. In straight, gliding flight the intermediate-scale,

twin keel parawings demonstrated a maximum lift-to-drag ratio of 2.5 to 2.75, depending on wing loading. Lift-to-drag modulation capability, using either rear-keel-suspension line retraction or tip-suspension-line retraction, was limited to approximately 0.5 less than maximum L/D on the parawing configurations flown. These results were generally consistent with free-flight gliding performance measured on the small-scale parawings.

INTRODUCTION

A deployable, aerodynamic-deceleration device capable of controlled, gliding flight is a promising approach to the problem of providing a land-landing capability for manned spacecraft. One such candidate device, called the "All Flexible Parawing," was initially developed by the NASA Langley Research Center. Further parawing technology development was carried out by the Northrop Corporation, Ventura Division, under Contract NAS 1-7467, administered by the Langley Research Center. The overall plan of this program was to develop progressively larger parawings, beginning with "small-scale" parawings of 400 sq ft size, next with "intermediate-scale" parawings of 4000 sq ft size, and finally, with "full-scale" parawings of 10,000 to 12,000 sq ft size suitable for use with large spacecraft. The results of the small-scale program were reported in Reference 1. The results of the intermediate-scale program constitute the primary subject of this report. A secondary subject of this report is a comparison of the results of the intermediate-scale program with the results of the small-scale program.

The intermediate-scale parawing program encompassed a series of twenty aerial drop tests of 4,000 sq ft parawings. Both single keel and twin keel parawing models were flown in these tests. However, twin keel parawings were flown in eighteen of the twenty tests. Two basic types of aerial tests were flown: 1) parawing deployment tests on an instrumented, bomb-type test vehicle with the parawing at a fixed rigging, and 2) parawing gliding-flight tests on an instrumented, controllable, sled-type test vehicle. In the latter tests the systems were provided with both turn control and pitch control. All the intermediate-scale aerial drop tests were conducted at the DOD Parachute Test Facility, El Centro, California.

SYMBOLS

b_o	flat pattern wing span, ft
C_D	drag coefficient, D/qS_W
$(C_DS)_p$	total drag area of parawing pilot parachute(s), ft^2
C_K	load factor. Calculated by dividing the peak total stage load by the product of dynamic pressure, q, at initiation of the stage and the average reference area, $(C_RS_W)_{AVE}$, for that stage of the deployment process
C_L	lift coefficient, L/qS_W
C_R	resultant force coefficient, $\sqrt{C_L^2 + C_D^2}$
C_RS_W	product of resultant force coefficient C_R, and reference wing area, S_W, ft^2. Calculated by dividing total parawing load by wind corrected dynamic pressure
$(C_RS_W)_{AVE}$	average C_RS_W for given deployment stage, ft^2
D	drag
d	diameter
F	force, lbs
F_ℓ	suspension line peak load, lbs
F_o	peak total parawing load, lbs. Calculated by multiplying the peak measured total load for each stage by the ratio of descent weight to suspended weight
F_{o_m}	peak measured total load in each deployment stage, lbs
G	ratio of acceleration to earth gravity
h	height above mean sea level
K	parawing keel
L	lift
LE	parawing leading edge

LS	parawing line stretch event
LT	parawing line transfer event
ℓ	length of suspension line from bottom of skirt or keel band to center of top cross bar of link to which suspension line is attached
ℓ_K	reference keel length
ℓ_{LT}	length of left tip suspension line
ℓ_{RK}	length of rear keel suspension line(s)
ℓ_{RL}	effective reefing line length, including end attachments for non-continuous reefing lines
ℓ_{RT}	length of right tip suspension line
ℓ_{RL}/ℓ_K	effective reefing ratio
ℓ_T	length of tip suspension line
$(\ell_T/\ell_K)_{AVE}$	average tip setting - ratio of the average length of the left and right tip suspension lines to the reference keel length
MSL	mean sea level
PD	programmer parachute disconnect event
p	angular velocity about X-axis, rad/sec
q	dyanmic pressure, lbs/ft^2
r	angular velocity about Z-axis, rad/sec
SK	single keel parawing type
S_W	reference canopy area of parawing, ft^2 $= 0.69148\ell_K^2$ for single keel models $= 0.7726\ell_K^2$ for twin keel models
TE	parawing trailing edge
TK	twin keel parawing type
t	time, sec

t_f	filling time for each stage, sec. Measured from initiation of stage to maximum inflated parawing size
t_{pl}	time from line stretch to peak load, sec
W_D	descent weight, lbs
W_S	suspended weight, lbs
W_D/S_W	unit canopy loading (wing loading), lbs/ft^2
X, Y, Z	reference axes system with origin at the moment reference center
x, y, z	displacement of a sensor from the reference center
1DR	first stage disreef event
2DR	second stage disreef event
3DR	third stage disreef event
δ	movement of tip control line or aft keel control line from neutral position
δ_{T/ℓ_K}	differential tip setting - ratio of difference in length of right and left tip suspension lines to reference keel length. Positive values indicate right tip suspension line is shorter than left tip suspension line (right turn input). Negative values indicate left tip suspension line is shorter than right tip suspension line (left turn input)
ρ	mass density of air, $slugs/ft^3$
$\dot{\psi}$	turn rate, deg/sec

SUMMARY OF SMALL-SCALE PARAWING PROGRAM

GENERAL

The small-scale parawing program was the first phase in a multi-phase technology program entitled, "Investigation of Large-Scale All-Flexible Parawings for Spacecraft Recovery." The purpose of the overall program was to establish the suitability of the all-flexible parawing as a primary descent system for large spacecraft.

SMALL-SCALE PROGRAM OBJECTIVES

The objectives of the small-scale parawing program were as follows:

1. Investigate and evaluate parawing deployment mechanics and deployment loads, define packing techniques, reefing methods and sequencing for satisfactory parawing deployment.
2. Demonstrate successful parawing deployment followed by steady, trimmed gliding flight.
3. Obtain verification of parawing rigging for steady glide.
4. Develop operational procedures and test crew training.
5. Obtain data for defining parawing scaling relationships.
6. Evaluate parawing materials and parawing fabrication techniques and revise as required.
7. Incorporate applicable new parawing technology established in small-scale tests to the design of large parawings.

SMALL-SCALE PROGRAM SCOPE

The small-scale parawing program encompassed two wind tunnel test programs, a free flight gliding test series, a set of aerial deployment verification tests and a deployment drop test series. Table 1 presents a summary of the small-scale parawing program. The first wind tunnel test program was conducted in the Langley Research Center's 30 foot by 60 foot full-scale tunnel; the second wind tunnel test program was conducted in the Ames 40 foot by 80 foot tunnel. The free flight gliding tests and the aerial deployment verification tests were conducted at El Mirage Dry Lake, California. The deployment drop test series was carried out at the DOD Joint Parachute Test Facility, El Centro, California. The small-scale parawing test program was accomplished in the period of September 1967 to August 1968.

SMALL-SCALE PARAWING TEST SPECIMENS

The wind tunnel tests in the LRC 30 foot by 60 foot full-scale tunnel utilized 15-ft ℓ_K single keel parawings of 156 sq ft planform area, and 15-ft ℓ_K twin keel parawings of 174 sq ft planform area. A total of six wings were fabricated for these wind tunnel tests, three single keel and three twin keel models. These six models were tested in 17 different configurations.

The wind tunnel tests in the Ames 40 ft by 80 ft tunnel utilized a 15-ft ℓ_K single keel parawing of 156 sq ft planform area, a 24-ft ℓ_K single keel parawing of 400 sq ft planform area, and two 22.7-ft ℓ_K twin keel parawings of 400 sq ft planform area each.

The free flight gliding tests at El Mirage Dry Lake investigated the flying characteristics of 24-ft ℓ_K single keel and 22.7-ft ℓ_K twin keel parawings, all of 400 sq ft planform area. A total of four different models were flown. None of these models had provision for reefing.

TABLE 1. - SUMMARY OF SMALL-SCALE PARAWING TEST PROGRAM

Category of test	Test facility	Test objectives	Parawing test specimens	Payloads	Type of wind tunnel run or aerial drop test	Number of wind tunnel runs or drop tests
Wind tunnel test	LRC 30 ft by 60 ft full scale tunnel	a. Evaluate performance of various candidate reefing systems b. Evaluate effects of parawing construction on gliding performance	a. 15 ft l_k (156 sq ft)* single keel b. 15 ft l_k (174 sq ft) twin keel		a. Deployment tests b. Tethered gliding tests	50 54
Wind tunnel Test	Ames 40 ft by 80 ft tunnel	a. Determine effects of canopy construction on gliding performance b. Provide comparative wind tunnel data on models used in free flight tests	a. 15 ft l_k (156 sq ft) single keel b. 24 ft l_k (400 sq ft) single keel c. 22.7 ft l_k (400 sq ft) twin keel		Tethered gliding tests	19
Aerial drop test	El Mirage Dry Lake, Calif.	a. Evaluate free flight L/D performance, including maximum L/D and L/D modulation capabilities b. Evaluate turn rate performance c. Evaluate flight performance	a. 24 ft l_k (400 sq ft) single keel b. 22.7 ft l_k (400 sq ft) twin keel	a. Non-instrumented, ballast vehicle b. Instrumented, controllable test vehicle	Helicopter launched, aerial drop tests	37
Aerial drop test	El Mirage Dry Lake, Calif.	Verify deployment and selected reefing system operation	a. 24 ft l_k (400 sq ft) single keel b. 22.7 ft l_k (400 sq ft) twin keel	Non-instrumented, ballast vehicle	Helicopter launched, aerial drop tests	2
Aerial drop test	DOD Joint Parachute Test Facility, El Centro, Calif.	a. Evaluate reefing system functioning and deployment performance b. Determine suspension line and reefing line loads information c. Obtain design data for larger parawing systems by means of scaled deployment tests d. Evaluate capability of the 400 sq ft parawings to withstand deployment within the specified deployment envelope e. Develop techniques for packing and rigging larger parwing specimens	a. 24 ft l_k (400 sq ft) single keel b. 22.7 ft l_k (400 sq ft) twin keel	Instrumented, bomb type test vehicle	Fixed wing aircraft launched, aerial drop tests	16

*Planform Area

The aerial deployment verification tests at El Mirage Dry Lake and the deploymment drcp tests at El Centro, California, were conducted with 24-ft ℓ_K single keel parawings and 22.7-ft ℓ_K twin keel parawings, each of 400 sq ft planform area. A total of six wings, three single keel and three twin keel models, were fabricated and flown. All six wings were provided with multi-stage reefing systems.

The reefing systems selected from this test program were four-stage systems, both for the twin keel and the single keel parawings. Characteristics of the selected reefing systems are:

1. All suspension lines initially equalized in length to that of the tip lines -- the shortest suspension lines on the wing.
2. Reefing lines arranged on the periphery of each lobe of the wing.
3. A gathering reefing line along the trailing edges of the wing.

Details of the selected reefing systems and the deployment sequence for the single keel and for the twin keel parawing are presented in Reference 1.

SUMMARY OF RESULTS

Significant results of the small-scale parawing program can be summarized as follows:

1. Maximum lift-to-drag ratio achieved with the single-keel parawing was 2.7 in the wind tunnel and 2.3 in free gliding flight. Comparable maximum L/D values for the twin keel were 3.4 in the wind tunnel and 2.97 in free gliding flight.

2. Maximum L/D for the small models was found to be significantly affected by tip-suspension-line length and by wing loading.

3. L/D modulation capability, using rear keel line(s) retraction, was limited to a reduction of approximately 0.5 from maximum L/D, both for single keel and twin keel models.

4. Successful deployment followed by steady, trimmed gliding flight was demonstrated for both single- and twin-keel models, at altitudes up to 18,000 ft and dynamic pressures up to 100 psf.

5. The selected multi-stage reefing systems for the single- and twin-keel models demonstrated the feasibility of maintaining deployment load factors in the range of 3 to 4 G's or less.

6. The selected reefing systems produced significant suspension-line-load variations from stage to stage, as a result of the non-uniform canopy area growth in the deployment sequence.

7. Maximum turn rates of 125 degrees per second with the single keel models and 110 degrees per second with the twin keel models were achieved, using single-tip-line retraction. Turn rate was found to be a linear function of control line movement for both wing types.

A complete description of the small-scale parawing program, including descriptions of the models flown, test results, data analyses, and conclusions, is contained in Reference 1.

SUMMARY OF INTERMEDIATE-SCALE PARAWING PROGRAM

GENERAL

The intermediate-scale parawing program was the second phase in a multi-phase technology program entitled, "Investigation of Large Scale All-Flexible Parawings for Spacecraft Recovery." The purpose of the overall program was to establish the suitability of the all-flexible parawing as a primary descent system for large spacecraft.

INTERMEDIATE-SCALE PROGRAM OBJECTIVES

The objectives of the intermediate-scale parawing program were as follows:

1. Demonstrate successful parawing deployment with a 5000 pound payload, at a wing loading of 1.25 psf in the altitude range of 3000 to 18,000 feet and at dynamic pressures from 30 to 100 psf. The developed parawing will have minimum weight and packed volume, consistent with safety.
2. Obtain deployment loads data and information on parawing design details, fabrication techniques, and deployment system for application to the full-scale parawing.
3. Demonstrate transition from deployment to stable, trimmed gliding flight for a wing loading of 1.25 psf.
4. Obtain quantitative effects of wing loading on parawing flight characteristics and rigging for trimmed flight.
5. Obtain quantitative data at a wing loading of 1.25 psf and evaluate the effects of wing loading on control forces, rates, travel, and vehicle response to control inputs.

6. Define a suitable control mode for pitch control.

7. Evaluate the system landing capabilities and obtain quantitative data pertinent to approach and landing touchdown conditions.

8. Obtain data for defining parawing scaling relationships.

9. Demonstrate that the parawing system can satisfy its design requirements without damage to the canopy, suspension lines or risers.

INTERMEDIATE-SCALE PROGRAM SCOPE

The intermediate-scale parawing program consisted of a series of aerial drop tests carried out at the DOD Joint Test Facility, El Centro, California. Two basic types of tests were conducted in this test series; (1) parawing deployment tests on an instrumented, bomb-type test vehicle with the parawing at a fixed rigging, and (2) parawing controlled, gliding flight tests on an instrumented, sled-type, radio controlled test vehicle. A total of twenty aerial tests was flown, of which fourteen were deployment tests and six were controlled, gliding flight tests. The intermediate-scale parawing test program was accomplished in the period from August 1968 to June 1969.

INTERMEDIATE-SCALE TEST PROGRAM RATIONALE

The test program conducted with the intermediate-scale parawings was devised to achieve the previously identified program objectives. In general, the tests of the parawing on the instrumented, bomb-type test vehicle were planned primarily to achieve the objectives associated with the deployment phase of parawing flight. However, the tests on the bomb-type test vehicle did also

provide some useful data on controlled gliding flight, particularly those tests in which the parawings were deployed at the higher altitudes. On the other hand, the tests of the parawing on the controllable, sled-type test vehicle were planned primarily to achieve the objectives associated with the controlled, gliding phase of parawing flight. However, the tests on the sled-type test vehicle did also provide some useful data on parawing deployment characteristics.

Parawing tests on the bomb-type test vehicle may be categorized as follows:

1. System validation tests
2. Scale point tests
3. Deployment demonstration tests
4. Controllable vehicle qualification tests.

The system validation tests were normally the first tests conducted in the series, with payload weight and parawing deployment conditions set at minimum levels. Primary purpose of these tests was to validate proper operation of the parawing system, test vehicle and associated test instrumentation.

The scale point tests were those tests for which the system descent weight and parawing deployment conditions were selected according to a previously formulated set of scaling laws. The scale point tests were designed to simulate the deployment loading and dynamic behavior of a full-scale parawing system at significant points in the prescribed deployment envelope. For the twin keel parawing, the scale point tests were selected to simulate a full-scale parawing with a planform area of 10,000 sq ft, at a wing loading of 1.5 psf (i.e., flown on a 15,000-lb descent weight system deployed at a dynamic pressure of 100 psf and 18,000 ft altitude). No scale point tests were conducted with intermediate-scale, single keel parawings.

The deployment demonstration tests were conducted to demonstrate the capability of the intermediate-scale parawings to be successfully deployed in the prescribed altitude-dynamic pressure deployment envelope. These tests normally included testing at conditions corresponding to the corners of the deployment envelope, i.e., at the maximum and minimum dynamic pressure and altitude conditions.

Finally, the qualification tests were tests conducted on the bomb-type vehicle to qualify the parawing system for use on the expensive, heavily-instrumented, controllable test vehicle. The descent weight and parawing deployment conditions used for these qualification tests were normally selected to exceed, by a fixed margin, the descent weight and deployment conditons planned for the controllable vehicle flights.

Parawing tests on the controllable, sled-type test vehicle were all in the same category, i.e., gliding flight demonstration tests. The one parameter that was varied in these tests was wing loading. Parawing deployment was carried out at the highest altitude practicable with the launch aircraft available, in order to provide the maximum amount of gliding flight data. Parawing deployment dynamic pressure was somewhat arbitrarily set in the low-to-moderate range to minimize the possibility of canopy damage during deployment. Maneuver plans were varied from flight to flight, in order to provide a balance between straight gliding flight data and turn maneuver data.

INTERMEDIATE-SCALE PARAWING TEST SPECIMENS

The intermediate-scale parawing test specimens, both single keel and twin keel, were designed with a flat pattern area of 4000 sq ft. This size represented an order-of-magnitude increase in wing size from the 400 sq ft parawings flown in the small-scale program. At the 4000 sq ft size these wings were designed for testing at a 5000-lb descent weight for a nominal wing loading of

1.25 psf. Ballasting provisions in the intermediate-scale test vehicles allowed variability of wing loading in test from a minimum of 0.72 psf (i.e., with a 2880-lb descent weight) to a maximum of 1.50 psf (i.e., with a 6000-lb descent weight). APPENDIX A provides detailed descriptions of the intermediate-scale test vehicles and their associated instrumentation.

Structurally, the intermediate-scale parawings were considerably more sophisticated than the small-scale wings. Design of the large wings required that the canopies have adequate structure in the direction of primary loads, where the load path direction changed appreciably with geometry changes in the wing during the deployment process. Also, these large wings with their asymmetric planforms presented problems in controlling canopy fabric during initial deployment. Indeed, parawing canopy structural problems and deployment damage were the only major problems encountered in the intermediate-scale test program. These problems manifested themselves in the single keel parawing specimen early in the test program. The single keel structural problems, coupled with the demonstrated higher gliding performance potential of the twin keel parawing, were the bases for discontinuing further testing with single keel parawings beyond the initial two tests. Later in the test program similar structural problems were encountered with the twin keel parawing specimen. A number of significant structural modifications were carried out on the twin keel wing to overcome these problems. The structural modifications included the addition of ten leading edge suspension lines, reinforcement of certain critically loaded areas in the canopy, and the addition of ripstop tape networks to the canopy. These structural modifications are described in detail in the section on INTERMEDIATE-SCALE PARAWING TEST SPECIMENS.

The reefing systems used on the intermediate-scale parawings, both single keel and twin keel, were essentially the same 4-stage, lobe-type reefing systems developed and flight tested in the small-scale parawing program (see Reference 1). These reefing systems

had demonstrated in small-scale parawing testing, the feasibility of maintaining deployment loads at or near the 3.0 G load factor level. Some relatively minor changes were made to the twin keel reefing system in the course of intermediate-scale parawing testing. One such change was the addition of reefing to the center section nose area of the wing. Details of the intermediate-scale parawing reefing systems are presented in the section on INTERMEDIATE-SCALE PARAWING TEST SPECIMENS.

INTERMEDIATE-SCALE PARAWING TEST SYSTEMS

SYSTEM DESCRIPTIONS

Bomb-Type Test Vehicle System

The flight test system consisted of a parawing test specimen and an instrumented, bomb-type test vehicle. Figure 1 illustrates the parawing/bomb vehicle flight test system in the gliding flight configuration. This figure shows the major dimensions of the test vehicle and the location of the suspension lines that were used to control the angle of attack of the parawing and the system flight direction. The parawing shown in the illustration is a twin keel model. The same test vehicle was used for single keel parawing deployment tests.

Reference dimensions for the parawings were as follows:

Twin keel models:

$\ell_T/\ell_K = 0.603$, $\ell_T = 43.4$ ft for all tests except 207T;
$\ell_T/\ell_K = 0.650$, $\ell_T = 46.8$ ft for Test 207T,
$\ell_{RK}/\ell_K = 0.954$, $\ell_{RK} = 68.7$ ft for all tests.

Single keel models:

$\ell_T/\ell_K = 0.781$, $\ell_T = 59.4$ ft for all tests,
$\ell_{RK}/\ell_K = 0.865$, $\ell_{RK} = 65.8$ ft for all tests.

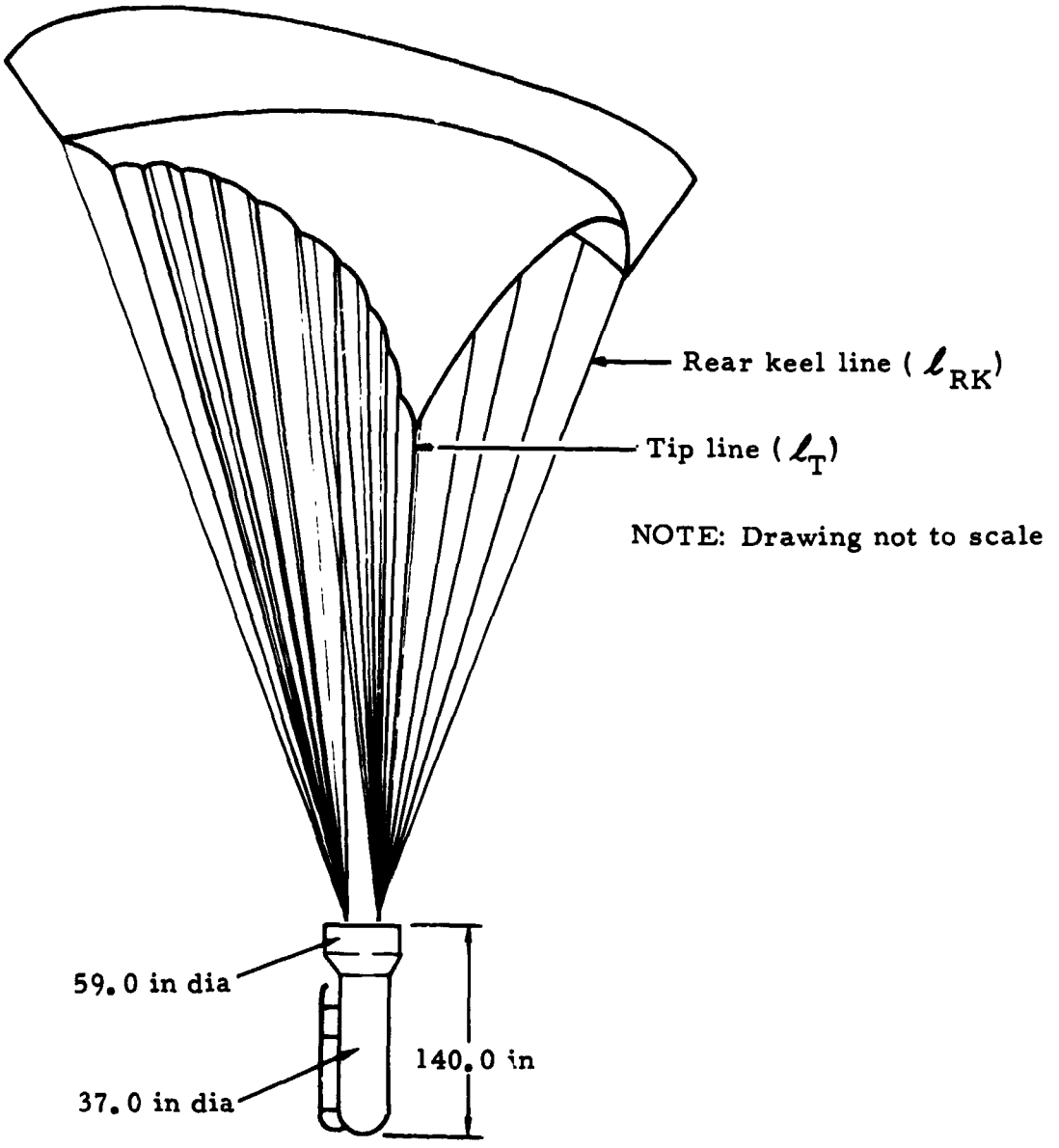

Figure 1. Side view of parawing/bomb-test-vehicle flight test system

Other sections of this report contain more detailed descriptions of the parawing test specimens, the bomb-type test vehicle and the interface between the parawing test specimen and the test vehicle.

Controllable Test Vehicle System

Figures 2 and 3 illustrate the parawing/controllable test vehicle system. The flight test system for the controllable vehicle tests consisted of a parawing test specimen and an instrumented, controllable test vehicle. Only twin keel parawing models were flown with the controllable test vehicle. Figure 2 gives the major dimensions of the test vehicle and the reference dimensions of the parawing test specimens flown with the controllable test vehicle. Figure 3 illustrates the positions of the control lines employed during the flight tests. Turn control was accomplished by retracting or extending control lines which changed the length of the tip suspension lines. The length of each tip suspension line could be controlled within limits. This allowed control of the average length of the two tip suspension lines and also the difference in length between the two tip suspension lines. Differences in the length of the tip suspension lines were used for turn control. Turns were made in the direction of the shorter tip suspension line. The two rear keel suspension lines were bridled and their length controlled by a single control cable. Detailed descriptions of the parawing test specimens, the controllable test vehicle and the interface between the parawing and the test vehicle are provided in other sections of this report.

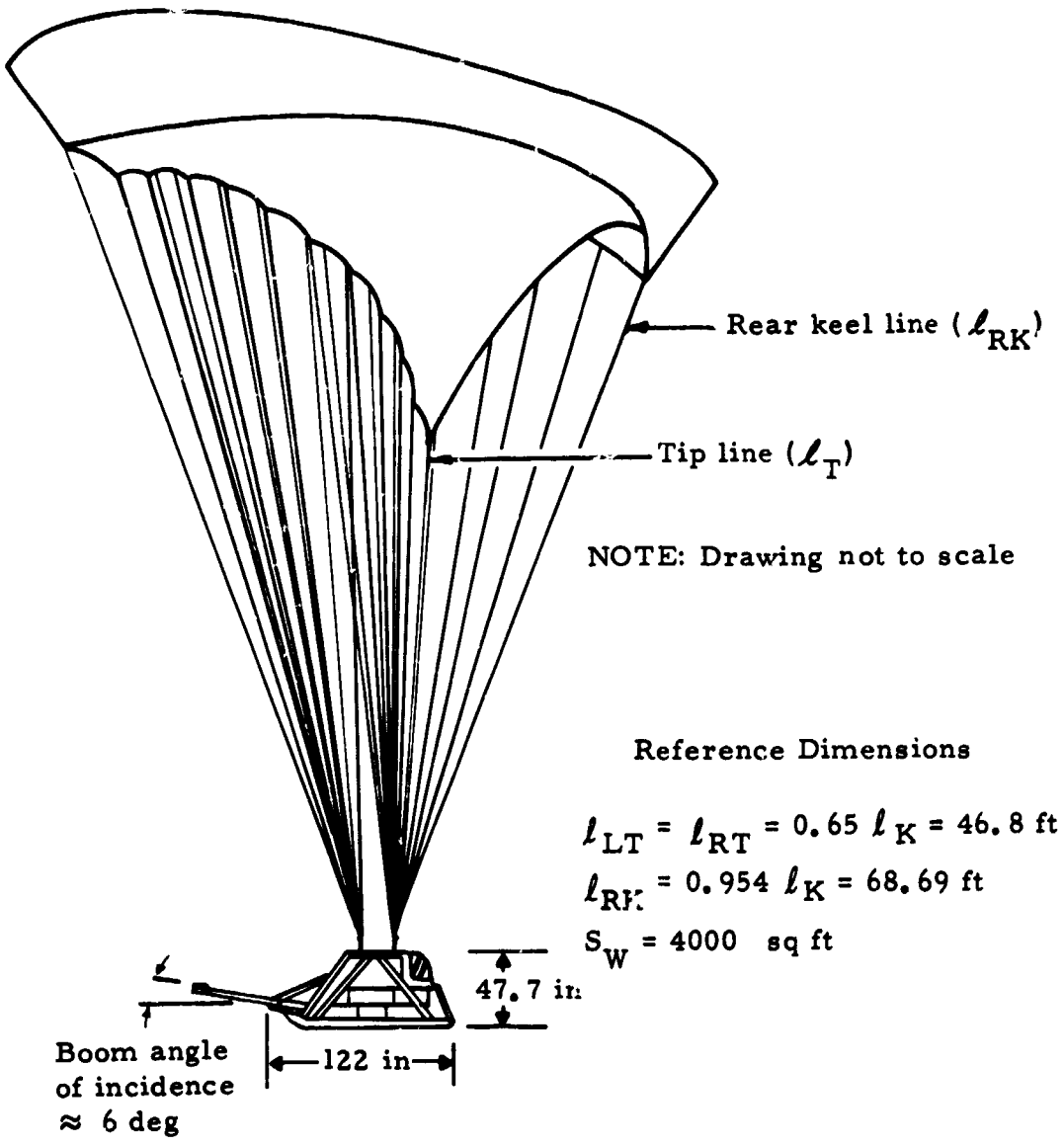

Figure 2. Side view of parawing/controllable-test-vehicle test system

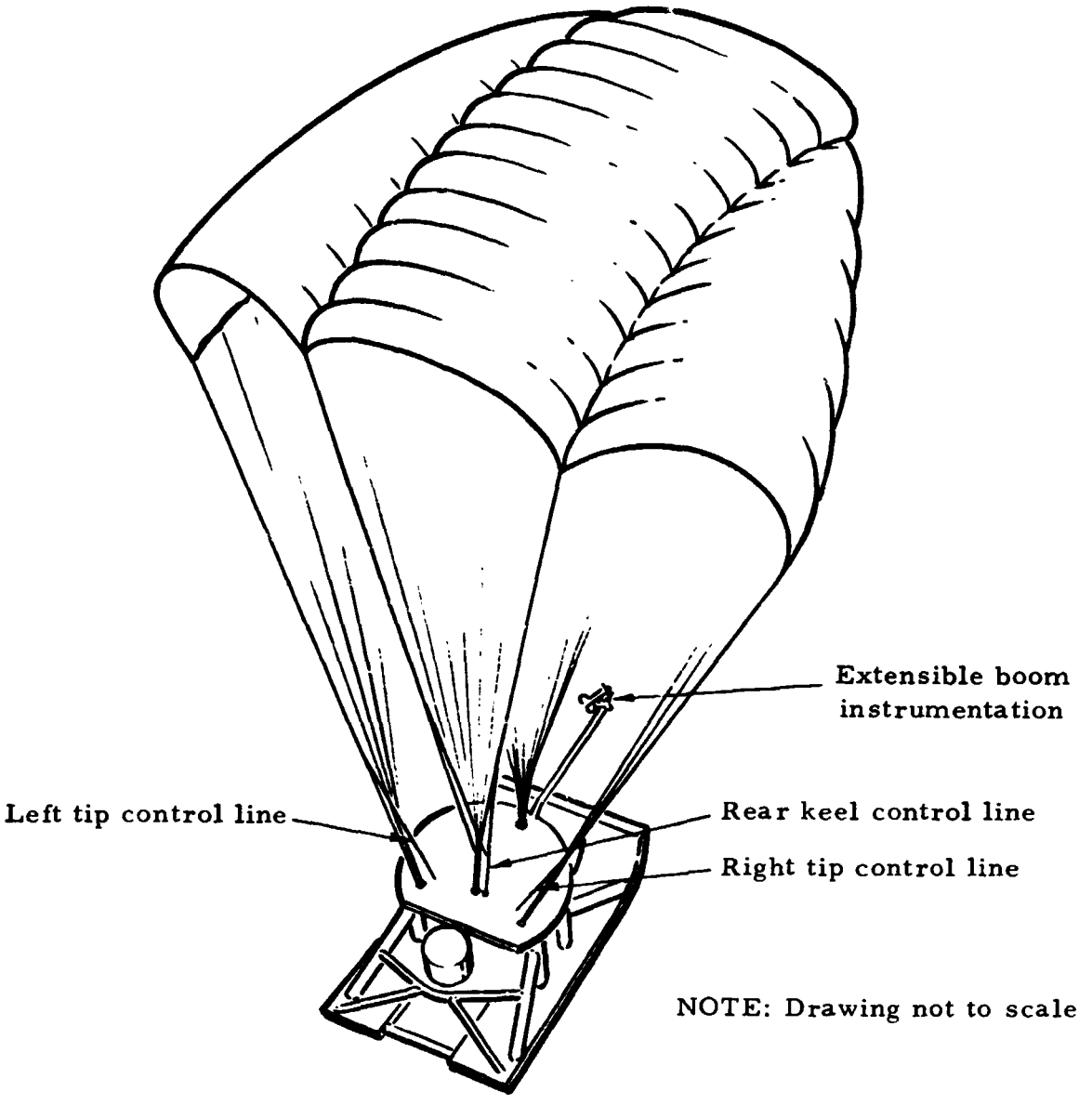

Figure 3. Rear quarter view from above the parawing/controllable test vehicle system

REEFING SEQUENCES

General

The basic reefing sequences used in the intermediate-scale parawing program were developed in the small-scale parawing program. Both the twin keel and the single keel parawing reefing sequences had been developed with the objective of maintaining peak opening loads during deployment at or below 3 G's. The reefing systems served to accomplish this objective by allowing the drag area of the system to increase in discrete steps.

A number of different reefing schemes for varying the drag area in a step-wise manner were evaluated in LRC wind tunnel tests, early in the small-scale program. Reference 1 describes the various reefing systems evaluated. The most promising reefing systems from this initial evaluation, one each for the single keel and the twin keel parawing models, were subsequently tested and suitably modified in aerial drop tests conducted at El Mirage Dry Lake, California (2 tests) and at the DOD Joint Parachute Test Facility, El Centro, California (16 tests). The resulting reefing systems were incorporated in the design of the intermediate-scale single keel and twin keel parawings. A latter section of this report provides detailed descriptions of these reefing systems.

Both of the intermediate-scale, single keel parawing tests were conducted with the same reefing sequence. In the intermediate-scale, twin keel parawing tests, some modifications were made to the reefing sequence originally developed in the small-scale program. The following pages describe the reefing sequences tested in the intermediate-scale parawing program.

Twin Keel Parawing Reefing Sequence

The twin keel parawing reefing sequence consisted of four stages of reefing, followed by the gliding configuration stage. The following paragraphs provide a stage-by-stage description of the reefing sequence.

Stage 1. - The wing surface was reefed into three lobes by use of a separate reefing line around the periphery of each section of the wing (i.e., the center and the two outboard sections), and by gathering the wing trailing edges with a separate reefing line. For those tests in which nose reefing was employed, the center section nose area of the wing was also gathered with a separate reefing line. Suspension lines were foreshortened to the length of the tip suspension lines, the shortest suspension lines on the wing. This was done to: (a) align the inlets to the three lobes in a plane perpendicular to the air stream; (b) eliminate loose suspension lines and their possible entanglement during the deployment process; (c) prevent abrasion damage of keel suspension lines against the skirt reinforcing band; and (d) provide a more uniform suspension line loading.

During stage 1, the parawing inflated to a three-lobed, balloon shape. Figure 4 shows a view looking up into the canopy with the wing fully inflated in the first reefed stage. As shown, three air inlets -- one for each lobe -- are formed by the reefing lines around the leading edges, the keels, and the trailing edges. In this stage the parawing performed basically as a ballistic drag device, similar to a parachute.

Stage 2. - To establish stage 2, the reefing lines on the periphery of the outboard sections of the wing were severed. All other reefing lines remained intact. The parawing inflated to the planform shape shown in Figure 4. Note that the center lobe maintained its balloon-like shape between the more fully inflated outboard lobes. During this stage the wing continued to perform basically as a ballistic drag device.

Stage 3. - To establish stage 3, the reefing line on the periphery of the center section of the wing was severed. The wing planform for this stage is shown in Figure 4. Two planforms are illustrated, one with and one without reefing of the center section nose area of the wing. During this stage the wing began gliding in a rearward direction.

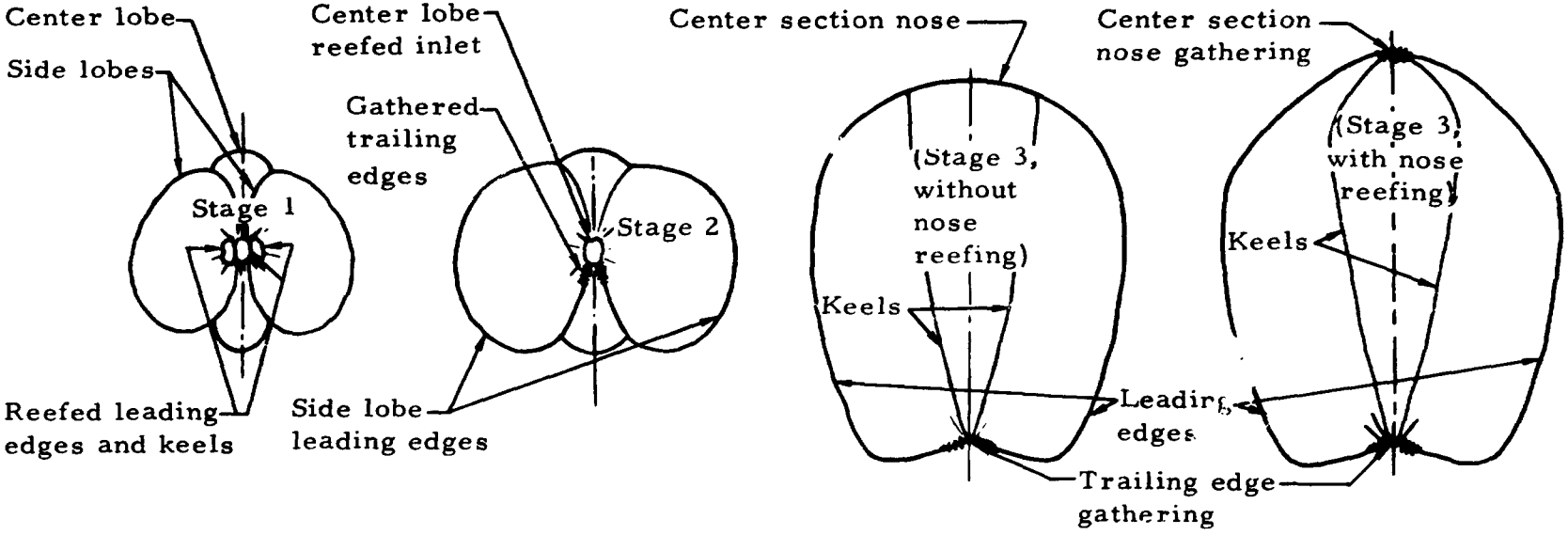

Note: All views are looking up into canopy; all views for fully inflated canopy during a stage

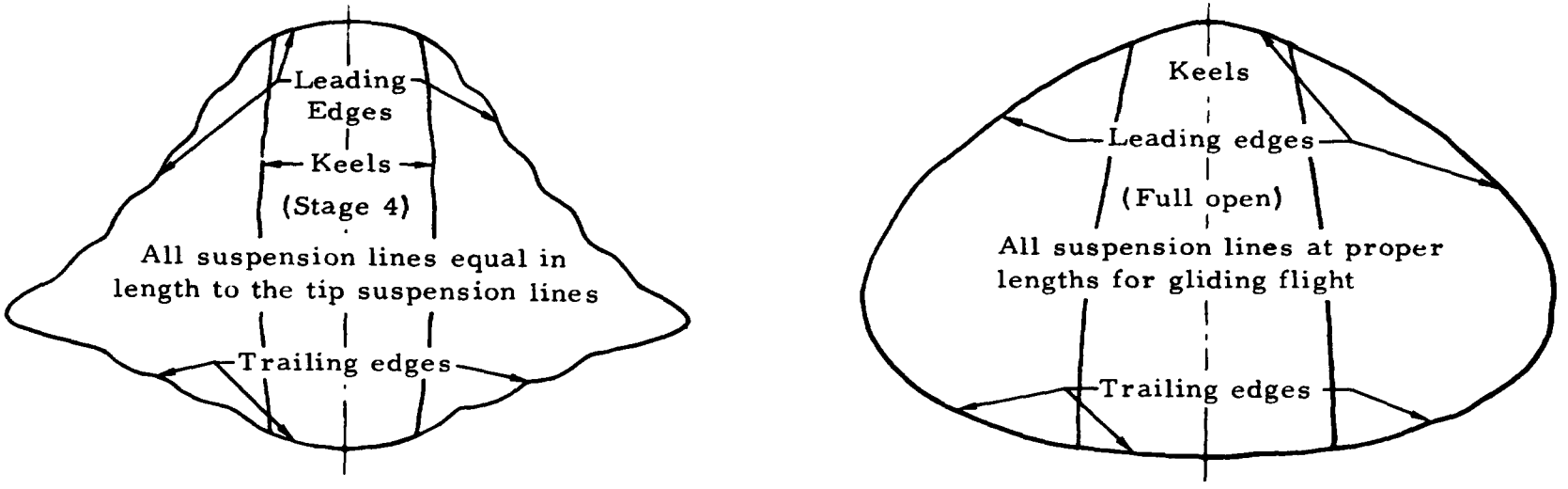

Figure 4. Typical planforms during reefing sequence for twin keel parawing

Stage 4. - To achieve stage 4, the trailing edge gathering line, and if used, the nose gathering line were severed. For this stage all reefing lines were removed and the wing inflated to the planform shown in Figure 4. The wing underwent a transition to forward gliding flight during this stage.

Full open. - The suspension lines were released to their gliding flight lengths, and the wing made a transition to the gliding flight planform shown in Figure 4.

Single Keel Parawing Reefing Sequence

The single keel parawing reefing sequence consisted of four stages of reefing, followed by the gliding configuration stage. The following paragraphs provide a stage-by-stage description of the reefing sequence.

Stage 1. - The wing surface was reefed into two lobes by reefing lines routed around the leading edge and trailing edge of each section, and by separate reefing lines which gathered the keel and the trailing edges of the wing. Suspension lines were foreshortened to the length of the tip suspension lines, for the reasons previously identified in the description of the twin keel reefing sequence.

During stage 1, the parawing inflated to a two-lobed, balloon shape. Figure 5 shows a view looking up into the canopy with the wing fully inflated in the first reefed stage. As shown, two lobes were formed with the gathered keel serving as a partition between the lobes. In this stage the parawing performed basically as a ballistic drag device, similar to a parachute.

Stage 2. - To establish stage 2, the reefing lines around the leading edge and trailing edge of each lobe were released, so that the leading edges were allowed to fully inflate. Figure 5 shows a planform view (from below) of the canopy in this stage. During this stage the wing continued to perform basically as a ballistic drag device.

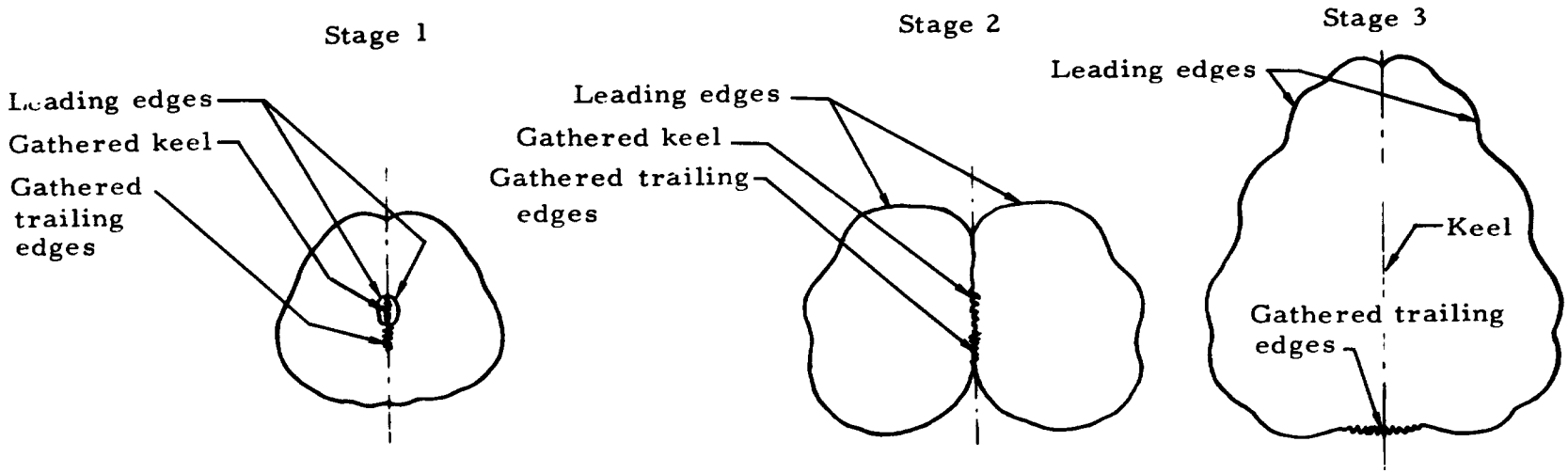

Note: All views are looking up into canopy; all views are for fully inflated canopy during a stage

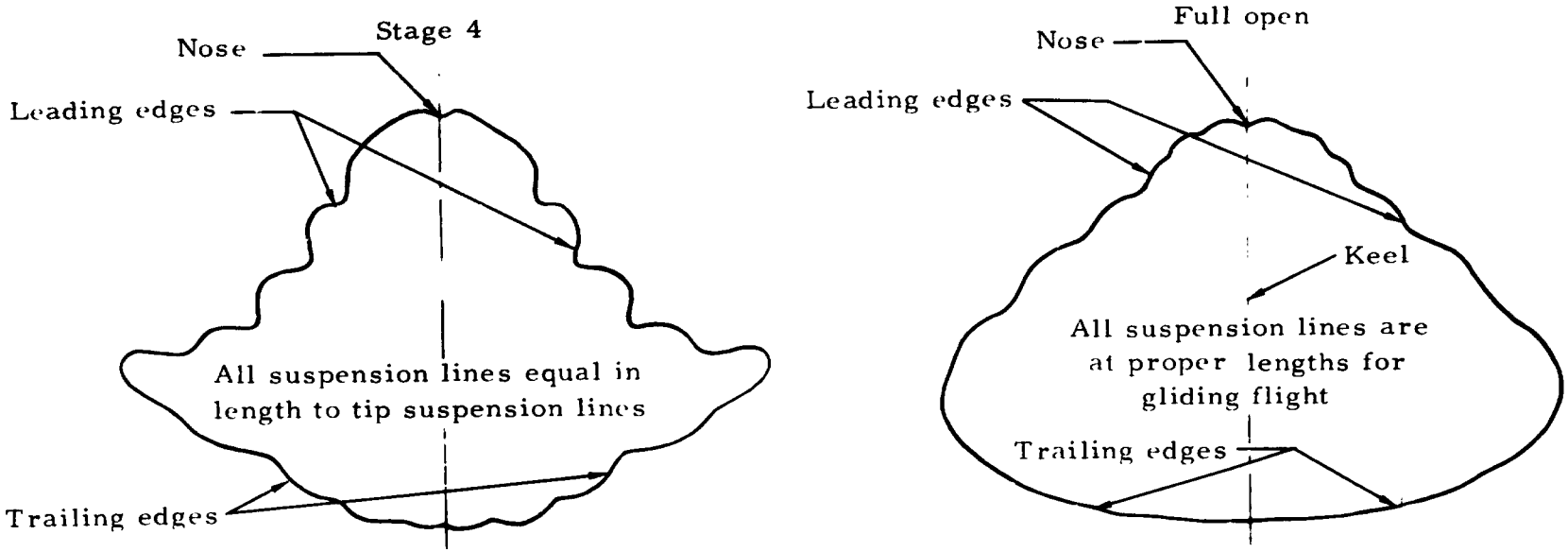

Figure 5. Typical planforms during reefing sequence for single keel parawing

Stage 3. - To achieve stage 3, the keel gathering line was severed. Figure 5 shows the planform for this stage. During this stage the wing began gliding in a rearward direction.

Stage 4. - For stage 4, the trailing edge gathering line was severed, removing all reefing lines from the wing. A transition to forward gliding flight occurred during this stage. The planform for this stage is shown in Figure 5.

Full open. - The suspension lines were released to their gliding flight lengths, and the wing made a transition to the gliding flight planform shown in Figure 5.

INTERMEDIATE-SCALE TEST SEQUENCES

LAUNCH AIRCRAFT

Two types of aircraft were used for the bomb-type vehicle tests. These were the C-119 and the C-130. For the controllable vehicle tests, only the C-119 aircraft was used.

PARAWING DEPLOYMENT SYSTEM AND TEST SEQUENCE

Bomb-Type Test Vehicle

For purposes of discussion in this section of the report, the deployment system is defined as all the equipment used from aircraft launch of the test system until the parawing-test-specimen-line-stretch event. Figure 6 shows a typical test sequence with the bomb-type test vehicle and illustrates the various components in the deployment system. For launch from the aircraft, the bomb-type test vehicle was initially mounted on a platform. The platform was a standard, cargo-delivery platform, sized to fit the rollers and guide rails on the floor of the aircraft. Launch of

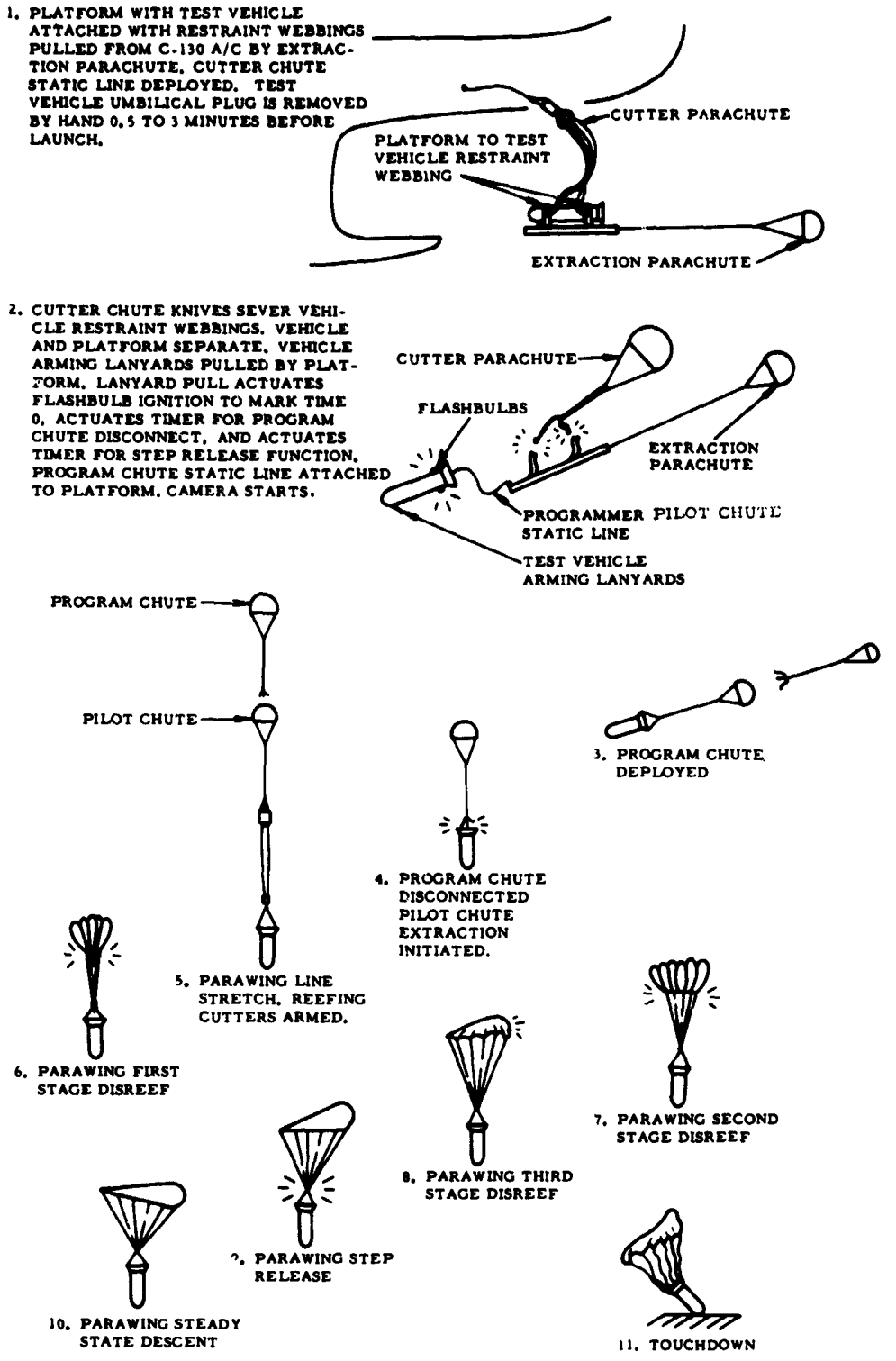

Figure 6. Sequence of events, C-130 and C-119 aircraft launch of bomb-type test vehicle

the test system from the drop aircraft was initiated by deploying an extraction parachute to the rear of the aircraft. This parachute in turn pulled the platform with the attached bomb-type test vehicle from the aircraft. As the bomb and platform moved away from the aircraft, another parachute, called the cutter chute, was static line deployed. This parachute was used to sever the lashings which held the bomb to the platform.

After the bomb restraint lashings were cut, the extraction parachute pulled the platform away from the bomb. As the bomb separated from the platform, a static line from the platform deployed a pilot chute which in turn deployed the programmer parachute. The function of the programmer parachute was to establish the proper dynamic pressure and flight path angle, prior to deployment of the parawing test specimen. After a predetermined length of programmer parachute operating time, the programmer parachute was released and used to deploy the parawing pilot chute. The pilot chute in turn extracted the parawing pack from the aft section of the bomb-type vehicle and deployed the parawing from its deployment bag. At this point in the sequence the parawing began the reefing sequence previously described. The time interval for each stage of the reefing sequence was controlled by pyrotechnic, reefing-line cutters. These cutters had a time-delay powder train which was lanyard initiated at parawing line stretch. At the end of the fixed time delay, the powder train ignited an explosive charge which actuated the reefing-line-cutter blade. Upon completion of the deployment sequence, the parawing/bomb vehicle system made an uncontrolled gliding descent.

During the flight, test data were telemetered from on-board instrumentation to a ground receiving station. Also, camera coverage and photo-theodolite data were obtained. A description of the data obtained during the flight is presented in APPENDICES A and B.

Controllable, Sled-Type Test Vehicle

Figure 7 illustrates a typical sequence with the controllable test vehicle. The vehicle was carried in the launch aircraft on an inclined ramp. Launch of the vehicle was initiated by release of the shackles which held the test vehicle to the launch ramp. Releasing the shackle allowed the test vehicle to slide down the inclined ramp and out of the aircraft. As the test vehicle separated from the aircraft, a static line deployed a programmer parachute. As with the bomb-type vehicle tests, the purpose of the programmer parachute was to establish the proper conditions for deployment of the parawing test specimen. After a predetermined period of time the programmer parachute was disconnected from the test vehicle and used to deploy the parawing pilot chute. The pilot chute in turn lifted the parawing pack off the test vehicle upper deck and deployed the parawing test specimen from its deployment bag. The parawing then proceeded through the previously described reefing sequence until the fully inflated, gliding-flight configuration was established.

The parawing/test vehicle system was then put through a series of maneuvers which involved changes in the lengths of the rear-keel-suspension-lines and the tip-suspension-lines. These maneuvers were performed to obtain data on flight performance during straight and turning flight. Flight test data from on-board instrumentation were telemetered to a ground receiving station during the flight. Motion picture coverage and photo-theodolite tracking data were also obtained.

More complete information on the data obtained during the flight is presented in APPENDICES A and B.

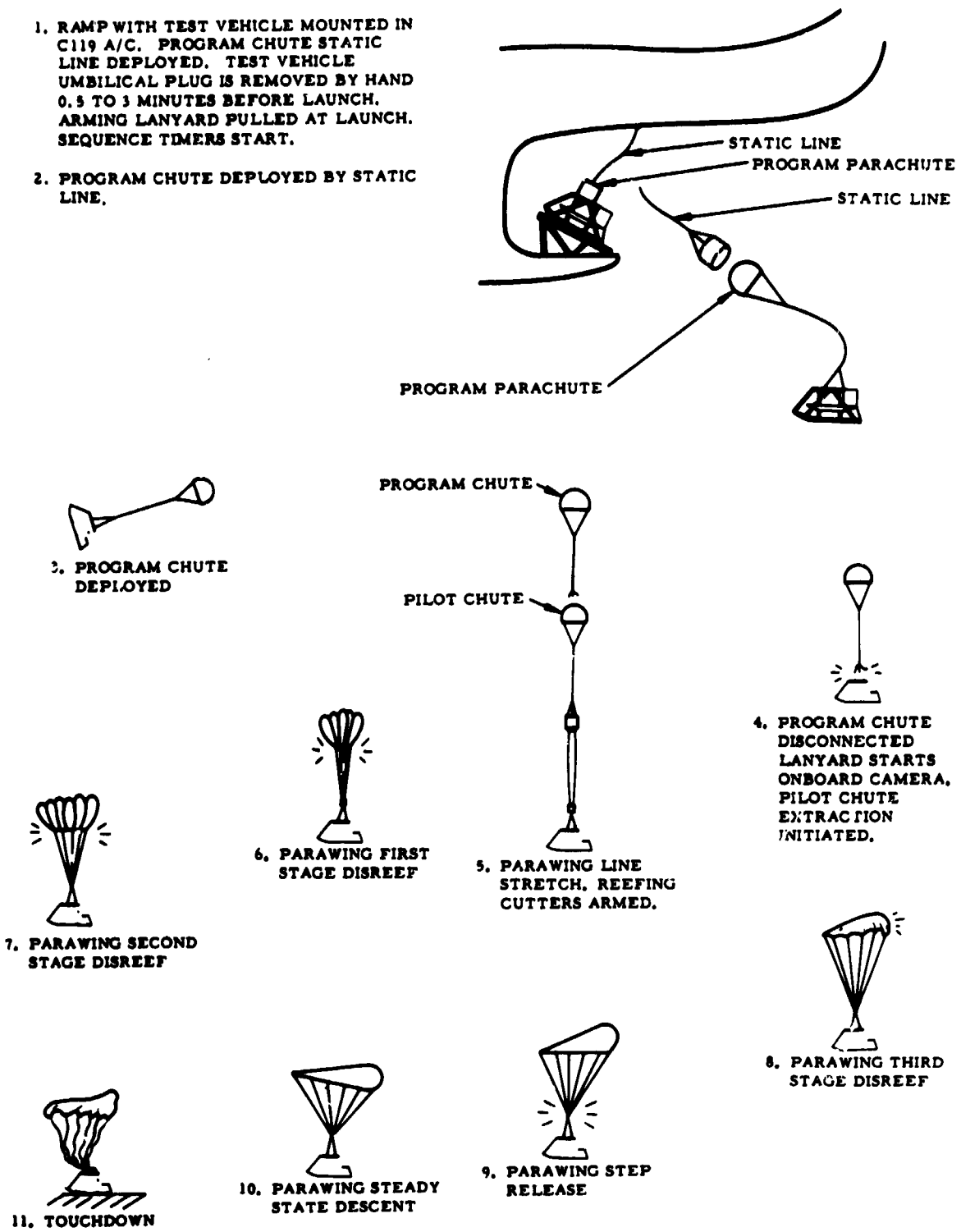

Figure 7. Sequence of events, C-119 aircraft launch of controllable test vehicle

INTERMEDIATE-SCALE PARAWING TEST SPECIMENS

GENERAL

The test specimens used in the intermediate-scale aerial drop test program consisted of seven versions of the twin keel parawing and one version of the single keel parawing. Early in the test program the single keel parawing was eliminated from further testing, due to canopy structural problems plus the demonstrated, higher gliding performance potential of the twin keel parawing. Changes to the twin keel parawing were mainly structural improvements to the canopy. In addition, functional and structural improvements were made to the reefing system and some minor changes made in suspension line lengths.

STRUCTURAL ARRANGEMENT

Basic canopy structures for the single and the twin keel parawings were similar in design. The canopies were constructed of 2.25 ounce per square yard, low permeability, nylon sailcloth, with the warp running parallel to the wing trailing edges. Main structural canopy seams were laid parallel to the trailing edges of the wing, joining leading edge suspension line or reefing ring attachment points with adjacent keel line attachment points. These seams were reinforced with layers of nylon tape as required. All the outer edges and the keels of the canopies were reinforced with multiple layers of the nylon tape. Highly stressed areas, such as the suspension line and reefing ring attachments, were reinforced with semicircular or eliptical shaped, load-distribution patches fabricated from the same basic canopy material. Where necessary, additional patch reinforcement was provided by overlaid radial tapes.

Twin Keel Parawing

The planform and structural arrangement for the seven versions of the twin keel parawing are shown in Figures 8 through 13. Version I, as shown in Figure 10, was the basic version from which all other versions were created by modification. Version I had a total of forty-two suspension lines; six lines equally spaced along each leading edge, twelve lines located along each keel and three lines spaced along the trailing edge of each outer section. The Version II model was identical to Version I, except for tip suspension lines L6 and R6, which were made 40.6 inches longer in order to provide a complete range of tip-control-line travel when used with the controllable test vehicle.

The Version III model shown in Figure 11 was identical to Version II, except for the addition of five leading edge suspension lines to each outer section, larger semicircular load distribution patches at leading-edge-line-attachment locations 2-1/2 through 4-1/2 and four longitudinal ripstop tapes sewn on each outer section. Version IV shown in Figure 12 was identical to Version II, except for the addition of five suspension lines to the leading edge of each outer section, five longitudinal ripstop tapes added to the wing center section, sixteen diagonal ripstop tapes added to each outer section and load distribution patches added at leading-edge-line-attachment locations 3, 3-1/2 and 4. Version V was identical to Version IV, except for 40.6 inches shorter tip suspension lines L6 and R6 on the Version V. Version VI shown in Figure 13 was identical to Version IV, except that the outer section radial tapes on the LK1 and RK1 reinforcing patches were lengthened to terminate at the intersections of two diagonal ripstop tapes. Version VII was identical to Version VI, except for 40.6 inches shorter tip suspension lines L6 and R6 on Version VII. The suspension line lengths and strengths for all versions are given in Table 2.

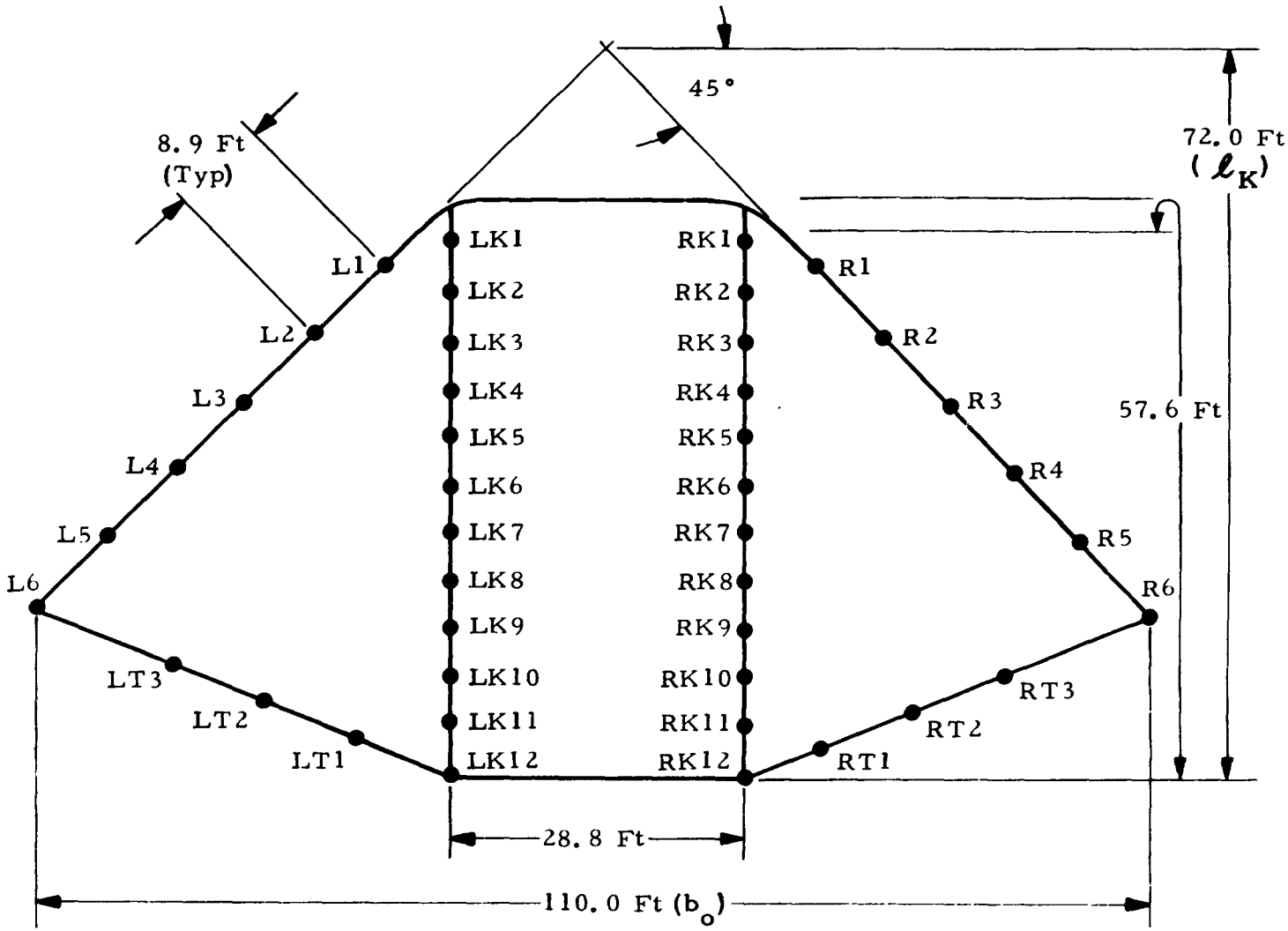

Figure 8. Planform layout for intermediate-scale, twin keel paiawing, Versions I and II

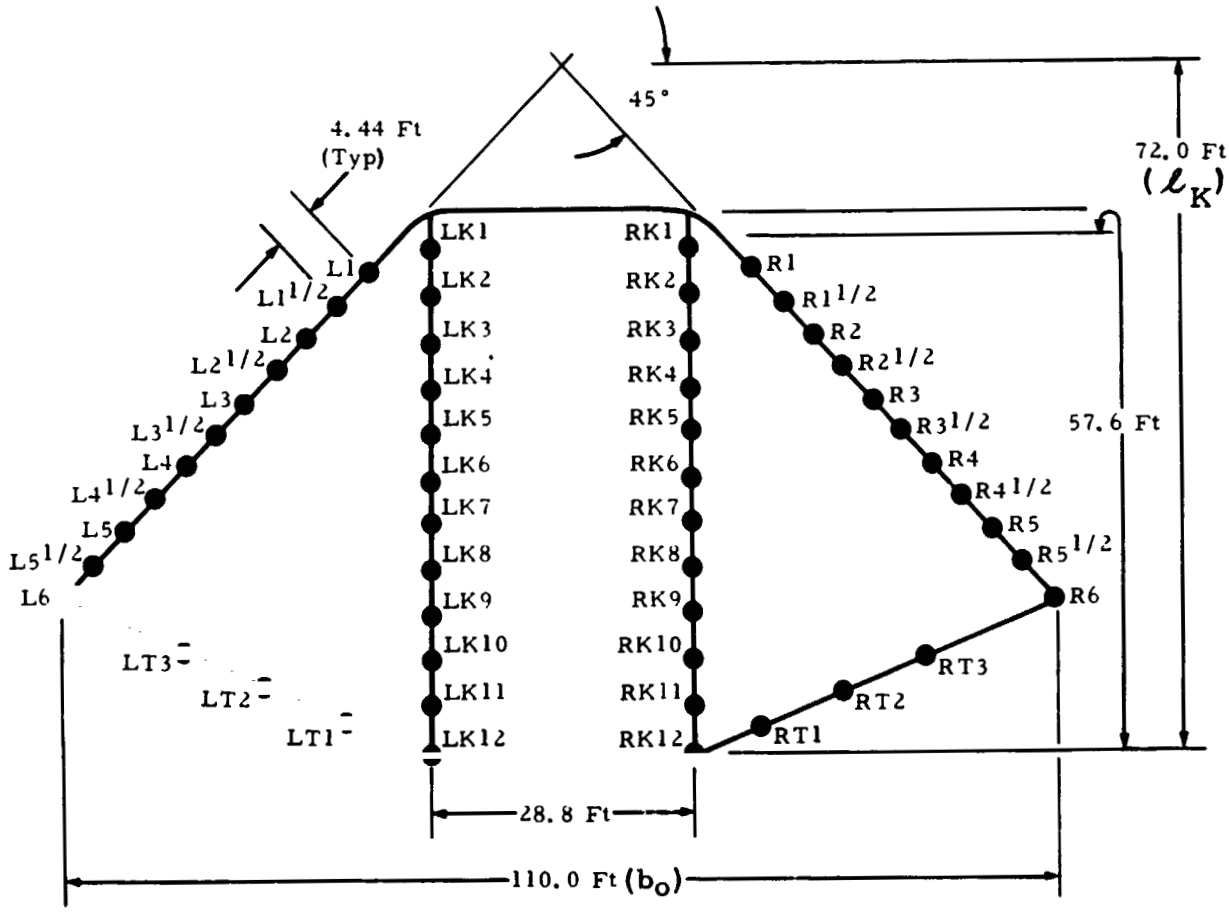

Figure 9. Planform layout for intermediate-scale, twin keel parawing, Versions III through VII

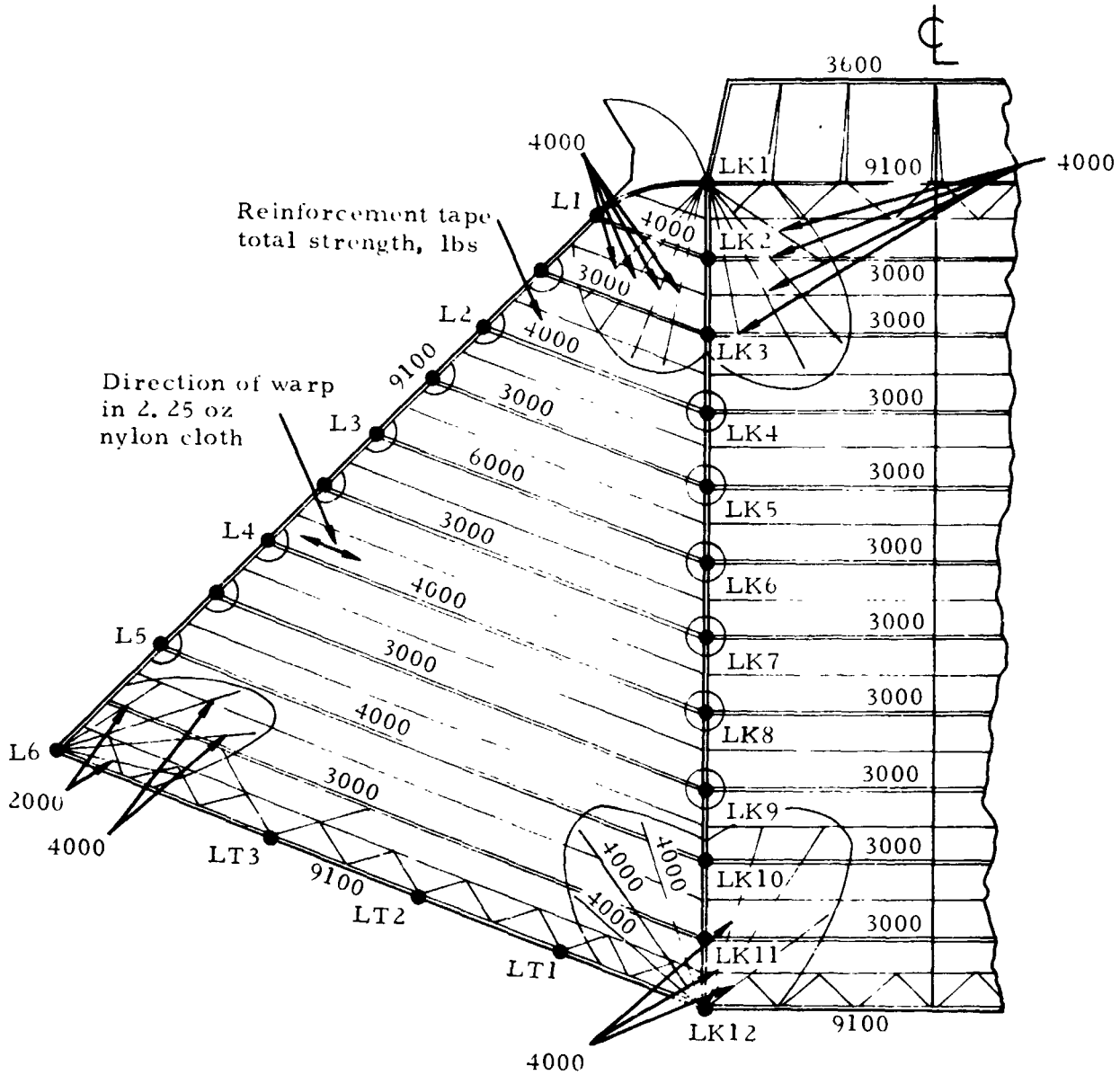

Figure 10. Structural diagram for twin keel parawing, Versions I and II

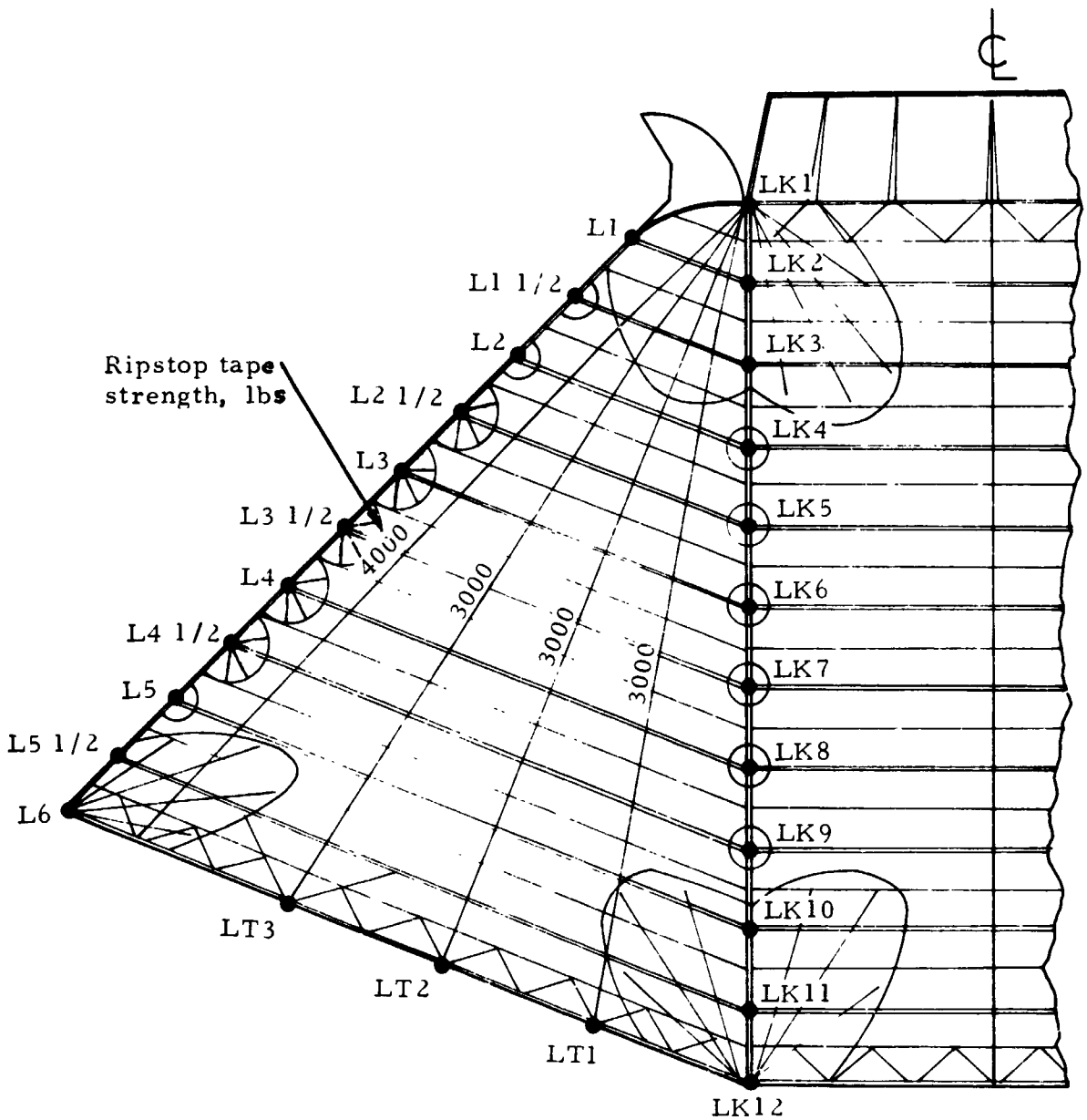

Figure 11. Structural diagram for twin keel parawing, Version III (identical with Versions I and II, except as noted above)

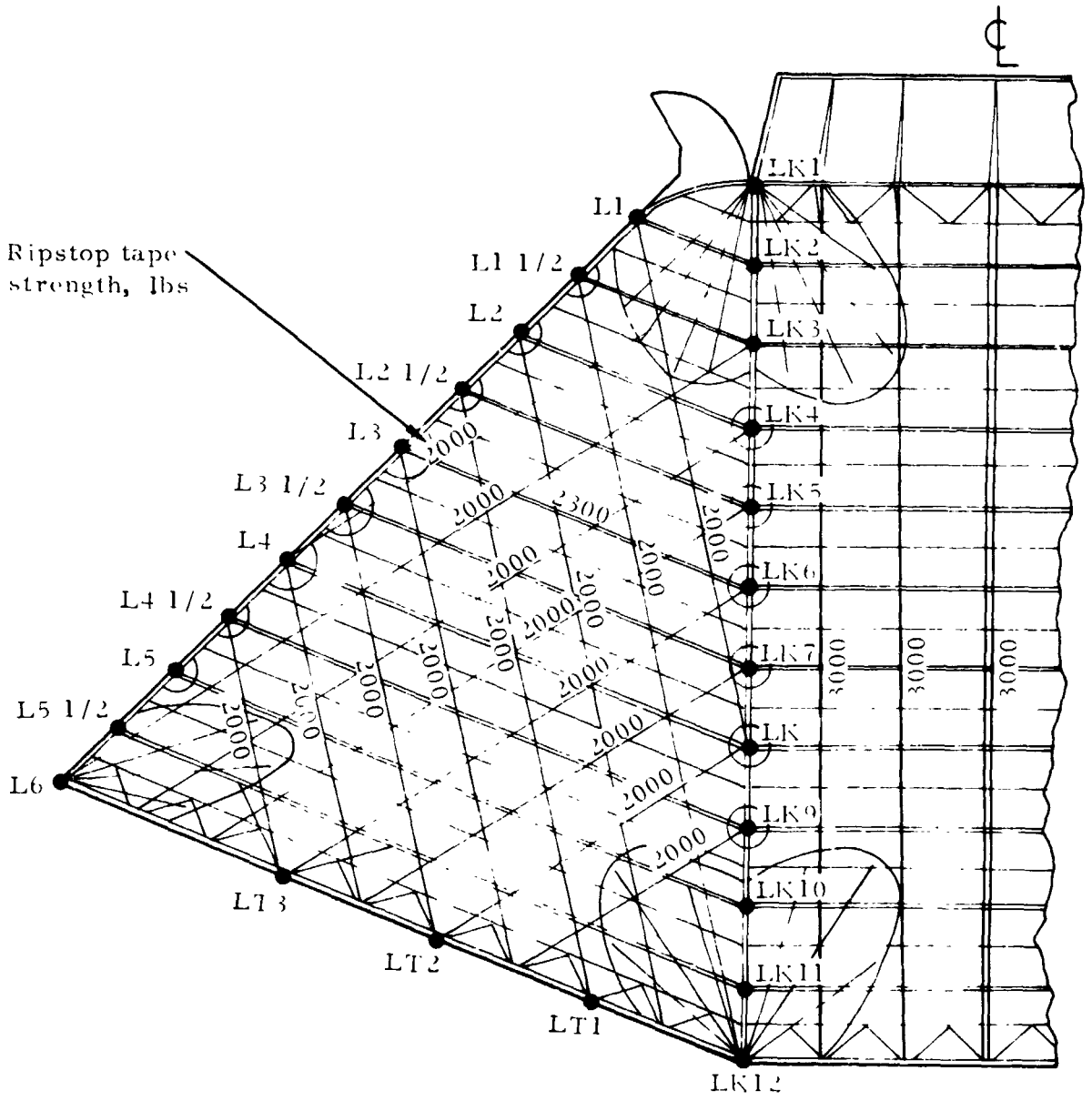

Figure 12. Structural diagram for twin keel parawing, Versions IV and V (identical with Versions I and II, except as noted above)

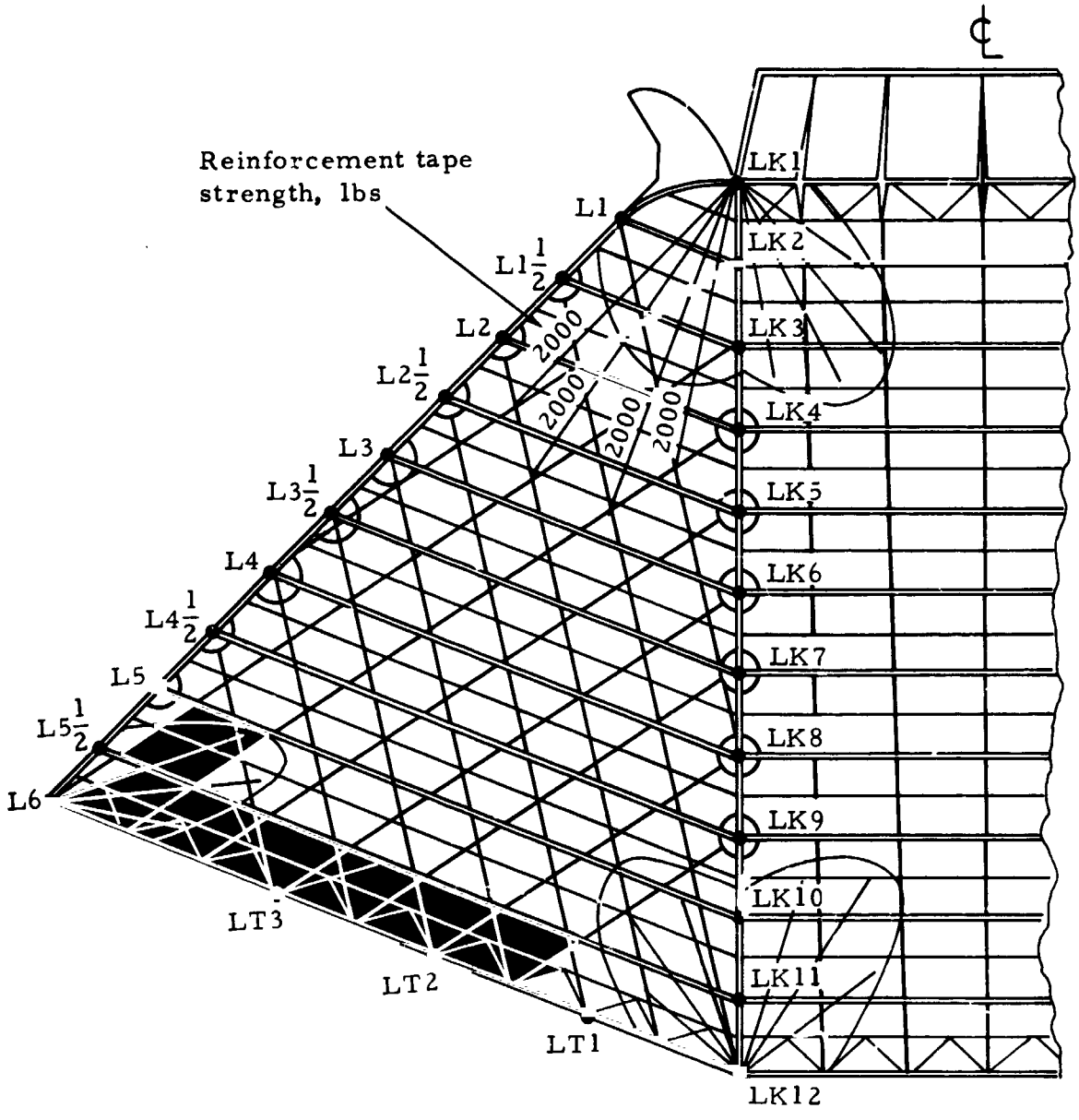

Figure 13. Structural diagram for twin keel parawing Versions VI and VII (identical with Versions IV and V, except as noted above)

TABLE 2. -TWIN KEEL PARAWING SUSPENSION LINE DESIGN LENGTHS & RATED STRENGTHS

Suspension line no.	Version I		Version II		Versions III, IV & VI		Versions V & VII	
	Design (a) length, in	Rated strength, lbs	Design (a) length, in	Rated strength, lbs	Design (a) length, in	Rated strength, lbs	Design (a) length, in	Rated strength, lbs
R1 & L1	803.5	5500	803.5	5500	803.5	5500	803.5	5500
R1 1/2 & L1 1/2	—	—	—	—	796.6	3500	796.6	3500
R2 & L2	786.2	5500	786.2	5500	786.2	5500	786.2	5500
R2 1/2 & L2 1/2	—	—	—	—	777.6	4500	777.6	4500
R3 & L3	769.0	10,000	769.0	10,000	769.0	5500	769.0	5500
R3 1/2 & L3 1/2	—	—	—	—	747.4	4500	747.4	4500
R4 & L4	730.1	5500	730.1	5500	730.1	5500	730.1	5500
R4 1/2 & L4 1/2	—	—	—	—	699.8	3500	699.8	3500
R5 & L5	673.9	5500	673.9	5500	673.9	5500	673.9	5500
R5 1/2 & L5 1/2	—	—	—	—	636.8	3500	636.8	3500
R6 & L6	521.0	5500	561.6	5500	561.6	5500	521.0	5500
RK1 & LK1	842.4	4500	842.4	4500	842.4	4500	842.4	4500
RK2 & LK2	855.4	4500	855.4	4500	855.4	4500	855.4	4500
RK3 & LK3	851.0	4500	851.0	4500	851.0	4500	851.0	4500
RK4 & LK4	842.4	4500	842.4	4500	842.4	4500	842.4	4500
RK5 & LK5	842.4	4500	842.4	4500	842.4	4500	842.4	4500
RK6 & LK6	842.4	4500	842.4	4500	842.4	4500	842.4	4500
RK7 & LK7	833.8	4500	833.8	4500	833.8	4500	833.8	4500
RK8 & LK8	833.8	4500	833.8	4500	833.8	4500	833.8	4500
RK9 & LK9	829.4	4500	829.4	4500	829.4	4500	829.4	4500
RK10 & LK10	820.8	4500	820.8	4500	820.8	4500	820.8	4500
RK11 & LK11	803.5	4500	803.5	4500	803.5	4500	803.5	4500
RK12 & LK12	758.9	5500	758.9	5500	758.9	5500	758.9	5500
RT1 & LT1	925.0	3500	925.0	3500	925.0	3500	925.0	3500
RT2 & LT2	925.0	3500	925.0	3500	925.0	3500	925.0	3500
RT3 & LT3	808.0	3500	808.0	3500	808.0	3500	808.0	3500

a skirt band attachment to riser leg connector link, except for RK12 and LK12 which were attached to an extension riser 65.4 inches long. The lengths of RK12 and LK12 from the skirt band attachment to the riser leg connector links where all other suspension lines were attached was 824.3 inches.

Single Keel Parawing

The planform and structural arrangement for the single keel parawing are shown in Figures 14 and 15, respectively. The single keel parawing had a total of thirty-two suspension lines, six lines equally spaced along each leading edge, twelve lines spaced along the keel and four lines equally spaced along each trailing edge. The length and strength of each suspension line are given in Table 3.

RIGGING ARRANGEMENT

The parawing was attached to the test vehicle with four risers located as shown in Figure 16. Each riser was attached to a group of suspension lines with a connector link. Multiple riser legs were used where necessary to accommodate a large number of lines. The number of riser legs at each attachment location is identified in Figures 17, 18 and 19. The suspension-line-to-riser arrangements are shown in Figures 20, 21, 22 and 23. To provide for the equal-suspension-line length parawing configuration required during the reefed phase of deployment, each suspension line was provided with a by-pass loop located equidistant from the canopy skirt. These loops were attached to the swing-arm release fittings located at the main fore and aft attach points. The excess length of each suspension line in the deployment configuration was stowed in individual sleeves attached to the suspension line above the by-pass loop. These stowed line segments were deployed following the line-transfer event. The parawing attachment arrangements to the test vehicle during the deployment phase and during the gliding flight phase are shown in Figures 24 and 25, respectively.

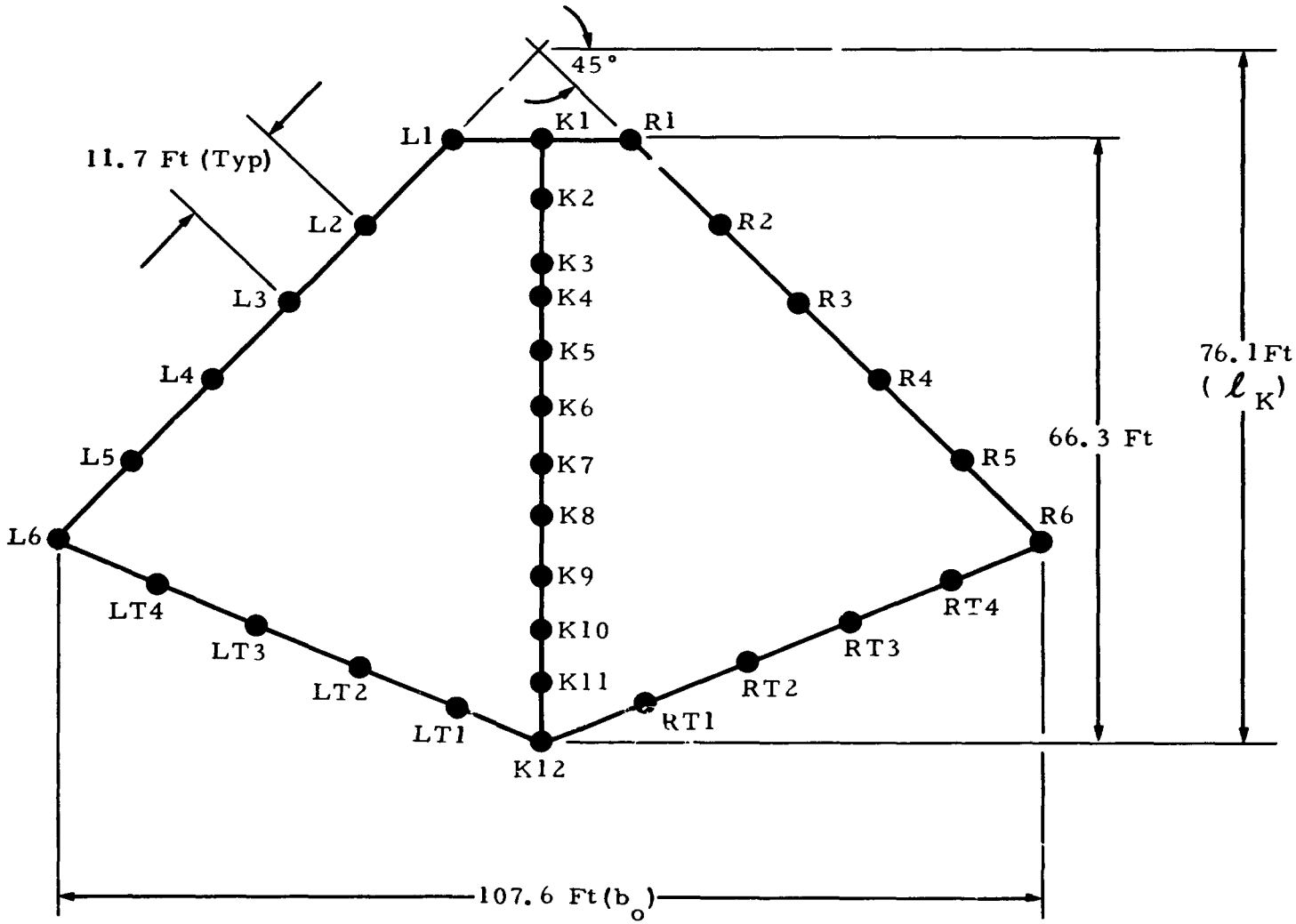

Figure 14. Planform layout for intermediate-scale single keel parawing

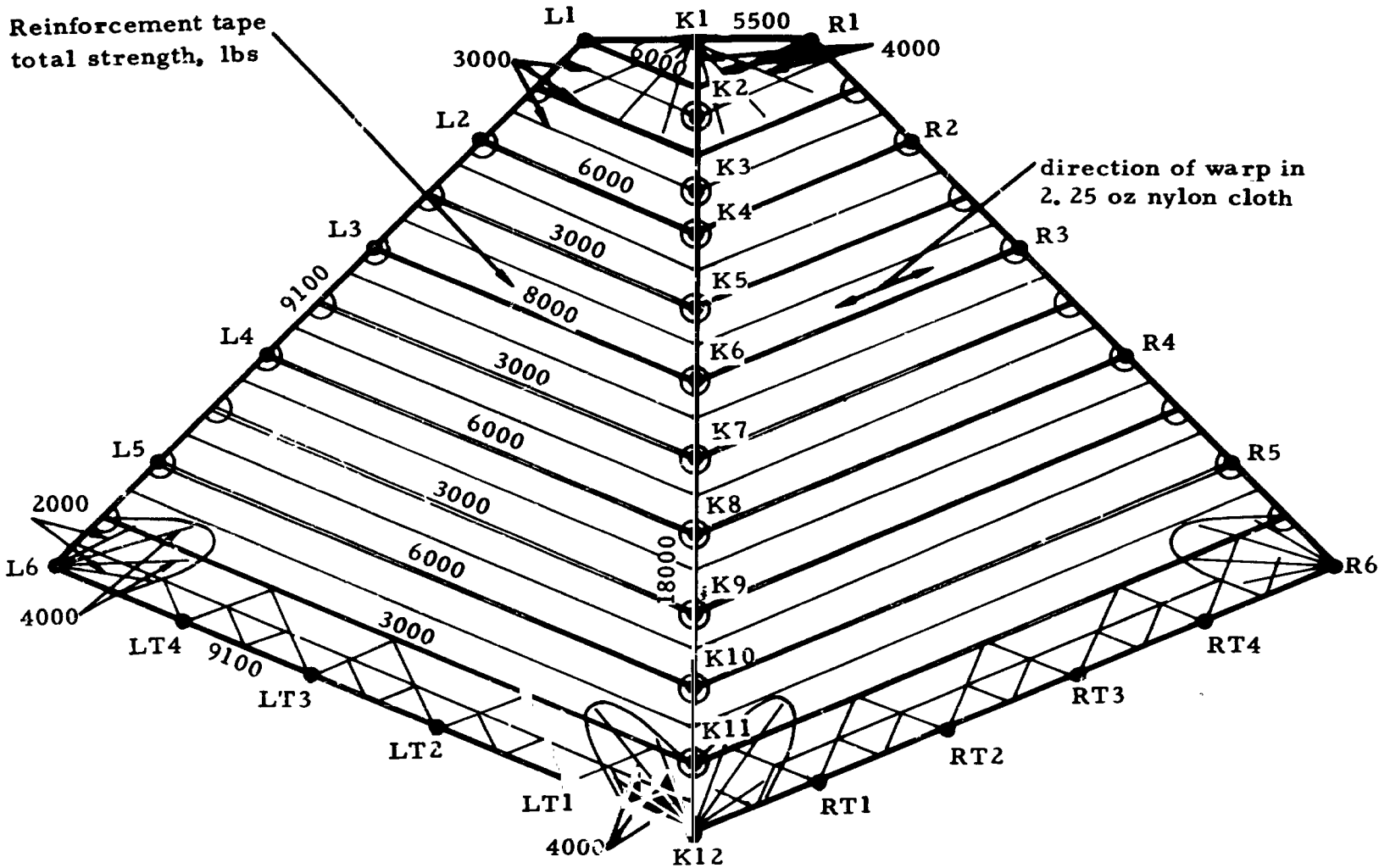

Figure 15. Structural diagram for single keel parawing

TABLE 3.-SINGLE KEEL PARAWING SUSPENSION LINE DESIGN LENGTHS AND RATED STRENGTHS

Suspension line no.	Design length (a) in	Rated strength lbs
R1 & L1	986.6	6000
R2 & L2	939.2	6000
R3 & L3	899.4	10000
R4 & L4	834.8	6000
R5 & L5	791.9	6000
R6 & L6	711.5	6000
K1	948.7	4500
K2	969.6	4500
K3	979.0	4500
K4	960.1	4500
K5	937.3	4500
K6	929.7	4500
K7	929.7	5500
K8	929.7	5500
K9	929.7	5500
K10	916.1	5500
K11	847.5	5500
K12	787.4	5500
RT1 & LT1	993.0	3500
RT2 & LT2	1040.4	3500
RT3 & LT3	1005.6	3500
RT4 & LT4	853.8	3500

(a)skirt band attachment to riser leg connector link

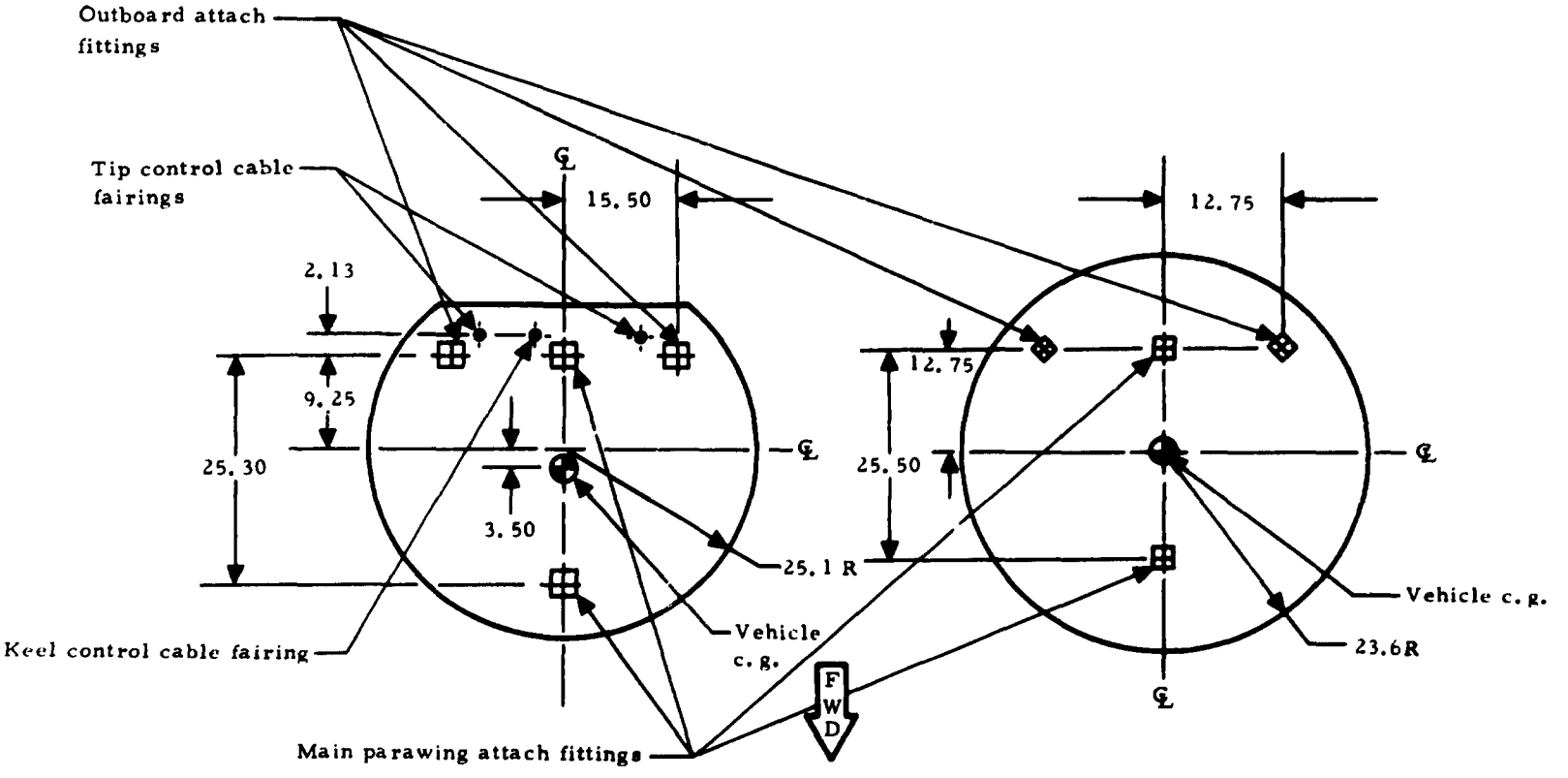

Controllable test vehicle (top view)

Bomb type test vehicle (top view)

Note: All dimensions in inches

Figure 16. Parawing attach fitting locations on the intermediate-scale test vehicles

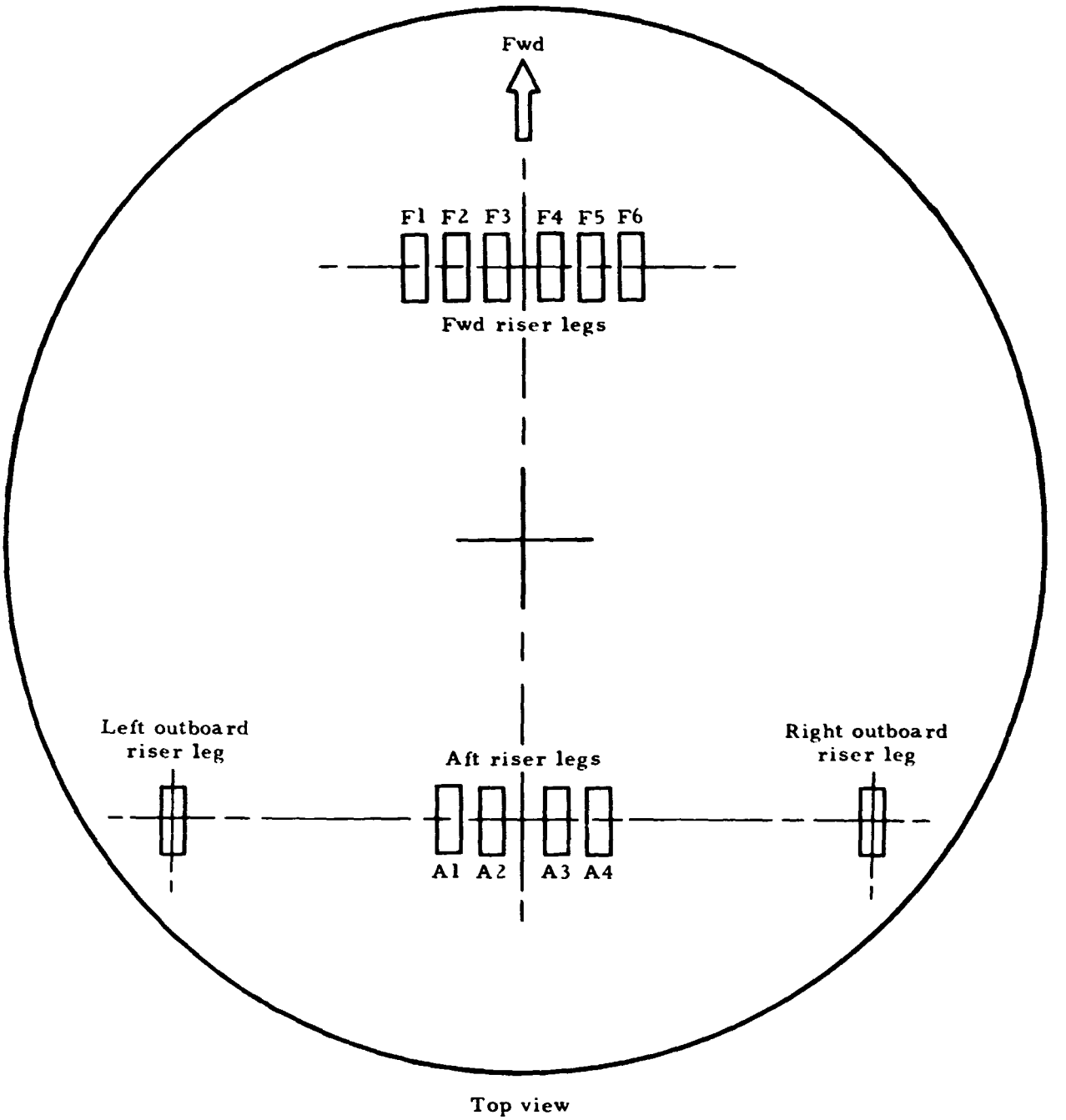

Figure 17. Riser arrangement for twin keel parawing, Versions I & II

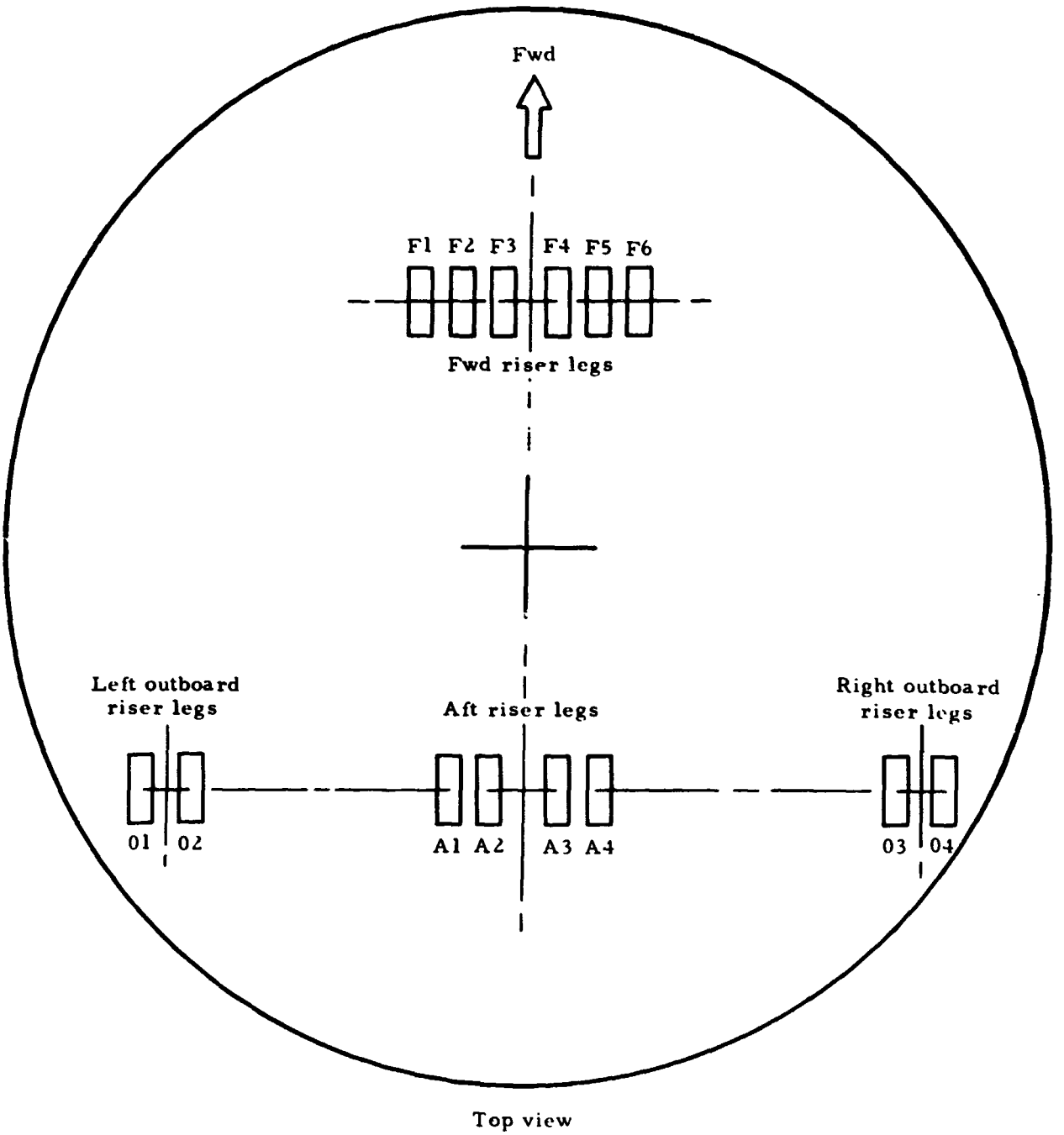

Figure 18. Riser arrangement for twin keel parawing, Version III through VII

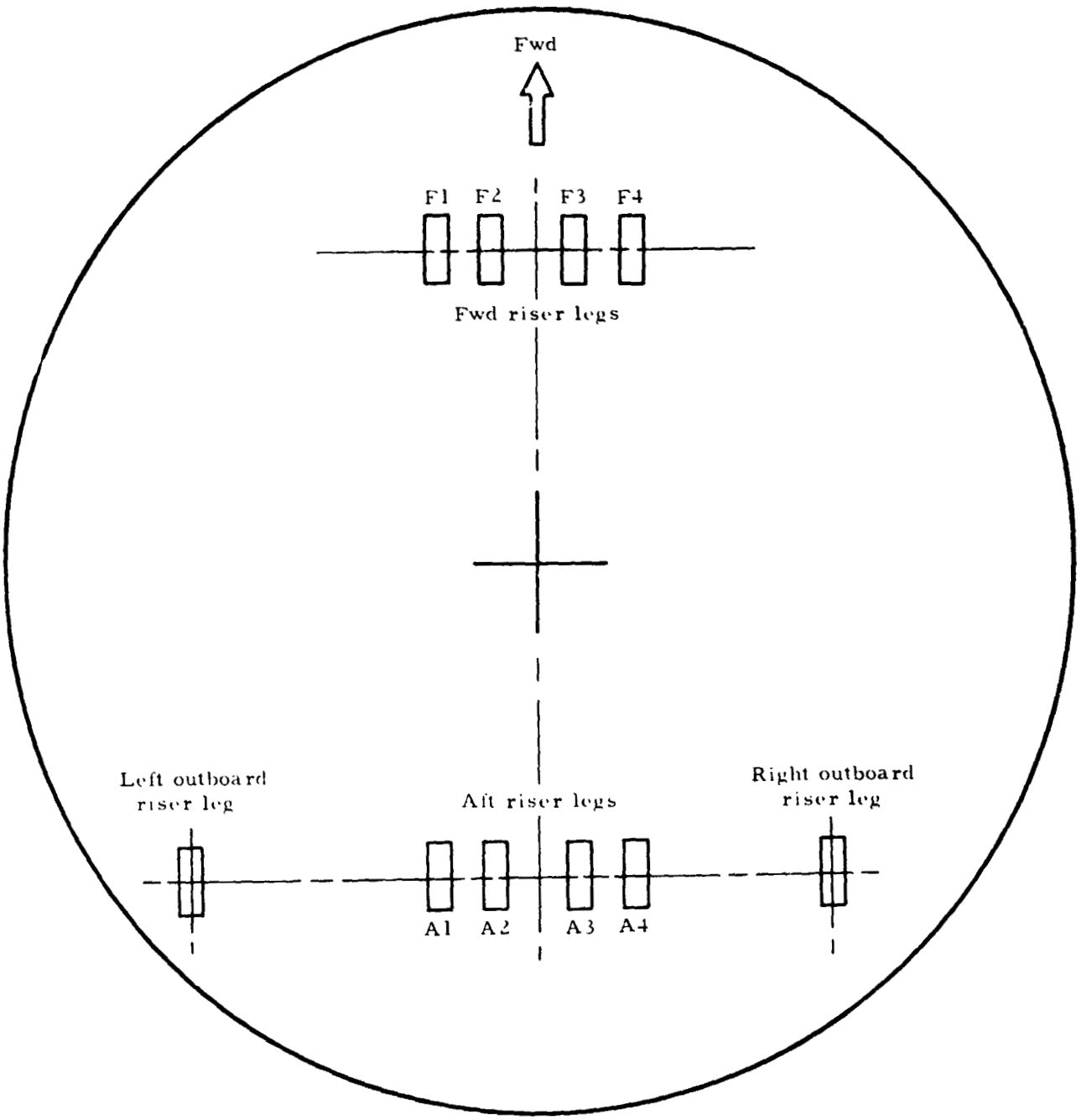

Top view

Figure 19. Riser arrangement for single keel parawing

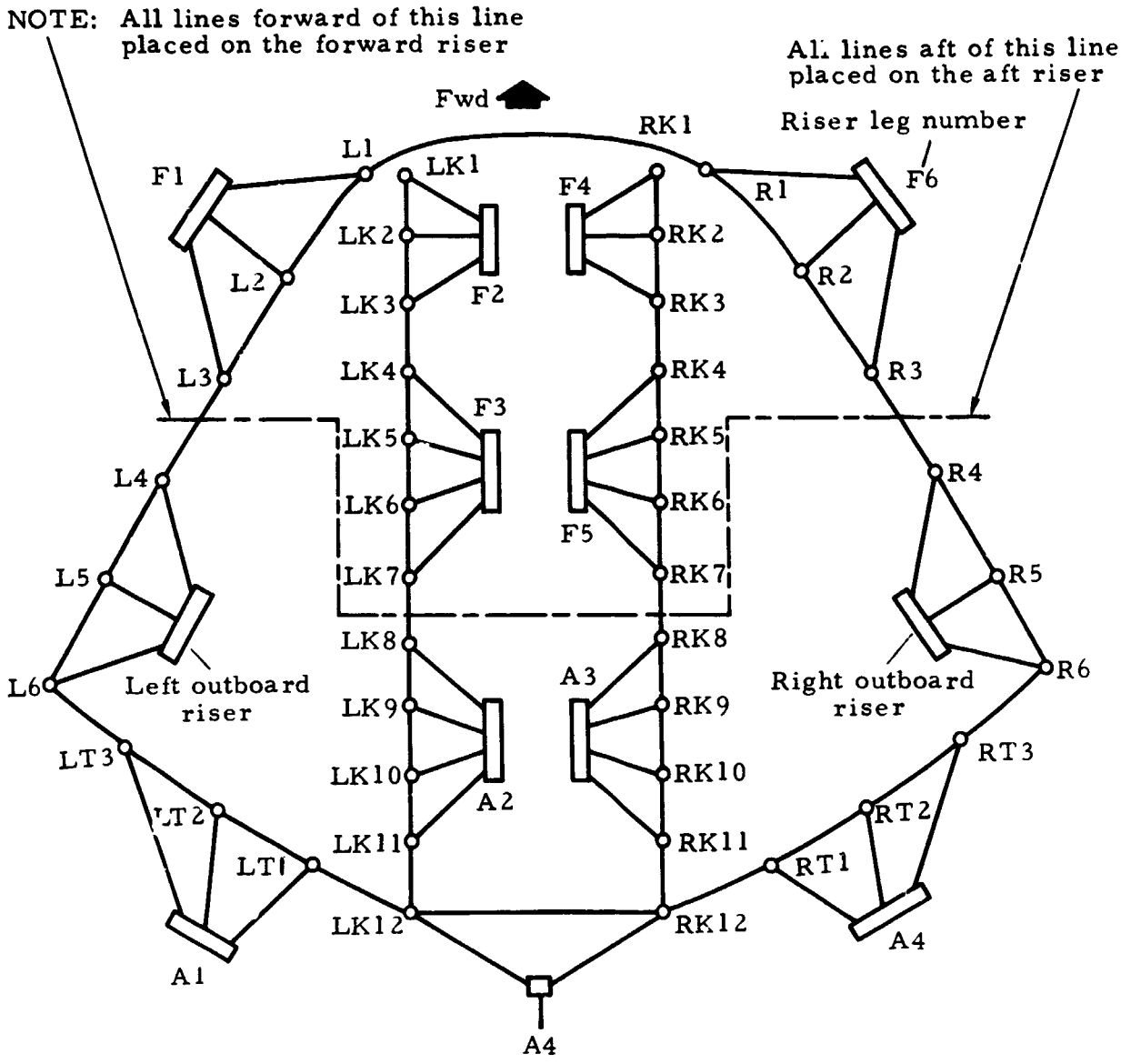

View from above

Figure 20. Suspension line/riser attachment arrangement for twin keel parawing, Version I

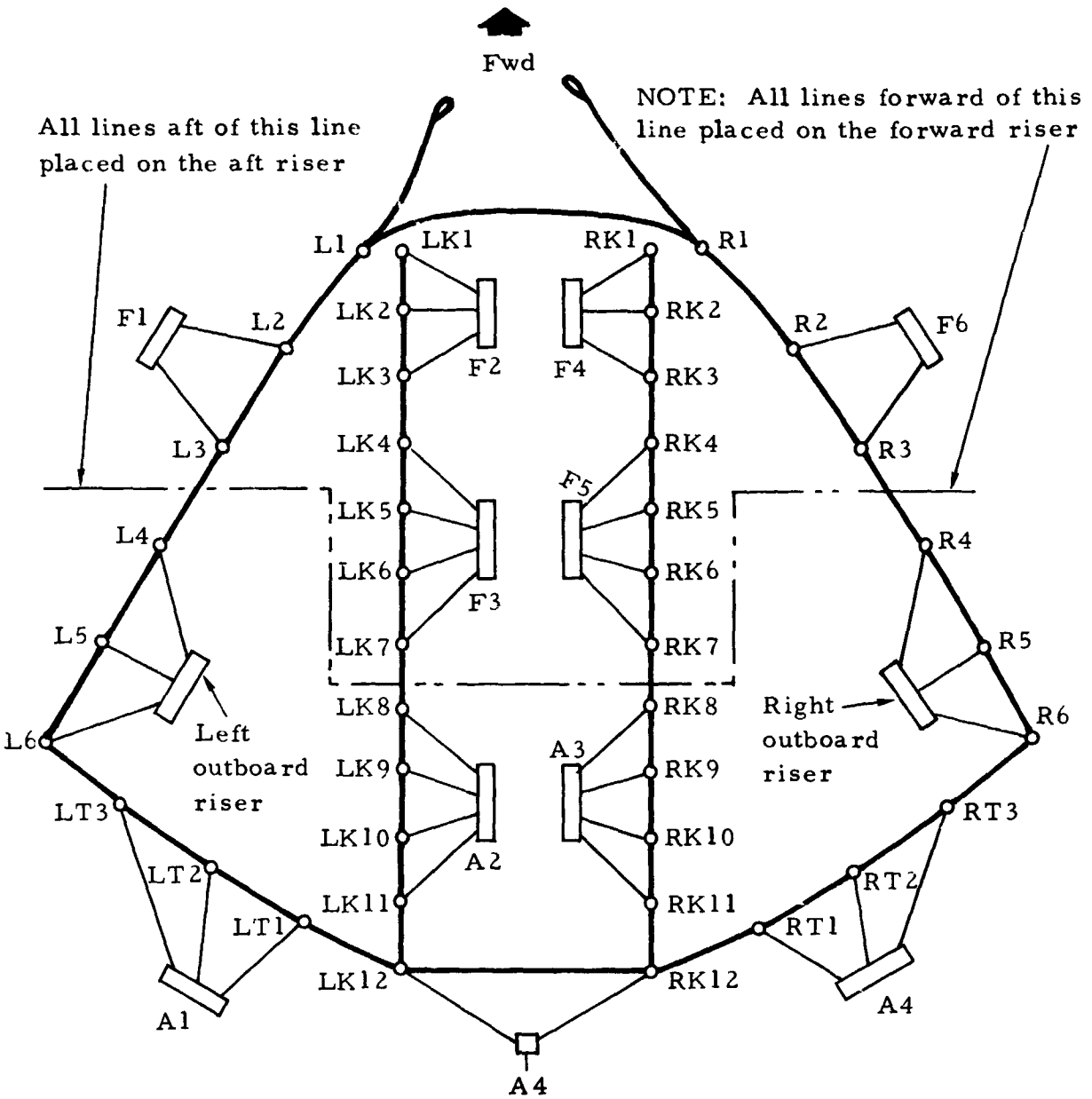

Figure 21. Suspension line/riser attachment arrangement for twin keel parawing, Version II

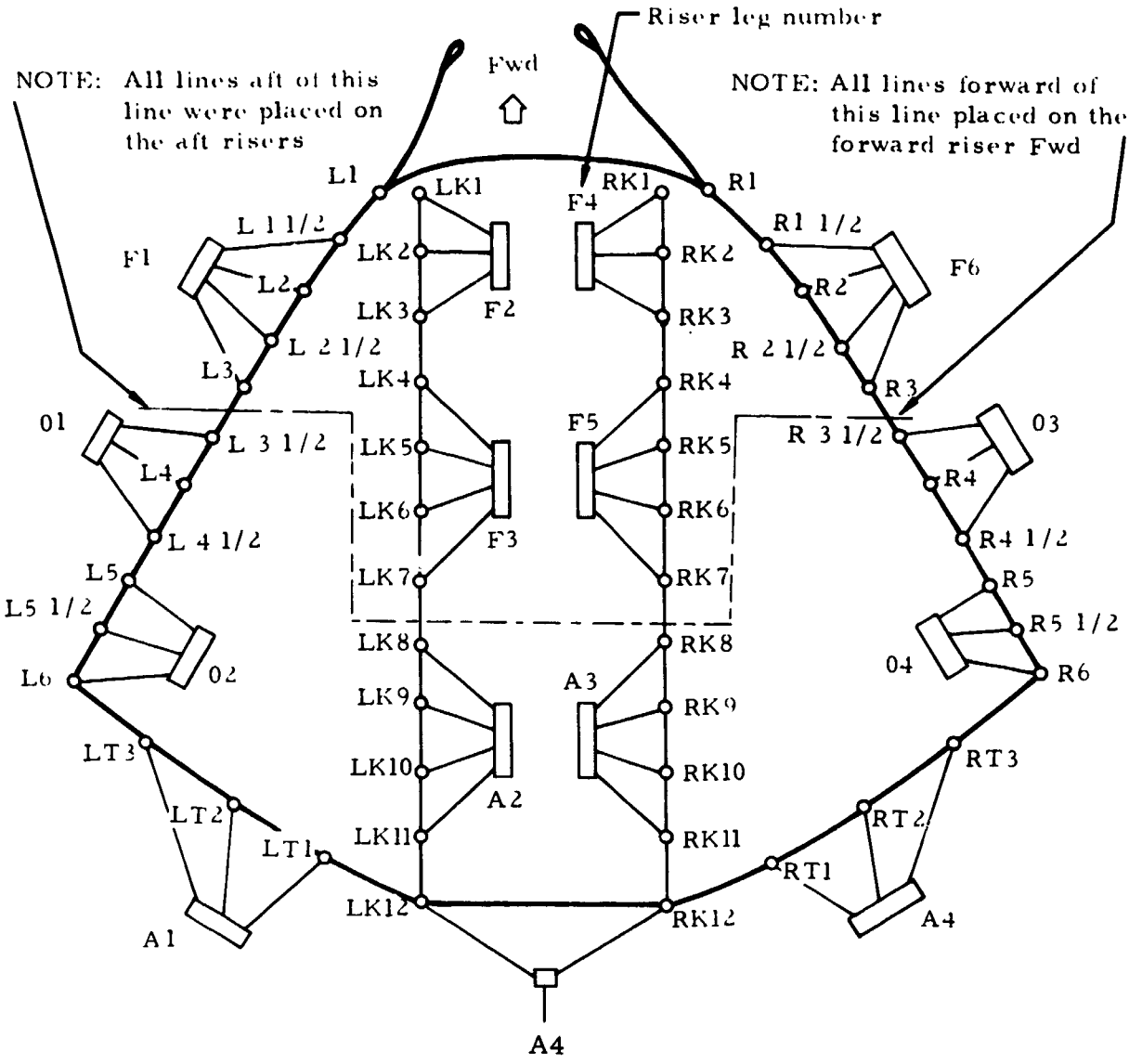

View from above

Figure 22. Suspension line/riser attachment arrangement for twin keel parawing, Versions III, IV, V, VI, and VII

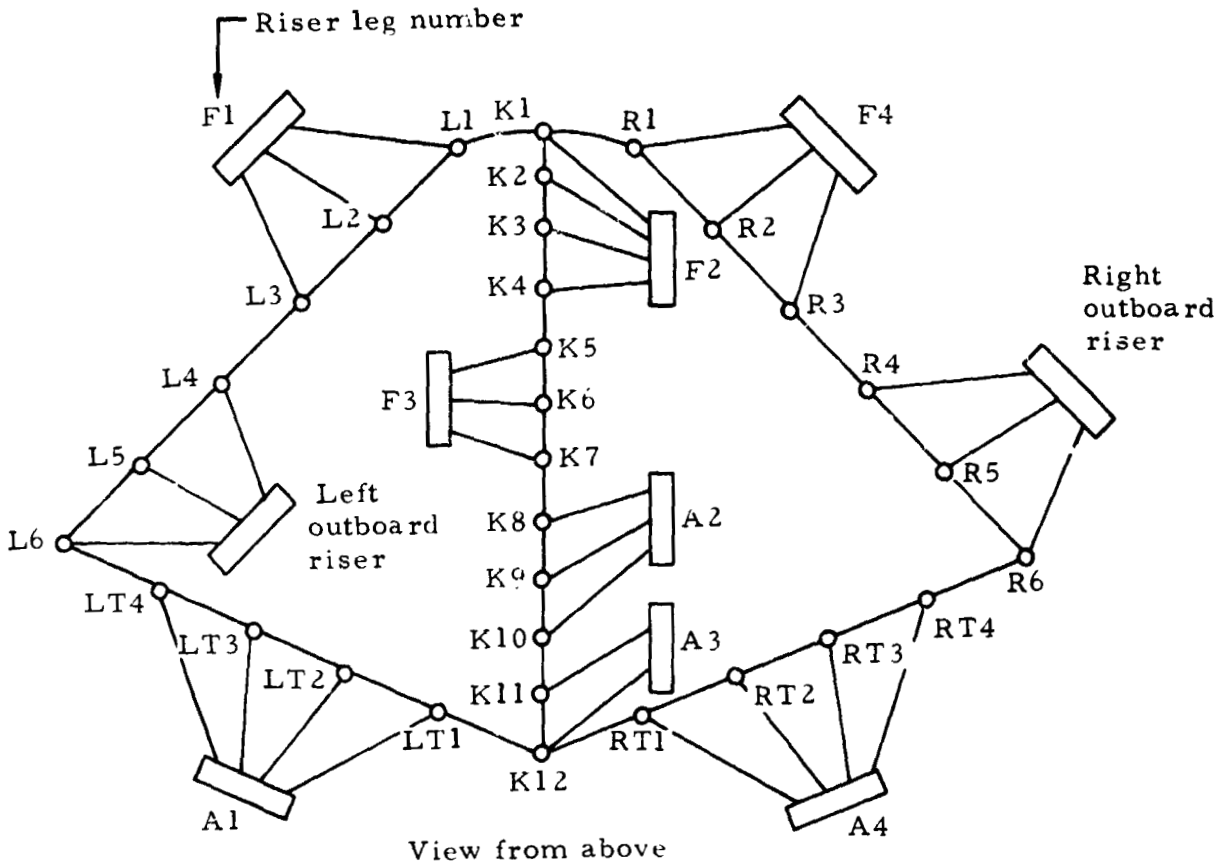

Figure 23. Suspension line/riser attachment arrangement for single keel parawing.

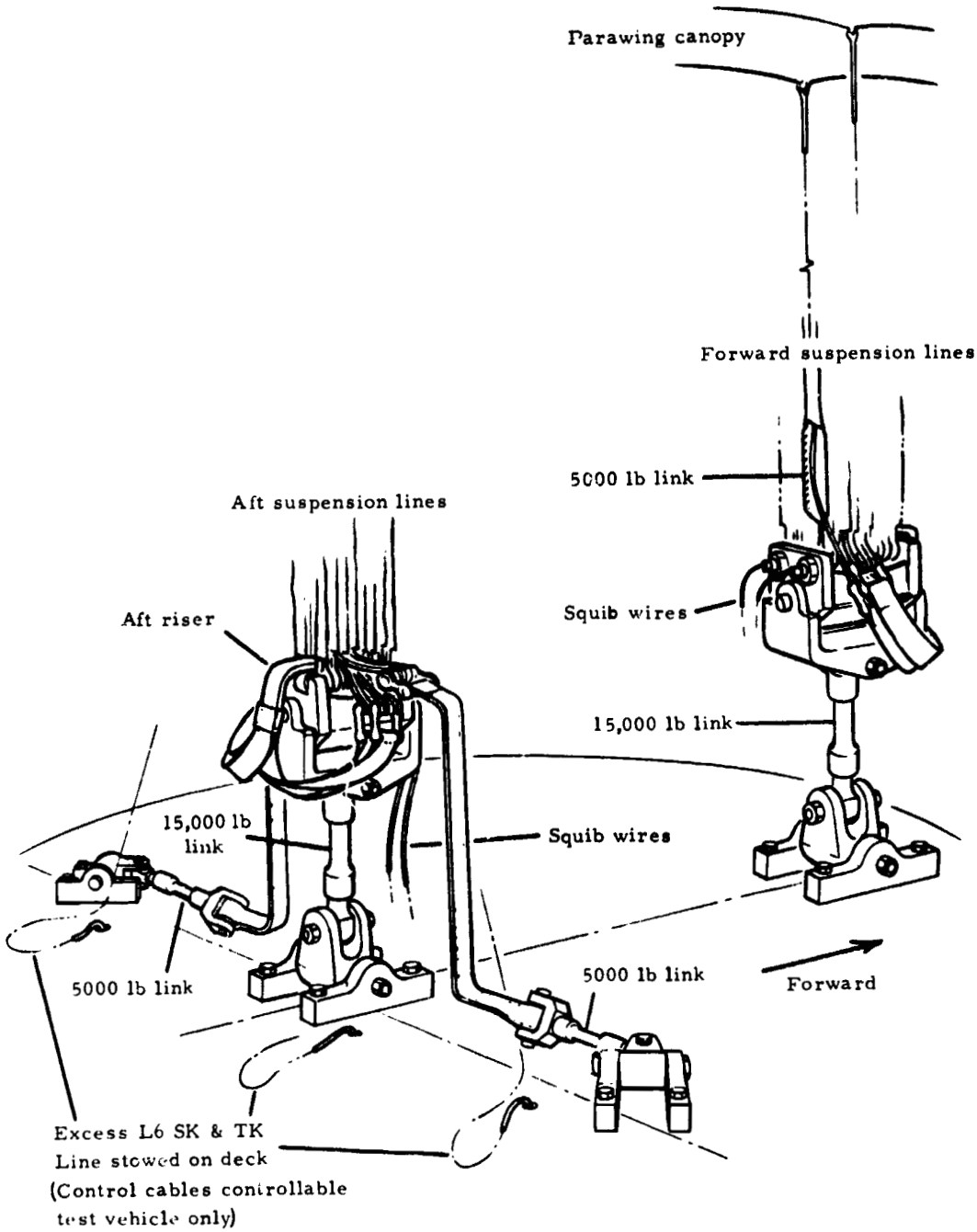

Figure 24. Intermediate-scale parawing deck attachment arrangement before line transfer

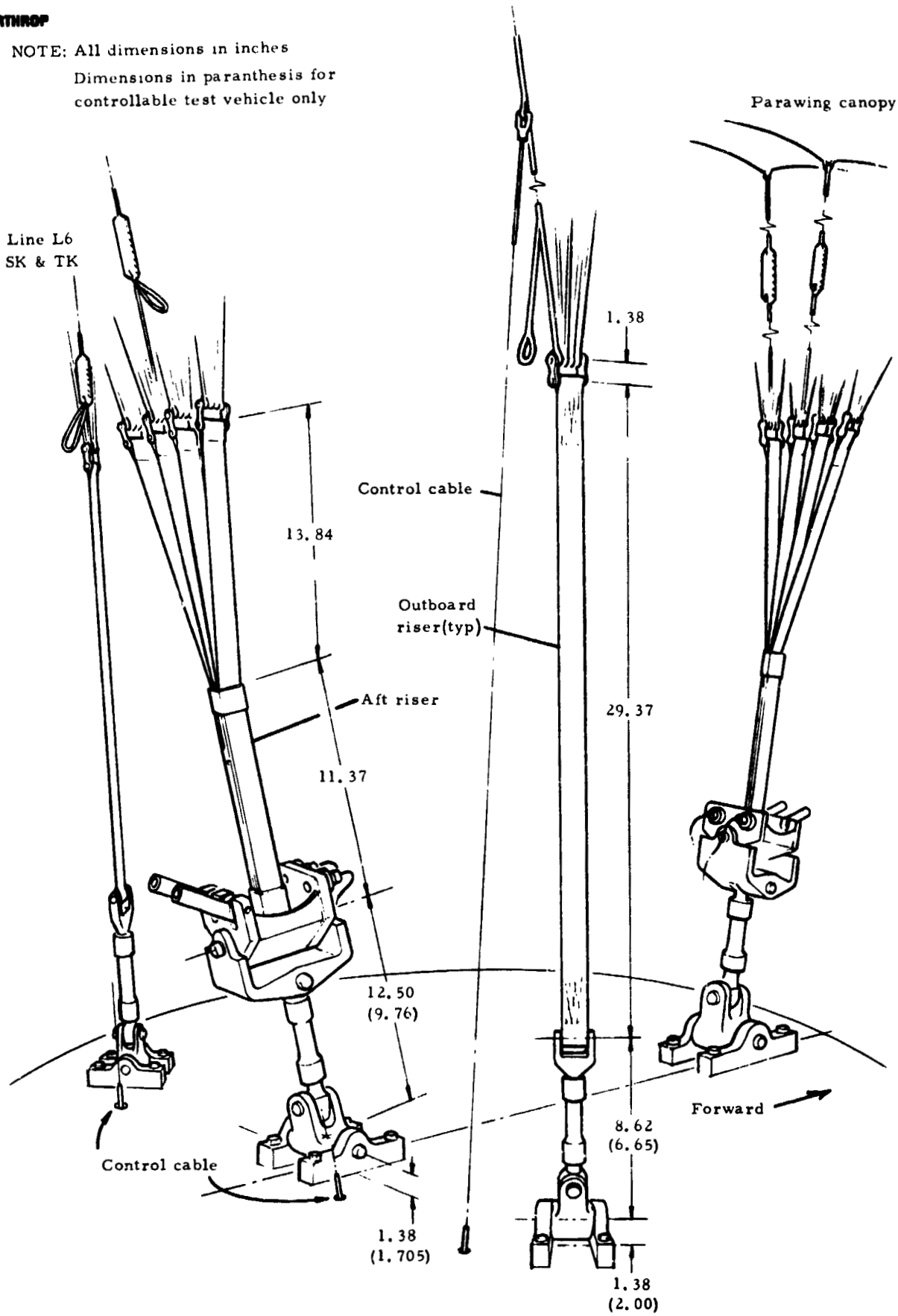

Figure 25. Intermediate-scale parawing deck attachment arrangement after line transfer

REEFING SYSTEM

Twin Keel Parawing

The basic reefing system for the twin keel parawing, designated reefing system A, was the four-stage system defined in Figure 26. The first-stage reefing system consisted of a separate line for reefing each outer lobe. Each reefing line was connected to a keel becket forward of K12, passed through all the outboard, keel reefing rings, the leading edge reefing rings and terminated at a connector loop located at K12. The connector loop passed through a reefing cutter and reefing ring at RK12 and at LK12. At cutter initiation the connector loop was severed, providing simultaneous disreef of both outer lobes.

The second-stage reefing system consisted of reefing the center lobe with one reefing line. The line was attached to a keel becket located forward of LK12, passed through all the left inboard keel reefing rings, nose reefing rings and the right inboard keel reefing rings. The end of the line was attached to a becket located forward of RK12. The line also passed through two, second stage, reefing cutters at RK2.

The third-stage reefing system consisted of a single reefing line used to gather the wing trailing edges. Each end of the line was attached to a becket located at L6 and at R6. The line was passed through all the trailing edge reefing rings and the third stage reefing cutters located at RK12 and LK12.

The fourth-stage reefing system was the aforementioned and described equalization of the suspension line lengths to the length of the tip lines. Although not a conventional reefing system arrangement, the line equalization was a separate stage in the deployment process and is, for purposes of this discussion, identified as a separate reefing stage. Initiation of deck mounted,

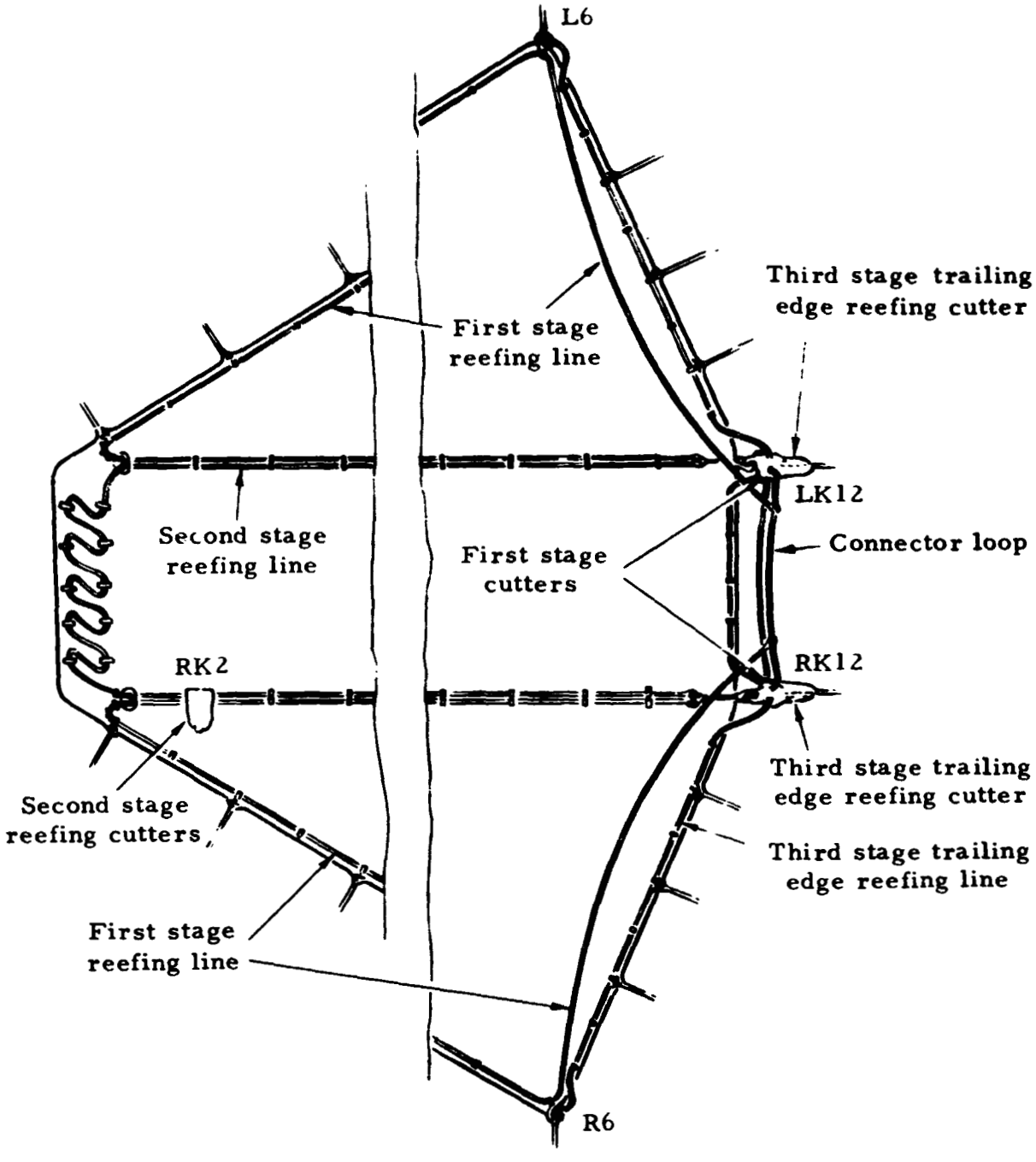

Viewed from below

Figure 26. Reefing system A, twin keel parawing

pyrotechnic operated, swing-arm disconnects released the suspension line by-pass loops, deployed the stowed suspension line lengths and allowed the wing to assume a gliding flight configuration.

Reefing system A was improved by adding a separate third stage nose reefing line to reduce third stage loads and reduce localized loads in the center section of the wing, particularly in the nose area. The first stage connector loop was routed through the reefing rings located at L6 and at R6 to eliminate possible hangup of the first stage reefing line at L6 and R6. This system was designated reefing system B and is identified in Figure 27.

Further improvement was made to the third stage reefing system by relocating the trailing edge reefing cutters at the tip suspension line locations L6 and R6. The reefing cutters in their original location could move relative to the trailing edge gathering line, causing possible abrasion of this line. The original reefing cutter location also required that the cutters be capable of severing two thicknesses of the line, due to the proximity of the reefing line eye splice to the cutter hole. With the third-stage reefing cutters relocated in the reefing-line eye splice at the wing tips, only one thickness of line was cut by each reefing line cutter. This permitted use of a stronger trailing-edge-gathering line. Also, the abrasion problem of gathering line against reefing cutter was eliminated with the cutters secured to each end of the gathering line. The reefing system which incorporated this third stage change was designated reefing system C and is identified in Figure 28.

Single Keel Parawing

The single keel parawing used a four-stage reefing system, as shown in Figure 29. The first stage reefing system consisted of a separate reefing line for each of the two lobes of the canopy. Each line was connected to the reefing ring at K1, passed

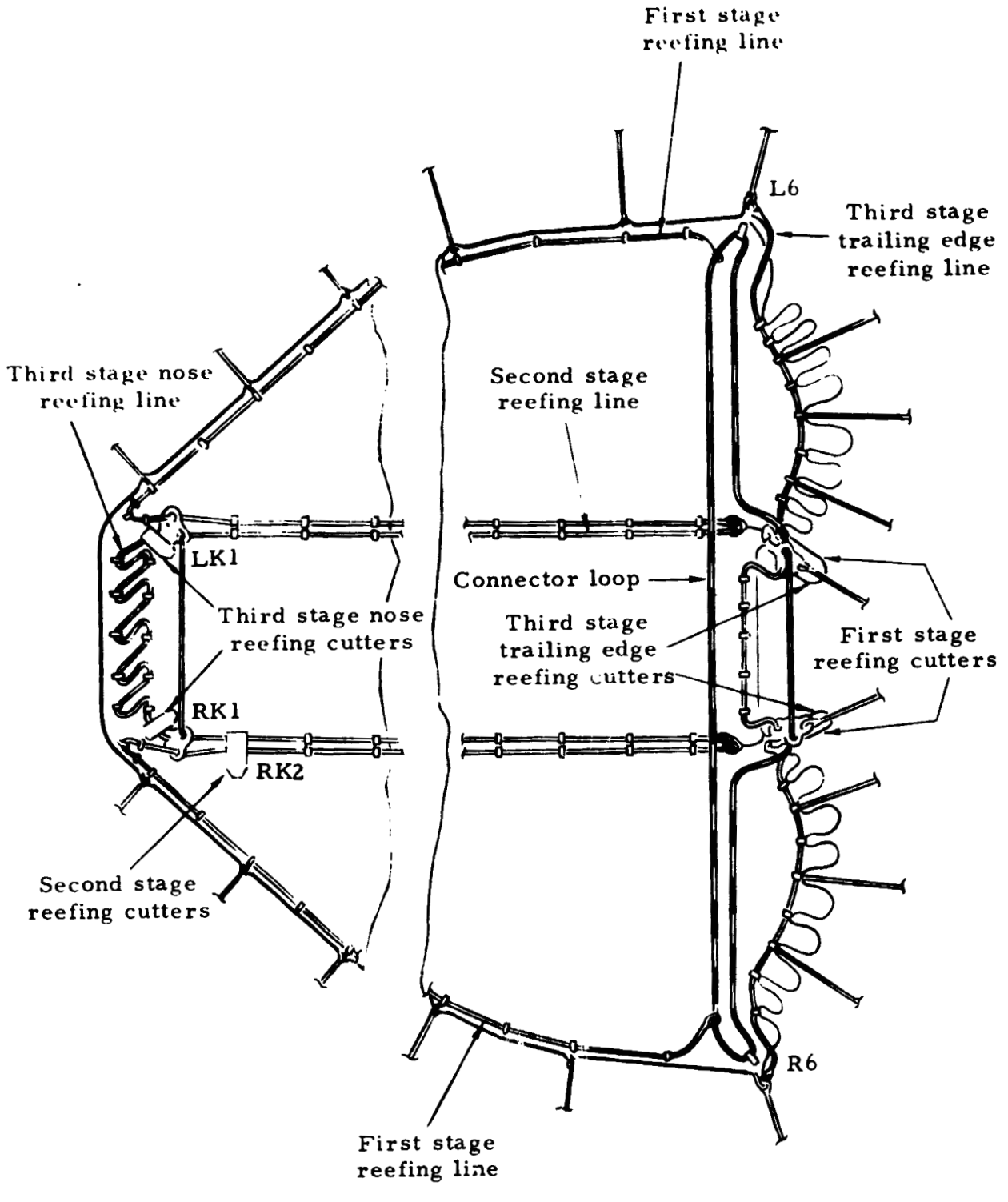

Figure 27. Reefing system B, twin keel parawing

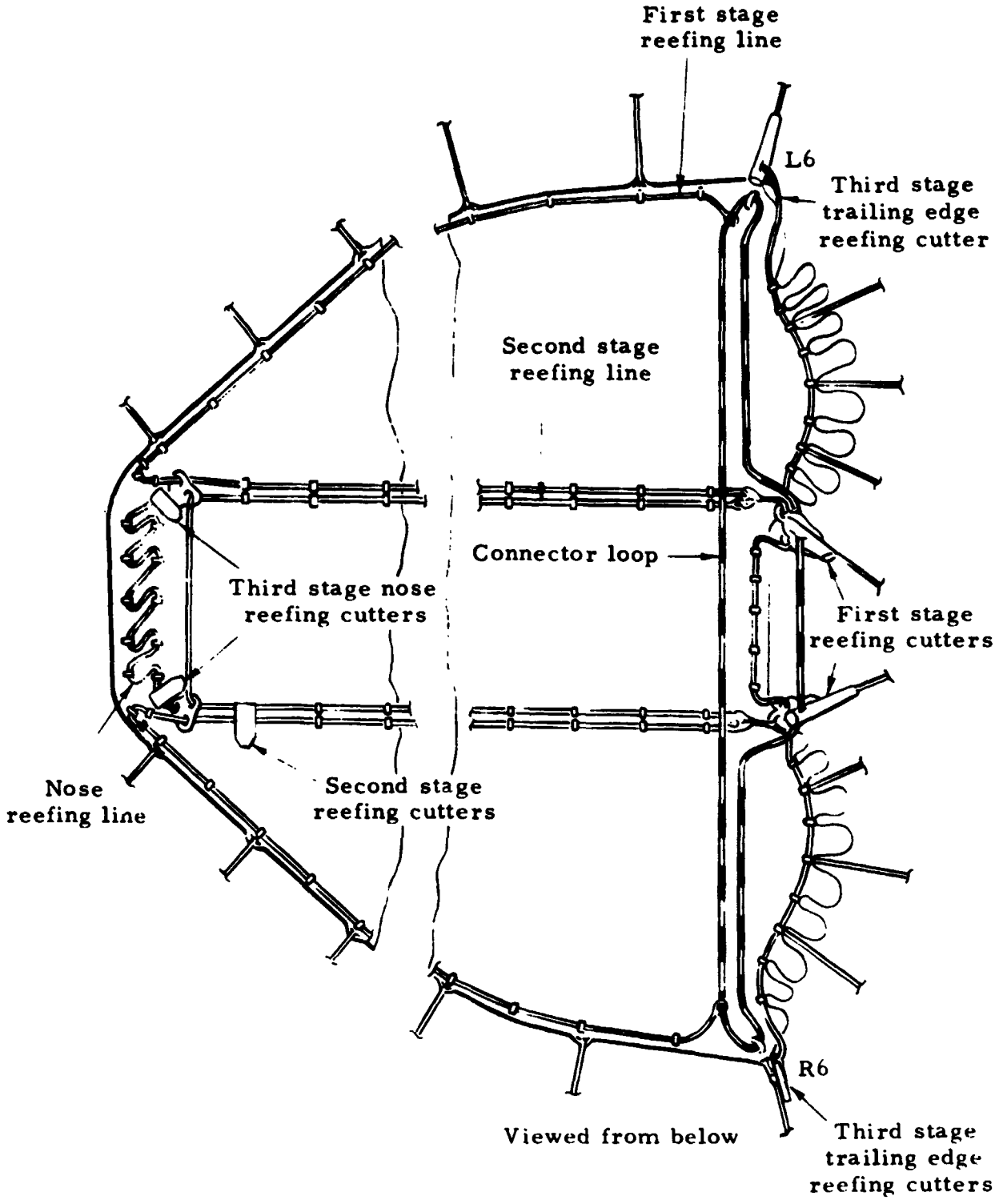

Figure 28. Reefing system C, twin keel parawing

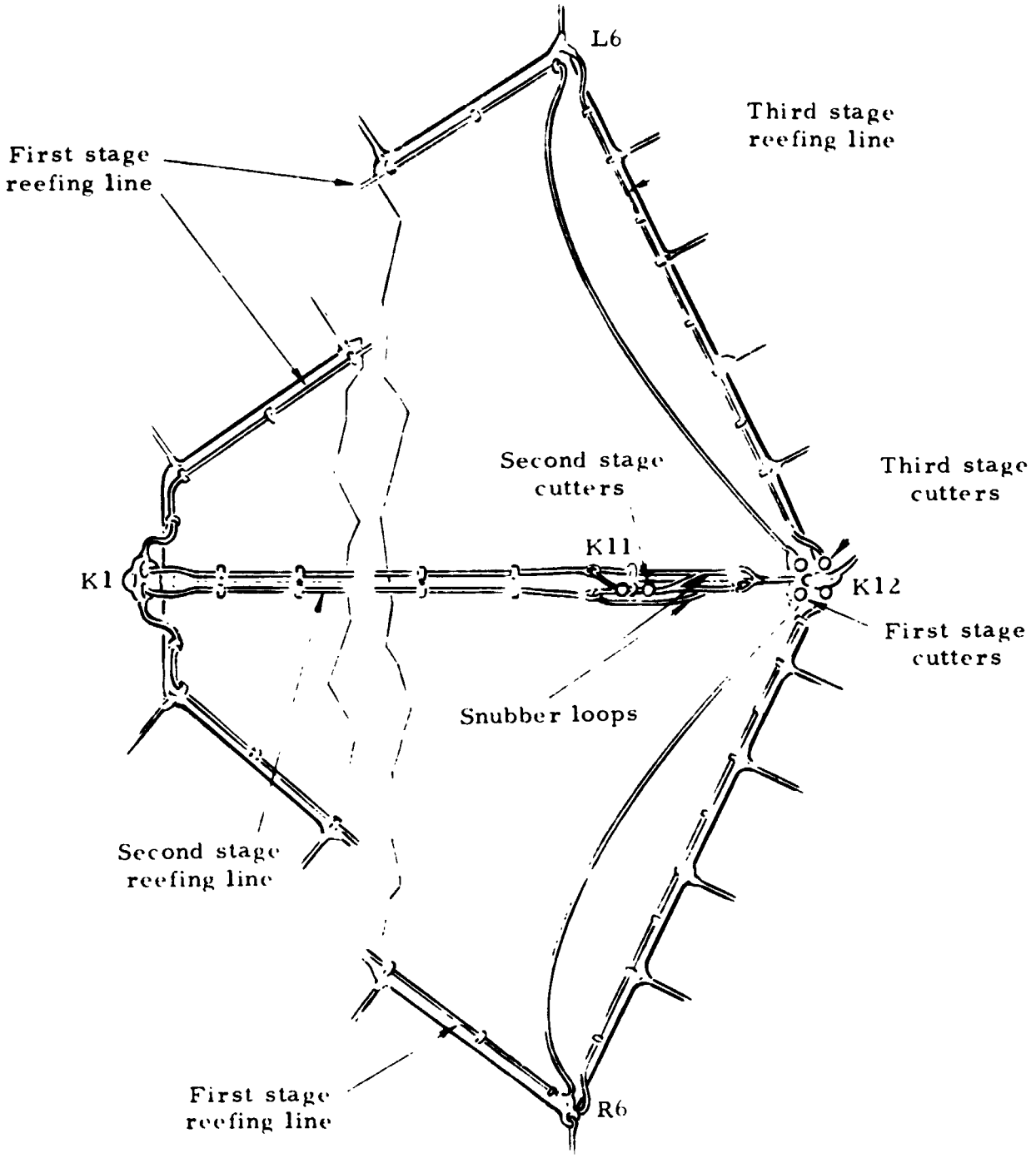

Viewed from below

Figure 29. Reefing system, single keel parawing

through all the leading-edge reefing rings and terminated at a connector loop located at K12. The connector loop passed through two reefing line cutters and the reefing ring at K12. At reefing cutter initiation, the connector loop was severed, providing simultaneous disreef of both lobes.

The second-stage reefing system consisted of a single reefing line used to gather the keel between K1 and K12. The reefing line was connected to a snubber loop on the left side of the keel at K11 and passed through all the reefing rings on the left side forward through K1 and then back through the keel reefing rings on the right side to a second snubber loop at K11. Each snubber loop was connected to its respective keel becket. These beckets were both located between K11 and K12 on the keel. Both snubber loops passed through two reefing cutters located at K11. At cutter initiation both snubber loops were severed, freeing both ends of the keel reefing line.

The third-stage reefing system consisted of one reefing line used to gather the trailing edges of the canopy. Each end of the line was attached to a tip becket at L6 and at R6 and passed through all the trailing-edge reefing rings, including two reefing cutters at K12. At cutter initiation the reefing line was severed in the center of the line, allowing the aft section of the wing to open and inflate.

As with the twin keel parawing, the fourth-stage reefing system was the suspension-line-length-equalization arrangement. Initiation of deck mounted, pyrotechnic operated, swing-arm disconnects released the suspension line by-pass loops, deployed the stowed suspension line lengths and allowed the wing to assume a gliding flight configuration.

SUMMARY OF INTERMEDIATE-SCALE AERIAL DROP TESTS

APPENDIX C presents a detailed description of each of the twenty aerial drop tests conducted with intermediate-scale parawings. The descriptions are arranged in chronological order of test. Each test description includes the primary objective of the test, test parawing identification, test vehicle identification and system weight, actual versus planned conditions at parawing deployment and significant measured performance. The test descriptions also include unusual or questionable occurrences, test anomalies, descriptions of failures and parawing damage, plus the results of failure analyses, in terms of conclusions and recommended corrective actions.

Of the twenty intermediate-scale parawing tests, eighteen tests were flown with twin keel parawing specimens and two tests were flown with single keel parawing specimens. Of the eighteen twin keel parawing tests, twelve tests were conducted with a bomb test vehicle with fixed rigging on the parawing; the remaining six twin keel parawing tests were conducted with a controllable test vehicle. Both single keel parawing tests were flown on a bomb test vehicle with fixed rigging on the parawing. Table 4 provides a summary of the intermediate scale parawing tests, and includes the test sequence, test number, parawing and test vehicle identification, primary test objective, planned and actual test conditions, and test comments.

TABLE 4.- SUMMARY OF INTERMEDIATE-SCALE PARAWING FLIGHT TESTS

Sequence no.	Test no.	Parawing version no.	Reefing system version - reef, %	Test vehicle type & serial no.	Test objective	Parawing line stretch deployment conditions						Test comments
						Q, psf		Alt, ft		W_D lbs		
						Plnd	Act	Plnd	Act	Plnd	Act	
1	200T	I	A - 14	Bomb #1	Validate system operation at minimum load	20	28	5000	4754	2880	2879	Abbreviated 4th reefed stage. Good test.
2	204T	I	A - 14	Bomb #1	Scale point test for full-scale system W_D = 15,000 lbs, q=70 psf, h=18,000 ft	44.3	49.2	18,000	18,784	3795	3786	Some vehicle oscillation after 1st stage inflation. Good test.
3	200S	I	11.6	Bomb #2	Validate system operation at minimum load	25	29.4	5000	4882	2880	2868	Parawing nose tucked under for entire gliding flight. Otherwise, good test.
4	201S	I	12	Bomb #1	Demonstrate deployment capability W_D = 5000 lbs, q=30 psf, h=3000 ft	30	32.6	3000	2627	5000	4997	Major canopy damage during parawing deployment.
5	201T	I	A - 10	Bomb #1	Demonstrate deployment capability W_D = 5000 lbs, q=30 psf, h-3000 ft	30	32.9	4000	3740	5000	5034	Left trailing edge failed to disreef. Wing spun to impact.
6	202T	I	A - 10	Bomb #2	Scale point test for full-scale system. W_D = 15,000 lbs, q=100 psf, h=13,000 ft	63.3	69.6	14,000	14,107	3795	3792	Some canopy damage in nose area. Good test.
7	205T	I	A - 10	Bomb #1	Demonstrate deployment capability W_D = 5000 lbs, q=70 psf, h=14,000 ft	70	76.3	14,000	14,326	5000	5031	Some canopy damage in nose area plus 20 inch tear in right lobe. Otherwise, good test.
8	203T	I	A - 14	Bomb #2	Scale point test for full-scale system W_D = 15,000 lbs, q=100 psf, h=14,000 ft	63.3	64	14,000	14,568	3795	3805	Major canopy damage in right lobe during deployment.
9	208T	II	A - 10	Bomb #1	Qualify wing for use on 4000 lb controllable test vehicle	36	27.5	18,000	18,882	5000	5024	Major canopy damage in right lobe during deployment.
10	207T	III	B - 10	Bomb #1	Qualify wing for use on 4000 lb controllable test vehicle	36	37.1	18,000	14,840	5000	4994	Nonsteady gliding flight, due to tip lines rigged too long. Otherwise, good test.
11	250T	III	B - 10	Controllable #1	Obtain parawing gliding flight data on minimum weight controllable vehicle	21	23.9	As high as possible	19,010	3400	3444	Good test.
12	251T	III	B - 10	Controllable #1	Obtain parawing gliding flight data at W_{D/S_W} = 1.0 psf	24	43.3	As high as possible	15,970	4000	3977	Prolonged parawing pack hangup, resulting in abnormal deployment. Good gliding flight.
13	209T	V	B - 8	Bomb #1	Scale point test for full-scale system: W_D = 15,000 lbs, q=100 psf, h=14,000 ft	63.3	62.5	14,000	14,175	3795	3811	3rd stage trailing edge reefing line failed in 2nd stage. Otherwise, good test.
14	211T	V	B - 10	Bomb #2	Qualify wing for use on 6000 lb controllable test vehicle.	50	49.3	18,000	18,320	6000	6009	Moderate canopy damage. Otherwise, good test.
15	252T	IV	B - 10	Controllable #1	Obtain parawing gliding flight data at W_{D/S_W} = 1.0 psf	27	23.5	As high as possible	22,345	4000	4007	Good test.
16	206T	VII	C - 8	Bomb #2	Demonstrate deployment capability W_D = 5000 lbs, q=100 psf, h=18,000 ft	100	94.7	18,000	18,115	5000	5001	Moderate canopy damage in all three lobes. Otherwise, good test.
17	253T	VI	C - 10	Controllable #2	Obtain parawing gliding flight data at W_{D/S_W} = 1.25 psf	32	27.8	As high as possible	22,640	5000	5011	Good test.
18	210T	VII	C - 8	Bomb #1	Scale point test for full-scale system: W_D = 15,000 lbs, q=100 psf, h=18,000 ft	63.3	62.1	18,000	18,600	3795	3813	Good test. Some vehicle oscillation during deployment.
19	254T	VI	C - 10	Controllable #2	Obtain parawing gliding flight data at W_{D/S_W} = 1.5 psf	36	31.4	As high as possible	22,075	6000	6011	Good test.
20	255T	VI	C - 10	Controllable #2	Obtain parawing gliding flight data at W_{D/S_W} = 1.5 psf; determine performance repeatability	36	31	As high as possible	23,260	6000	6014	Good test. Some high turn rates commanded.

TEST RESULTS AND ANALYSIS

DEPLOYMENT PHASE

Opening Loads

Riser loads were measured in each of the twenty intermediate-scale parawing, aerial drop tests. Figures 30 through 69 present total parawing load time histories and total parawing load divided by dynamic pressure time histories during the deployment phase for all tests that were conducted. Total parawing load was calculated by summing all riser-load-link measurements and multiplying by the ratio of descent weight to suspended weight. Multiplying by this ratio corrects the measured riser loads to loads that were developed in the parawing. The total load/dynamic pressure plots were developed by dividing the total parawing load at each time point by the wind corrected dynamic pressure. The wind correction was made by subtracting the horizontal velocity component, as measured by ASKANIA at first-stage disreef, from each measured total velocity datum point to determine true air velocity. This velocity was then used to calculate dynamic pressure. The correction is based on the assumption that the ASKANIA measured horizontal velocity at first stage disreef was due to wind, and that this velocity component would be essentially zero under a no-wind condition.

All of the plots are annotated to show the times of the line stretch event, the first-, second- and third-stage disreef events and the line transfer event. During Test 251T, the right- and forward-riser load transducers did not function. Therefore, the load data presented for this test are based on left- and aft-riser loads only and are not representative. In general, Figures 30 through 69 present all total load and total load/dynamic pressure data obtained, regardless of anomalies or, in some cases, structural failure of the parawing. Subsequent analysis of the data to obtain load factors, reference areas, fill rates, etc., did not include those data obtained during unusual circumstances.

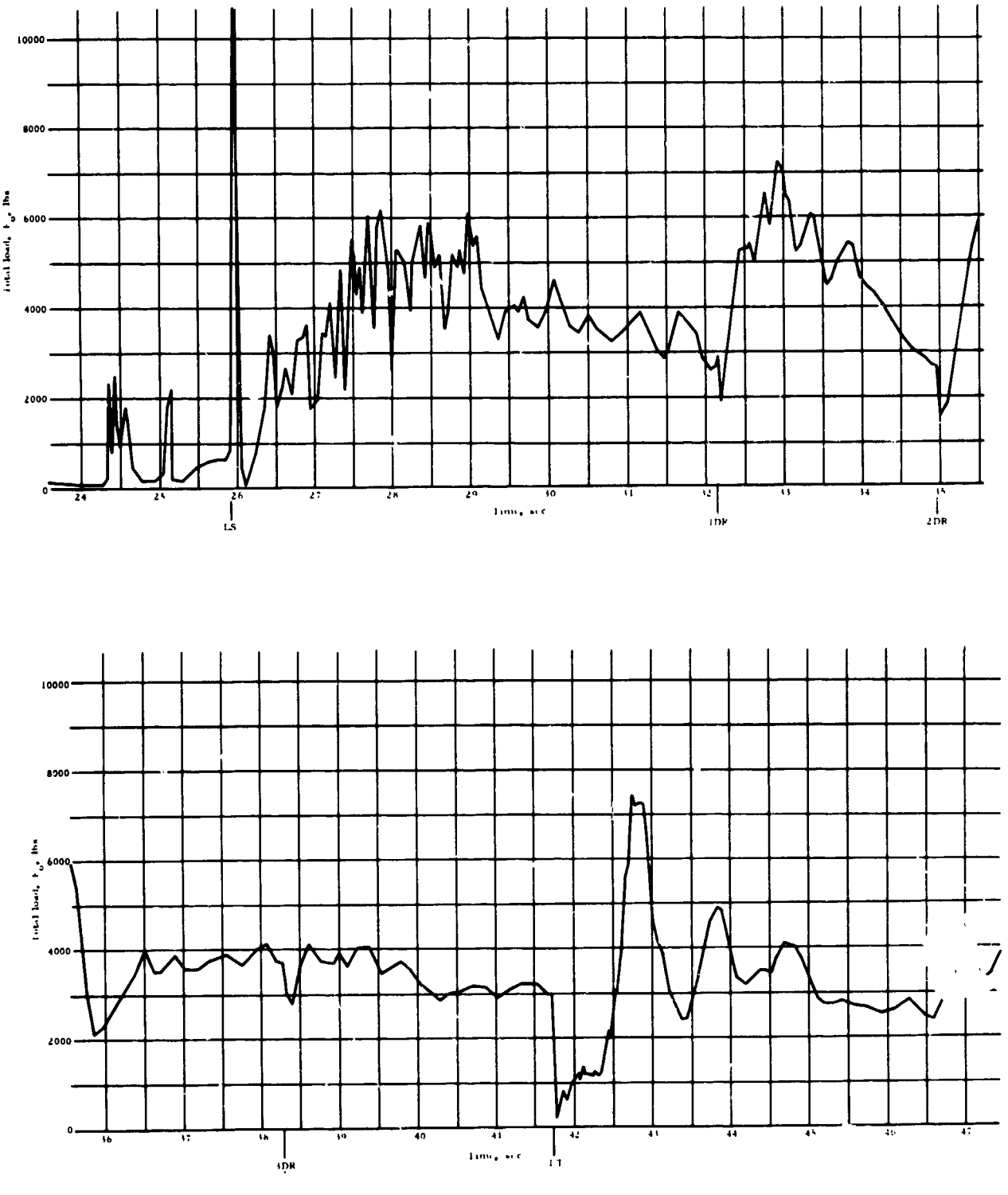

Figure 30. Total parawing load versus time from launch, single keel parawing, Test 200S

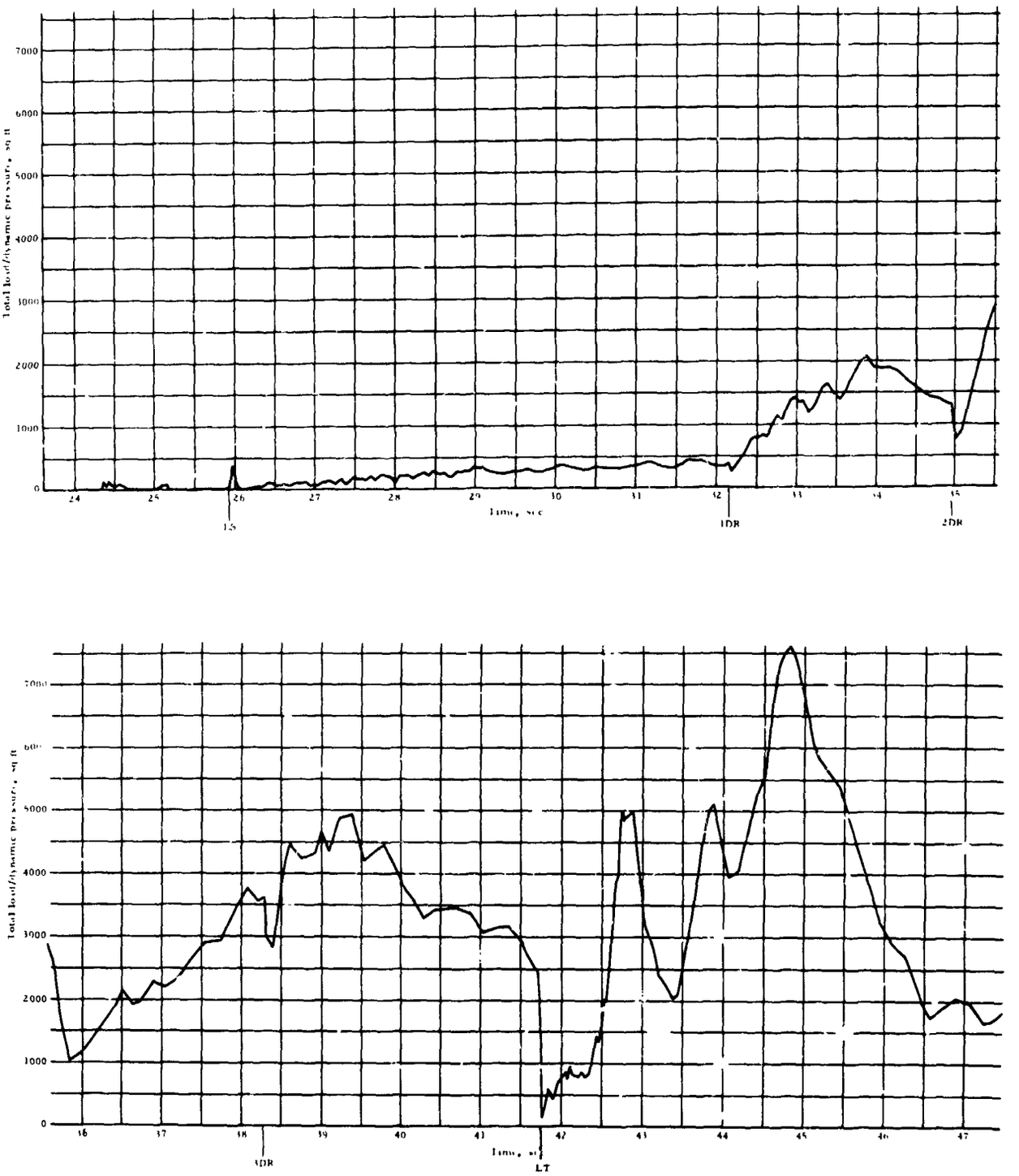

Figure 31. Total parawing load/dynamic pressure versus time from launch, single keel parawing, Test 20ᴜS

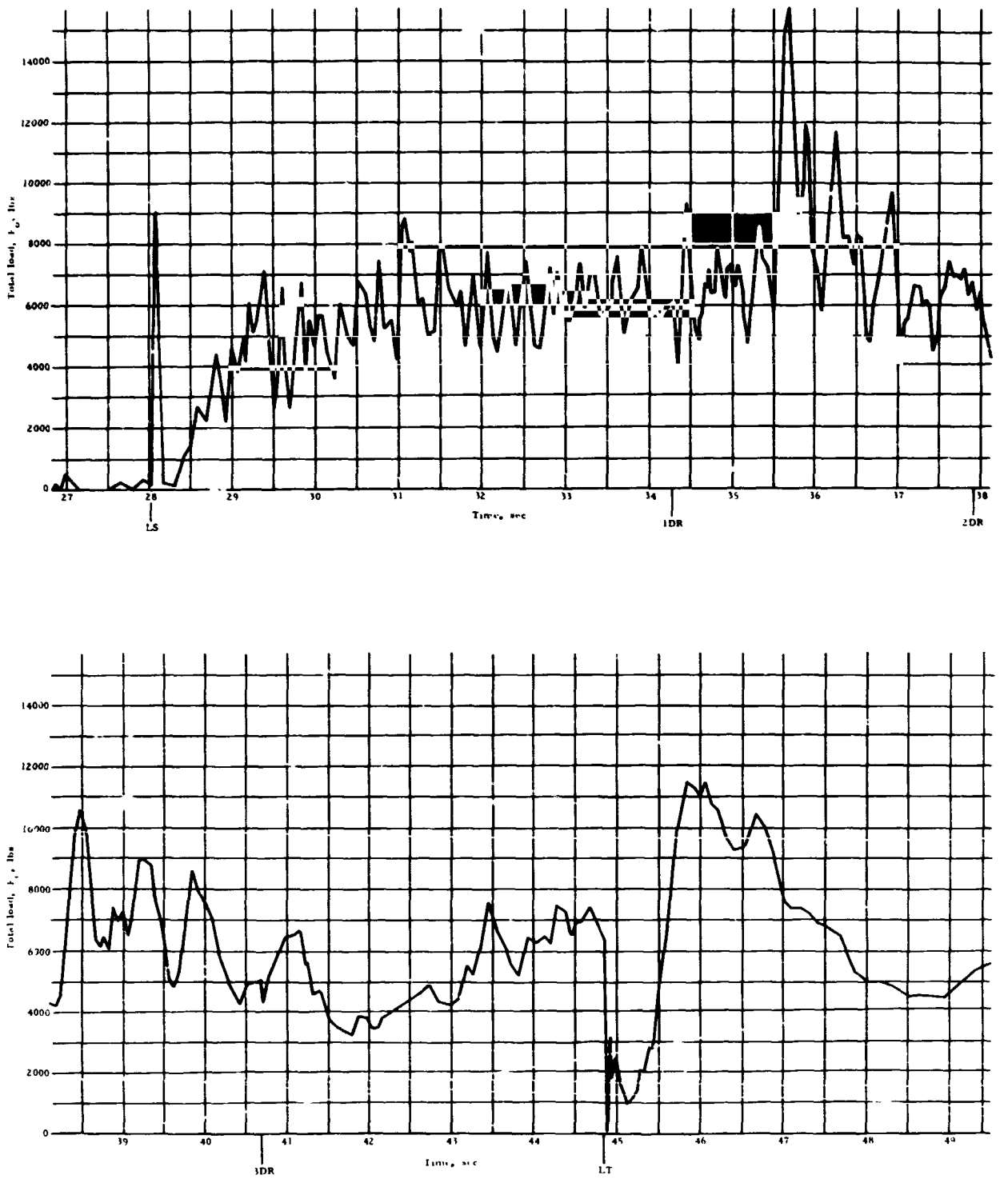

Figure 32. Total parawing load versus time from launch, single keel parawing, Test 201S

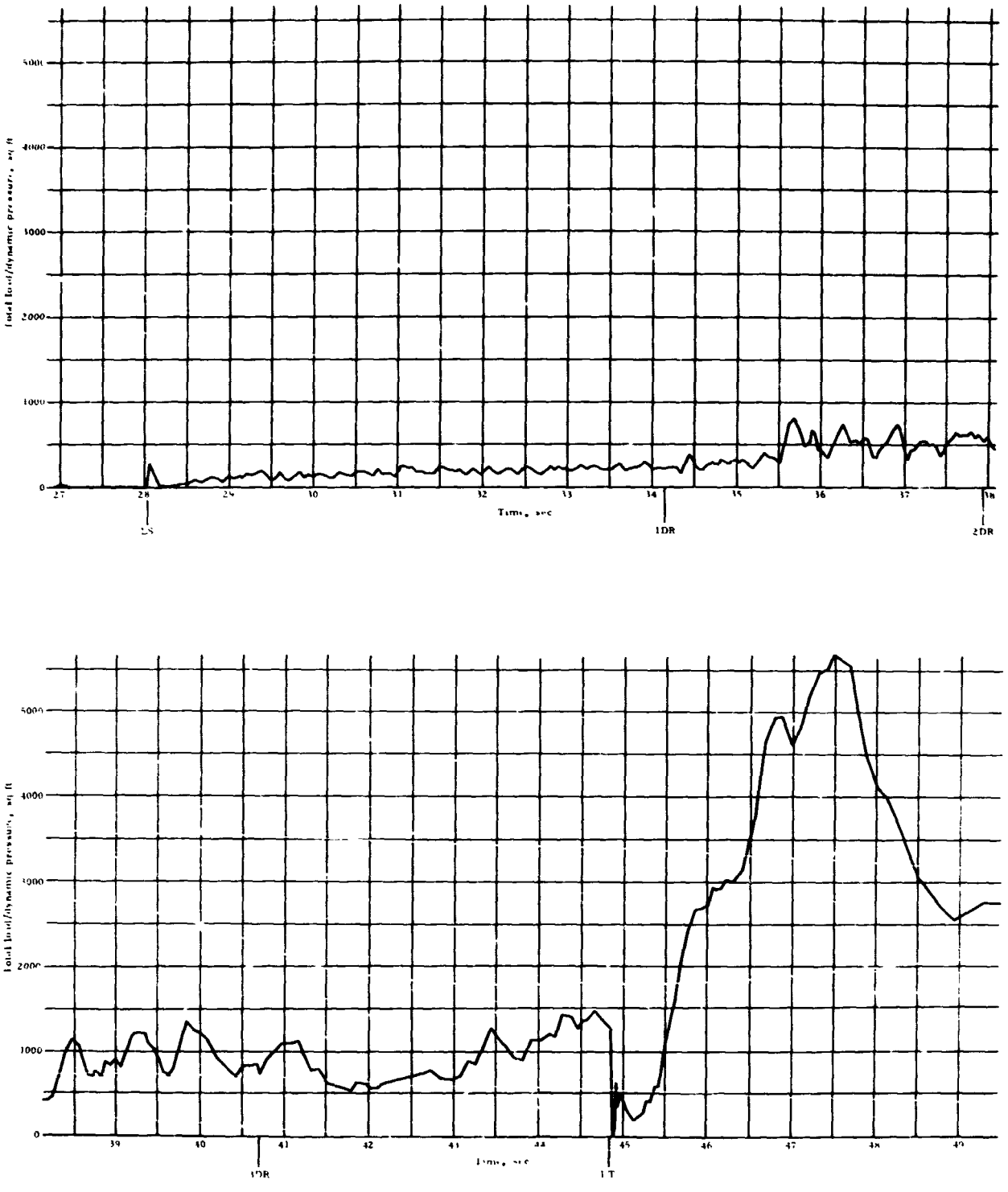

Figure 33. Total parawing load/dynamic pressure versus time from launch, twin keel parawing, Test 201S

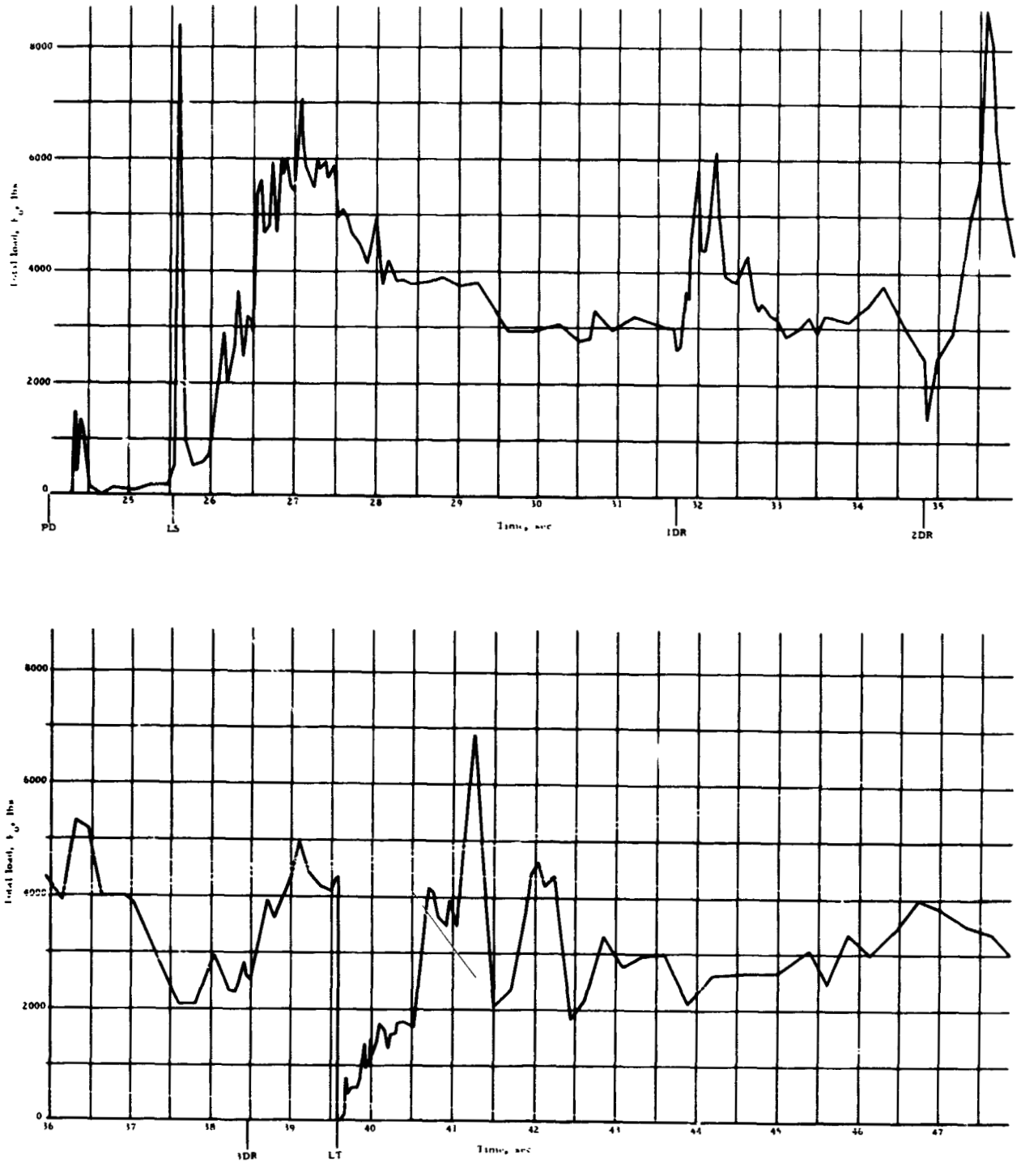

Figure 34. Total parawing load versus time from launch, twin keel parawing, Test 200T

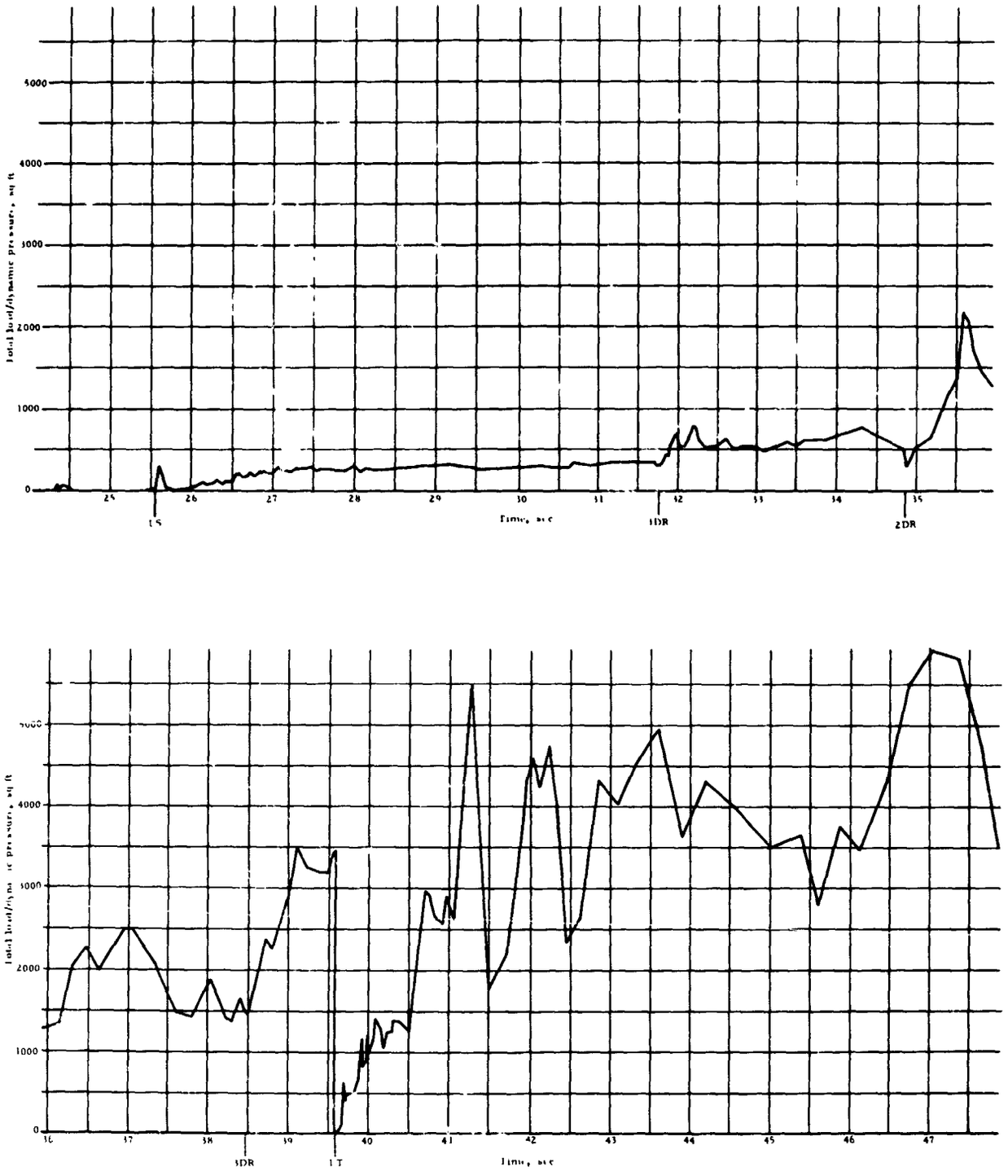

Figure 35. Total parawing load/dynamic pressure versus time from launch, twin keel parawing, Test 200T

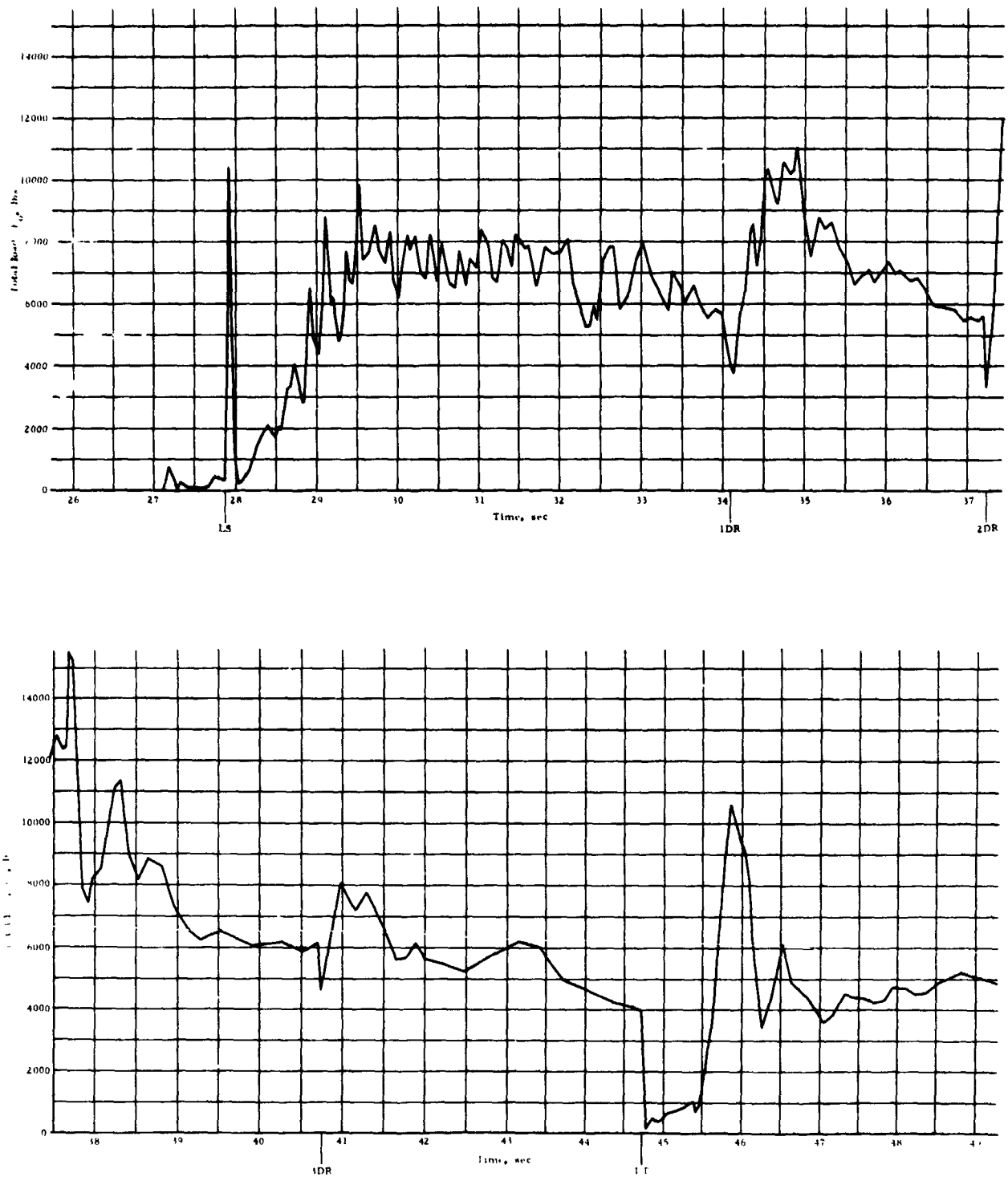

Figure 36. Total parawing load versus time from launch, twin keel parawing, Test 201T

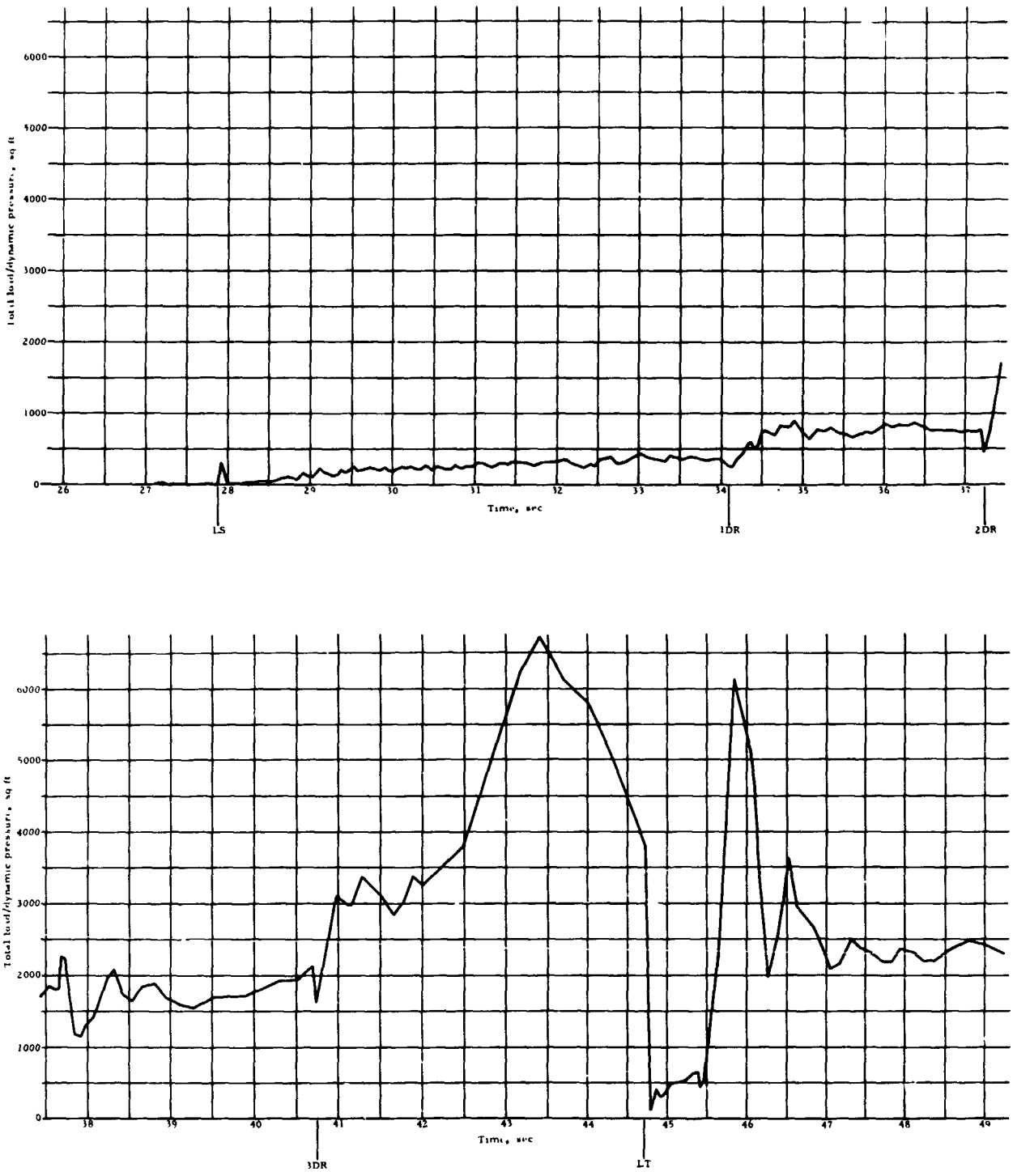

Figure 37. Total parawing load/dynamic pressure versus time from launch, twin keel parawing, Test 20iT

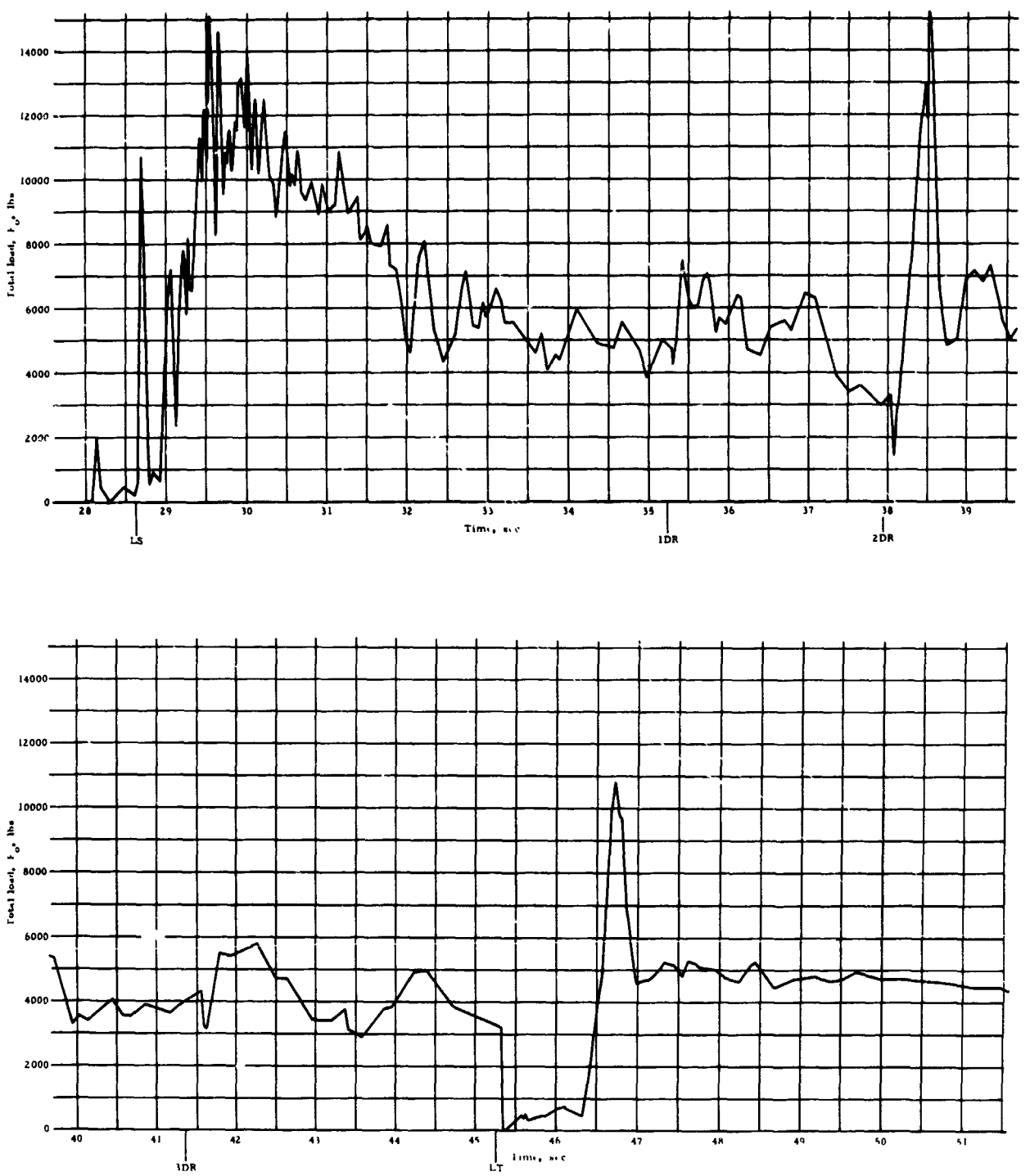

Figure 38. Total parawing load versus time from launch, twin keel parawing, Test 202T

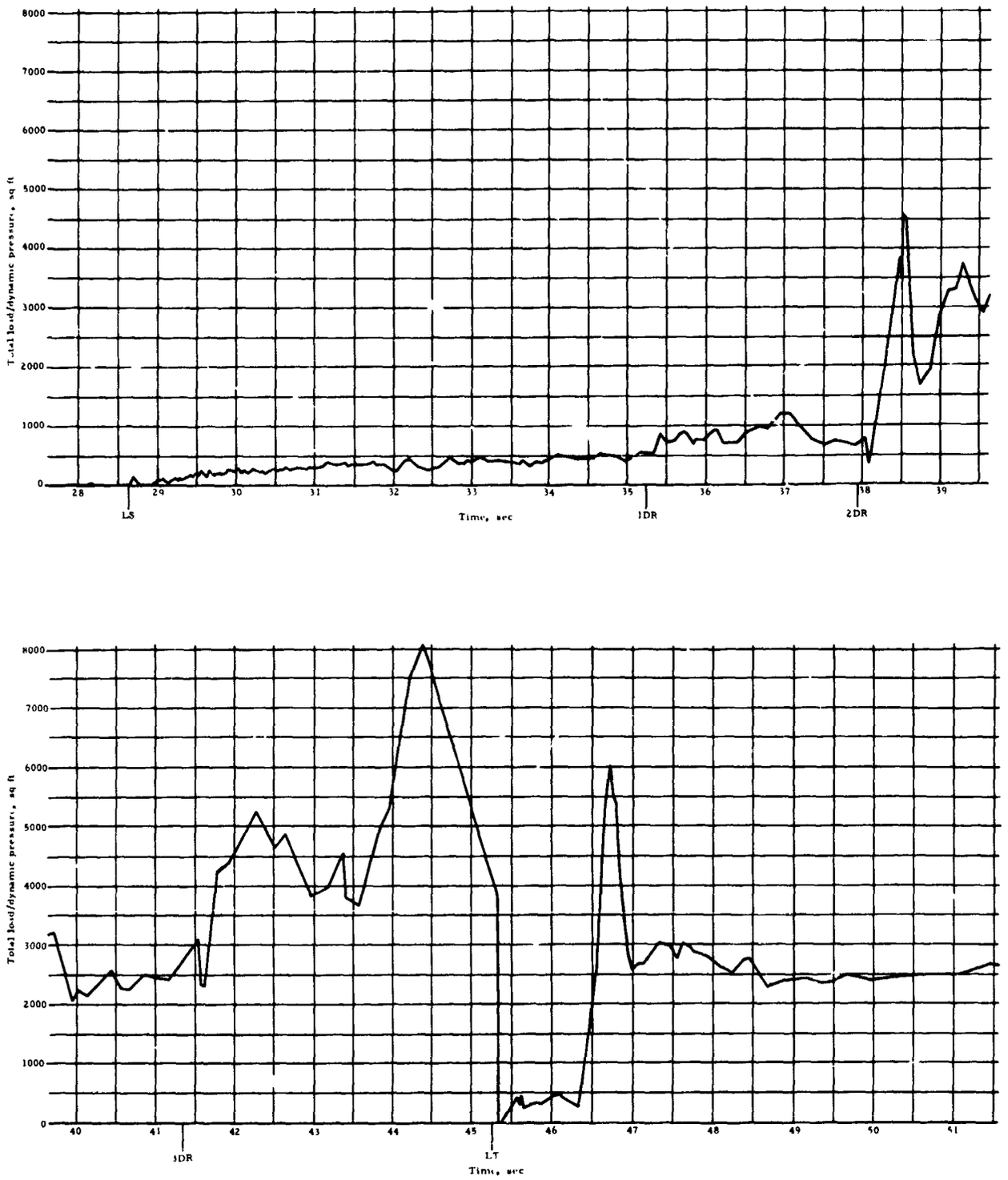

Figure 39. Total parawing load/dynamic pressure versus time from launch, twin keel parawing, Test 202T

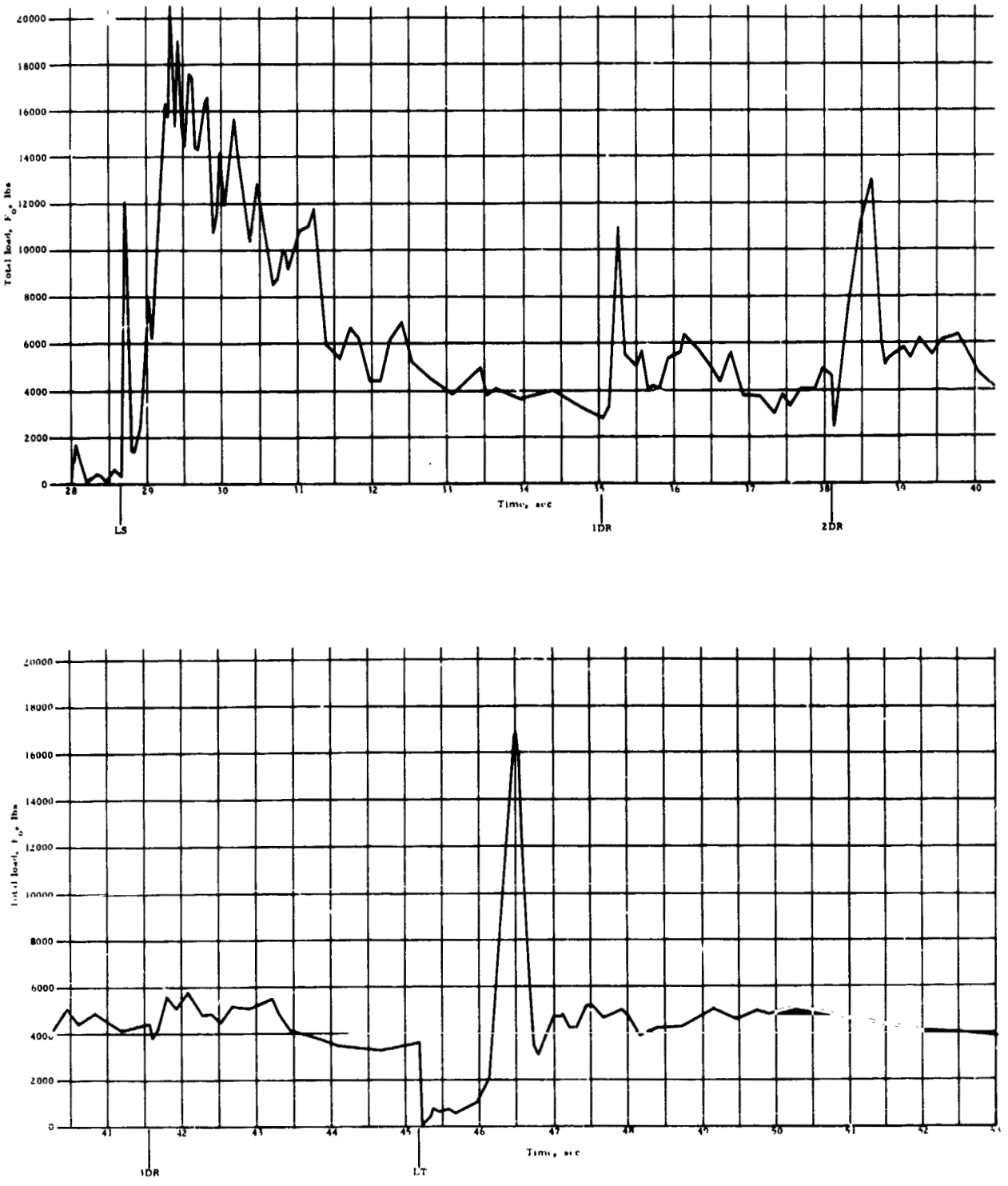

Figure 40. Total parawing load versus time from launch, twin keel parawing, Test 203T

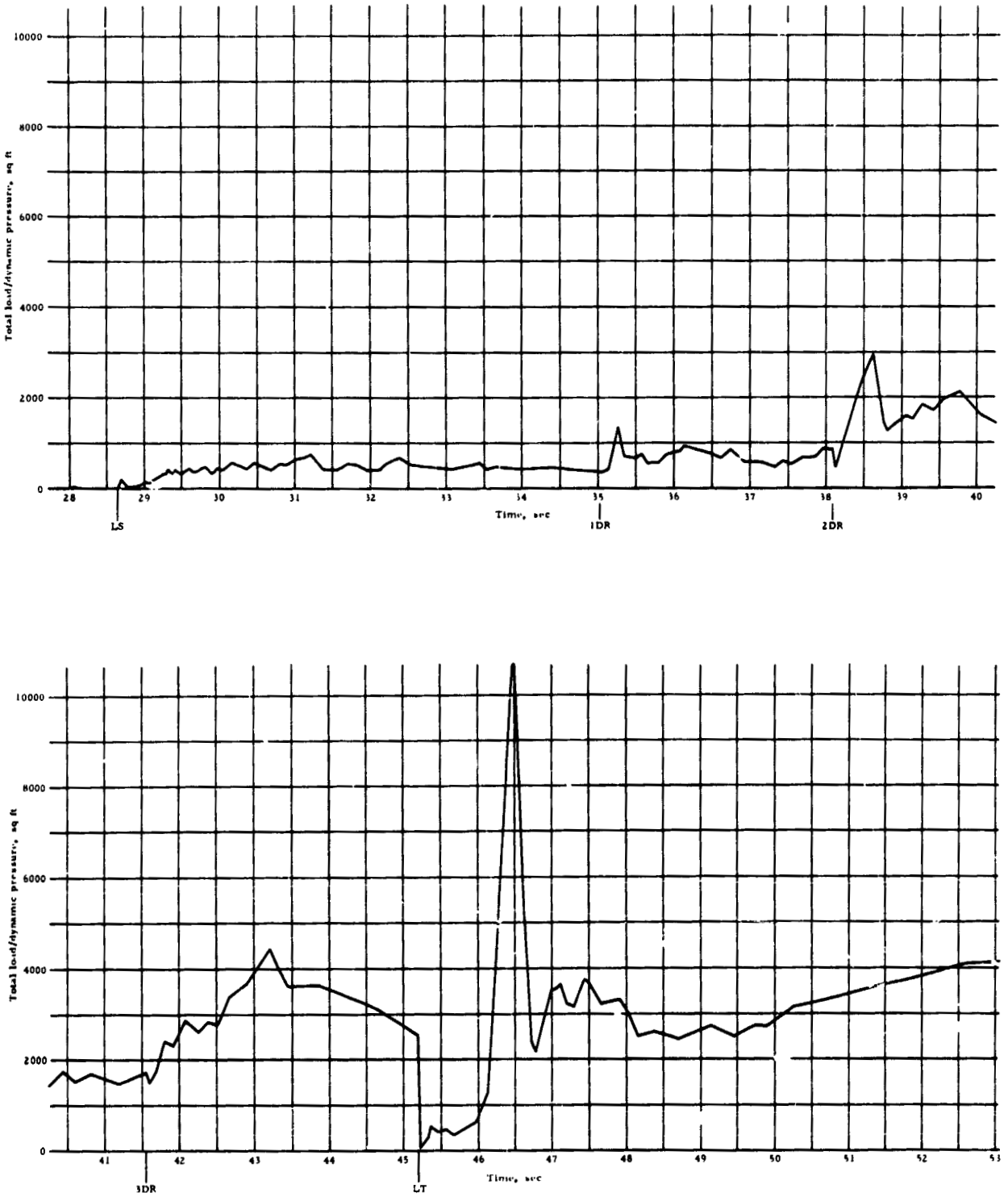

Figure 41. Total parawing load/dynamic pressure versus time from launch, twin keel parawing, Test 203T

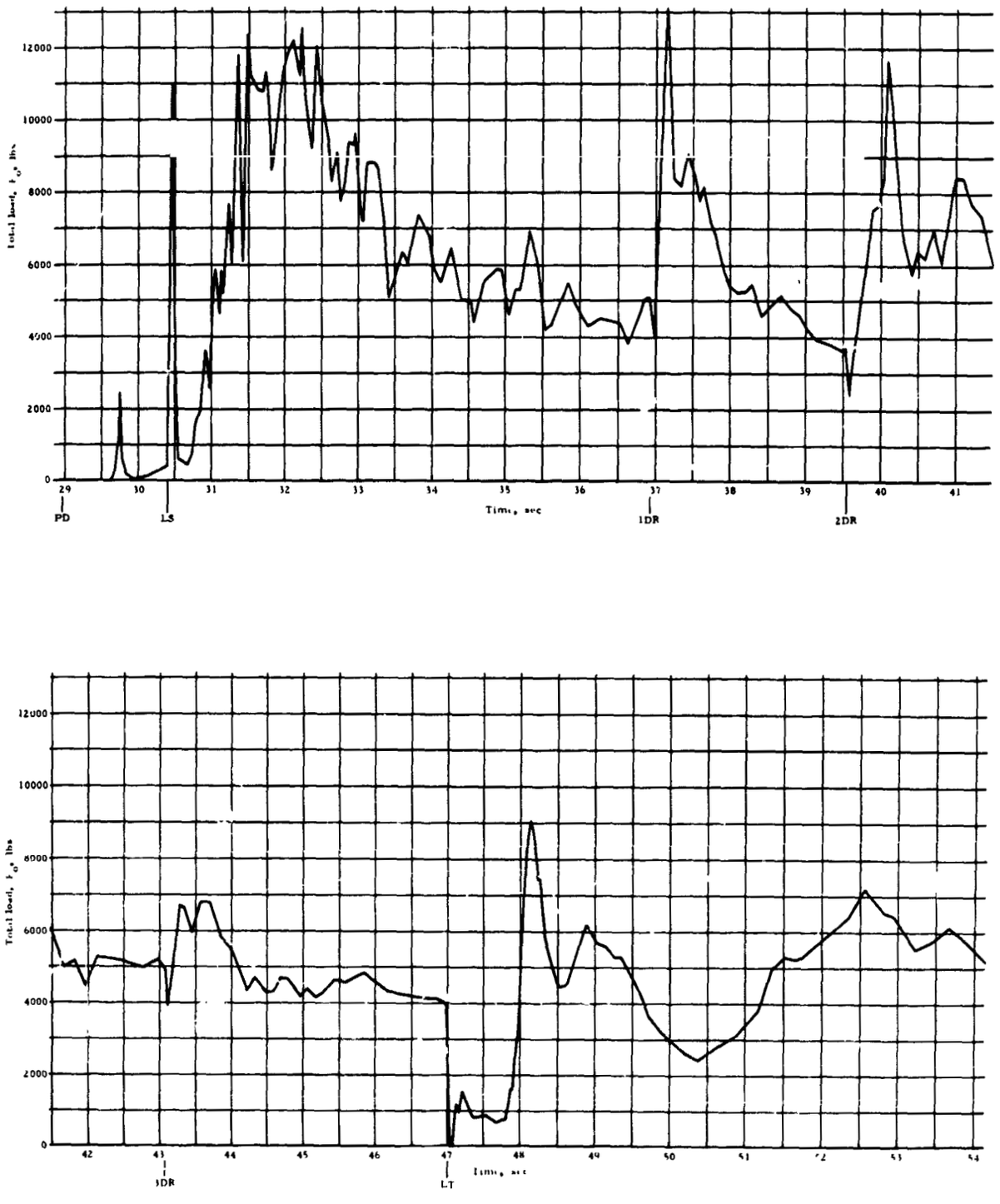

Figure 42. Total parawing load versus time from launch, twin keel parawing, Test 204T

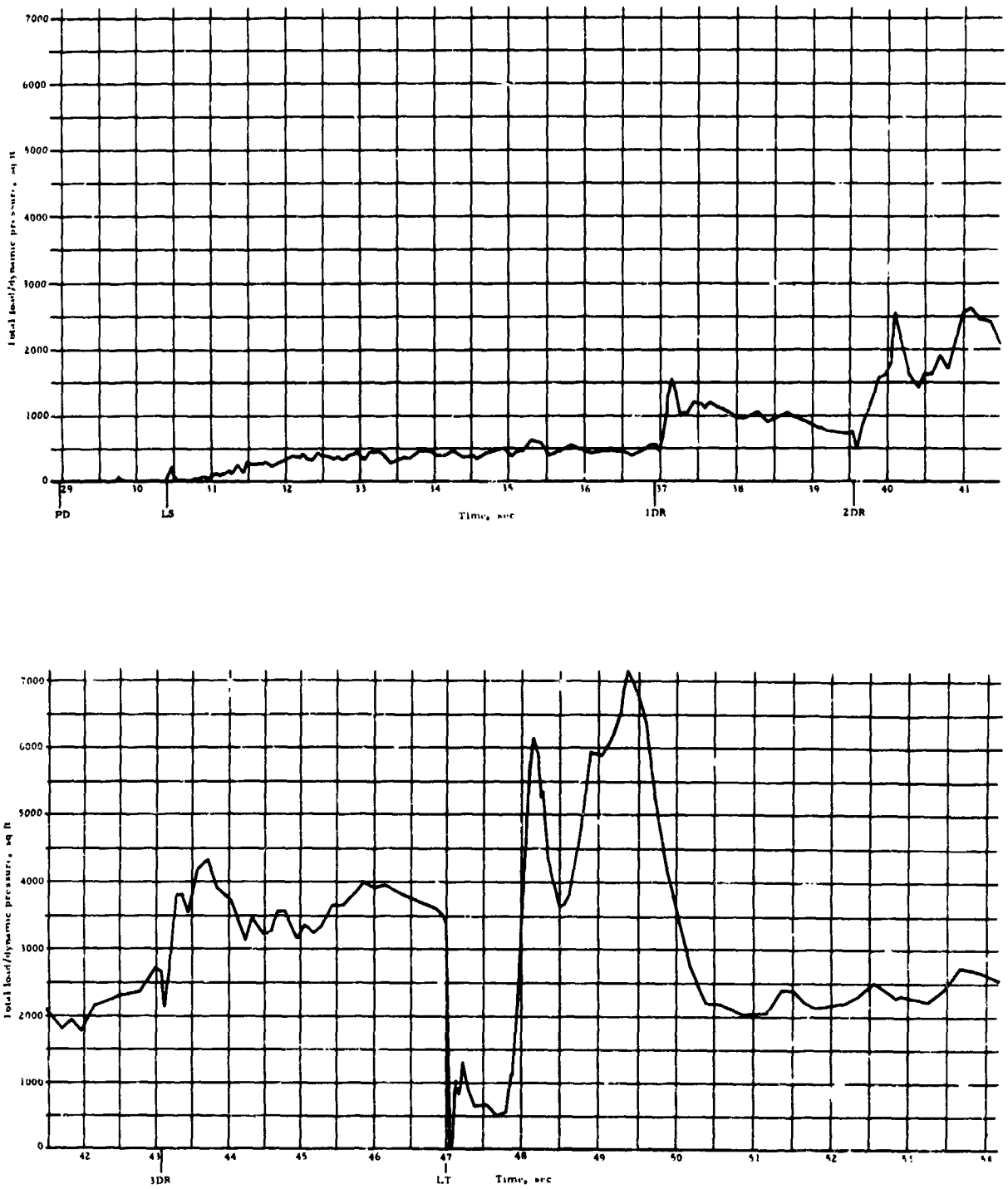

Figure 43. Total parawing load/dynamic pressure versus time from launch, twin keel parawing, Test 204T

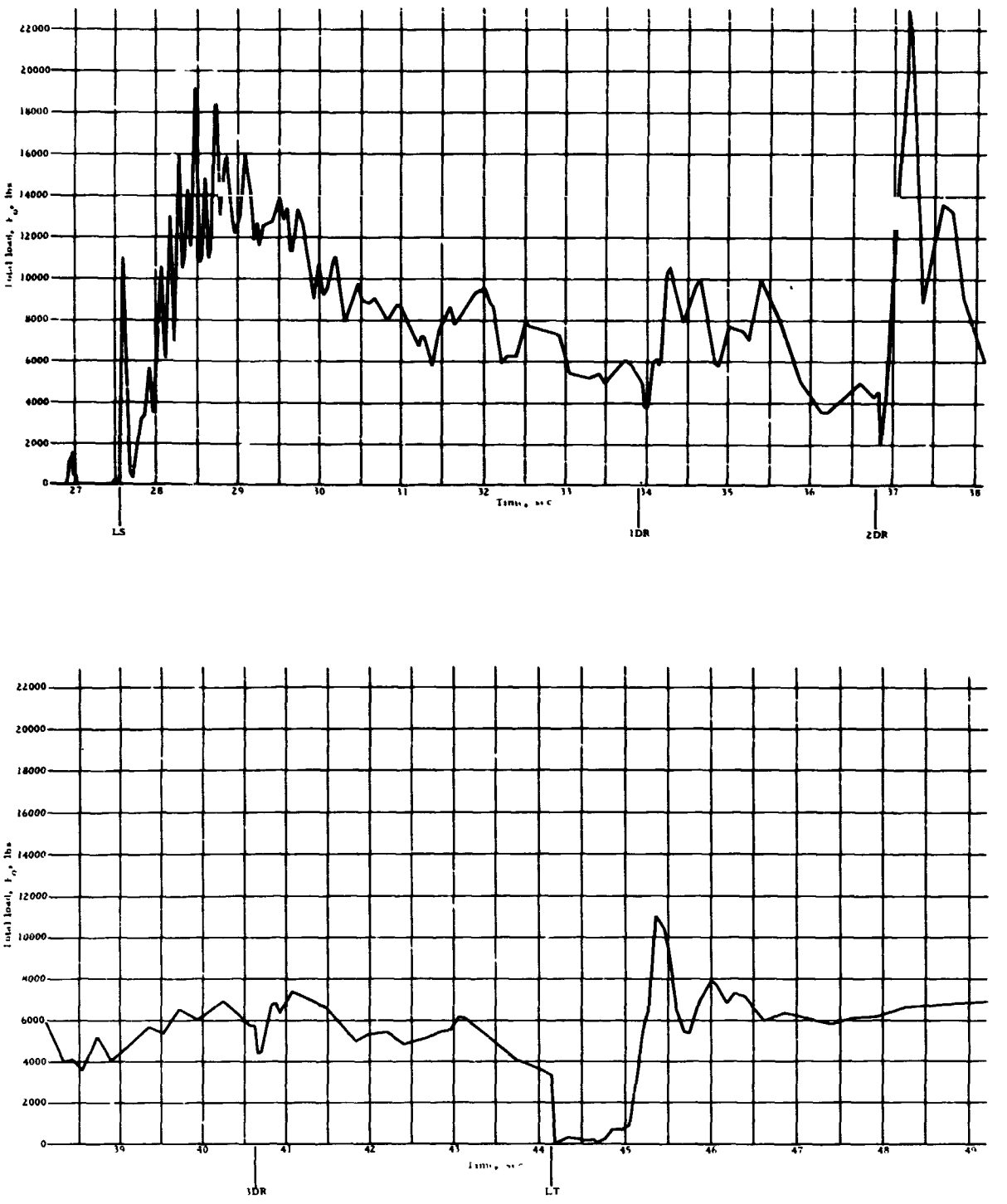

Figure 44. Total parawing load versus time from launch, twin keel parawing, Test 205T

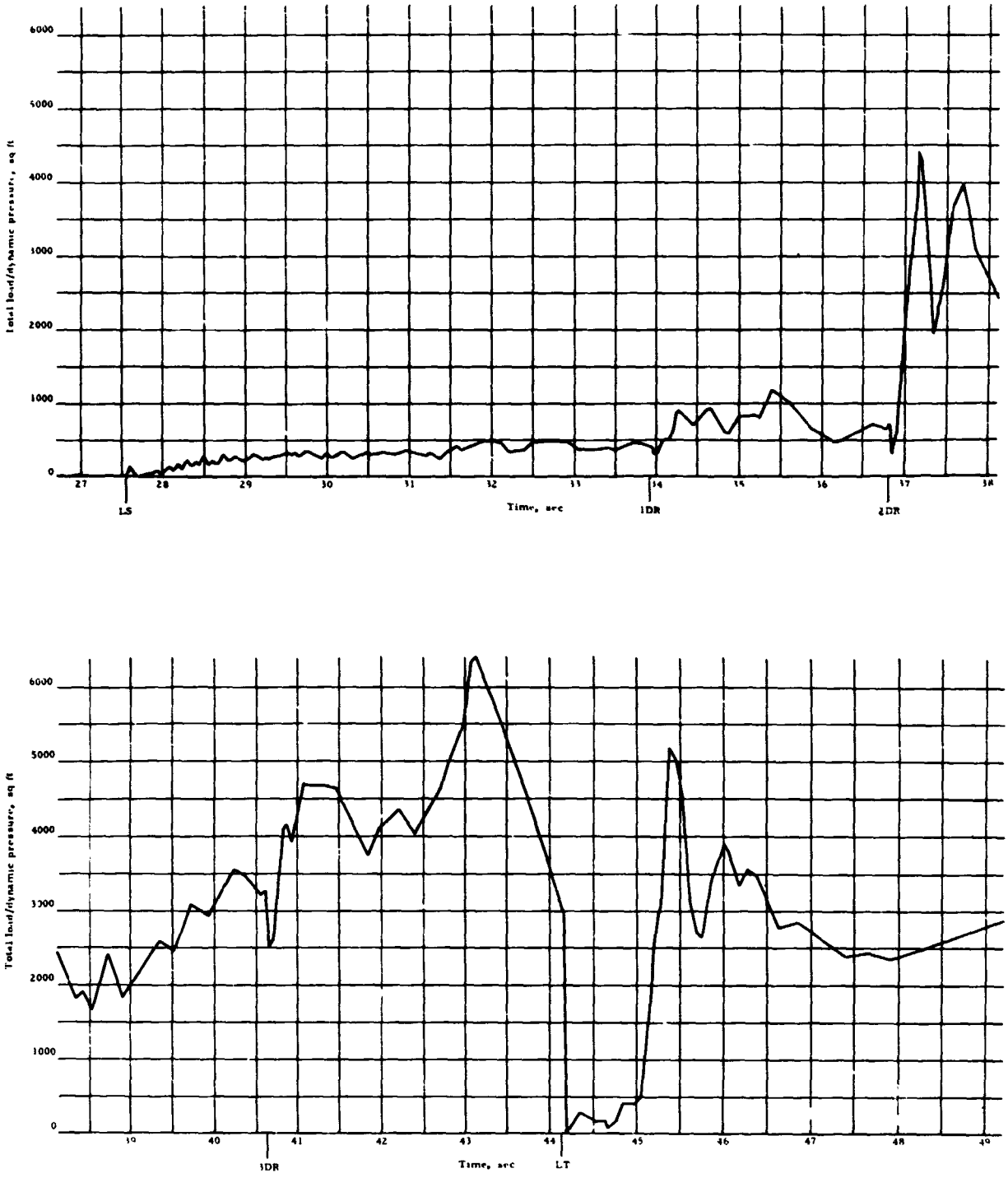

Figure 45. Total parawing load/dynamic pressure versus time from launch, twin keel parawing, Test 205T

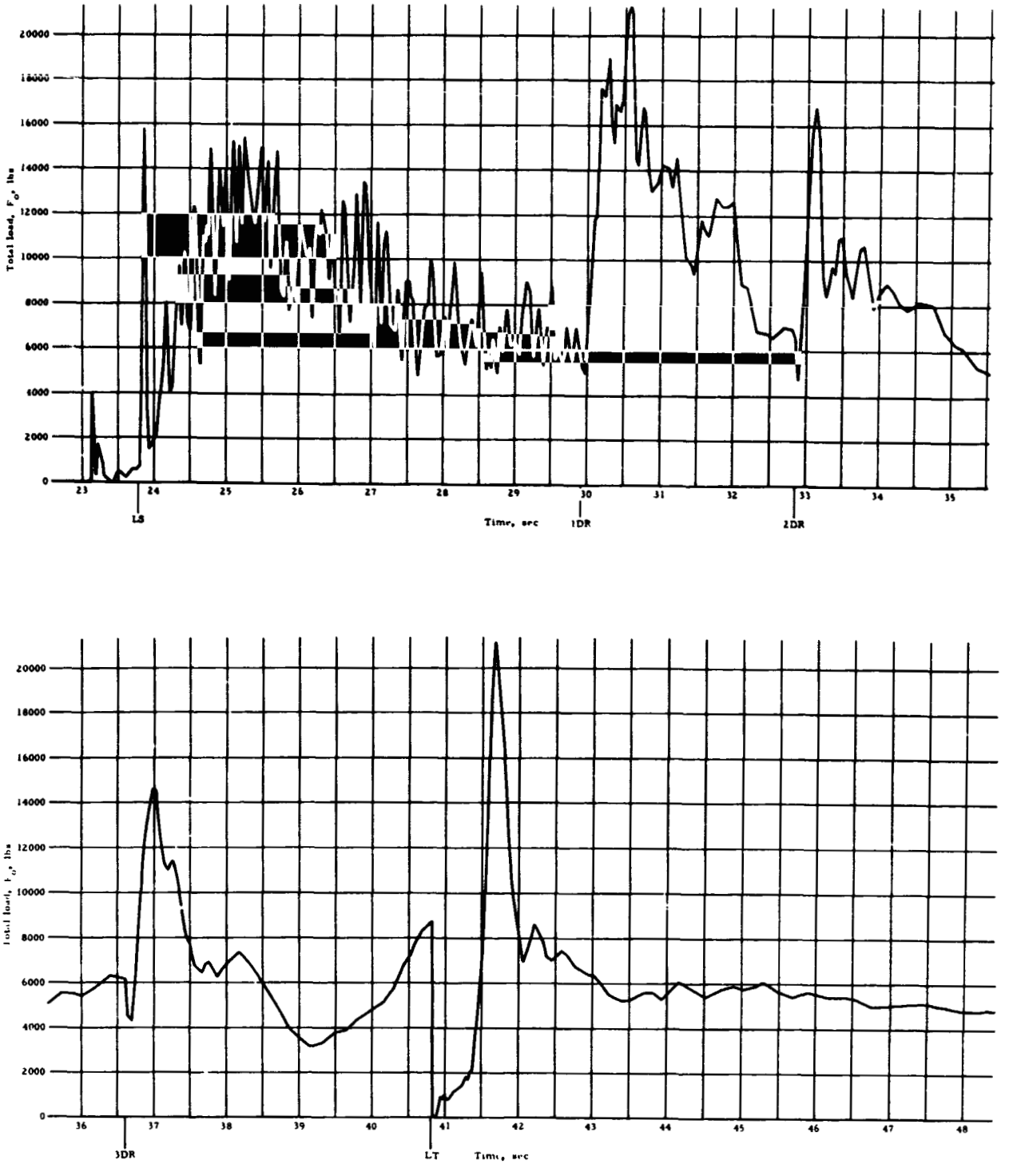

Figure 46. Total parawing load versus time from launch, twin keel parawing, Test 206T

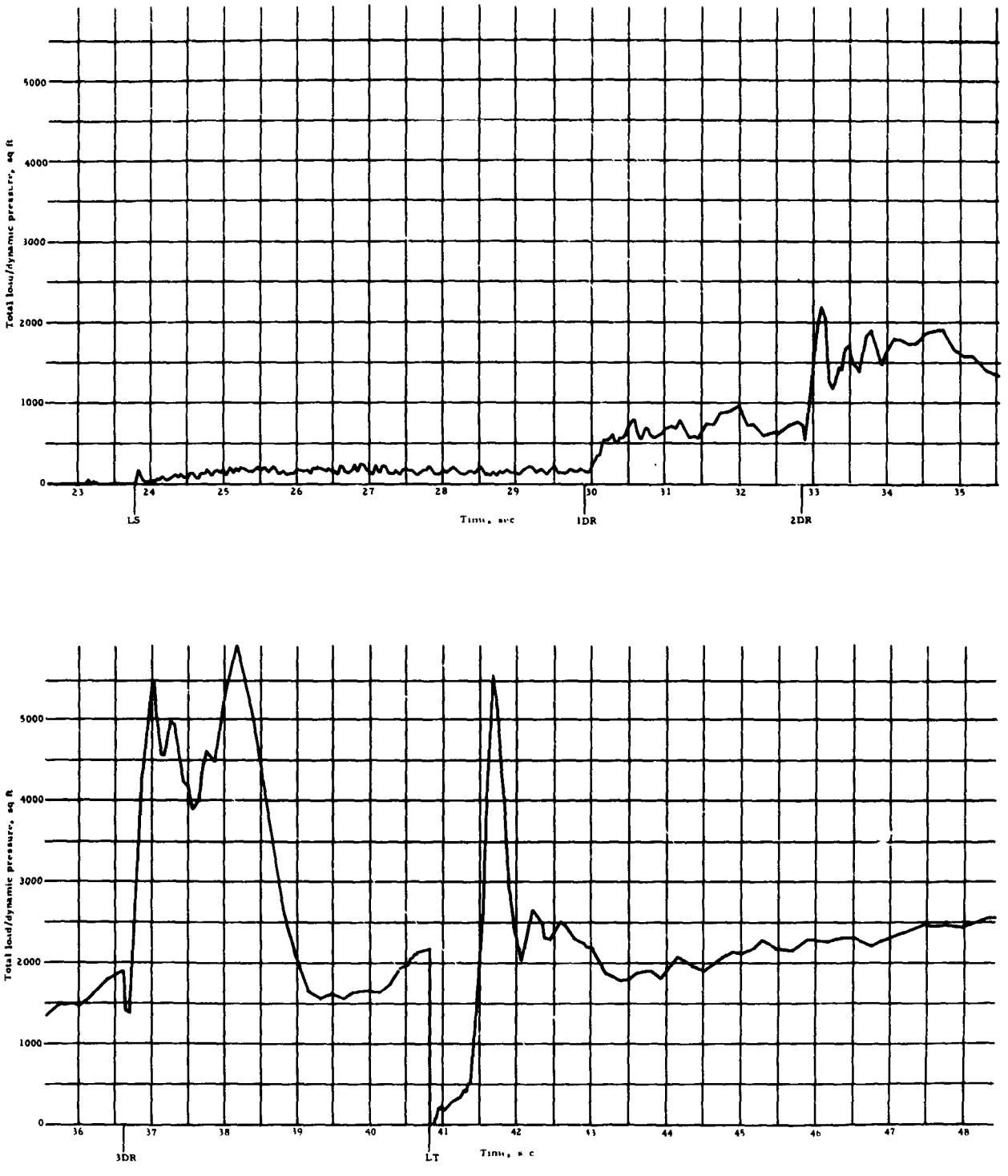

Figure 47. Total parawing load/dynamic pressure versus time from launch, twin keel parawing, Test 206T

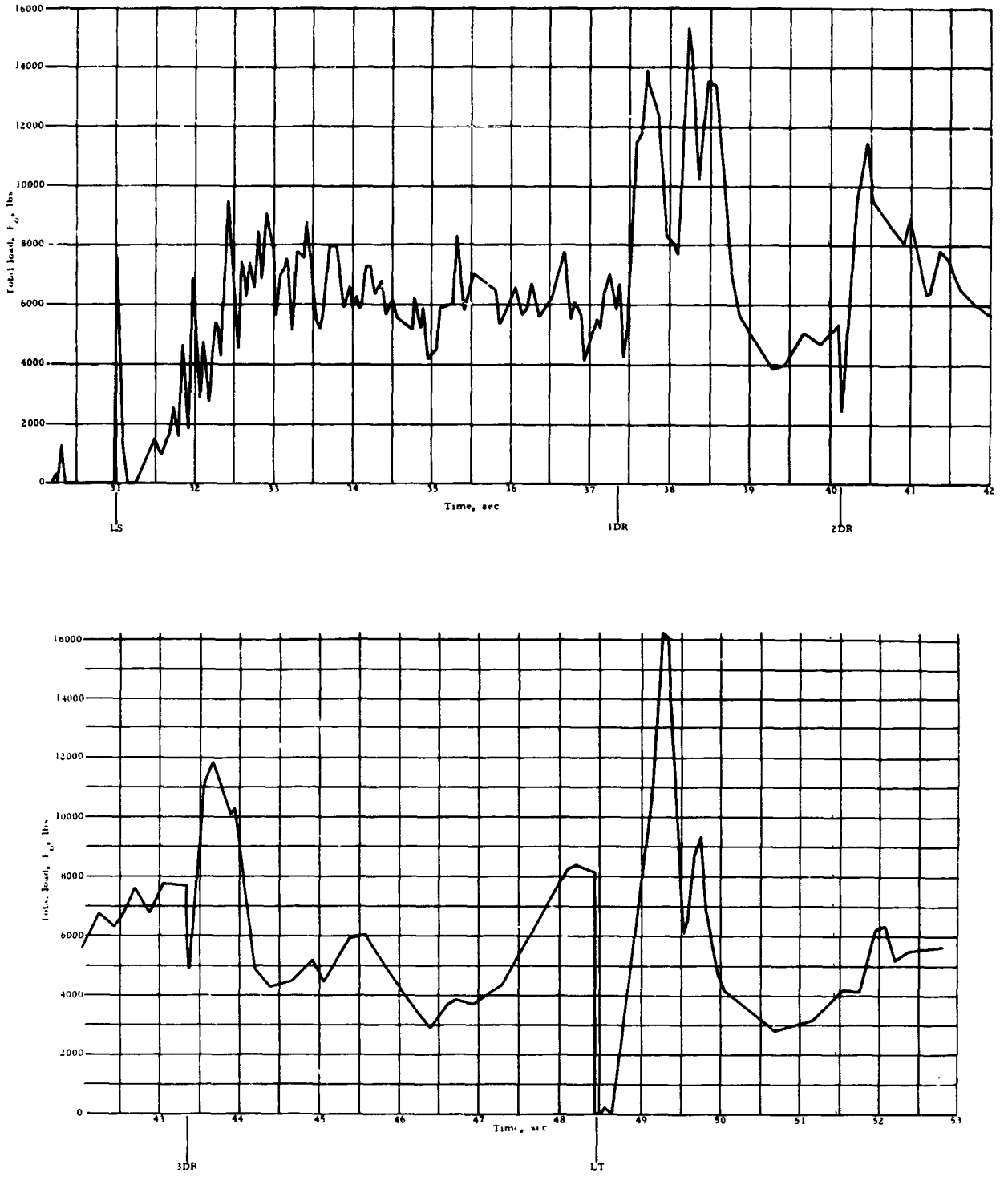

Figure 48. Total parawing load versus time from launch, twin keel parawing, Test 207T

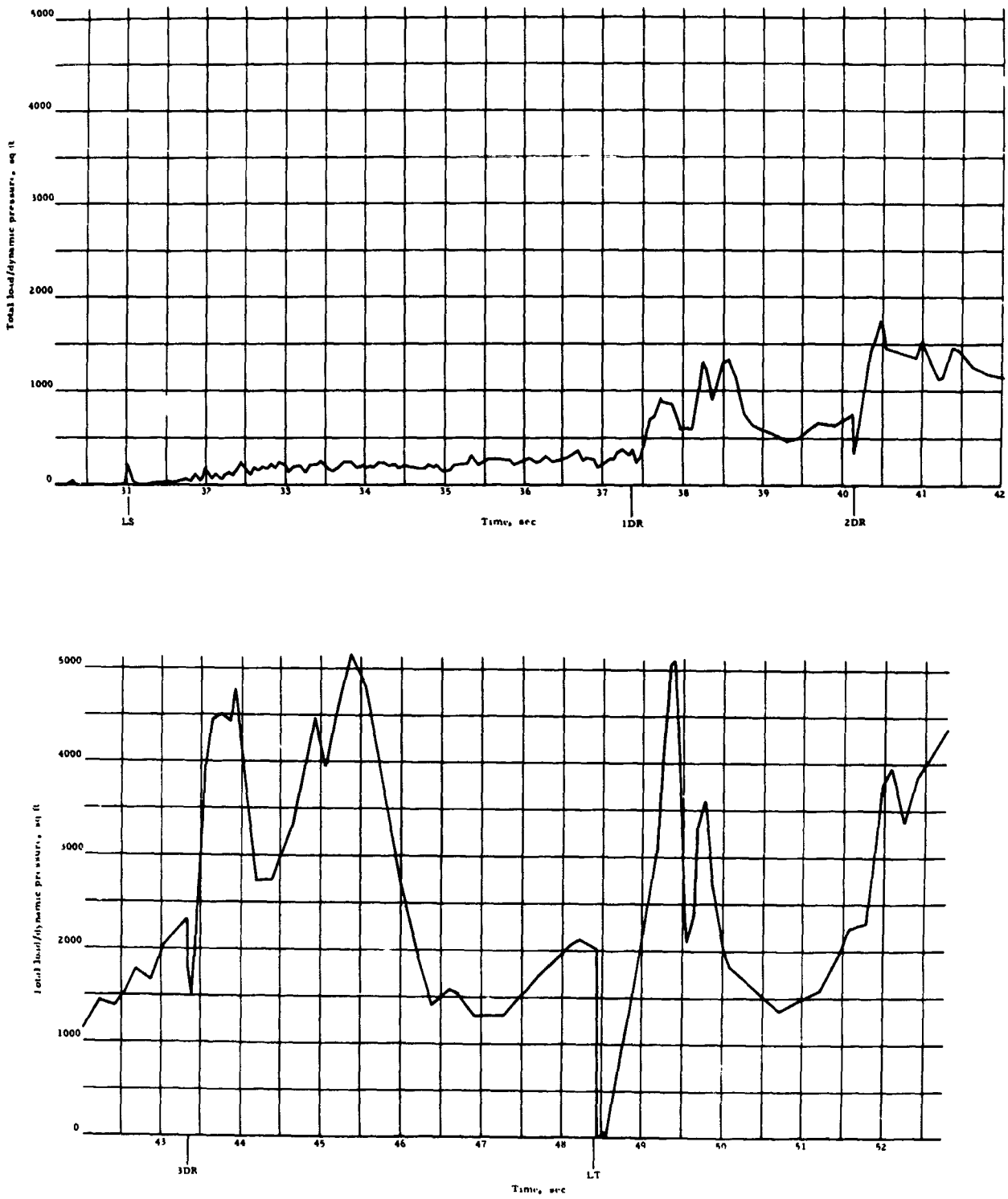

Figure 49. Total parawing load/dynamic pressure versus time from launch, twin keel parawing, Test 207T

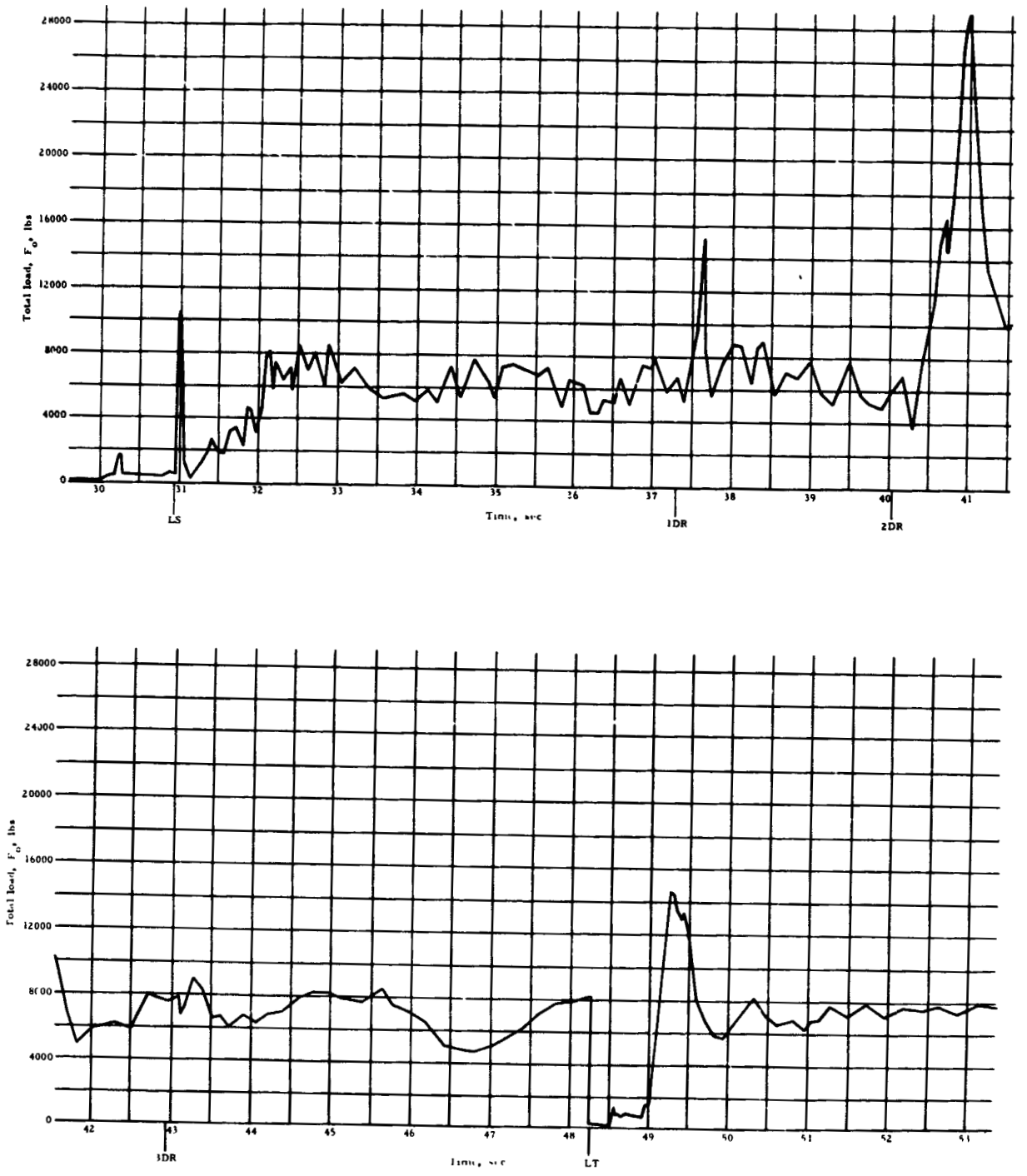

Figure 50. Total parawing load versus time from launch, twin keel parawing, Test 208T

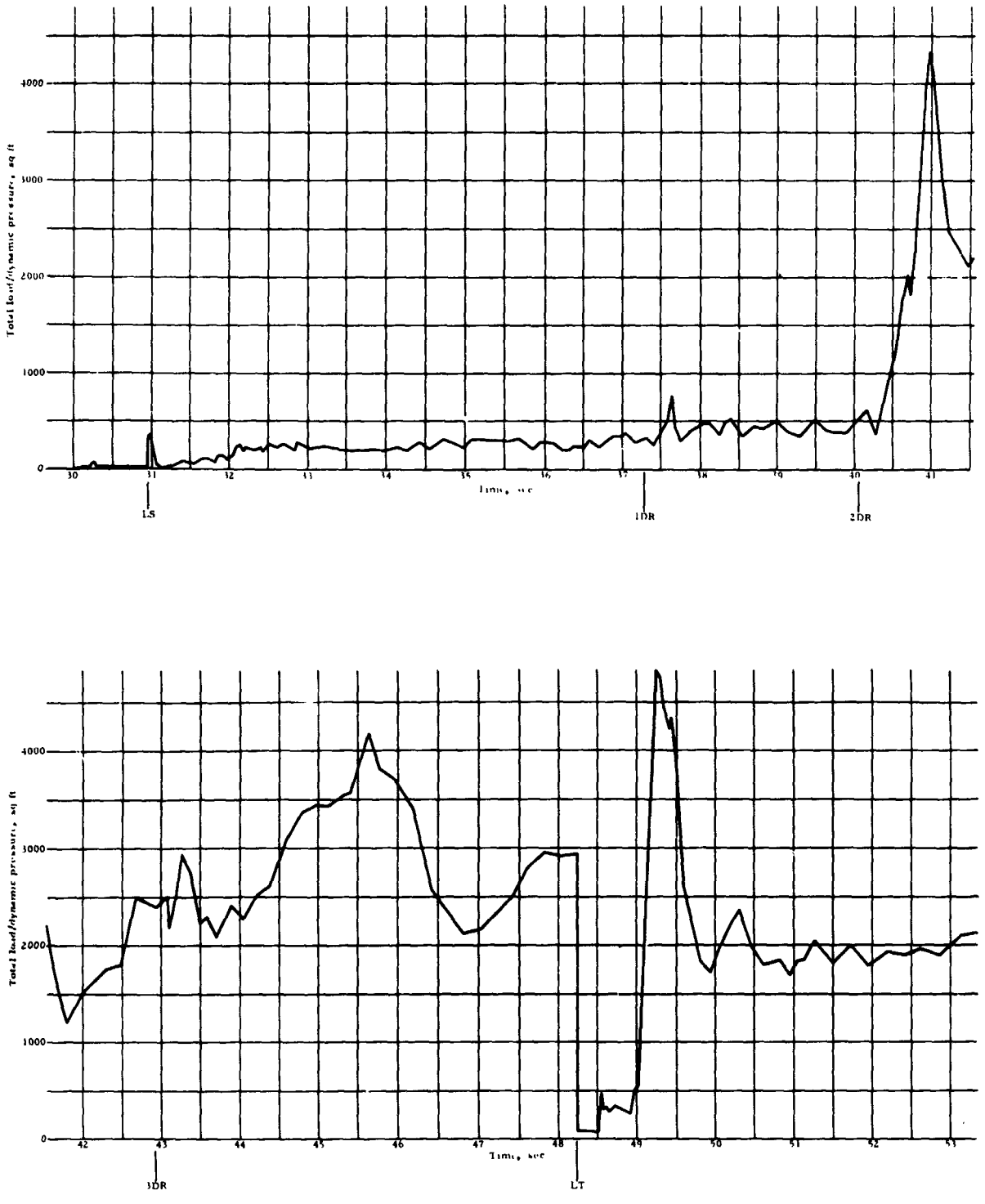

Figure 51. Total parawing load/dynamic pressure versus time from launch, twin keel parawing, Test 208T

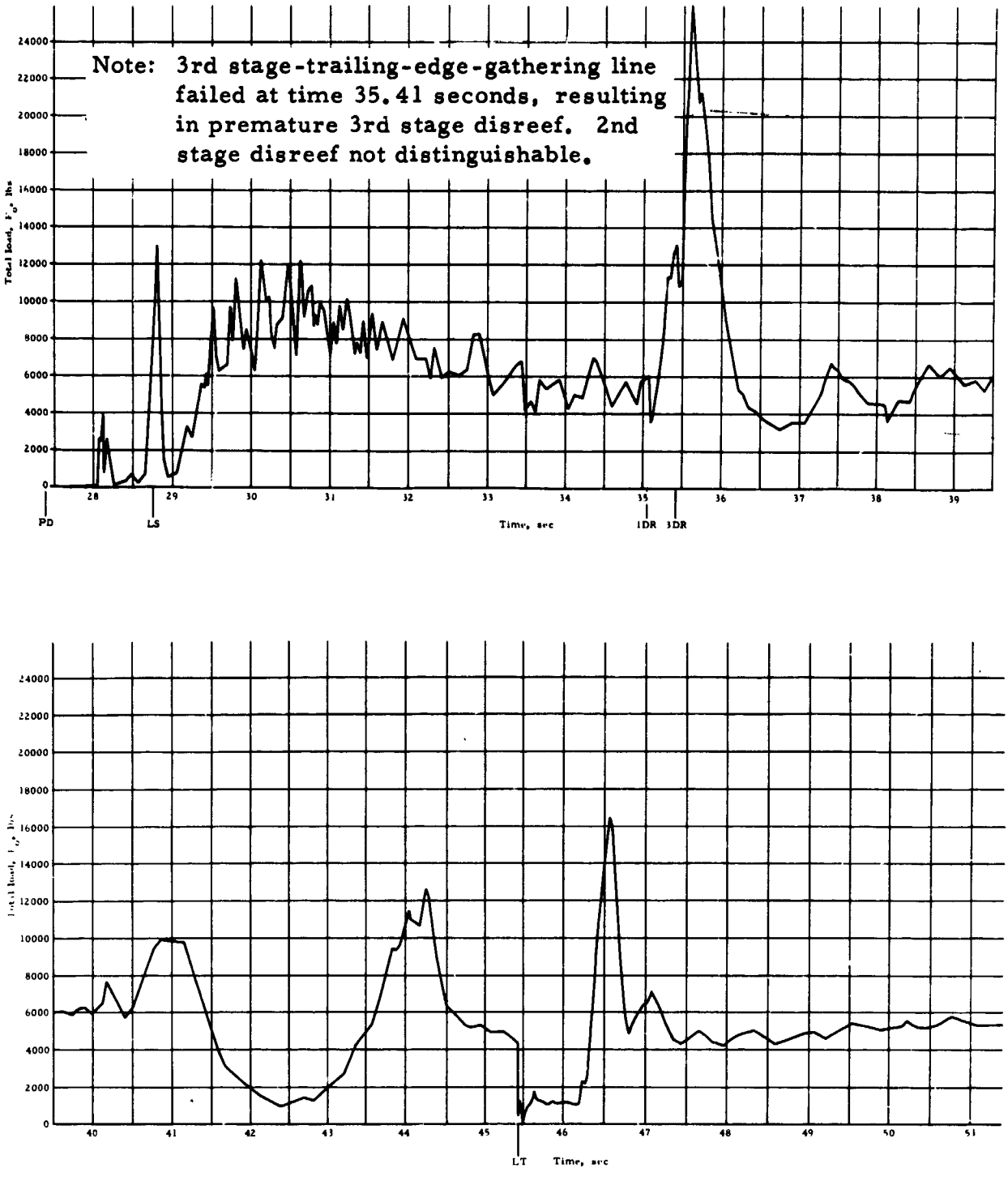

Figure 52. Total parawing load versus time from launch, twin keel parawing, Test 209T

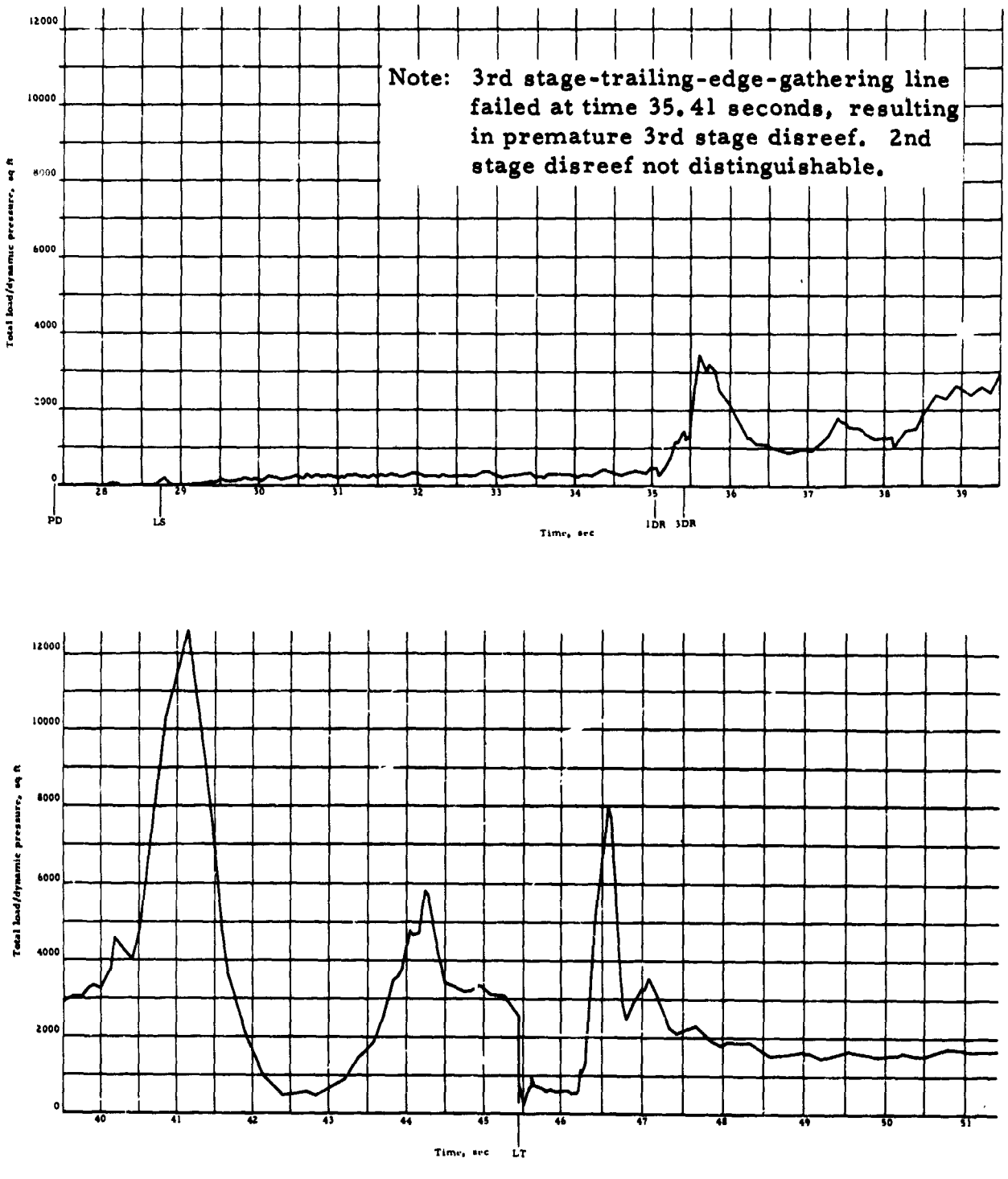

Figure 53. Total parawing load/dynamic pressure versus time from launch, twin keel parawing, Test 209T

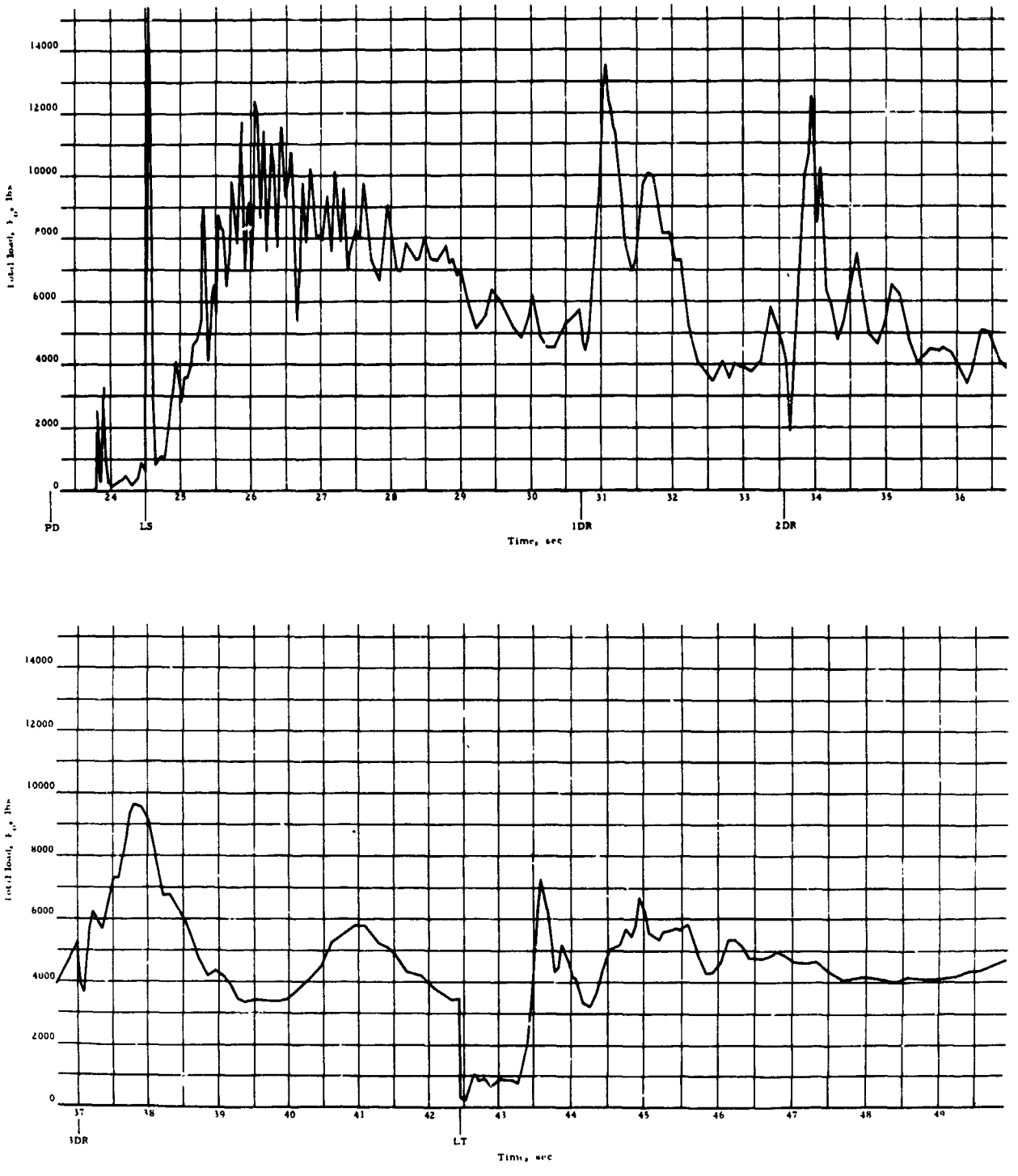

Figure 54. Total parawing load versus time from launch, twin keel parawing, Test 210T

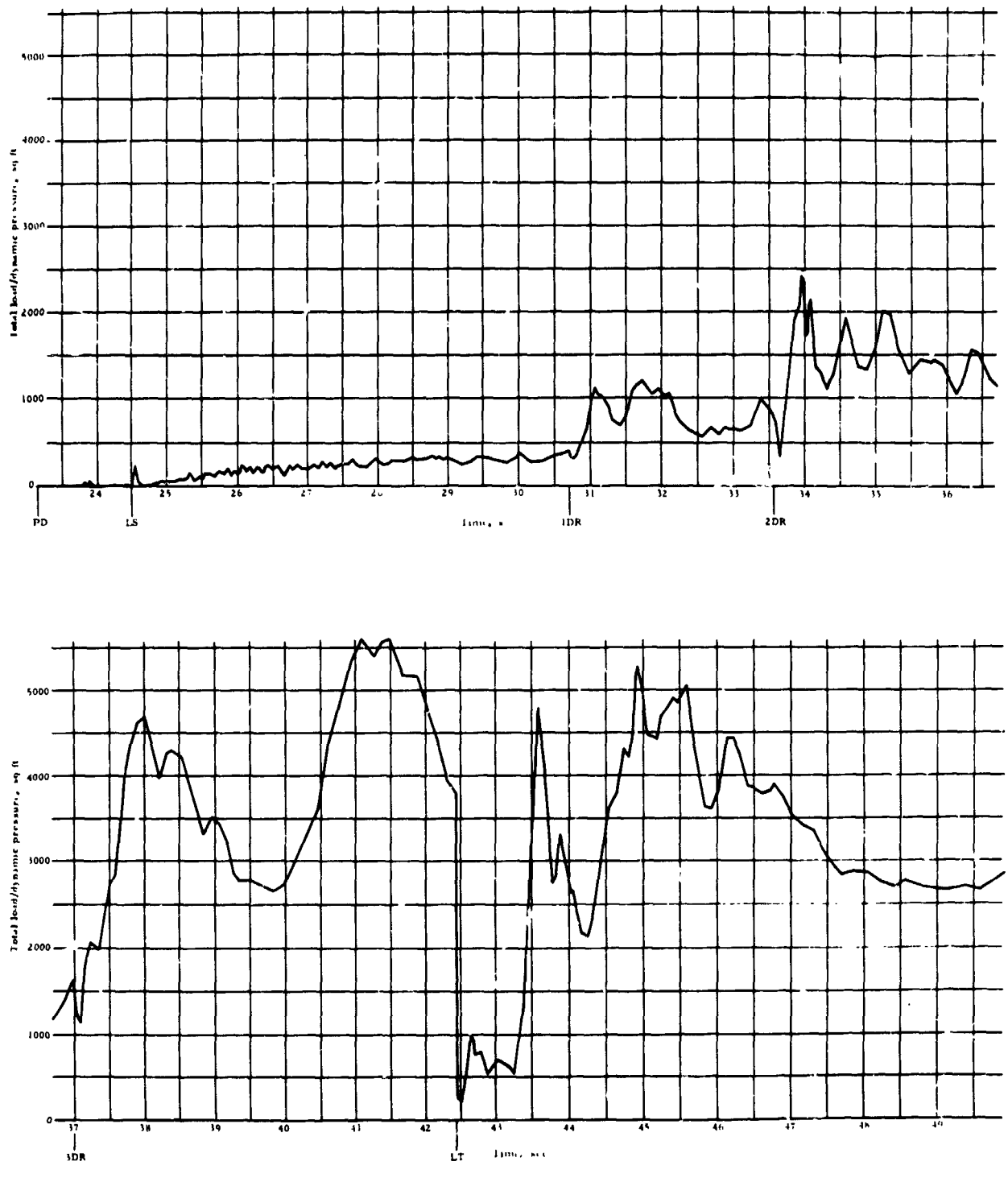

Figure 55. Total parawing load/dynamic pressure versus time from launch, twin keel parawing, Test 210T

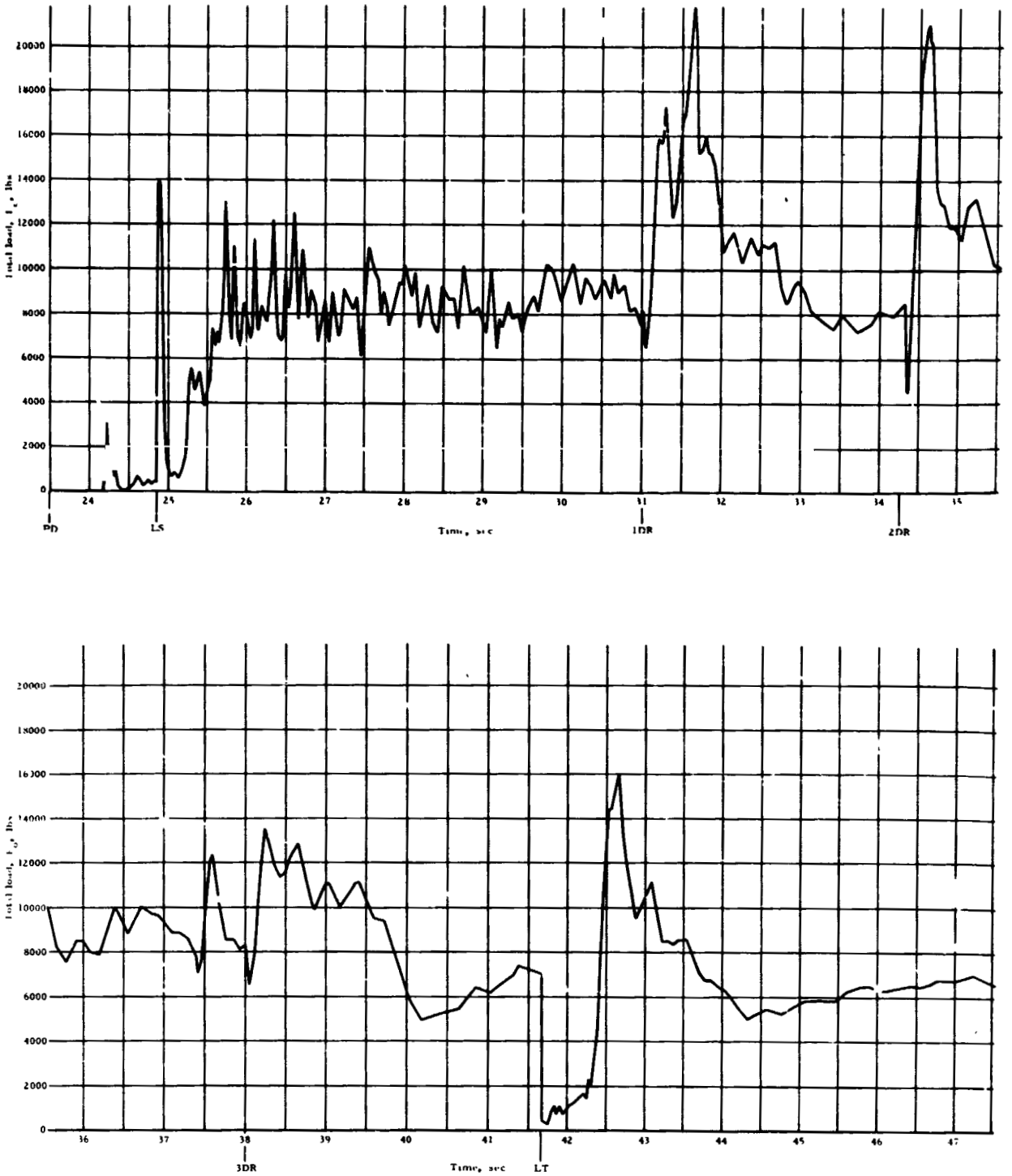

Figure 56. Total parawing load versus time from launch, twin keel parawing, Test 211T

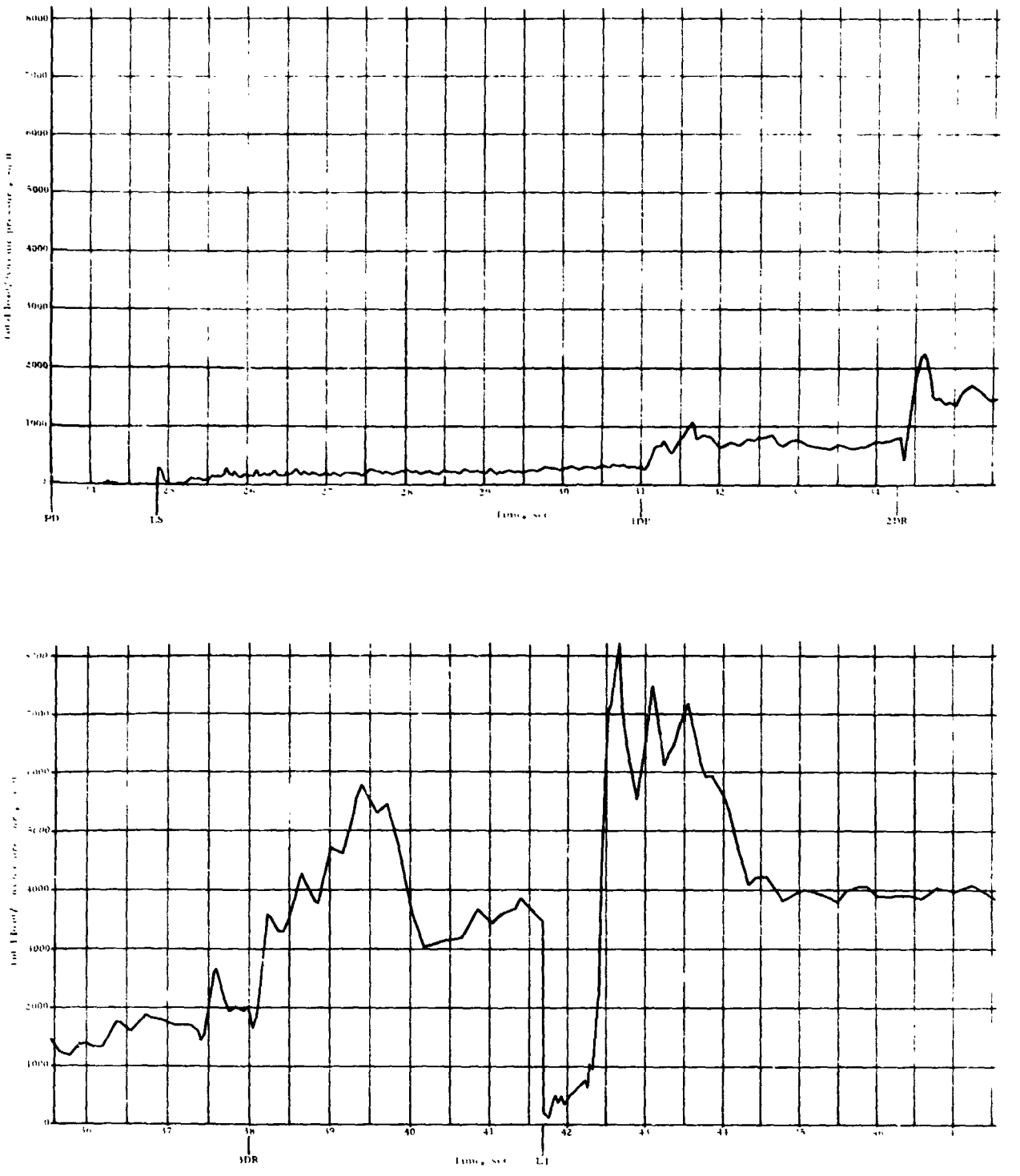

Figure 57. Total parawing load/dynamic pressure versus time from launch, twin keel parawing, Test 211T

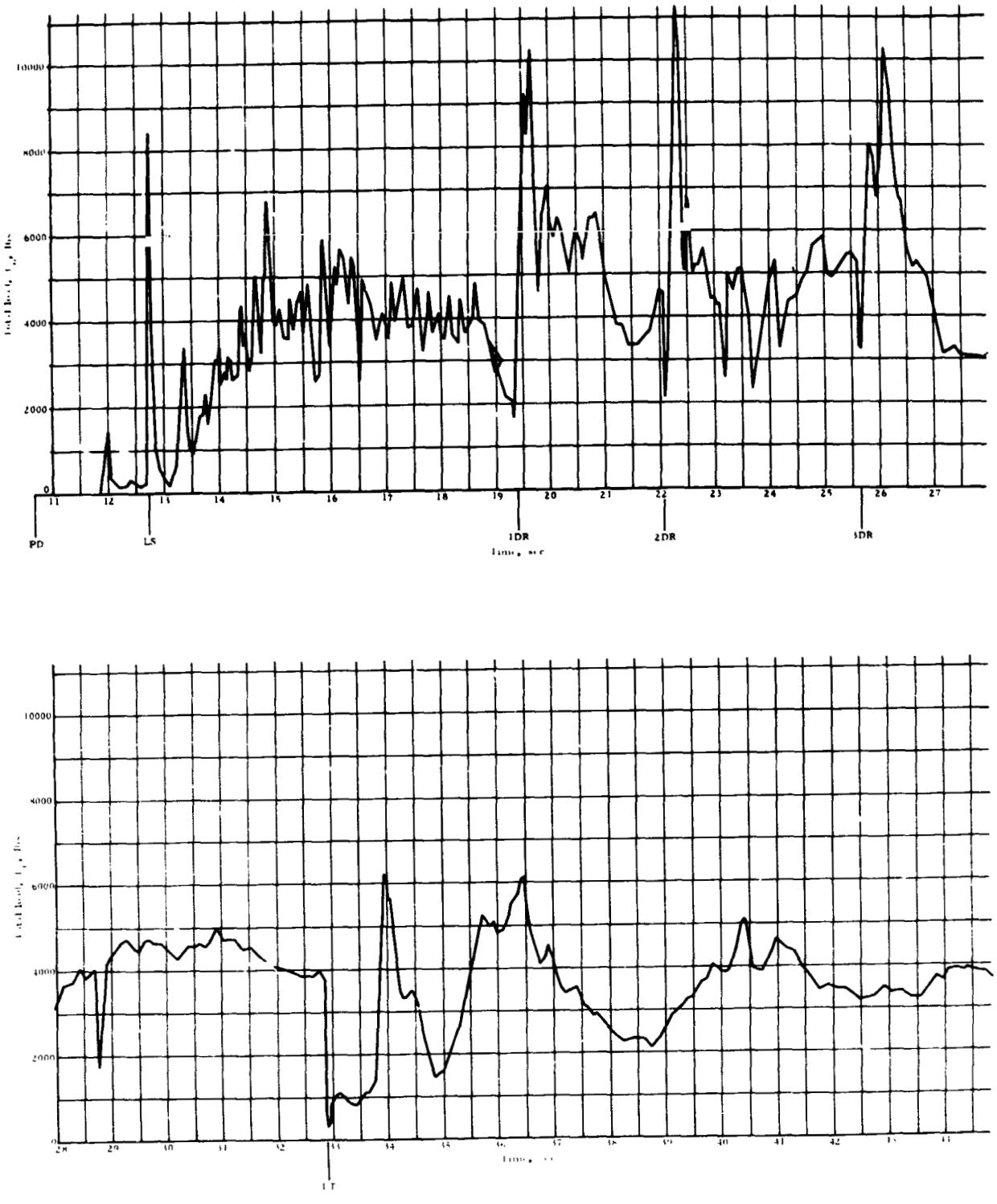

Figure 58. Total parawing load versus time from launch, twin keel parawing, Test 250T

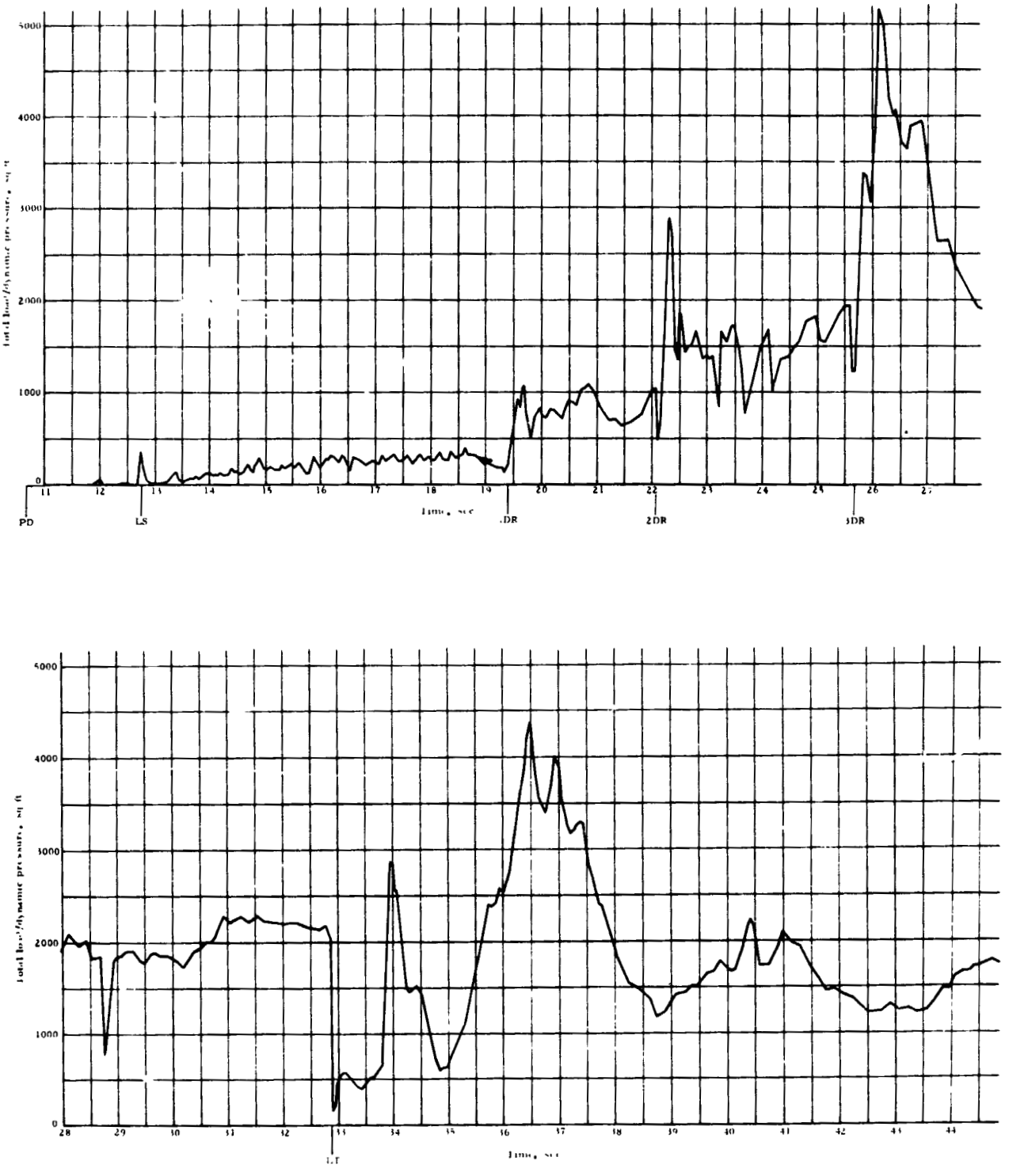

Figure 59. Total parawing load/dynamic pressure versus time from launch, twin keel parawing, Test 250T

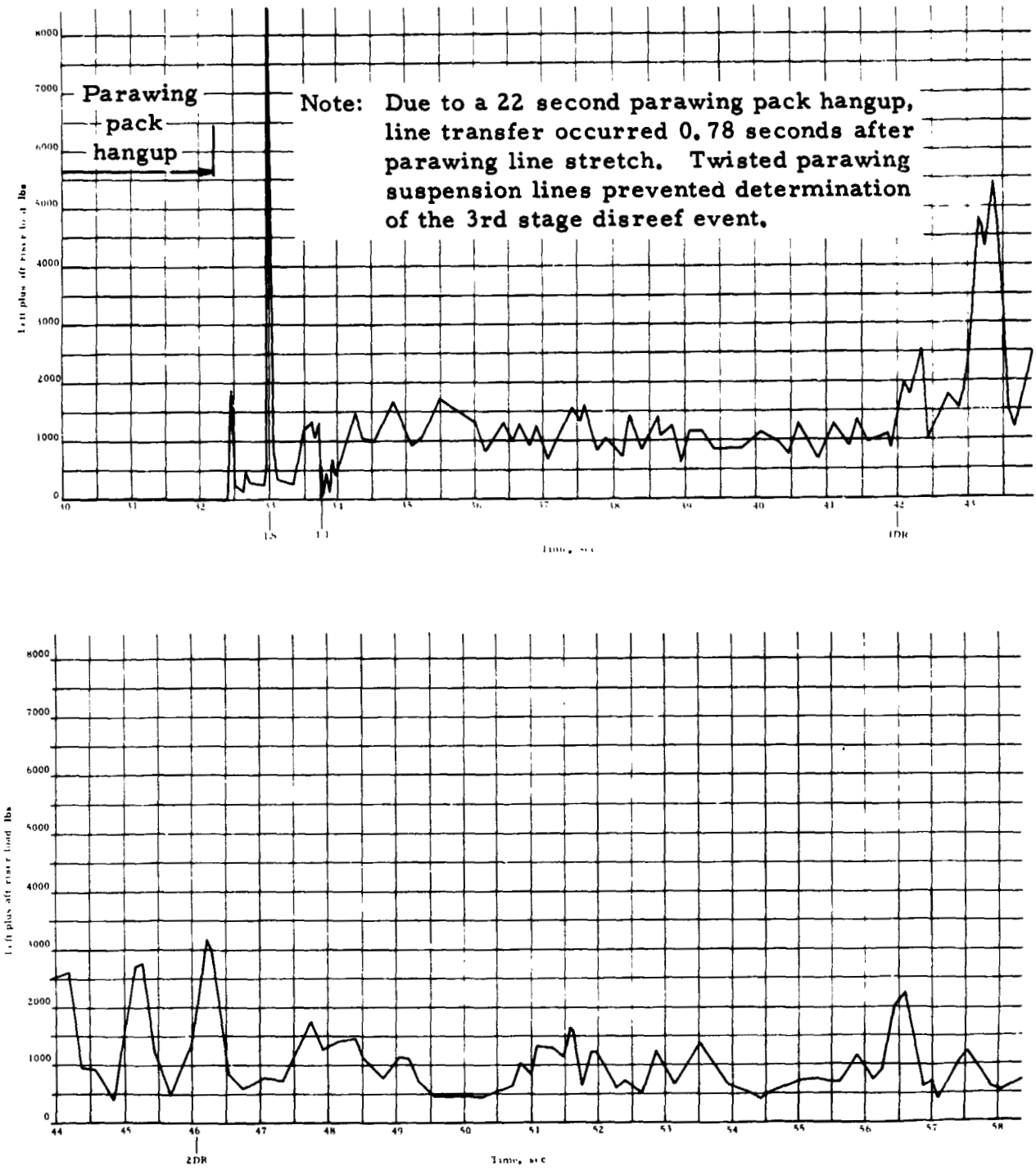

Figure 60. Left plus aft riser load versus time from launch, twin keel parawing, Test 251T

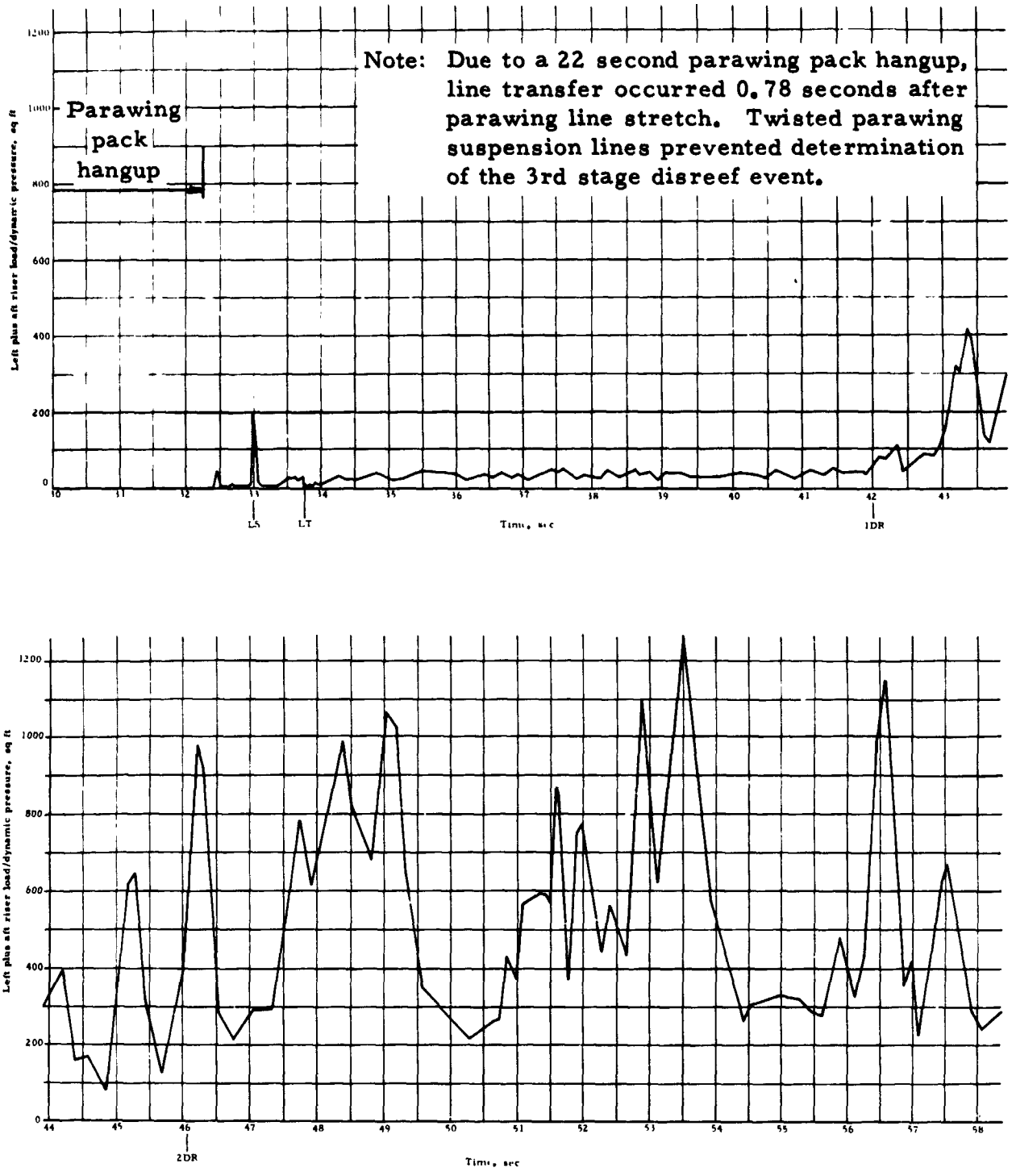

Figure 61. Left plus aft riser load/dynamic pressure versus time from launch, twin keel parawing, Test 251T

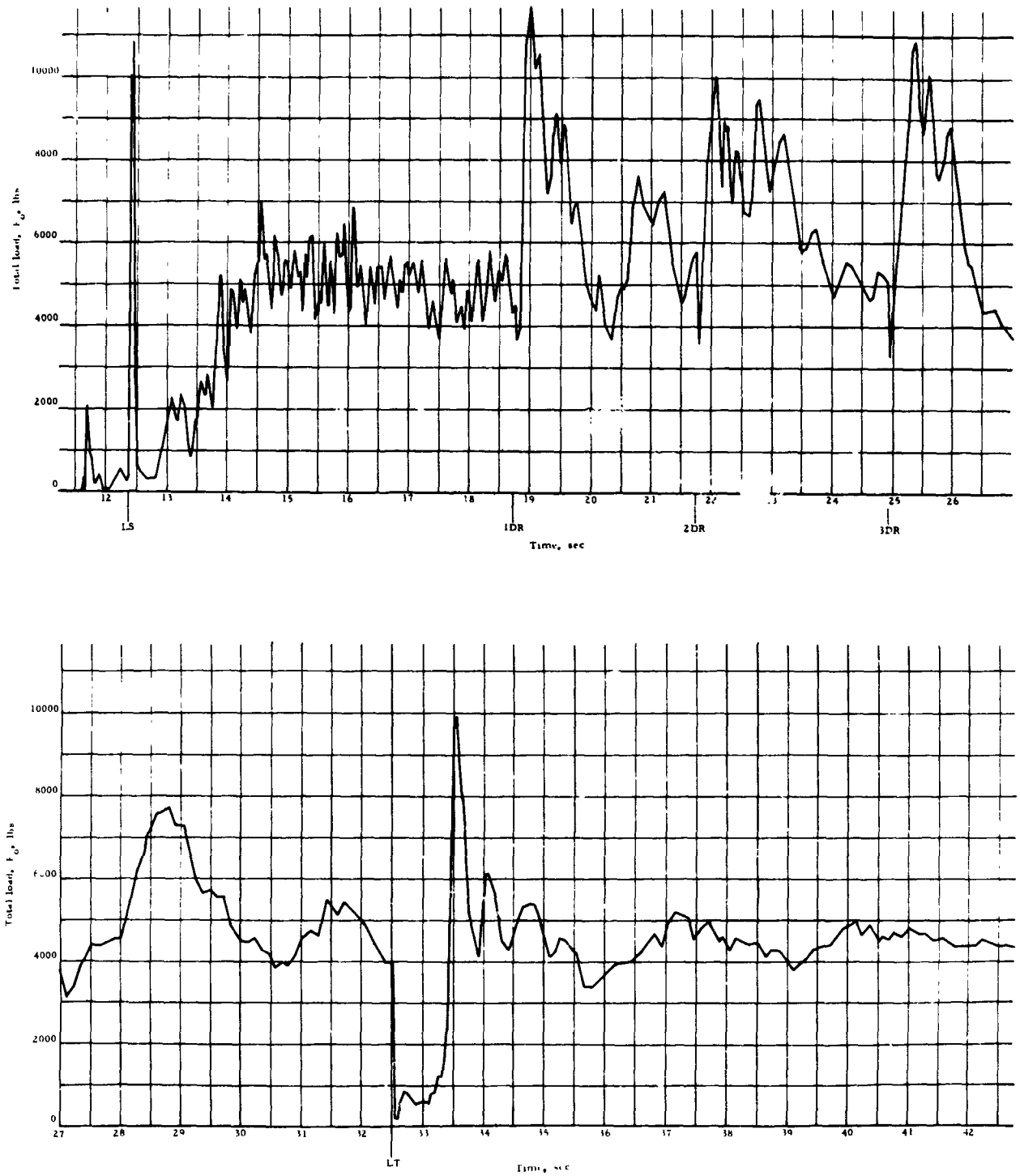

Figure 62. Total parawing load versus time from launch, twin keel parawing, Test 252T

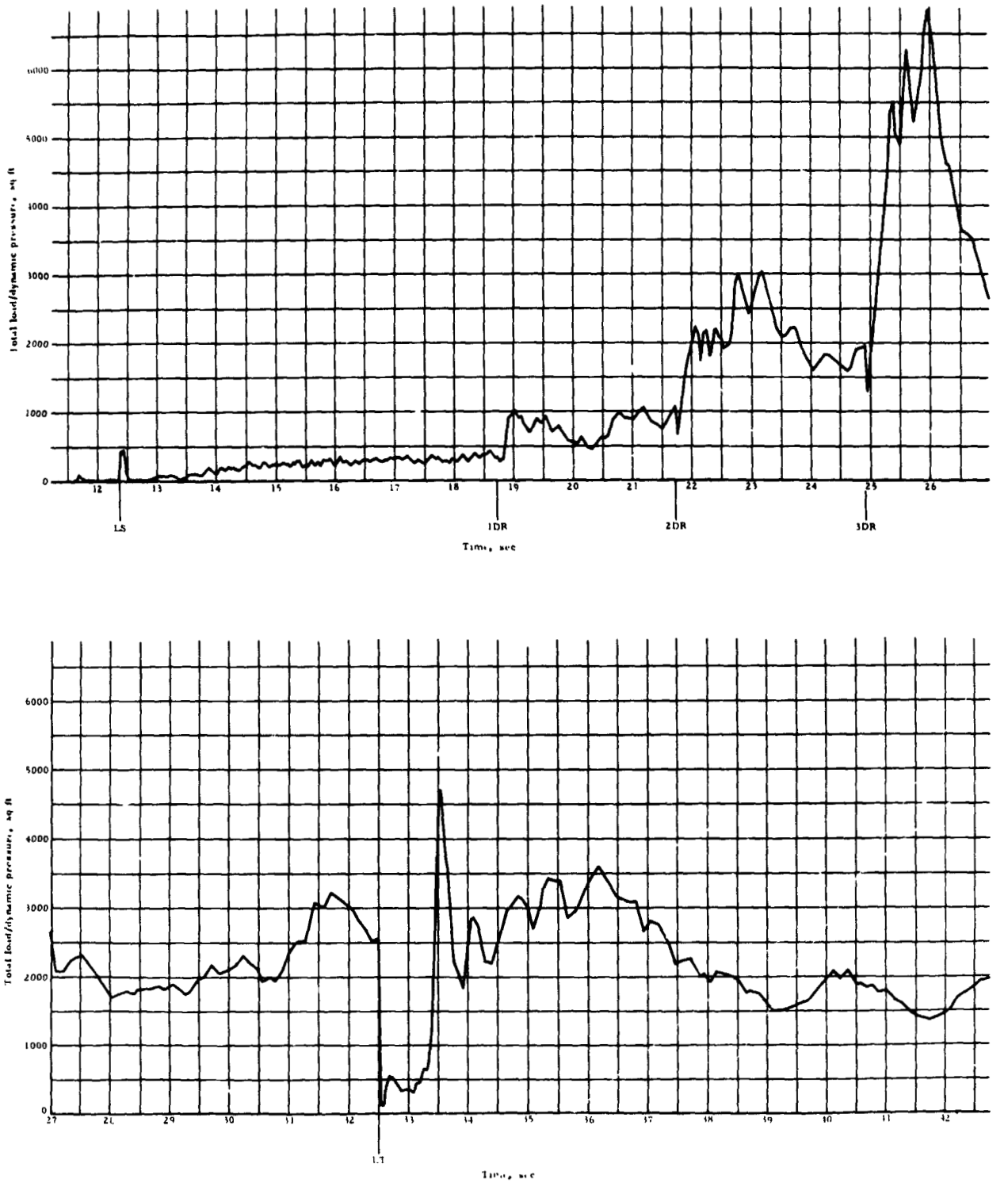

Figure 63. Total parawing load/dynamic pressure versus time from launch, twin keel parawing, Test 252T

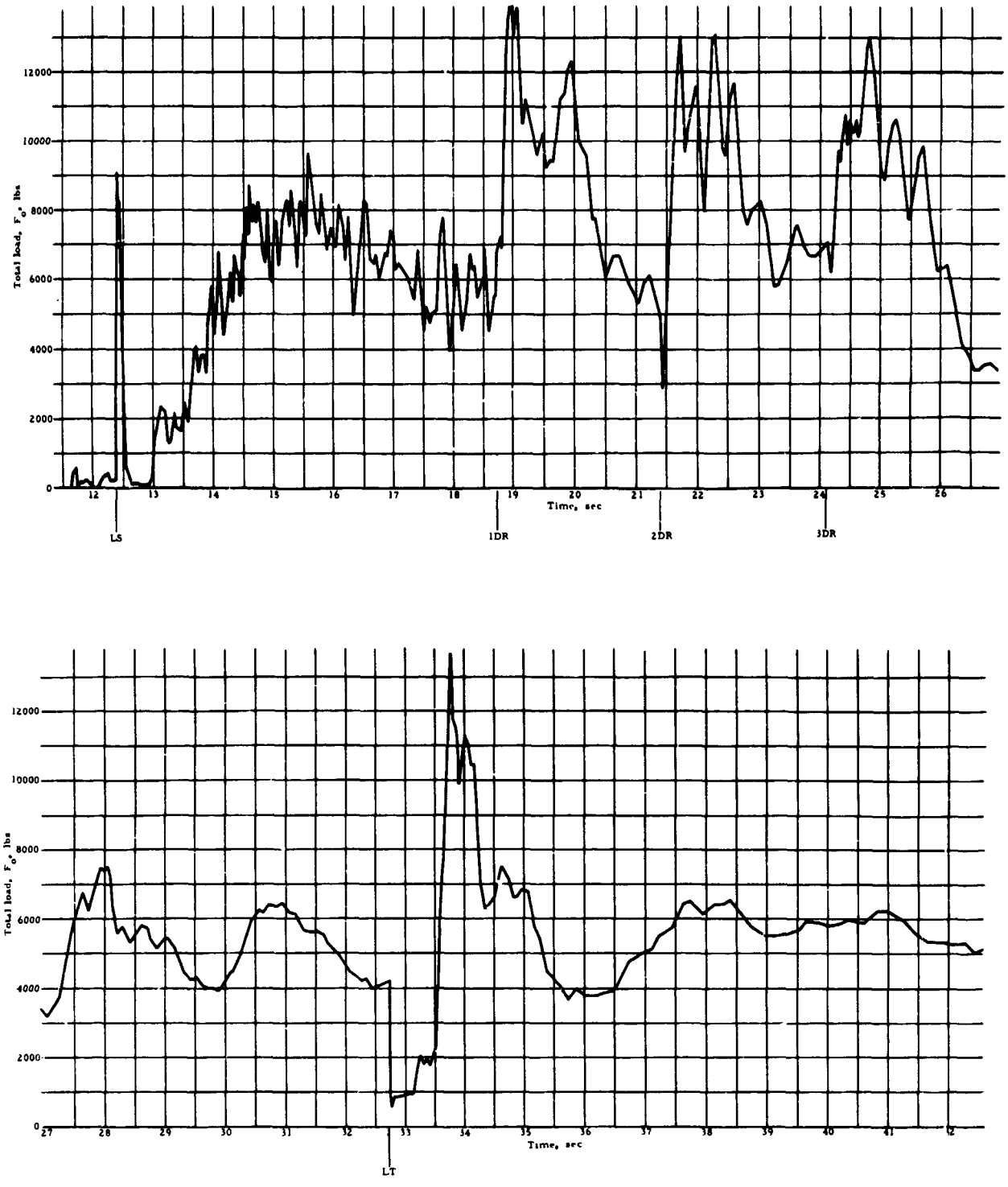

Figure 64. Total parawing load versus time from launch, twin keel parawing, Test 253T

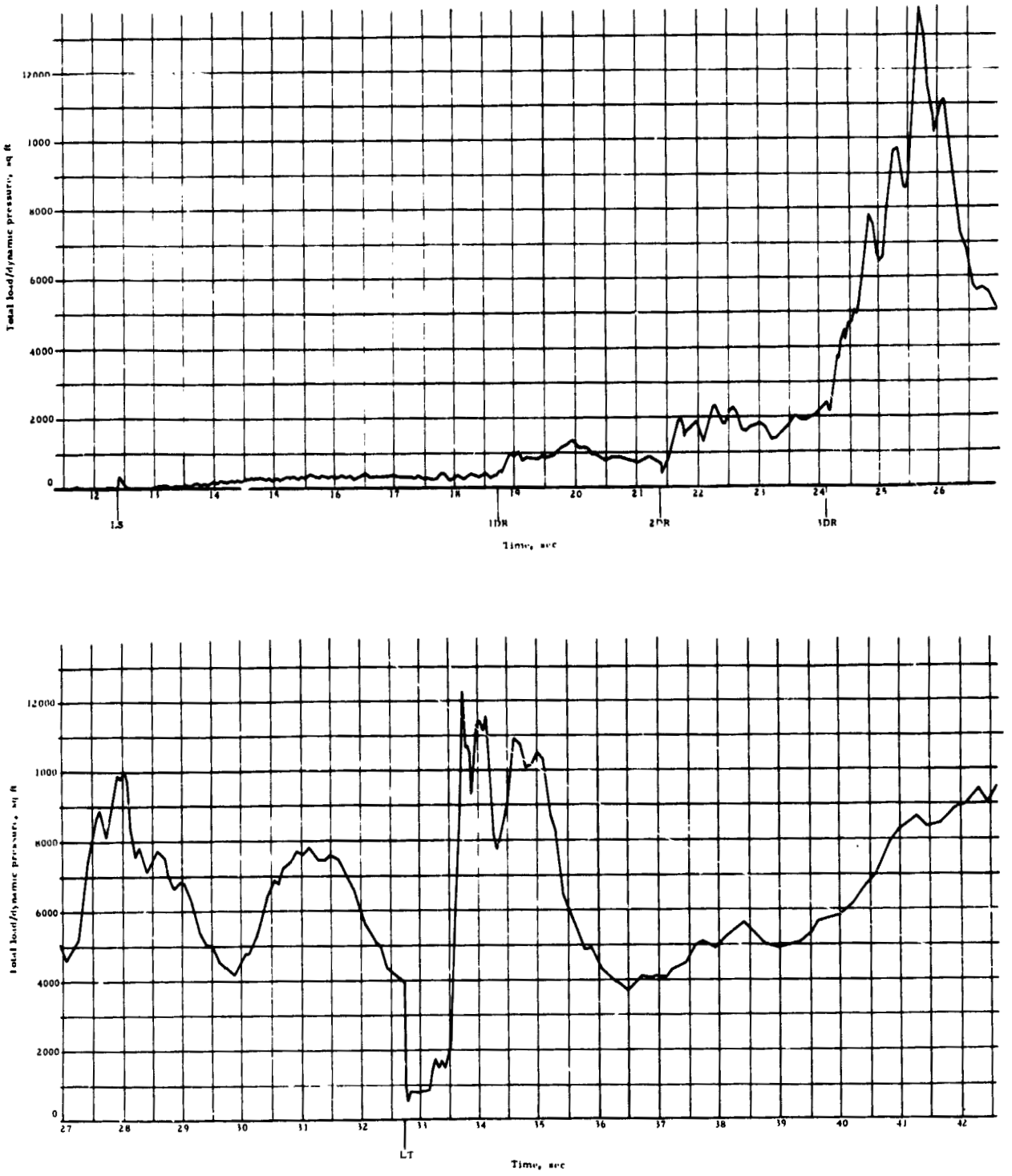

Figure 65. Total parawing load/dynamic pressure versus time from launch, twin keel parawing, Test 253T

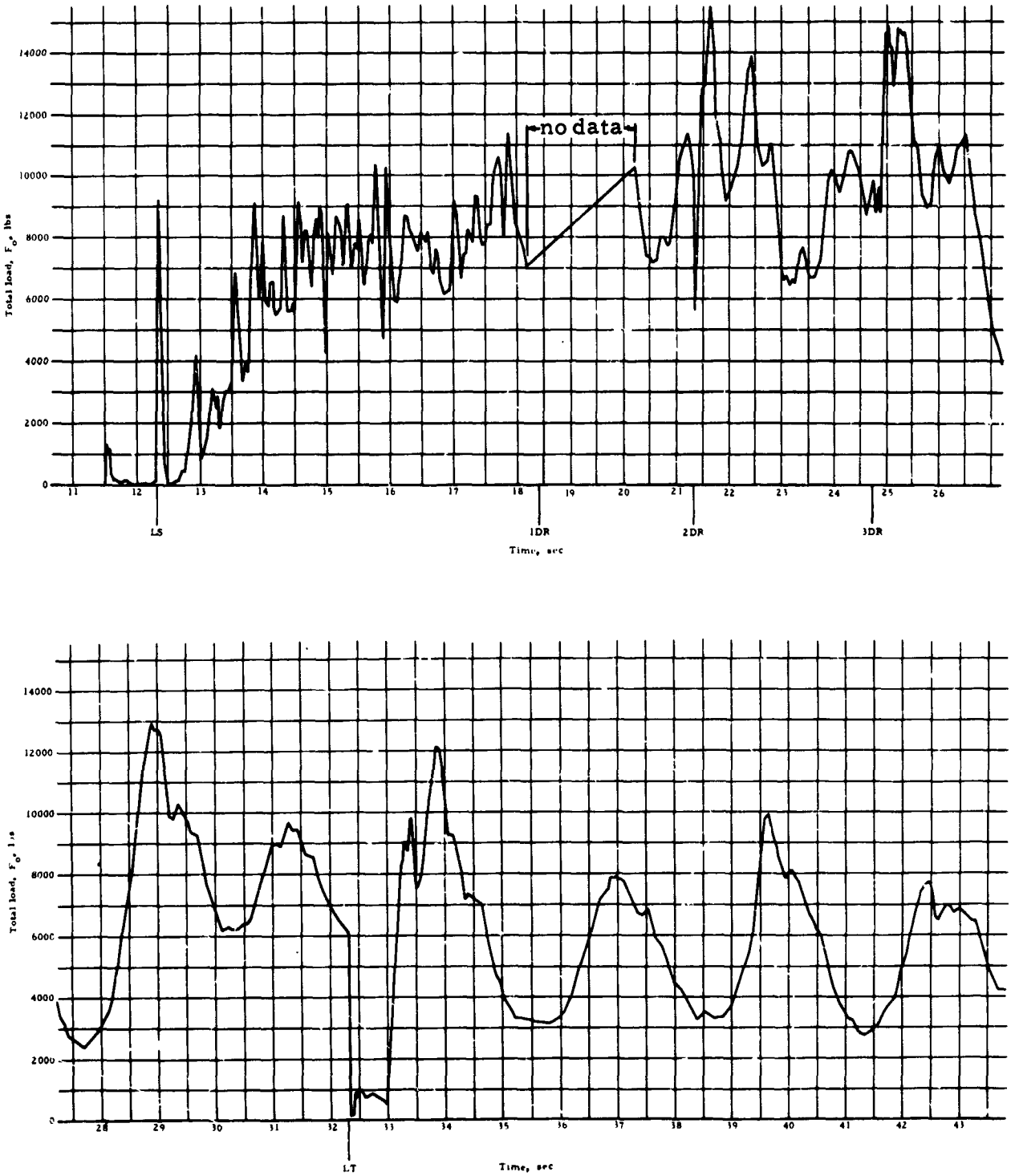

Figure 66. Total parawing load versus time from launch, twin keel parawing, Test 254T

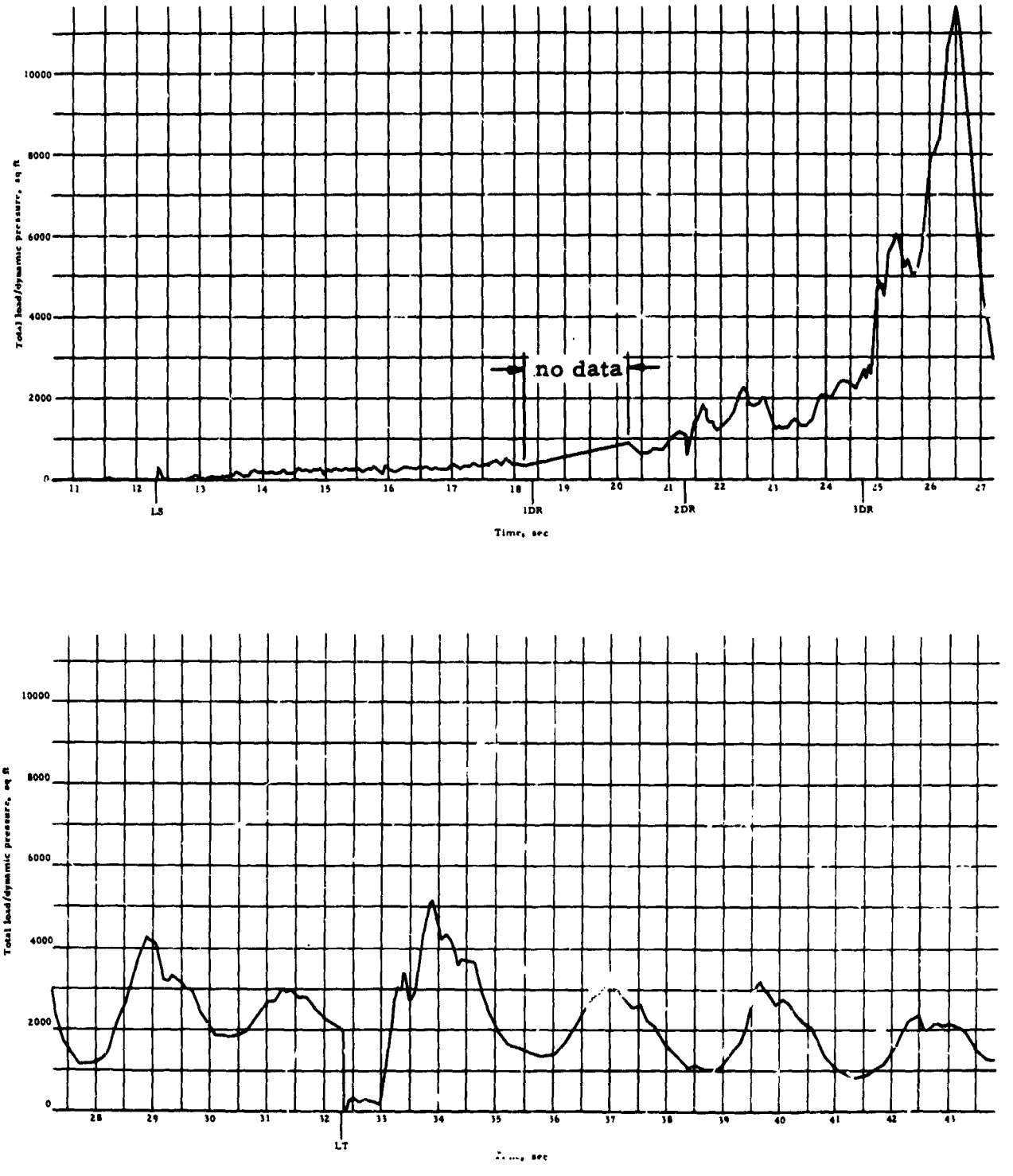

Figure 67. Total parawing load/dynamic pressure versus time from launch, twin keel parawing, Test 254T

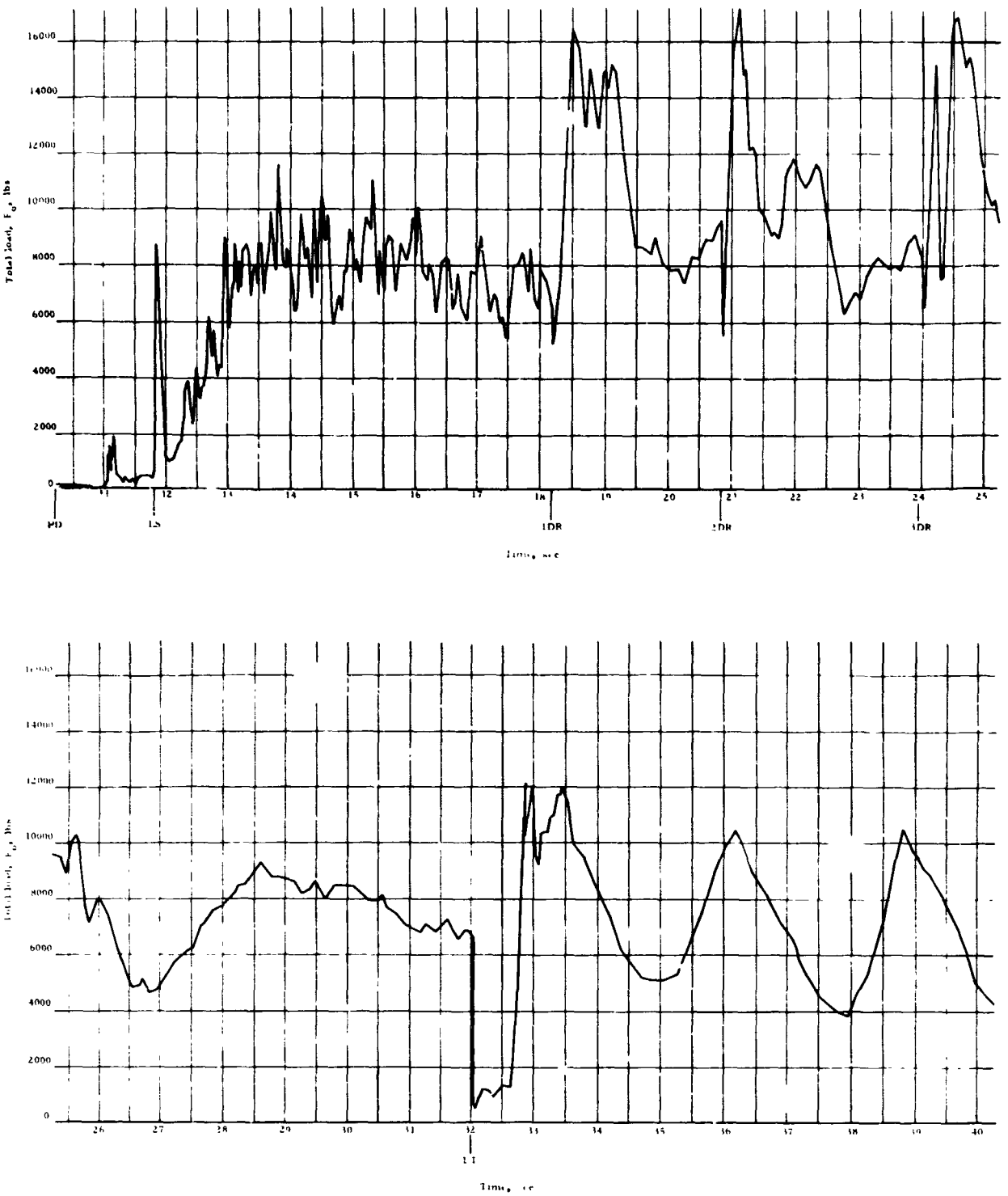

Figure 68. Total parawing load versus time from launch, twin keel parawing, Test 255T

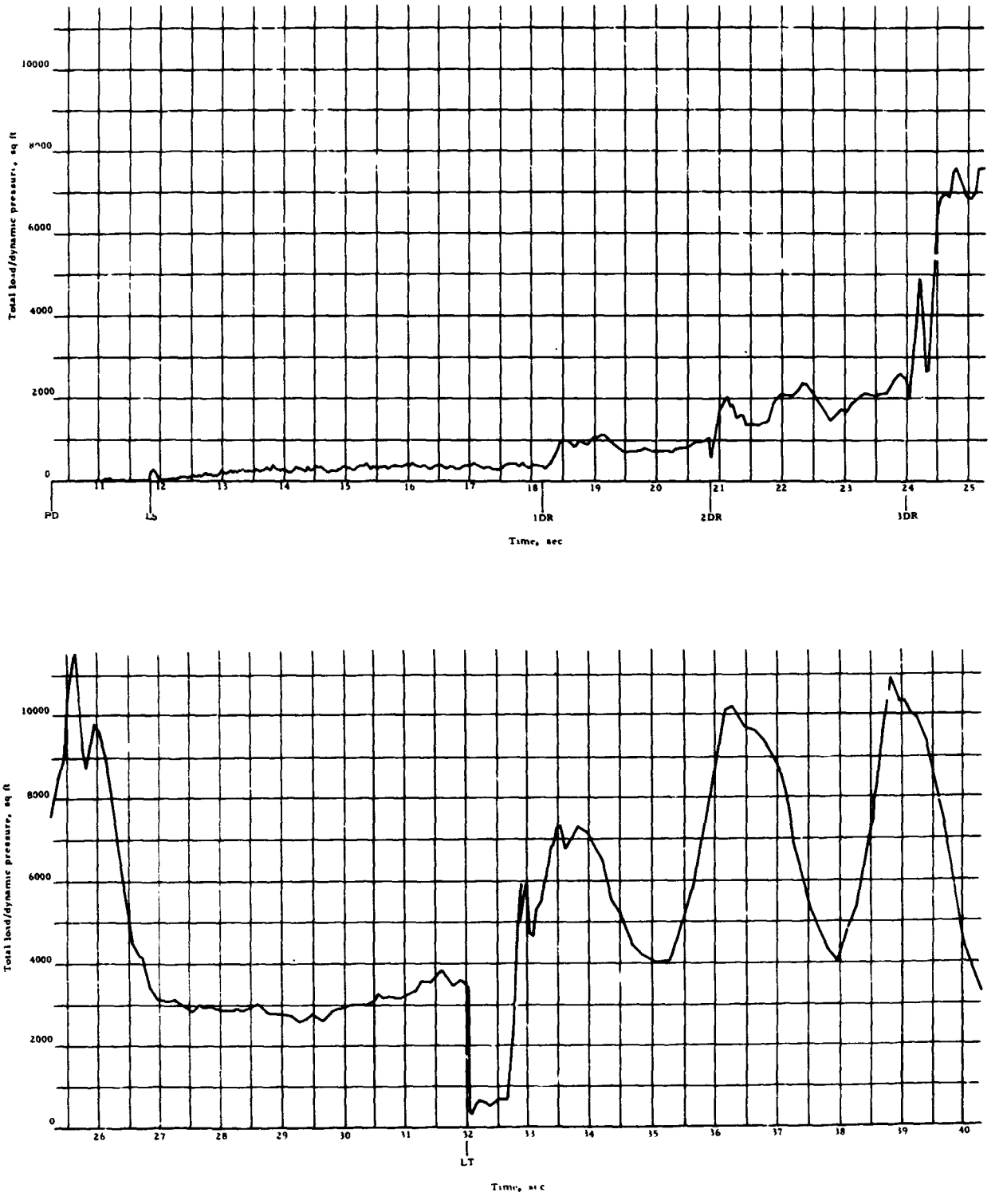

Figure 69. Total parawing load/dynamic pressure versus time from launch, twin keel parawing, Test 255T

Table 5 presents a summary of the deployment data obtained during the intermediate-scale test program. The table lists the following information for each test:

a. Descent weight, W_D, and suspended weight, W_S

b. Type and percent reefing

c. Peak deceleration ratio, G, at line stretch and during each stage, calculated by dividing the peak stage parawing load, F_o, by the descent weight

d. Reference area, $C_R S_W$, during each deployment stage. The values were obtained from the total load/dynamic pressure plots

e. Dynamic pressure, q, at line stretch, at first, second and third stage disreef, and at line transfer

f. Identification of anomalies, if any, that occurred during the test.

As noted in Table 5, the single keel parawings in the two bomb-type vehicle tests utilized 11.6 and 12.0 percent first-stage reefing. The twin keel parawings in the bomb-type vehicle tests utilized 8, 10 and 14 percent first-stage reefing, and the twin keel parawings in the controllable-vehicle tests utilized 10 percent first-stage reefing. Figure 70 presents a plot of first-stage reference area, $C_R S_W$, versus percent reefing for all twin keel parawing tests, except for Tests 206T, 208T, 211T and 251T. These tests were not included for the reasons noted in Table 5. The curve shown in Figure 70 is drawn through the average $C_R S_W$ value for the bomb-type vehicle tests, at each reefing pertentage. The average $C_R S_W$ value for 8 percent reefing is 295 ft^2. For 10 and 14 percent reefing these values are 355 and 400 ft^2, respectively. The $C_R S_W$ values for the controllable vehicle tests vary from 280 to 310 ft^2, with an average value of 295 ft^2. The lower average $C_R S_W$ value for these tests, in comparison with the bomb-type vehicle tests, is attributed to the wake produced by the controllable test vehicle.

TABLE 5.- SUMMARY OF INTERMEDIATE-SCALE DEPLOYMENT DATA

Test no.	Descent weight, W_D, lbs	Suspended weight, W_S, lbs.	Reefing system version-1st stage reefing, %	Line stretch, G	q_{LS}, psf	1st stage			2nd stage			3rd stage			4th stage			Full open	
						G	$C_R S_W$, ft^2	q_{1DR}, psf	G	$C_R S_W$, ft^2	q_{2DR}, psf	G	$C_R S_W$, ft^2	q_{3DR}, psf	G	$C_R S_W$ ft^2	q_{LT}, psf	G	$C_R S_W$, ft^2
200S	2868	2561	11.6	3.71	29.4	2.14	300	8.2	2.50	1350	2.1	2.08	2210	1.0	1.43	3760	1.2	2.59	4000
201S	4997	4678	12.0	1.81	32.6	1.76(4)	180(4)	27.5(4)	3.14(4)	500(4)	10.7(4)	2.11(4)	950(4)	5.8(4)	1.52(4)	900(4)	5.0(4)	2.29(4)	3500(4)
200T	2679	2521	A-14	2.91	28.6	2.45	299	9.0	2.12	598	4.7	3.00	1908	1.7	1.73(1)	3120(1)	1.2	2.39	3736
201T	5034	4692	A-10	2.06	32.9	1.95	350	15.1	2.20	735	7.2	3.08	1705	2.8	1.60(2)	4395(2)	1.1(2)	2.11(2)	2300(2)
202T	3792	3444	A-10	2.81	69.6	3.98	400	9.2	1.98	820	4.4	4.01	2580	1.5	1.52	5000	0.8	2.84	2500
203T	3805	3454	A-14	3.17	64.0	5.39	450	9.0	2.86(3)	660(3)	6.9(3)	3.39(3)	1700(3)	2.9(3)	1.52(3)	3150(3)	1.7(3)	4.38(3)	3000(3)
204T	3786	3433	A-14	2.91	49.2	3.32	450	9.2	3.47	960	5.0	3.09	1950	1.9	1.79	3590	1.2	2.39	2500
205T	5031	4678	A-10	2.19	76.3	3.80	375	13.7	2.10	715	6.6	4.56	2745	1.8	1.47	4555	1.1	2.19	2700
206T	5001	4585	C-8	3.15	94.7	3.07(5)	170(5)	38.5(5)	4.26(5)	670(5)	8.5(5)	3.35(5)	1630(5)	3.4(5)	2.92(5)	3160(5)	4.0(5)	4.21(5)	2500(5)
207T	4994	4609	B-16	1.52	37.1	1.90	300	17.8	3.07	740	6.9	2.29	1480	3.3	2.38	2720	4.0	3.23(11)	2700(11)
208T	5024	4668	A-10	2.08	27.5	1.70(9)	245(9)	21.2(9)	3.03(9)	435(9)	12.0(9)	5.77(9)	1935(9)	3.2(9)	1.78(9)	2855(9)	2.8(9)	2.91(9)	2000(9)
209T	3811	3396	B-8	3.40	62.5	3.20	300	15.0	3.43	(6)	(6)	(6)	(6)	9.0(6)	(6)	(6)	1.8(6)	4.33(6)	1600(6)
210T	3813	3394	C-8	4.03	62.1	3.23	290	15.5	3.55	820	5.7	3.27	1560	3.2	2.53	3780	0.9	1.88	2900
211T	6009	5597	B-10	2.30	49.3	2.15(10)	300(10)	25.0(10)	3.60(10)	700(10)	11.1(10)	3.48	1630	4.6	2.23	3890	2.0	2.64	3900
250T	3444	3196	B-10	2.45	53.9	1.95	280	11.0	2.98	780	4.5	3.27	1530	2.6	2.98	2300	1.8	1.78	1500
251T	3977	3637	B-10	2.13	43.3	(7)	(7)	25.8(7)	(7)	(7)	3.3(7)	(7)	(7)	(7)	(7)	(7)	44.8(7)	(7)	(7)
252T	4007	3637	B-10	2.70	23.5	1.73	285	14.6	2.91	780	5.3	2.49	2080	2.6	2.71	2840	1.5	2.47	2000
253T	5011	4638	C-10	3.81	27.8	1.92	300	16.7	2.76	890	7.2	2.61	1740	3.0	2.60	6860	1.0	2.72	6000
254T	6011	5639	C-10	1.52	31.4	1.89	300	18.7	1.72(8)	900(8)	9.4	2.58	1750	3.7	2.48	3700	3.2	?	2000
255T	6014	5639	C-10	1.45	31.0	1.92	310	19.2	2.73	840	9.6	2.86	1860	3.7	2.82	4330	2.0		6500

Notes:

(1) Line transfer occurred before peak load achieved
(2) The left trailing-edge did not disreef at end of third stage
(3) The wing panel between R3 and R3.5 tore from skirt band to keel at time of 1st stage disreef
(4) As the parawing neared or reached first stage reefed inflation, the right lobe split and collapsed. At 0.18 seconds after first stage disreef the left lobe split.
(5) Several holes and large tears occurred during first stage filling
(6) The third stage trailing edge reefing line failed 0.25 seconds after first stage disreef at a dynamic pressure of 9.0 psf. The peak load following this was 6.8 G's.
(7) The right tip and forward riser load transducers failed. Suspension lines twisted throughout deployment phase. Line transfer occurred 0.78 seconds after line stretch.
(8) The peak second stage load was not recorded because a calibrate cycle was run during most of the second stage interval
(9) The left lobe of parawing did not inflate solidly during first stage and did not disreef until end of second stage. The right lobe split at first stage disreef.
(10) A large hole appeared in the right lobe during first stage loading
(11) Long tip suspension lines render this test unrepresentative after line transfer

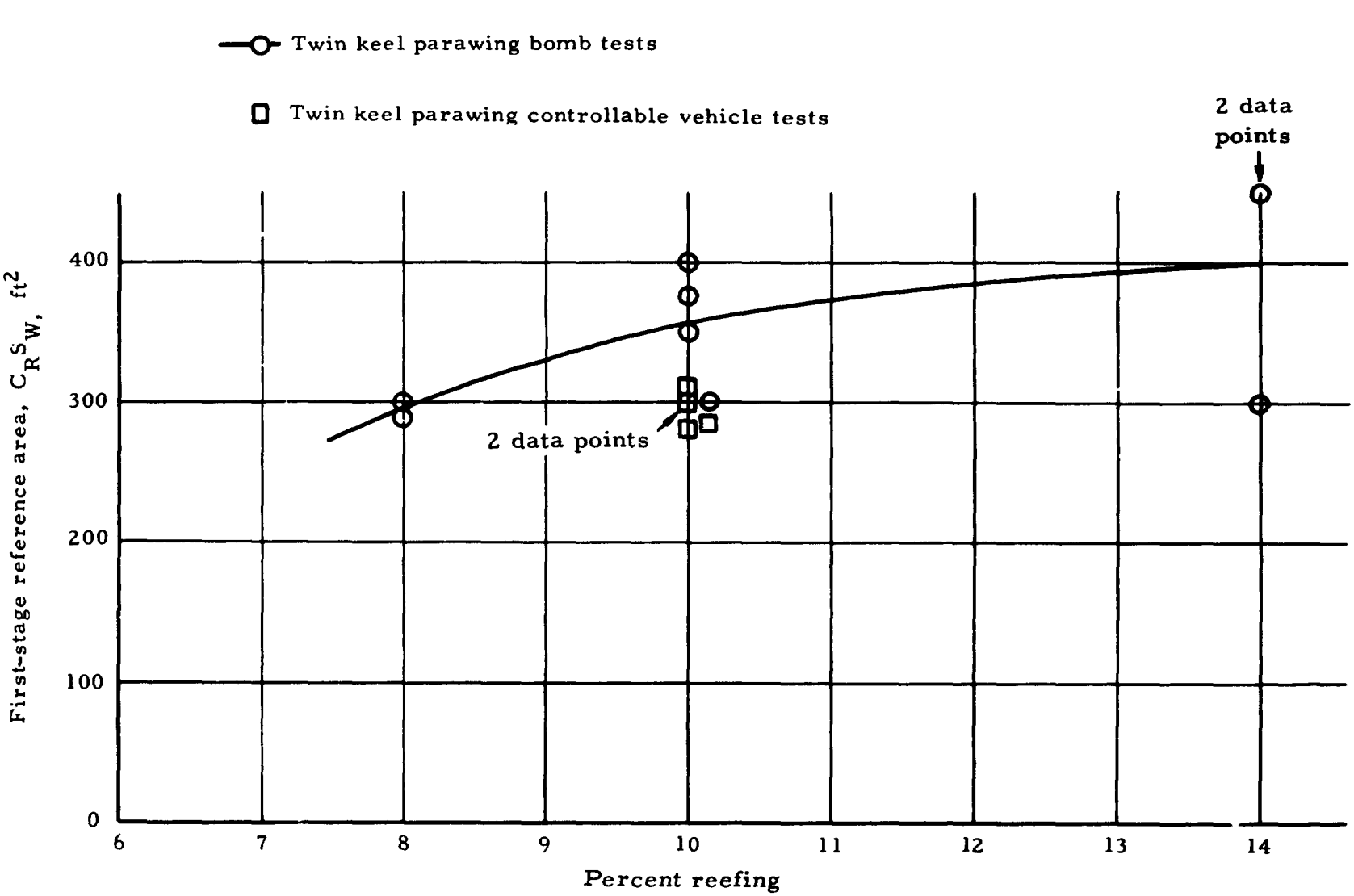

Figure 70. First-stage reference area versus percent reefing

Figure 71 presents a plot of first-stage resultant force coefficient versus percent reefing for the twin keel parawing intermediate-scale free flight tests, small-scale free flight tests and small-scale wind tunnel tests. Test points shown for the intermediate-scale bomb and controllable vehicle free flight tests are the same as those presented in Figure 70, with a solid line fairing through the bomb-type vehicle test data. The dashed line curve shown in Figure 71 is faired through the small-scale bomb-type vehicle test data that extend from about 15 through 22 percent reefing. The curve for the small-scale wind tunnel tests extends from about 10 through 22 percent reefing and was taken from Reference 1. Comparison of the three curves shows that the first-stage resultant force coefficient data were reasonably consistent in the three different phases of testing.

The peak deceleration ratio, G, for each reefing stage of each test, as presented in Table 5, is plotted in Figure 72. Review of Figure 72 shows:

a. The G values for first stage range between 3.0 and 4.0 for tests conducted at the higher line stretch dynamic pressures. The G value of 5.39 for Test 203T appears abnormally high when compared with other tests conducted at similar conditions.

b. Second-stage G values are about 3.0 or less, except for the two tests conducted at 8 percent reefing (209T and 210T) plus Test 204T. The 3.47 value for Test 204T appears high.

c. Two third-stage G values were over 4.0 (Tests 202T and 205T); all others were less than 3.3. Both Tests 202T and 205T utilized reefing Version A where the nose was not reefed. Reefing Version A allowed the third stage to inflate to a larger reference area than for reefing Versions B and C where the nose was reefed.

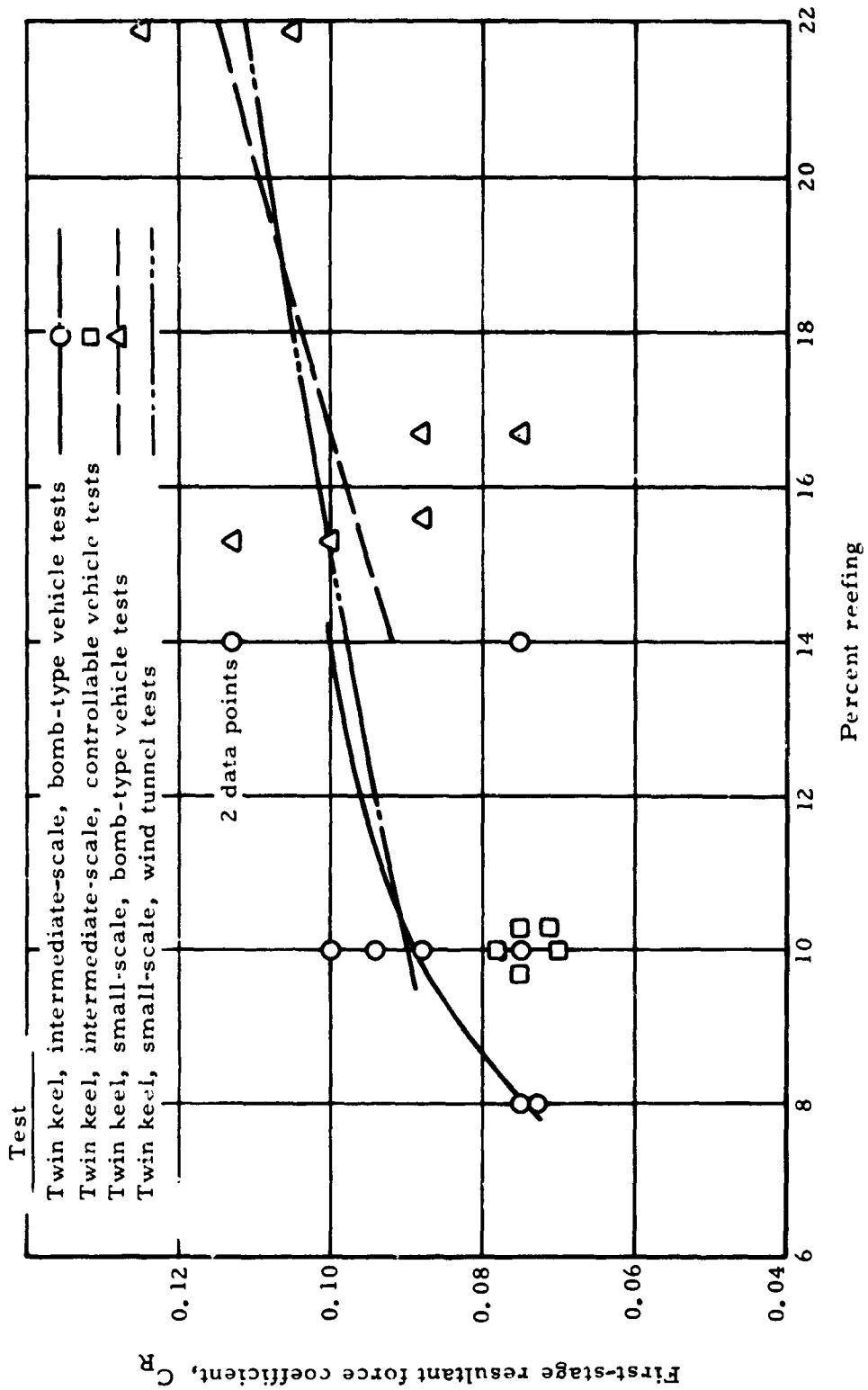

Figure 71. First-stage resultant force coefficient versus percent reefing for twin keel parawing, intermediate and small-scale tests

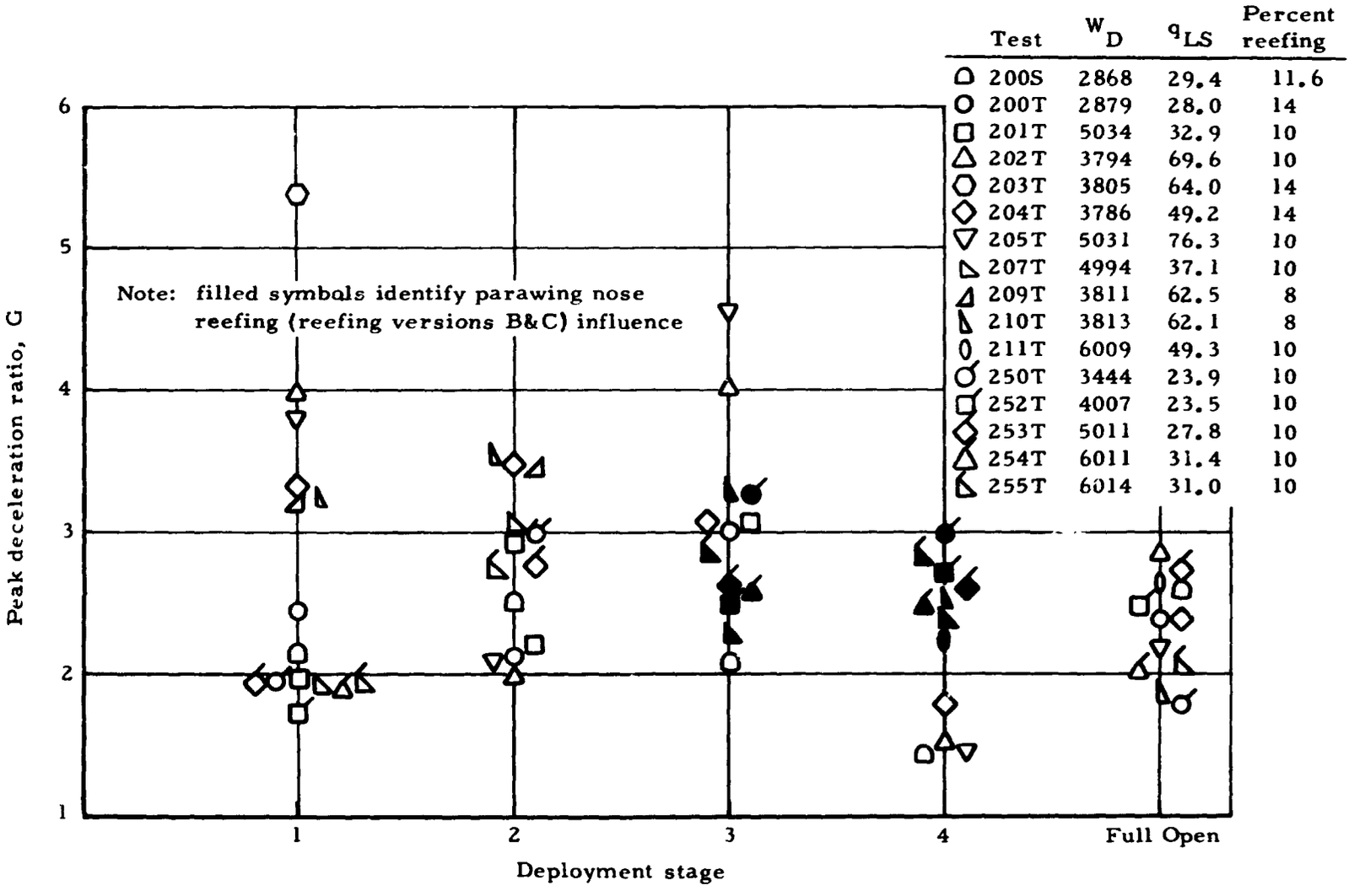

Figure 72. Peak deceleration ratio, G, versus deployment stage

d. All tests that used reefing Version A (larger third stage reference area) developed fourth-stage loads that were less than 2.0 G's. Tests that utilized reefing Versions B or C developed larger loads, but these loads were less than 3 G's in all cases.

e. All full-open loads were less than 3 G's.

Thus, it may be concluded that the first-stage G values were limited to a maximum of 4 G's with 10 percent reefing and deployment dynamic pressures of 76 psf or less. Second-stage G values were about 3.0 G's or less, except for Test 204T and for tests where 8 percent reefing was used (8 percent reefing resulted in higher dynamic pressure at first-stage disreef). For tests where nose reefing was used, all third-stage G values were less than 3.3 G's. Fourth-stage and full-open G values were less than 3.0 in all tests.

Figure 73 presents a plot of first-stage peak deceleration ratio, G, versus dynamic pressure at line stretch for the intermediate-scale bomb tests. The fairings shown in Figure 73 represent 8, 10 and 14 percent reefing and were drawn through the data points from tests that were conducted at these reefing percentages on a "best fit" basis. In general, Figure 73 shows that G load increases with dynamic pressure with each of the reefing percentages used in test. However, the number of tests conducted at the same reefing percentage and descent weight is considered insufficient to firmly establish the fairings shown. Previous experience with parachute-type decelerators indicates that the slopes of the fairings should decrease with increasing dynamic pressure.

In order to compare the loads data from tests conducted at various descent weights, reefing ratios and dynamic pressures at event initiation, an empirical method utilizing the load factor, C_K, was employed. In this empirical method, load factor is defined as:

$$C_K = \frac{G\, W_D}{(C_R S_W)_q}$$

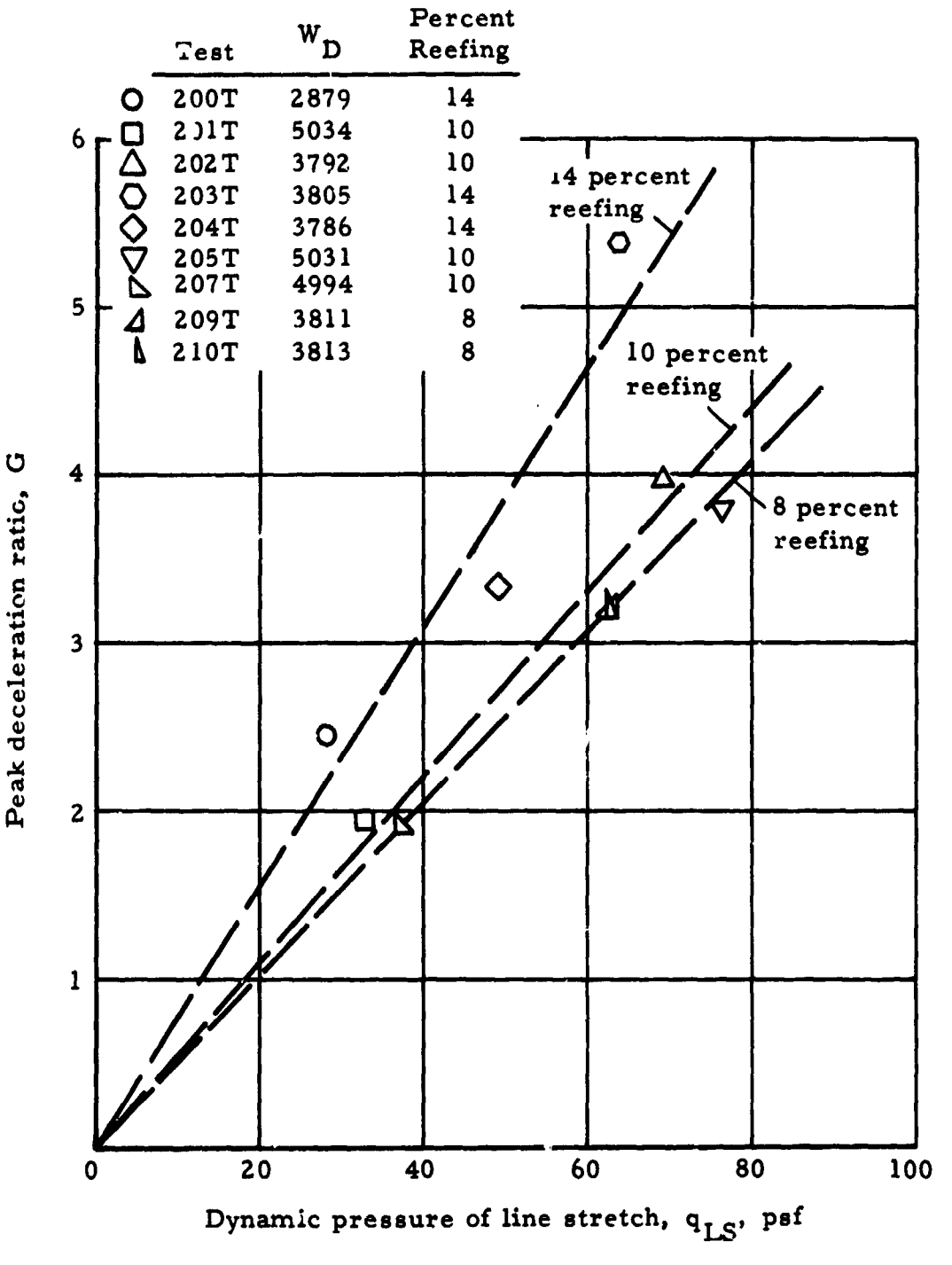

Figure 73. First-stage peak deceleration ratio versus dynamic pressure at line stretch

This factor relates the peak total parawing load, G W_D, for each stage to the reference area, $C_R S_W$, and the dynamic pressure, q, at the start of the reefing stage under consideration. The load factor, C_K, is the ratio of the actual peak force during an opening process to the force that would have been generated, had there been no velocity decay during the opening process and had the force been equal only to the product of reference area and dynamic pressure. The load factor also includes the effect of velocity decay during the opening process and the dynamics of the opening process.

The data required to calculate load factor for each test are presented in Table 5. The load factors computed from these data are tabulated in Table 6. Inherent limitations in ASKANIA phototheodolite measurements of space position, velocity, and acceleration during periods of rapid velocity change make computations of reference area difficult. Therefore, in the calculation of C_K, average reference areas, $(C_D S_W)_{AVE}$, based on the results of all applicable tests of the same reefing configuration, were used. In addition to load factors, Table 6 presents a summary of these average reference areas and canopy loadings, $W_D/(C_D S_W)_{AVE}$, for each test. Data from tests where structural failures or anomalies occurred during deployment are not included. First stage $(C_R S_W)_{AVE}$ values were calculated for the twin-keel parawing, bomb-type vehicle tests at each reefing ratio. Since only one reefing ratio (10 percent) was used for the controllable vehicle tests, the average $C_R S_W$ value shown is based on all tests of this type. Since second-stage reefing was essentially the same for all twin keel parawing tests, the average reference area shown is an average from all tests. Third-stage values were calculated in two groups -- tests that utilized nose reefing, and tests that did not. Average reference areas for the fourth stage and for the full-open stage were calculated by using all intermediate-scale, twin keel parawing test data.

TABLE 6. - SUMMARY OF REFERENCE AREA, LOAD FACTOR AND CANOPY LOADING DATA

Test no.	Reefing system version 1st stage reefing, %	Average reference area, $(C_R S_W)_{AVE}$, ft^2					Load factor, C_K					Canopy loading, $W_D/(C_R S_W)_{AVE}$, lbs/ft^2				
		1st stage	2nd stage	3rd stage	4th stage	Full open	1st stage	2nd stage	3rd stage	4th stage	Full open	1st stage	2nd stage	3rd stage	4th stage	Full open
200S	11.[illegible]	300	1350	2210	3760	4000	0.696	0.648	1.285	1.091	1.548	9.56	2.12	1.30	0.76	0.72
201S	12	(1)	(1)	(1)	(1)	(1)	(1)	(1)	(1)	(1)	(1)	(1)	(1)	(1)	(1)	(1)
200T	A-14	400	790	2175	(1)	3245	0.630	0.8[illegible]80	0.845	(1)	1.767	7.20	3.64	1.32	(1)	0.88
203T	A-14	400	(1)	(1)	(1)	(1)	0.801	(1)	(1)	(1)	(1)	9.51	(1)	(1)	(1)	(1)
204T	A-14	400	790	2175	3960	3245	0.639	1.714	1.076	0.901	2.324	9.46	4.79	1.75	0.96	1.17
201T	A-10	355	790	2175	(1)	(1)	0.840	0.928	0.990	(1)	(1)	14.18	6.37	2.31	(1)	(1)
202T	A-10	355	790	2175	3960	3245	0.611	1.033	1.589	0.970	4.14[illegible]	10.68	4.80	1.73	0.96	1.17
205T	A-10	355	790	2175	3960	3245	0.706	0.976	1.598	1.038	[illegible]	[illegible].17	6.37	2.31	1.27	1.55
208T	A-10	(1)	(1)	(1)	(1)	(1)	(1)	(1)	(1)	(1)	(1)	(1)	(1)	(1)	(1)	(1)
207T	B-10	355	790	1700	3960	3245	0.720	1.090	0.975	0.91[illegible]	[illegible]3	14.07	6.32	2.94	1.26	1.53
211T	B-10	(1)	(1)	1700	3960	3245	(1)	(1)	(1)	0.736	2.444	(1)	(1)	3.53	1.52	1.85
209T	B-8	295	(1)	(1)	(1)	(1)	0.661	(1)	(1)	(1)	(1)	12.92	(1)	(1)	(1)	(1)
206T	C-8	(1)	(1)	(1)	(1)	(1)	(1)	(1)	(1)	(1)	(1)	(1)	(1)	(1)	(1)	(1)
210T	C-8	295	790	1700	3960	3245	0.672	1.105	1.287	0.761	2.453	12.92	4.82	2.24	0.96	1.18
250T	B-10	295	790	1700	3960	3245	0.953	1.181	1.472	0.997	1.050	11.67	4.36	2.03	0.87	1.06
251T	B-10	(1)	(1)	(1)	(1)	(1)	(1)	(1)	(1)	(1)	(1)	(1)	(1)	(1)	(1)	(1)
252T	B-10	295	790	1700	3960	3245	1.000	1.011	1.107	1.055	2.033	13.58	5.07	2.36	1.01	1.23
253T	C-10	295	790	1700	3960	3245	1.173	1.048	1.069	1.097	4.200	16.99	6.34	2.95	1.27	1.54
254T	C-10	295	(1)	1700	3960	3245	1.226	(1)	0.970	1.017	1.247	20.38	(1)	3.54	1.52	1.85
255T	C-10	295	790	1700	3960	3245	1.[illegible]63	1.082	1.054	1.157	1.872	20.39	7.61	3.54	1.52	1.85

Notes

(1) Because of structural failure or anomalies during deployment, this test was not used in calculation of average-reference area, load factor or canopy loading.

The load factor (C_K) and the canopy loading, $W_D/(C_R S_W)_{AVE}$, for each stage and for each intermediate-scale test were presented in Table 6. The load factor method may be used to predict loads by using the relation:

$$F_o = C_K \, (C_R S_W)_{AVE} \, q,$$

provided the relationship between C_K and descent weight, reefing ratio, and dynamic pressure is known. Extensive work with parachute-type flexible decelerators has established that a consistent correlation exists between load factor, unit canopy loading, and initial dynamic pressure, for a given decelerator configuration. The general method of presenting this correlation is a plot of load factor, C_K, versus unit canopy loading, $W_D/C_R S_W$, with dynamic pressure (or equivalent velocity) as an independent parameter. Typical load factor plots for ringsail parachutes are presented in Reference 2. Figure 74 presents such a plot for the intermediate-scale parawing first stage. For the bomb-type vehicle tests, constant line-stretch-dynamic-pressure lines from 30 to 100 psf are shown as solid lines. The controllable vehicle tests were conducted at line-stretch-dynamic-pressure values that varied over a small range (23.9 to 31.4 psf) or at an average of about 28 psf. A dashed line for this average value is also shown in the plot. This dashed line is independent of the solid lines and pertains only to the controllable vehicle tests. The higher C_K values for these tests is attributed to a controllable vehicle wake effect. The value shown following each test number is the dyanmic pressure at parawing line stretch for that test.

The slope and spacing of the constant dynamic-pressure lines are based on the data that are plotted. Except for infinite mass cases, past experience has shown that load factor decreases with increasing dynamic pressure at any constant unit canopy loading. This same effect is seen for the data plotted in Figure 74.

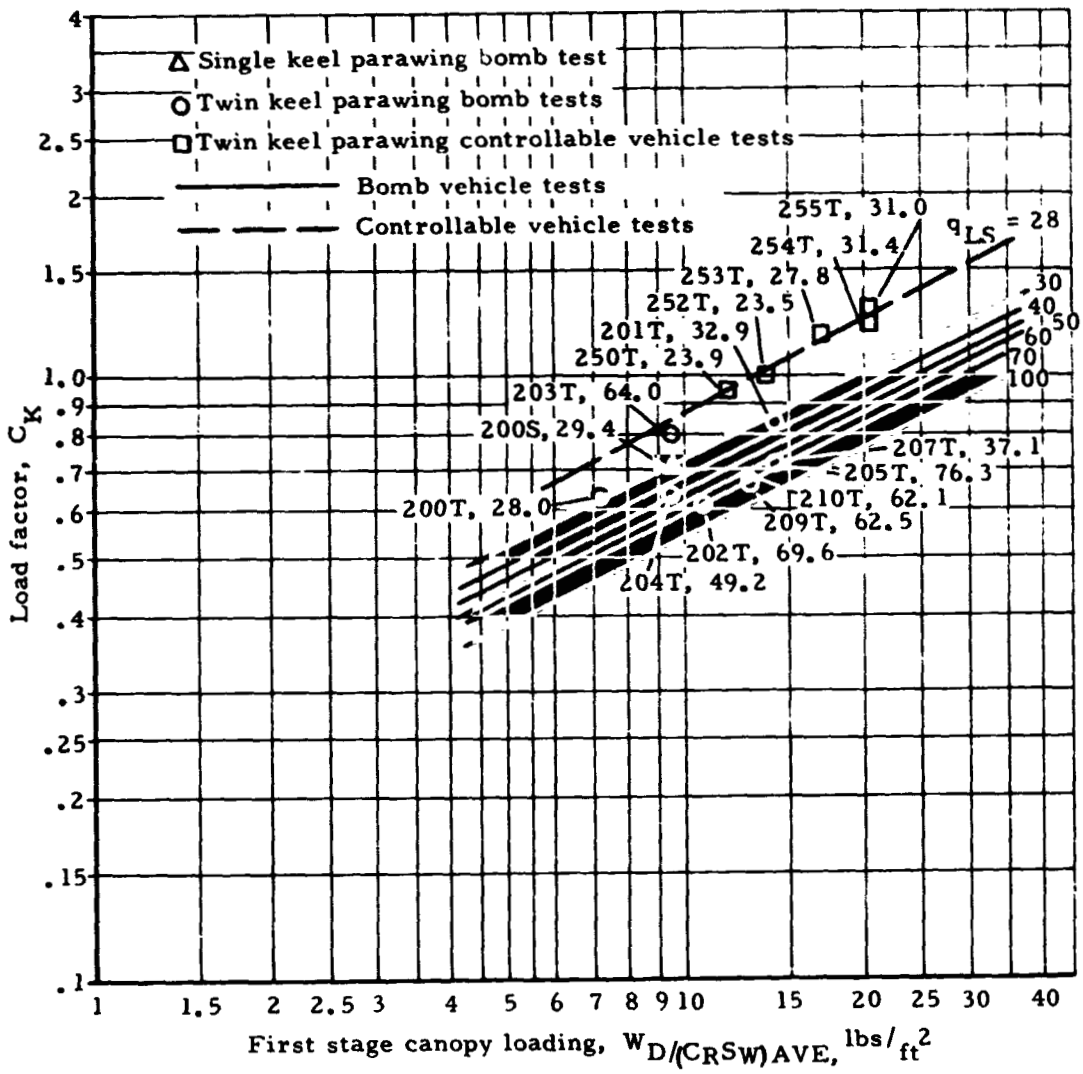

Figure 74. Load factor versus canopy loading, first stage

Review of the data indicates that there is good agreement among tests, and that the load factor method for predicting first-stage parawing loads is usable. The C_K values from the twin-keel parawing, controllable vehicle tests were about 22 percent higher than those from the bomb-type vehicle tests.

Figures 75 and 76 present plots of load factor (C_K) versus second- and third-stage canopy loading, respectively. Examination of the plot for the second stage indicates that there is, as for the first stage, a controllable-vehicle wake effect. As the parawing opens into third stage, this effect appears to be small. Because of the greater variability of opening during the second and third stage, the data did not follow as consistent a pattern as the data for the first stage. The two highest calculated C_K values for the third stage were from Tests 202T and 205T. The third-stage G loads for these tests, which utilized reefing Version A (without nose reefing) were also the highest values of all the applicable tests (see Figure 72).

Figure 77 presents plots of peak deceleration ratio, G, versus canopy loading for the fourth-reefed stage and for full open. For the fourth stage, a small controllable-vehicle wake effect is still evident. The G values appear to decrease with increasing canopy loading. All tests that utilized reefing Version A (larger third-stage reference area than for reefing Versions B and C) resulted in a lower dynamic pressure at third-stage disreef and a correspondingly lower fourth-stage load. The highest fourth-stage load measured was in Test 250T, where the value was 2.98 G. For full open, a controllable-vehicle-wake effect does not appear to exist. The G values decrease with increasing canopy loading and the highest G value (2.85) was recorded during Test 202T.

Figure 78 presents a plot which shows the ratio of parawing snatch load to descent weight versus $(C_D S)_p^{3/4} q_{LS}/W_D$ for the twin

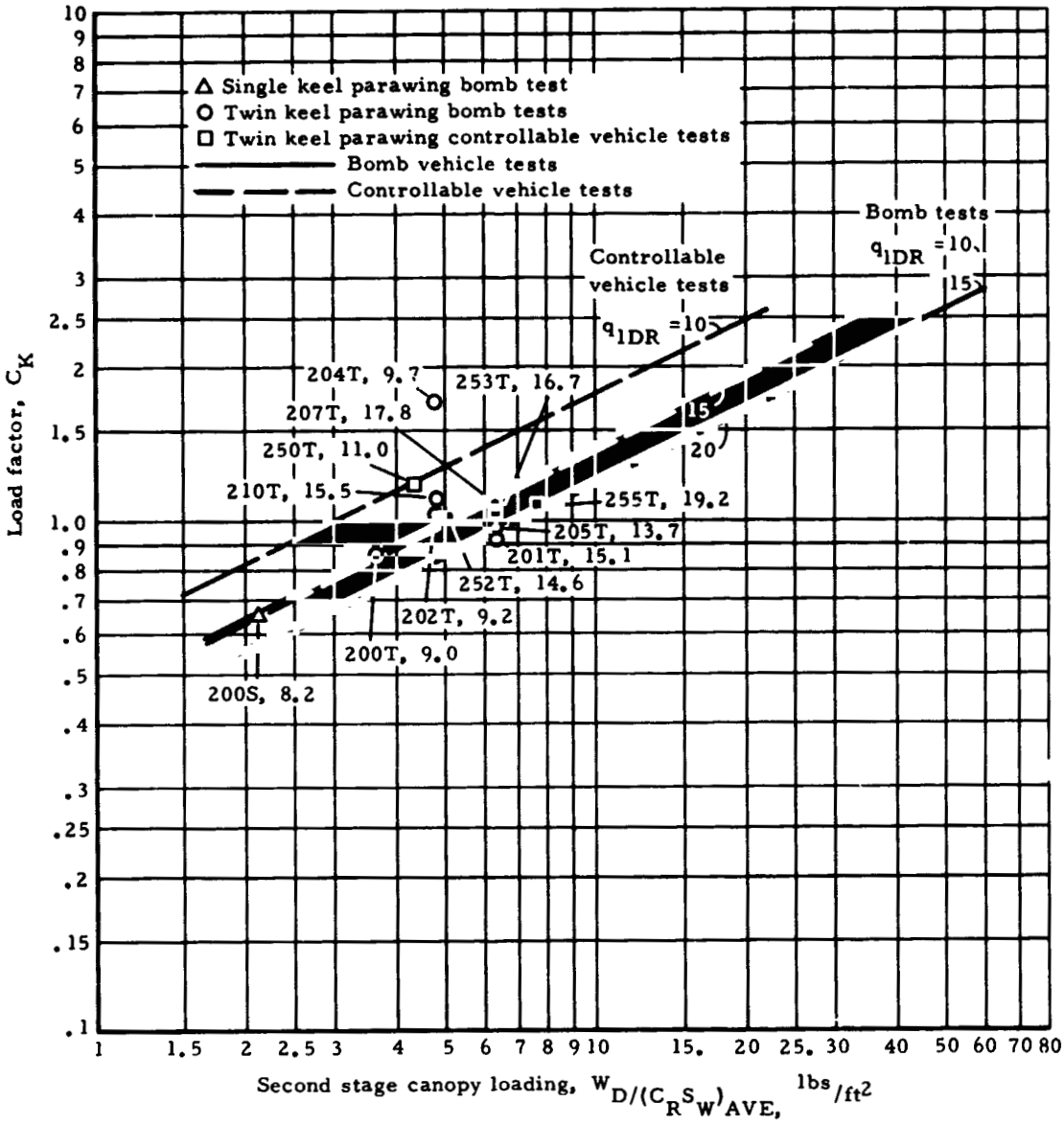

Figure 75. Load factor versus canopy loading, second stage

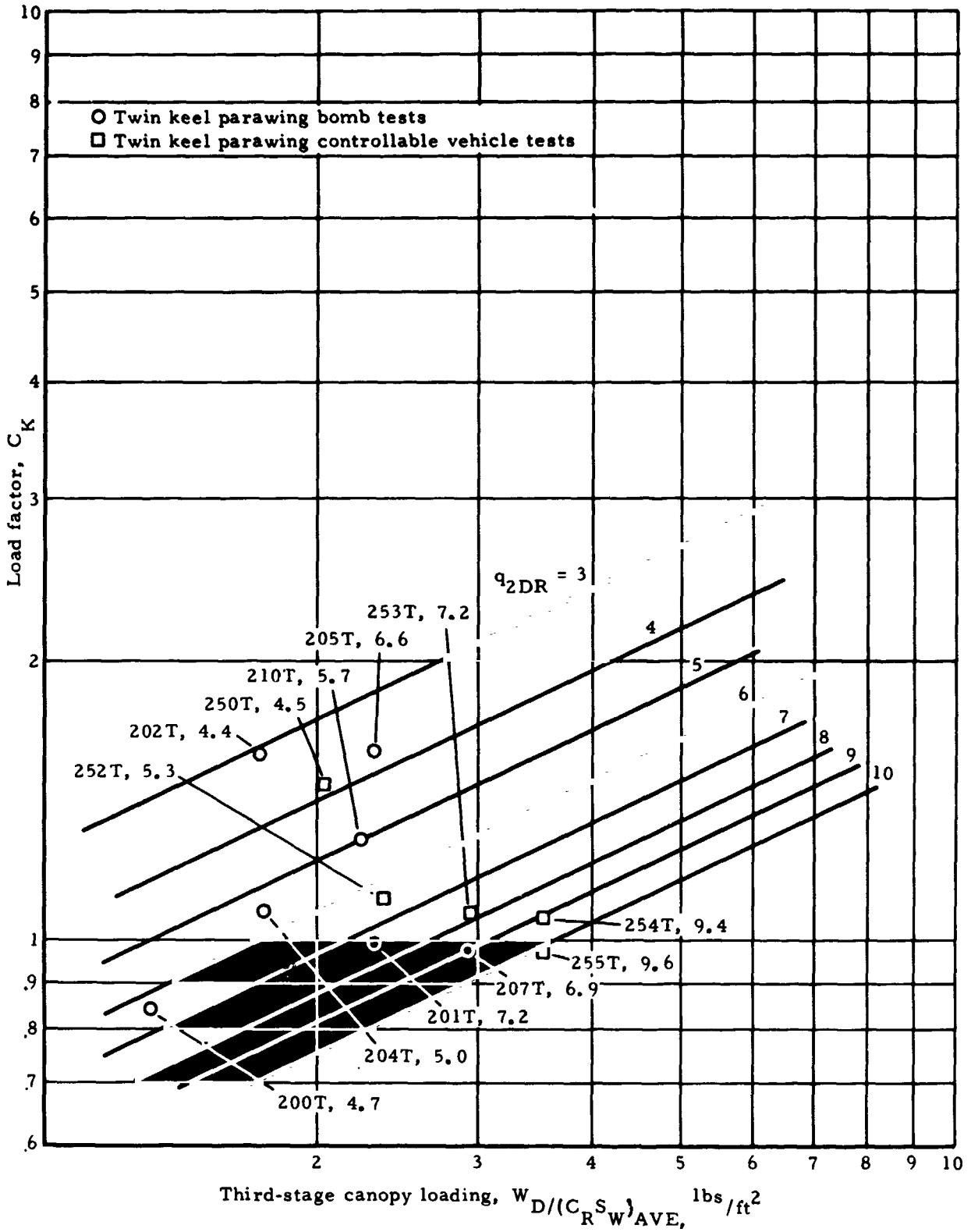

Figure 76. Load factor versus canopy loading, third stage

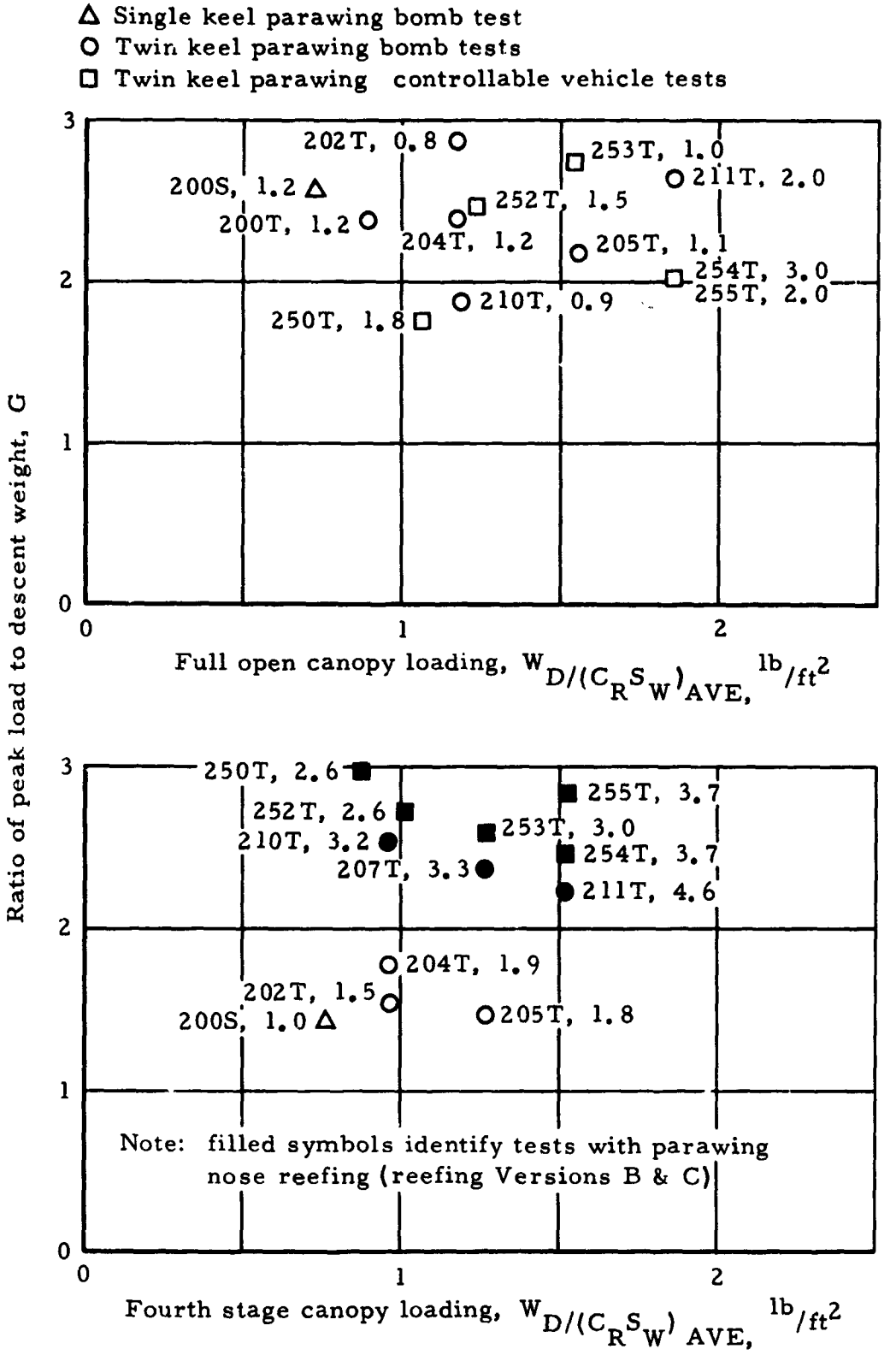

Figure 77. Ratio of peak load to descent weight versus canopy loading, fourth stage and full open

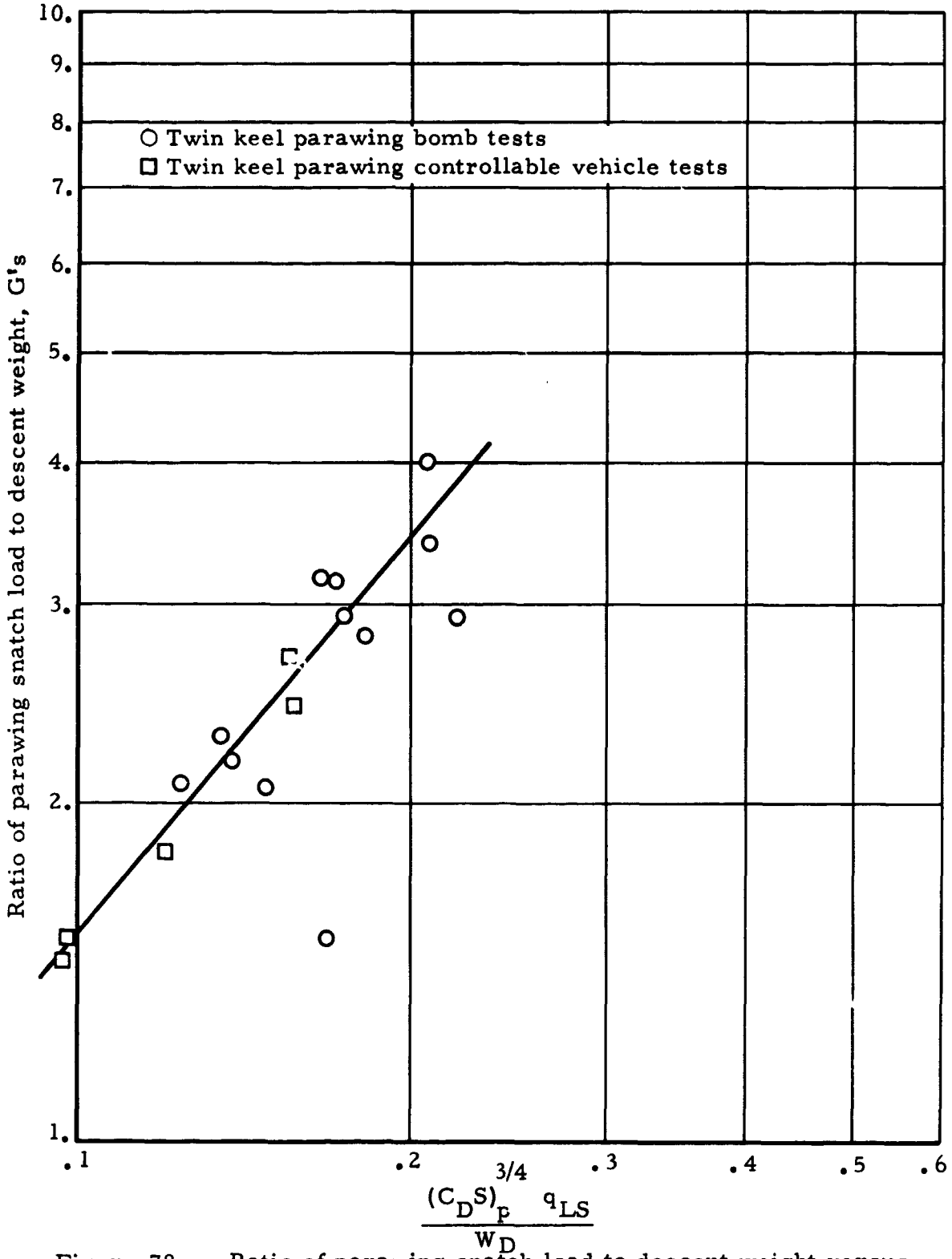

Figure 78. Ratio of parawing snatch load to descent weight versus $(C_D S)_p^{3/4} q_{LS}/W_D$

keel parawing tests. Snatch load varies as the difference in velocity at line stretch between the parawing and the vehicle, times the square root of the product of the parawing spring constant and the parawing mass. For all twin keel parawing tests, the spring constant and mass were essentially constant. The difference in velocity between the parawing at line stretch and the vehicle is a function of the drag area of the pilot parachute(s), $(C_DS)_p$, and the dynamic pressure during the deployment process. Figure 78 shows that if this differential velocity is represented by $(C_DS)_p^{3/4} q_{LS}$, correlation with snatch load is good. Figure 78 also shows that snatch load can be maintained at or near the 3 G level. The two tests that exceeded this level were Tests 209T and 210T where snatch loads of 3.4 and 4.0 G's, respectively, were measured. For these tests, the product of $(C_DS)_p q_{LS}$ produced a parawing-pack-extraction force of nearly 5 G's. Since past experience indicates that a parawing-pack-extraction force of 4 to 4.5 G's, computed in this manner, is sufficient for parawing deployment, the two high snatch loads could have been reduced to near the 3 G level by reducing the drag area of the pilot chute. The empirically derived equation for the line faired through the data in Figure 78 is:

$$G = 22.44 \left[(C_DS)_p^{3/4} q_{LS}/W_D\right]^{1.166}$$

Scale Point Tests

As identified in the subsection entitled INTERMEDIATE-SCALE TEST PROGRAM RATIONALE, four categories of parawing tests were conducted on the bomb-type test vehicle. Of prime importance in a discussion of first-reefed-stage loads are the scale point tests and the deployment demonstration tests. The deployment demonstration tests, in addition to providing intermediate-scale parawing deployment demonstrations at selected points in the prescribed

deployment envelope, also served as end point tests. That is, they were tests conducted at test point conditions to which certain of the small-scale parawing tests had been scaled. Thus, these tests served as bases for comparing the results of small-scale parawing tests scaled to those intermediate-scale end point conditions.

On the other hand, the scale point tests were intermediate-scale parawing tests scaled to full-scale parawing end point conditions. These tests provided information on the anticipated performance of a full-scale parawing system at selected end point conditions. The validity of this information and data is a function of the scaling method used and how well it could be followed to establish the simulated test conditions. The scaling method applied in the parawing program is presented in Reference 1.

Table 7 provides a comparison of the planned test conditions for intermediate-scale, twin keel, end-point-demonstration tests and the planned test conditions for intermediate-scale, twin keel scaled tests for full-scale parawing end point simulation.

Several twin keel, end-point-demonstration tests were conducted using a 5000 pound descent weight. However, none of the tests that resulted in usable data were conducted at the exact conditions shown in Table 7 and at a first-stage reefing ratio that would permit direct comparison with the small-scale parawing tests that had been scaled to intermediate-scale test conditions. The line-stretch dynamic pressure for Test 205T was 76.3 psf, the test altitude was about 14,000 ft and the first-stage reefing ratio was 10 percent. This test closely simulates Test 102T, except for reefing ratio. The first-stage reefing ratio for Test 102T was 21.9 percent. A comparison of these tests is possible, if actual test conditions are corrected to scaled values and to the same reefing ratio. Since 14 percent was the smallest reefing ratio used during small-scale testing and the largest used during

TABLE 7. - INTERMEDIATE-SCALE, TWIN KEEL END POINT TEST CONDITIONS AND TEST CONDITIONS FOR FULL-SCALE PARAWING SIMULATION

Parameter	Intermediate-scale end point conditions of small-scale simulation	Intermediate-scale conditions for full-scale simulation	Full-scale end point conditions for intermediate-scale simulation
Parawing canopy area, ft^2	4,000	4,000	10,000
q_{LS}, psf	70	44.3	70
W_D, lbs	5,000	3,795	15,000
Altitude, ft	18,000	18,000	18,000
Parawing canopy area, ft^2	4,000	4,000	10,000
q_{LS}, psf	100	63.3	100
W_D, lbs	5,000	3,795	15,000
Altitude, ft	18,000	18,000	18,000

intermediate-scale testing, it is possible to extrapolate both sets of data to this point. For the intermediate-scale tests, the relationship between parawing load and reefing ratio may be determined from Figure 74. This figure presents load factor, C_K, as a function of canopy loading and line stretch dynamic pressure, for all tests. The relationship that has been established between the parawing first-stage average reference area, $(C_R S_W)_{AVE}$, and reefing ratio (Figure 70), permits calculation of canopy loading and thus, the load for 14 percent reefing. The following illustrative computations identify the end point conditions, and the method of calculating the first stage intermediate-scale load that simulates small-scale Test 102T. Test 205T is the intermediate-scale reference test.

$$G = C_K (C_D S_W)_{AVE} \, q_{LS}/W_D$$

C_K = 0.66, as determined from Figure 74 for a

$W_D/(C_R S_W)_{AVE}$ = 5000/400 = 12.5 lb/ft^2 and a q_{LS} of 70 psf.

$(C_D S_W)_{AVE}$ = 400 ft^2 for 14 percent reefing (Figure 70)

q_{LS} = 70 psf, which is an end point condition.

$G = 0.66 \ (400) \ 70/5000 = 3.7$

The corresponding load for Test 102T is:

$$G = C_K \ (C_D S_W)_{AVE} \, q_{LS}/W_D$$

C_K = 0.52, as corrected to 14 percent reefing in Reference 1.

$(C_D S_W)_{AVE}$ = 40 ft^2

q_{LS} = 35 psf

W_D = 254 lbs

$G = 0.52 \ (40) \ 35/254 = 2.9.$

The previous computations show that the intermediate-scale load is about 28 percent higher than the small-scale load. A small portion (two to three percent) of the difference between the two may be due to the fact that several of the intermediate-scale bomb-type vehicle type tests were conducted at 14,000 feet, rather than the planned 18,000 feet.

If a similar procedure is used to calculate loads for the second set of end point conditions used in small-scale simulation, as shown in Table 7, the following comparison results:

For intermediate-scale:

$$G = C_K \ (C_D S_W)_{AVE} \, q_{LS}/W_D$$

$G = 0.60 \ (400) \ 100/5000 = 4.8.$

For small-scale:

$$G = 0.52\ (40)\ 50.8/254 = 4.2$$

or

$$G = 0.52\ (40)\ 38/190 = 4.2.$$

For this case the intermediate-scale load is about 15 percent higher than the corresponding small-scale load.

The previous two cases tend to indicate that the scaling method utilized may not be wholly valid. However, the problem could lie in the difficulty in providing test specimens that were alike. The mismatch in the actual test reefing ratios has already been discussed. Even if the reefing ratios had been identical in the small- and intermediate-size scaling tests, the effective inlet mouths may have been different. The intermediate-scale parawings had more reefing rings than the small-scale parawings. Thus, the geometry of the scallops (or cloth folds) around the reefing line periphery were different for these two wing sizes. Since the wing probably fills through these scallops, as well as through the reefing-line-defined mouth area, the effective mouth sizes for the two wing sizes could have been somewhat dissimilar, even at identical reefing ratios. Other factors that could account for the G load differences in the scale point tests are, 1) variations from the prescribed scaled test conditions (descent weight, dynamic pressure, deployment altitude), 2) normal variability of test measurements which could cause apparent differences in results when only the results of a few tests are available, and 3) factors not considered in the scaling method used, such as canopy flexibility, material thicknesses, etc.

Table 8 presents a summary of loads in G's, for each deployment stage, for the following scale point test conditions:

a. Small-scale conditions for intermediate-scale simulation (listed in Table 8 under Small-scale).

TABLE 8.-SUMMARY OF SCALE POINT TESTS

Small-scale	Intermediate-scale	Full-scale

First stage

G	C_K	Reference test no.	Reefing ratio, %	Weight, W_D, lbs	$(C_R S_W)_{AVE.}$, ft^2	$W_D/(C_R S_W)_{AVE.}$, lbs/ft^2	q_{LS}, psf	G	Weight, W_D, lb	$(C_R S_W)_{AVE.}$, ft^2	G	q_{LS}, psf
4.2	.60	–	14	5000	400	12.5	100	4.8				
2.9	.66	–	14	5000	400	12.5	70	3.7				
	.64	205T	10	5000	355	14.1	100	4.5				
	.70	–	8	5000	295	16.9	100	4.1				
	.59	203T 204T	14	3795	400	9.5	61.3	3.9	15,000	1000	3.9	100
	.625	202T	10	3795	355	10.7	61.3	3.7	15,000	887	3.7	100
	.69	209T 210T	8	3795	295	12.9	61.3	3.4	15,000	738	3.4	100
	.645	203T 204T	14	3795	400	9.5	44.3	3.0	15,000	1000	3.0	70
	.68	202T	10	3795	355	10.7	44.3	2.8	15,000	887	2.8	70
	.75	209T 210T	8	3795	295	12.9	44.3	2.6	15,000	738	2.6	70

Second stage

G	C_K	Reference test no.	Reefing ratio %	Weight, W_D lbs	$(C_R S_W)_{AVE.}$, ft^2	$W_D/(C_R S_W)_{AVE.}$, lb/ft^2	q_{1DR}, psf	G	Weight W_D, lbs	$(C_R S_W)_{AVE.}$, ft^2	G	q_{1DR}, psf
2.53	1.09	201T 205T 207T 251T	10	5000	790	6.3	15.8	2.7				
	1.18	204T	14	3795	790	4.8	9.4	2.3	15,000	1970	2.5	15.9
	1.18	202T 250T 252T	10	3795	790	4.8	11.6	2.8	15,000	1970	2.8	18.4
	1.18	210T	8	3795	790	4.8	15.3	3.8	15,000	1970	3.4	23.7

Third stage

G		Reference test no.	Reefing version	Weight, W_D, lbs	$(C_R S_W)_{AVE.}$, ft^2	$W_D/(C_R S_W)_{AVE.}$, lbs/ft^2	q_{2DR}, psf	G	Weight, W_D, lbs	$(C_R S_W)_{AVE.}$, ft^2	G	
2.89		205T	A	5000	2175	2.3	7.0	4.6				
		251T	C	5000	1700	2.9	7.0	2.6				
		202T	A	3795	2175	1.7	5.0	4.0				
		210T	C	3795	1700	2.2	5.0	3.3	15,000	4250	3.3	

Fourth stage

G		Reference test no.	Reefing version	Weight, W_D, lbs	$(C_R S_W)_{AVE.}$, ft^2	$W_D/(C_R S_W)_{AVE.}$, lb/ft^2	q_{1DR}, psf	G	Weight, W_D, lbs	$(C_R S_W)_{AVE.}$, ft^2	G	
1.98		205T	A	5000	3960	1.3	3.8	1.5				
		251T	C	5000	3960	1.3	3.1	2.6				
		204T	A	3795	3960	1.0	1.7	1.8				
		250T	C	3795	3960	1.0	2.8	3.0	15,000	9900	3.0	

Full open

G		Reference test no.	Reefing version	Weight, W_D, lbs	$(C_R S_W)_{AVE.}$, ft^2	$W_D/(C_R S_W)_{AVE.}$, lb/ft^2	q_{LT}, psf	G	Weight, W_D, lbs	$(C_R S_W)_{AVE.}$, ft^2	G	
2.61		251T	C	5000	3245	1.5	1.1	2.7				
		202T	A	3795	3245	1.2	1.2	2.8	15,000	8110	2.8	

b. Intermediate-scale end point conditions of small-scale simulation (listed in Table 8 under Intermediate-scale and on the same line as G's shown for Small-scale).

c. Intermediate-scale conditions for full-scale simulation (listed in Table 8 under Intermediate-scale and on the same line as G's shown for Full-scale).

d. Full-scale end point conditions for intermediate-scale simulations (listed in Table 8 under Full-scale).

Table 8, under Intermediate-scale, also lists the reefing configuration, weight, average reference area, canopy loading, and dynamic pressure. These parameters are either:

a. End point conditions of small-scale simulation, e.g., lines one and two (these are the same conditions that were previously used for the two example computations).

b. Scale conditions for full-scale simulation, e.g., lines five through ten.

Under Full-scale, the weight, average drag area and dynamic pressure are end point conditions for intermediate-scale simulation.

The load factors (C_K), listed under Intermediate-scale, first stage (Table 8), are determined from Figure 74 for the canopy loading and line stretch dynamic pressure values shown. These load factors, along with the average reference areas, line stretch dynamic pressures and descent weights, are used to compute the G loads shown. The C_K load factors relative to scale conditions for full-scale simulation (lines five through ten), along with full-scale average reference areas, line stretch dynamic pressures and descent weights are used to compute the full-scale G loads shown.

Figure 79 presents a plot of first-stage load factor versus percent reefing for all bomb-type vehicle tests. The figure also shows the relationship between load factor and percent reefing for:

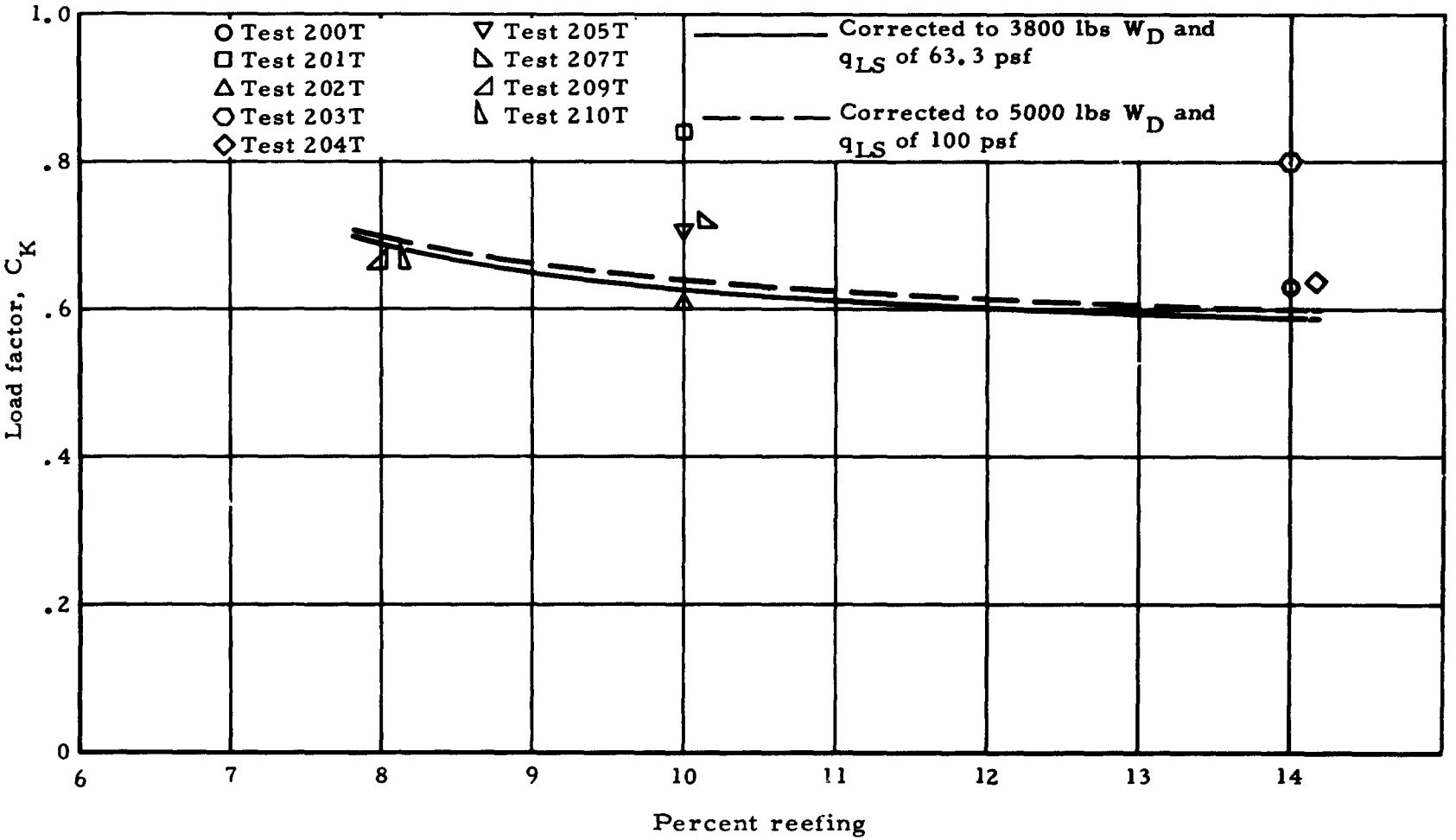

Figure 79. First-stage load factor versus percent reefing

a. Intermediate-scale tests corrected to 5000 pounds and a line stretch dynamic pressure of 100 psf (end-point conditions of small-scale simulation).

b. Intermediate-scale tests corrected to 3800 pounds and a line stretch dynamic pressure of 63.3 psf (conditions for full-scale simulation).

The load factor values for both of the above conditions were determined from Figure 74 and are presented to show the effect of reefing on load factor for these scale point tests. The decrease in load factor with percent reefing is consistent with a decrease in canopy loading, $W_D/(C_R S_W)_{AVE}$, which is due to an increase in first stage reference area (see Figure 70). The load factor values for 8, 10 and 14 percent reefing are listed in Table 8.

The results of intermediate-scale tests at end point conditions for small-scale simulation indicated that the first stage intermediate-scale loads were 15 to 28 percent higher than the small-scale loads. The first-stage results of intermediate-scale tests at conditions for full-scale simulation (Table 8) show:

a. Tests conducted at a line-stretch dynamic pressure of 63.3 psf (to simulate a full-scale parawing line-stretch dynamic pressure of 100 psf) result in first-stage peak loads that vary from 3.9 to 3.4 G's, for reefing ratios that vary from 14 to 8 percent, respectively.

b. Tests conducted at line stretch dynamic pressures of 44.3 psf to simulate a full-scale parawing dynamic pressure of 70 psf result in peak loads that vary from 3.0 to 2.6 G's for the same reefing ratio range.

These results indicate that at a deployment dynamic pressure of 100 psf a full-scale parawing must be reefed to less than 8 percent to maintain a 3 G peak load level in first stage. For a deployment dynamic pressure of 70 psf, the 3 G level could be maintained with a reefing ratio as high as 14 percent.

The accuracy of the above predictions for the full-scale parawing is subject to the same limitations in scaling that were previously discussed.

Relative to the second reefing stage, the dynamic pressure at first-stage disreef shown in Table 8 is the average measured value for the type of test being considered, i.e., categorized according to descent weight and reefing ratio. Since all 5000 pound tests (at end point conditions for small-scale simulation) that resulted in usable data were conducted with 10 percent reefing, this is the only reefing percentage shown. The second-stage load factor (C_K) of 1.09 for the 5000 pound tests was taken from Test 207T. The C_K factor of 1.18 for the 3800 pound tests, (for full scale simulation) for all reefing ratios, was taken from Test 250T. These factors were the highest calculated for the reference tests shown in Table 8, with the exception of Test 204T. The calculated C_K value of 1.7 for this test was so high in comparison with the next highest value of 1.18, as to be considered a wild point. Choosing C_K values based on the higher values calculated in any weight category is conservative, in comparison with using a load-factor, canopy-loading plot directly. However, in this case, the load factor data were not sufficiently consistent to do otherwise. The 2.7 G load shown for the 5000 pound case compares favorably with the 2.53 G value indicated from small-scale tests. Had a 14 percent reefing test been conducted, the dynamic pressure at first-stage disreef would have been lower. In all likelihood, this would have reduced the G load to 2.5 G's or less. The G values shown for the full-scale parawing are based upon the use of a 9 second first-stage reefed interval. The second stage G load value, using 8 percent first-stage reefing, is 3.4.

The third, fourth and full-open stage dynamic pressure values shown in Table 8 are average values. Note that use of nose reefing

(reefing Versions B and C) reduces the third-stage and increases the fourth-stage G values substantially, and permits holding a near 3 G level for both stages. G values shown for the third, fourth and full-open stages are maximum values and refer to the reference tests shown in the table. The third-stage G value of 4.6, for a 5000 pound test without nose reefing, is high in comparison with the 2.89 value predicted from small-scale tests. The fourth-stage and full-open values are about the same or lower than expected, based on small-scale tests. The full-scale values shown for the last three stages are based on the assumption that nose reefing would be used on the full-scale parawing.

Parawing Geometry During the Opening Sequence

Figure 80 presents sketches of the disreefing-sequence geometry for a typical twin keel parawing. The sketches, which were made from on-board camera films, show the projected parawing planform for each deployment stage and for full open. The three views shown for first stage represent the three reefing percentages (8, 10 and 14 percent) that were used during testing. The two views for third stage represent the wing planform with and without nose reefing. The dimensions shown in Figure 80 are in terms of the reference keel length (ℓ_K).

Figures 81 through 83 provide plots of the parawing first stage projected area versus time. These plots are presented to show the characteristic first-stage filling process for the parawing. This filling process is shown for the three reefing percentages tested, namely 14, 10 and 8 percent. For comparison purposes the plotted data in these figures are nondimensionalized. Projected area is expressed as the ratio of instantaneous projected area to fully-inflated projected area and plotted versus the nondimensional time parameter, t/t_f. The projected area values were determined

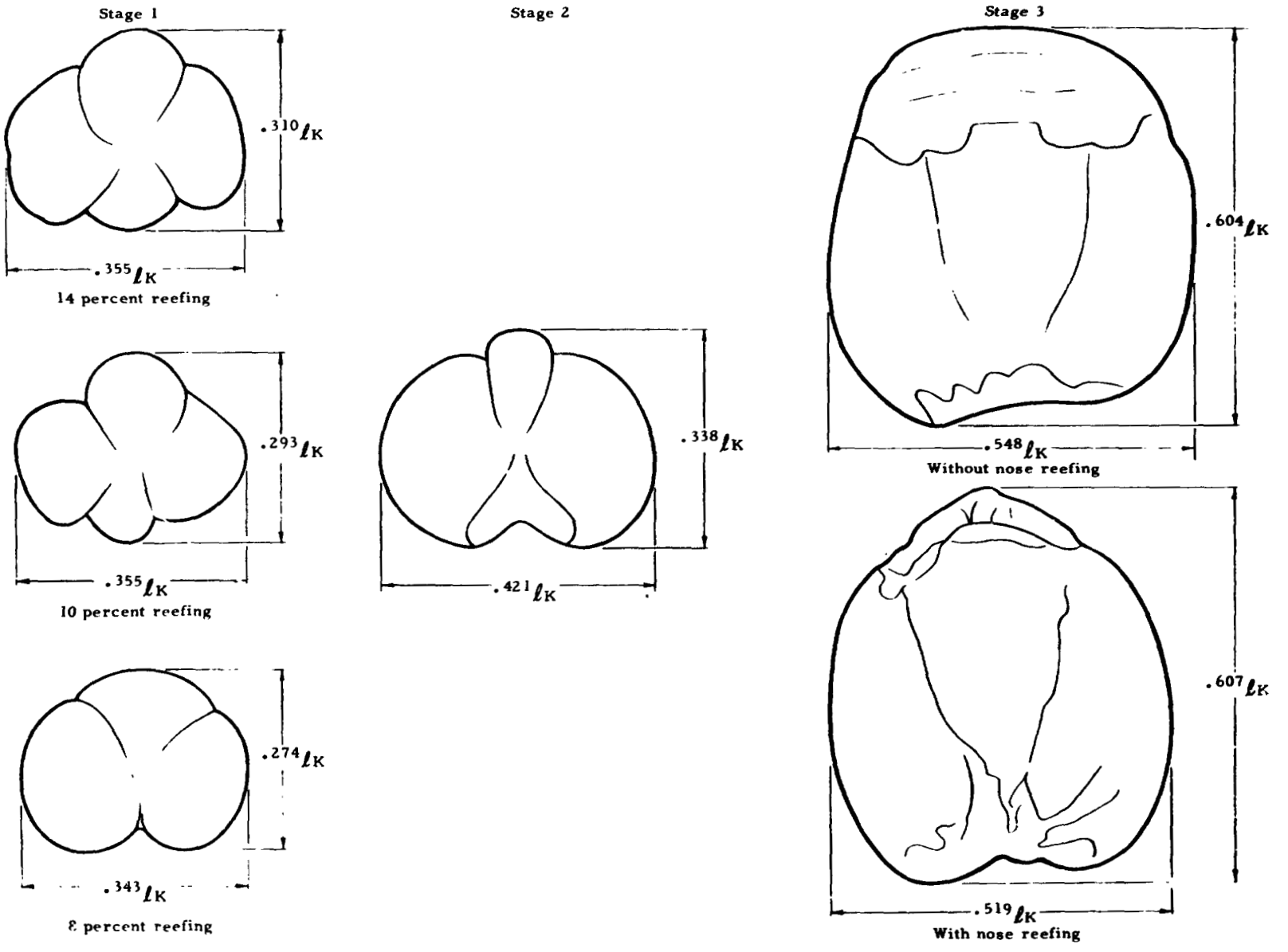

Figure 80. Disreefing sequence geometry, twin keel parawing, reefing stages one through full open

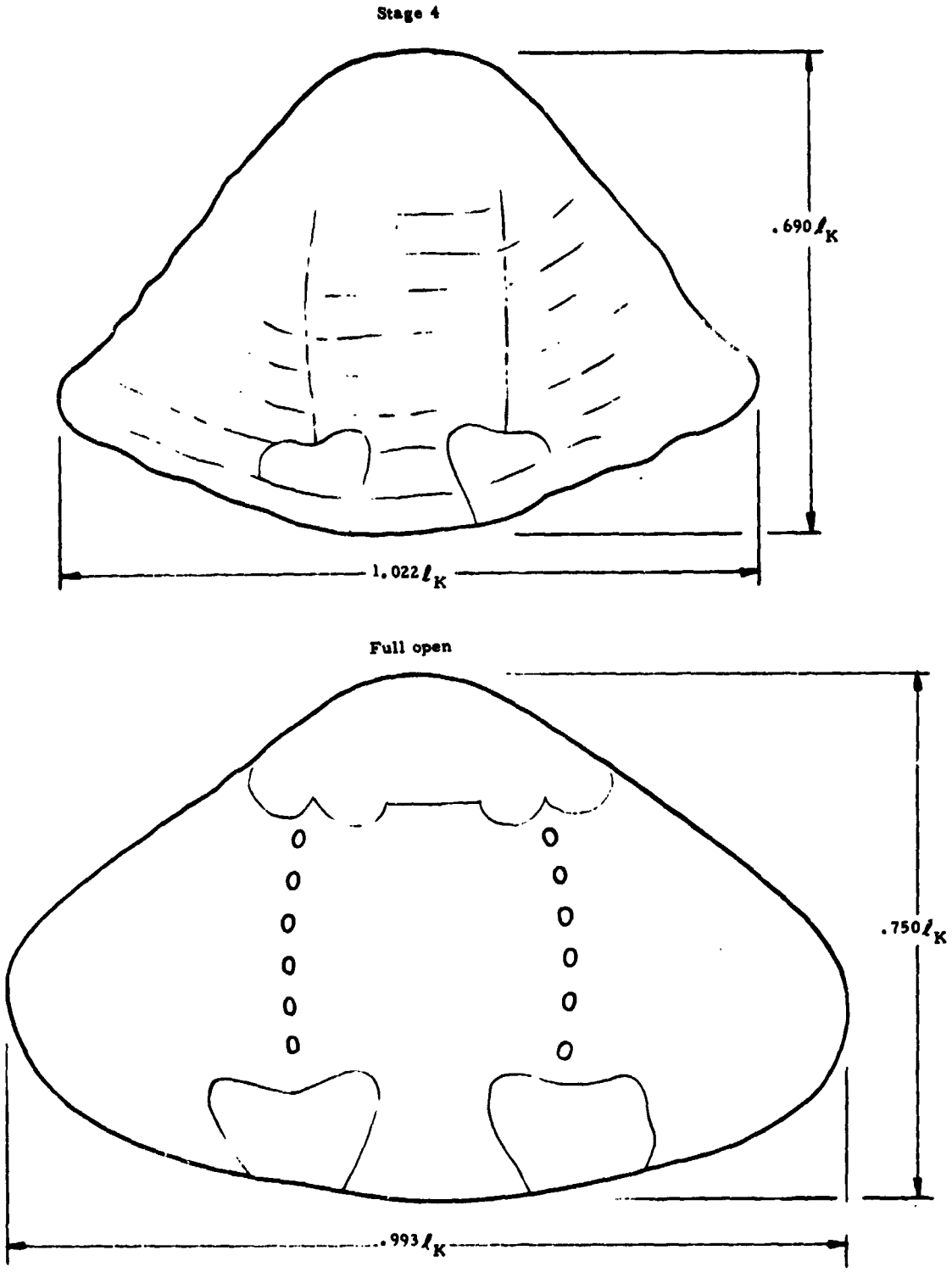

Figure 80. (concluded)

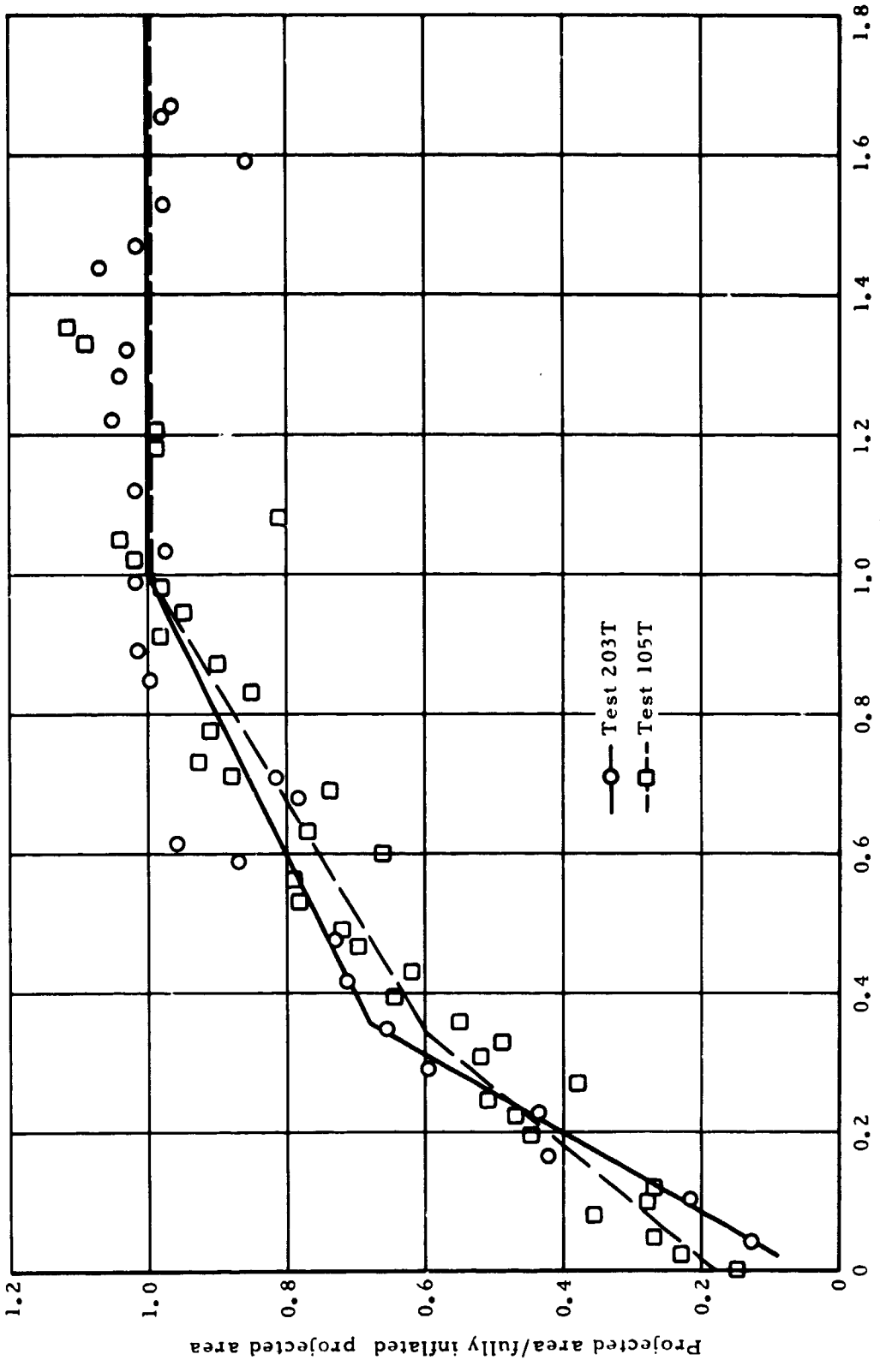

Figure 8 . mparison of projected area ratio during first reefed stage versus ...e, between Tests 203T and 105T, 14 percent reefing

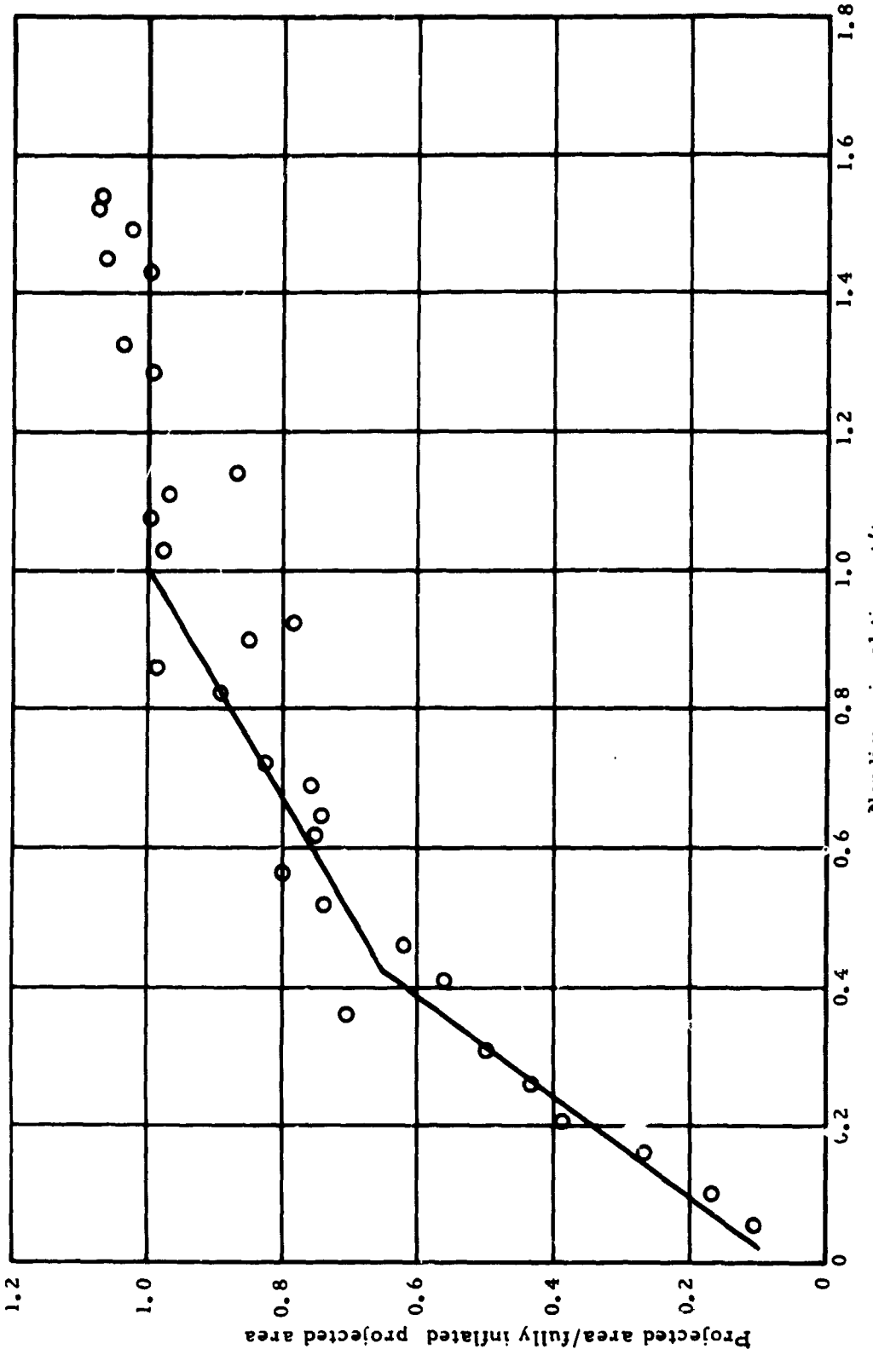

Figure 82. Projected area ratio during first reefed stage versus time for Test 202T,10 percent reefing

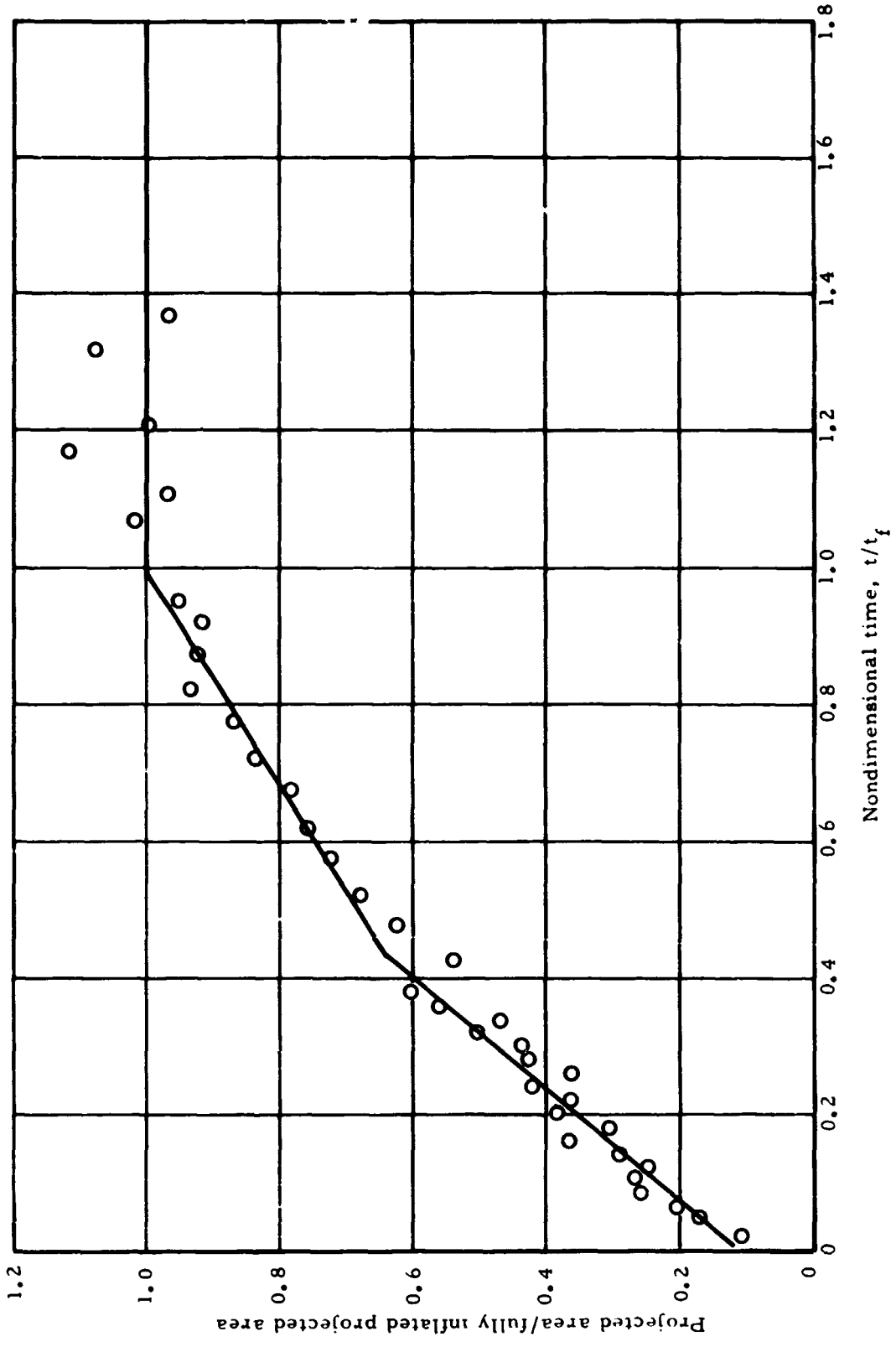

Figure 83. Projected area ratio during first reefed stage versus time for Test 210T, 8 percent reefing

from film analysis, using on-board film coverage. The fully-inflated projected area was determined by averaging the areas from the instant of parawing full reefed inflation until first-stage disreef. The first-stage filling time, t_f, was established as the time from parawing line stretch to the time when the projected-area-ratio time curve intersected the full inflation line. All three intermediate-scale tests shown in Figures 81 through 83 were conducted with a 3800 pound descent weight, at a line-stretch dynamic pressure of about 65 psf. The scatter shown by the data is due both to actual fluctuations of the parawing canopy and to inaccuracies in the measurement of the projected areas.

Figures 81 through 83 show that the first-stage inflation process can best be represented by two, straight-line segments. This is the same filling characteristic that was exhibited in the Langley small-scale parawing wind tunnel tests and in the small-scale drop tests. To illustrate this fact, Figure 81 provides a comparison of the first-stage filling process for Test 203T with small-scale Test 105T. Both tests were conducted with 14 percent first-stage reefing. Note the close similarity of these two inflations processes. The change-in-slope point for both tests occurred at a t/t_f value of about 0.35.

The effect of reefing percentage on the first-stage fill rate can be seen by comparing the slopes of the initial straight-line segments of the three intermediate-scale tests in Figures 81 through 83. Test 203T with 14 percent reefing (Figure 81) shows the steepest initial inflation rate. Test 202T with 10 percent reefing (Figure 82) shows a less steep initial inflation rate. Test 210T with 8 percent reefing (Figure 83) shows the least steep initial inflation rate of the three tests. Computer simulations confirm that the magnitude of the peak reefed load is a function of the slope of the initial reefed inflation rate. Thus, the observed trend of lower peak-first-stage loads with decreasing reefing ratio is logical and consistent with these inflation characteristics data.

Table 9 presents a summary of first-stage filling time and time to peak load, along with the parameters which influenced filling time, for all applicable twin keel bomb-type vehicle tests. Parameters that influence filling time include descent weight and velocity at line stretch, both of which influence the average velocity during the inflation process, plus reefing ratio.

Figures 84 and 85 show the effects of reefing ratio and velocity at line stretch on parawing first-stage filling time, based on selected data from Table 9. From simple volumetric flow considerations for an incompressible gas, parawing filling time is proportional to the reciprocal of the average velocity during the filling process and the mouth area. In Figure 84 filling time is plotted versus the inverse of reefing ratio squared (where reefing ratio squared is a measure of the mouth area) for Tests 203T, 202T, 209T and 210T. These tests were conducted at essentially the same descent weight and at approximately the same velocity at line stretch. Thus, the basic variable is reefing ratio. Figure 84 shows that filling time increased linearly with the inverse of reefing ratio squared. This same observation was noted during both wind tunnel and aerial testing of small-scale parawings.

Figure 85 presents a plot of filling time versus velocity at parawing line stretch. The plot shows the combined effects of reefing ratio and line-stretch velocity on filling time. (The constant-reefing-ratio lines were developed from a plot of filling time versus the inverse of line-stretch velocity, which provided straight line fairings. Data from Tests 205T, 207T and 201T, which were conducted at the same 10 percent reefing ratio and descent weight, but in a range of line-stretch velocities, were used to develop the slope of the fairings.) Figure 85 shows that first-stage filling time, t_f, decreased both with increasing line-stretch velocity and increasing reefing ratio. The manner in which first-stage filling time decreased with increasing reefing ratio, at a given velocity and descent weight, was shown in Figure 84.

TABLE 9. - SUMMARY OF FIRST STAGE FILLING TIME, TWIN KEEL PARAWING BOMB-TYPE VEHICLE TESTS

Test no.	Descent weight, W_D, lbs	Percent reefing $(\ell_{RL}/\ell_K) \times 100$	$\frac{1}{(\ell_{RL}/\ell_K)^2}$	t_{pl}, sec	t_f, sec	V_{LS}, ft/sec
200T	2879	14	51	1.53	3.77	168
203T	3805	14	51	0.66	3.50	295
204T	3786	14	51	1.82	(1)	276
201T	5034	10	100	1.64	5.34	181
202T	3792	10	100	0.90	4.25	306
205T	5031	10	100	0.92	4.42	319
207T	4994	10	100	1.42	4.47	224
209T	3811	8	156	1.36	5.58	287
210T	3813	8	156	1.54	4.50	308

NOTE:

(1) Data invalid because of twisted suspension lines.

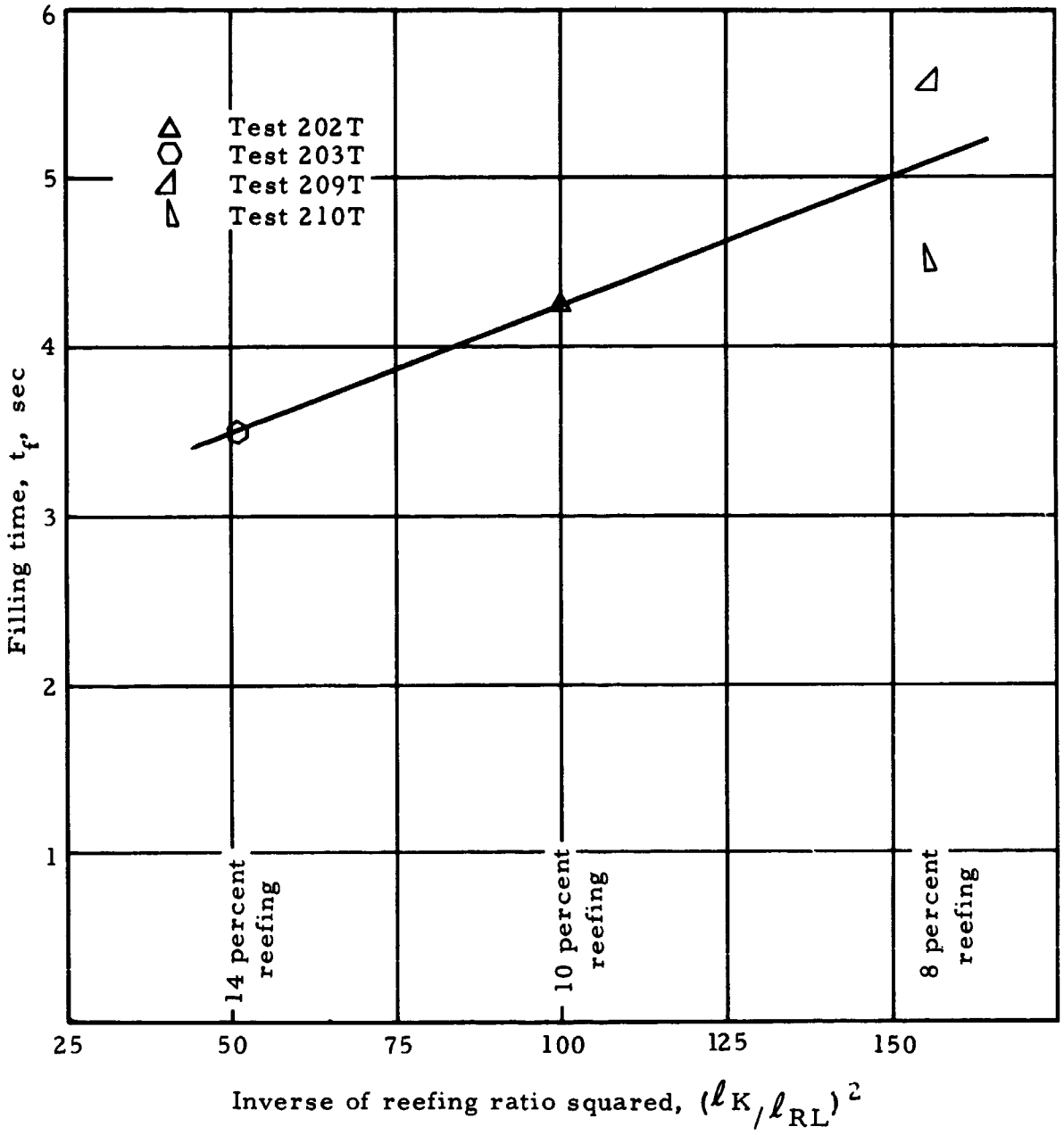

Figure 84. First-stage filling time versus inverse of reefing ratio squared

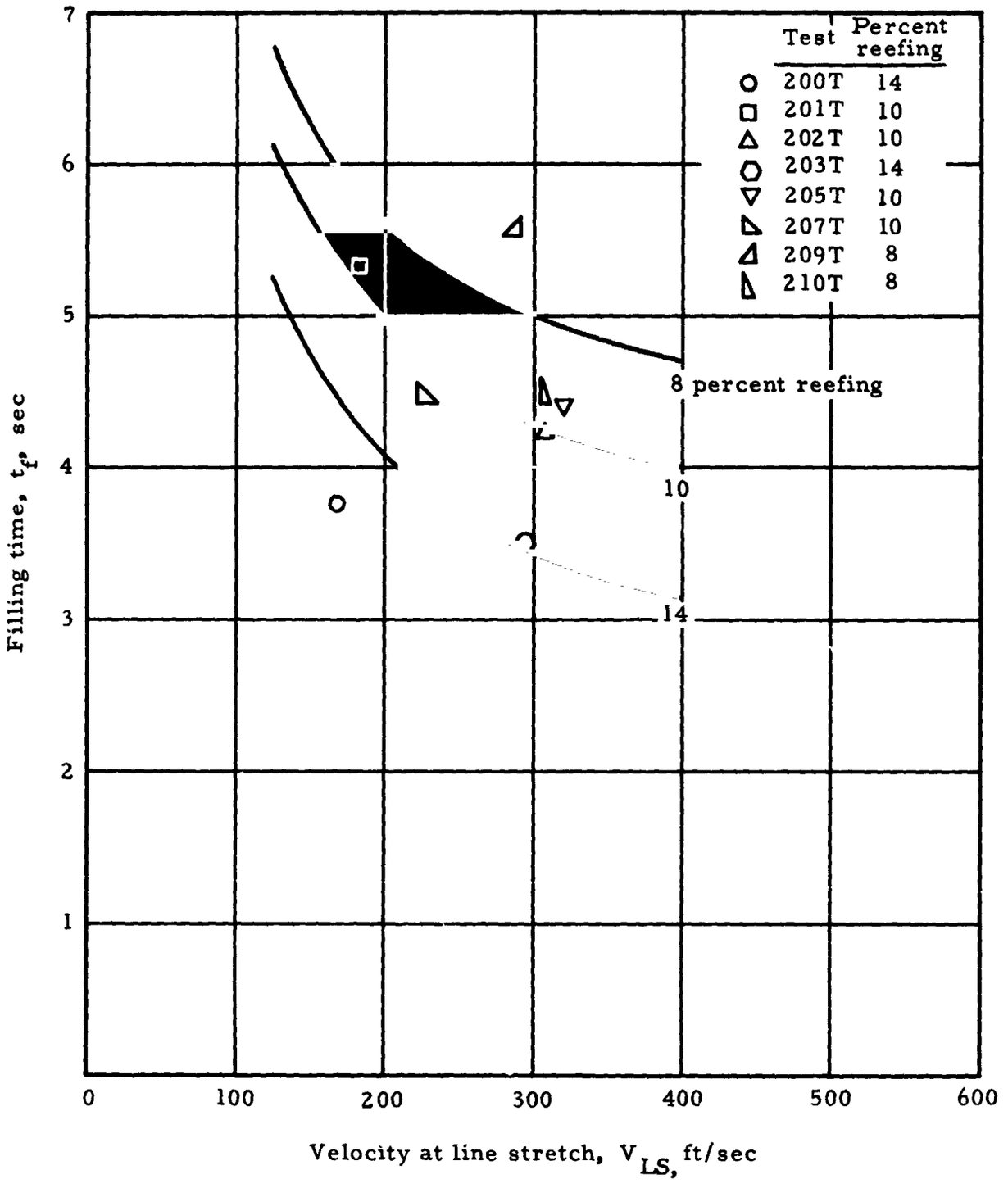

Figure 85. First-stage filling time versus velocity at line stretch

Suspension Line Loads

Suspension line loads were measured in all the intermediate-scale drop tests which utilized a bomb-type test vehicle. Table 10 presents the data obtained from single keel parawing Test No. 200S -- the only single keel parawing test with usable suspension-line-loads data. Figures 86 through 90 present the data obtained from the twin keel parawing tests.

TABLE 10. - RATIO OF PEAK-SUSPENSION-LINE LOAD TO PEAK-STAGE-TOTAL LOAD FOR 6-LINE-LEADING-EDGE, SINGLE KEEL PARAWING, TEST NO. 200S

	Deployment stage				
Line no.	1	2	3	4	Full open
L1	.015	.006	.039	.016	.009
L6	.052	.039	.032	.046	.064
K7	.061	.045	.073	.071	.092
K12	.047	.031	.028	.027	.110

L - Leading edge line

K - Keel line

Suspension line loads are presented as ratios of peak force in each deployment stage to peak measured total parawing load for that stage. (Peak line load, in lbs, can be obtained by multiplying the line load ratio by the product of the suspended weight and the G load for the given stage. Suspended weight and G load per stage are listed in Table 5 for all the intermediate-scale tests conducted.) All measured loads representative of the parawing configuration tested are presented. Loads not presented include tests or stages of tests where:

a. The parawing did not disreef in a normal manner, e.g., the fourth and full-open stage of Test 201T, where the left trailing edge did not disreef at the end of the third stage.

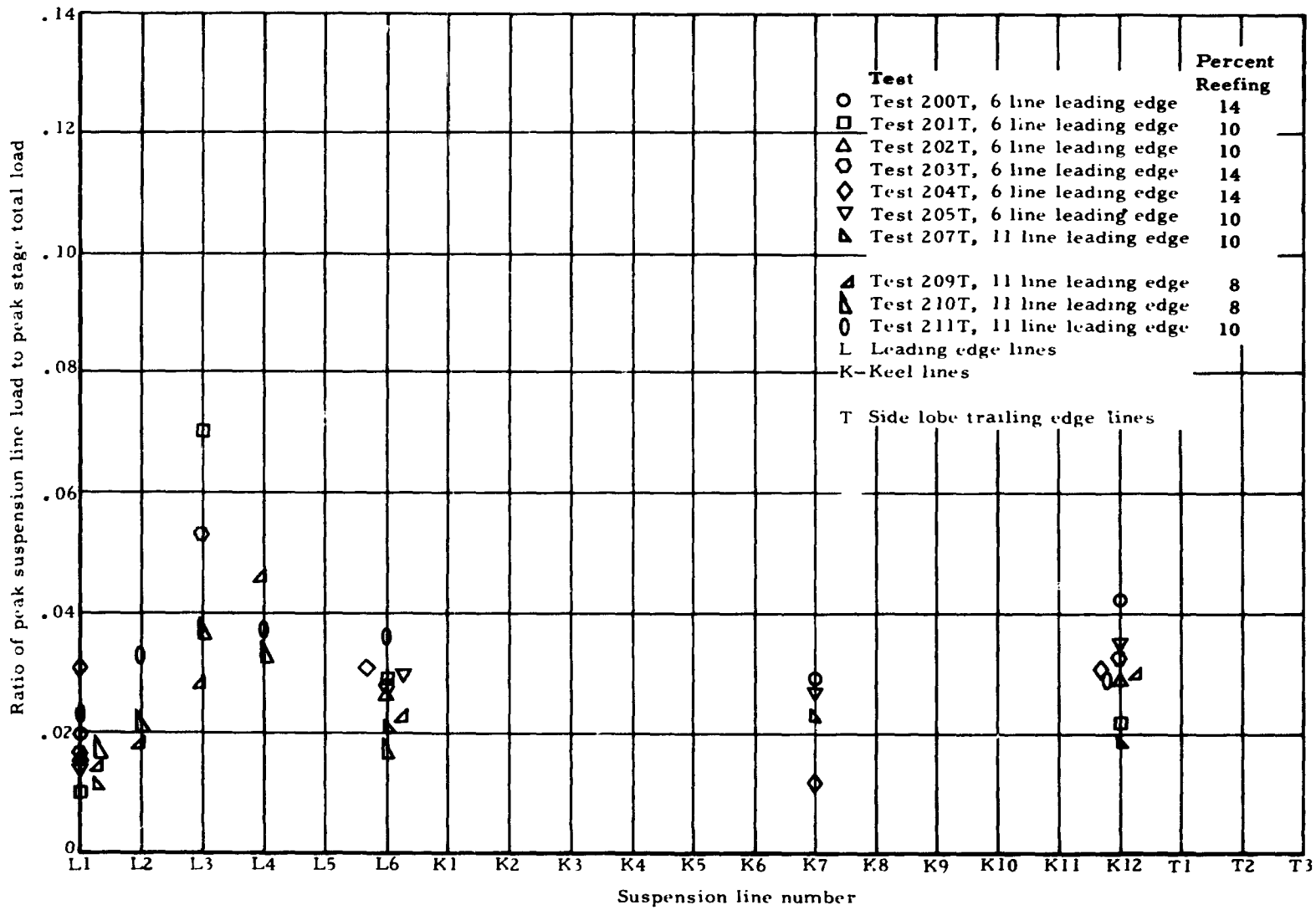

Figure 86. Twin keel parawing, stage 1 suspension-line-load-ratio data

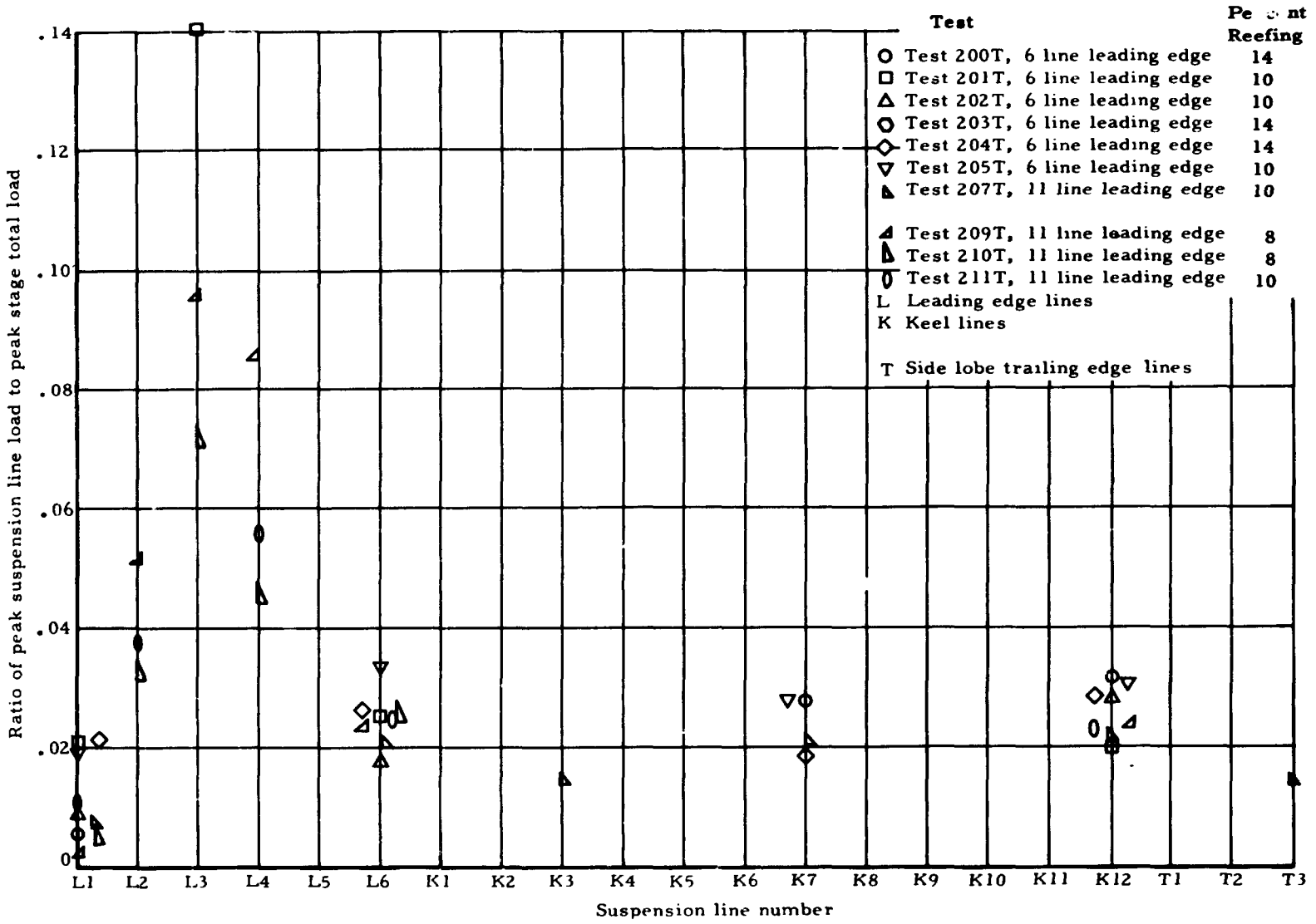

Figure 87. Twin keel parawing, stage 2 suspension-line-load-ratio data

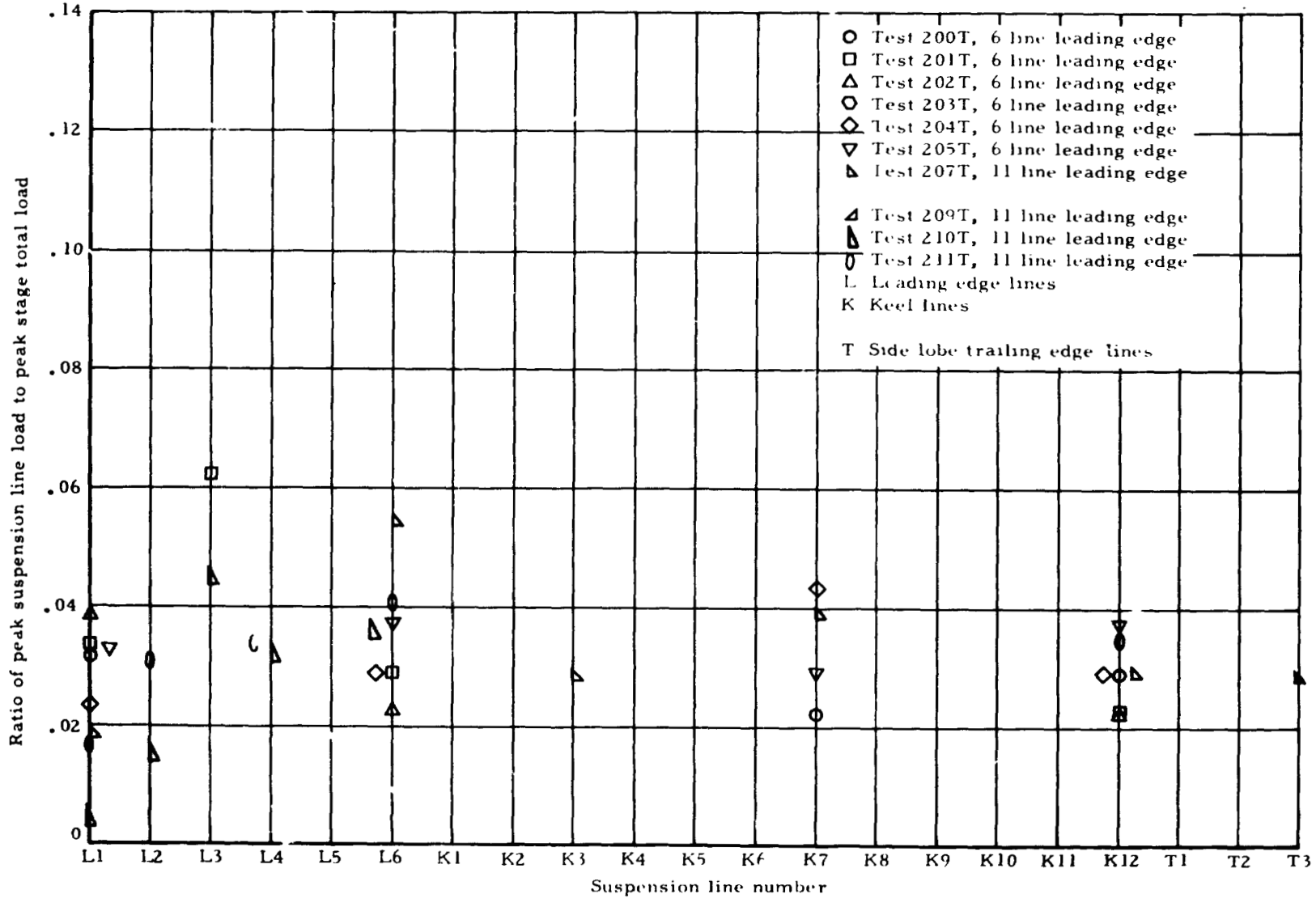

Figure 88. Twin keel parawing, stage 3 suspension-line-load-ratio data

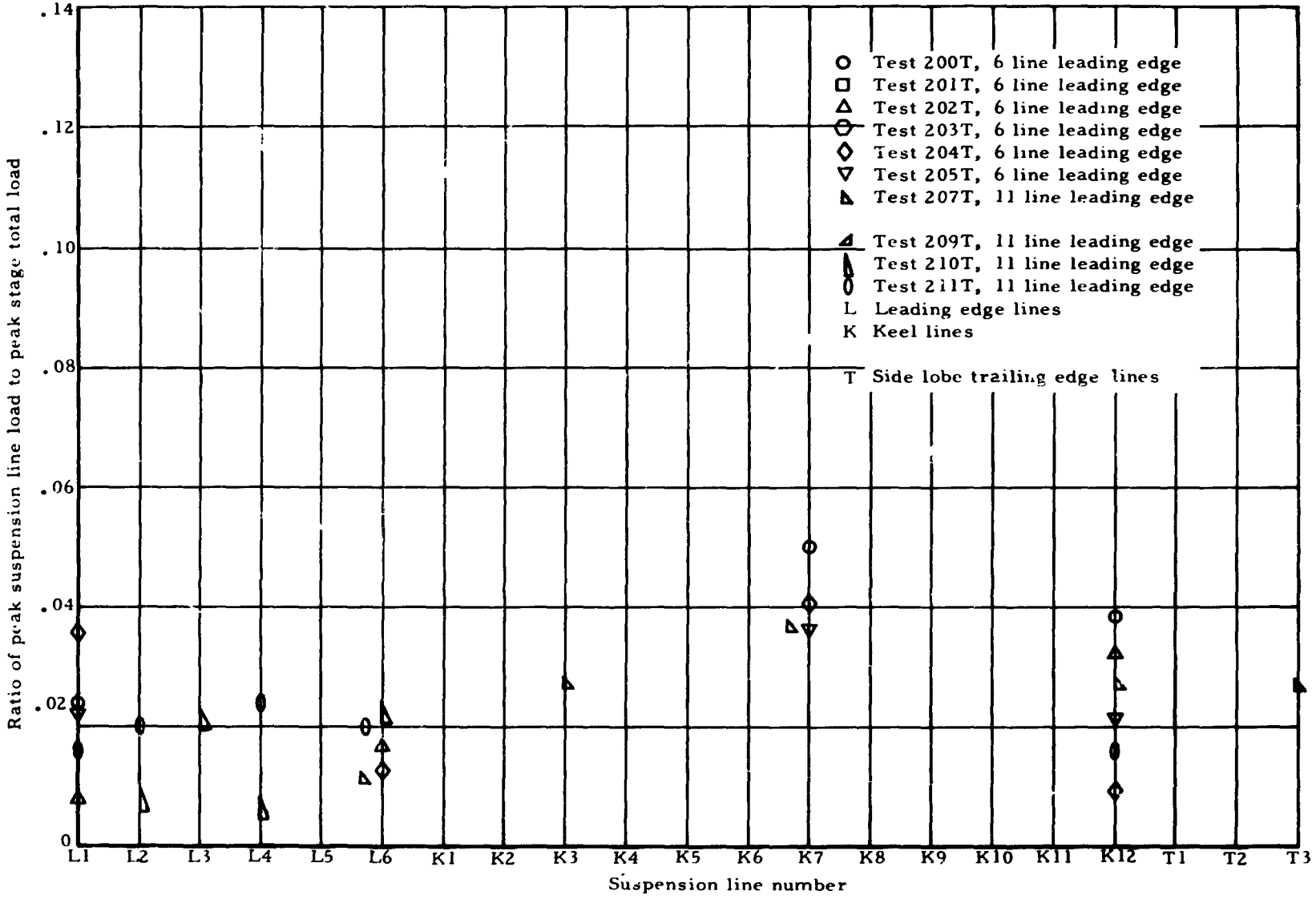

Figure 89. Twin keel parawing, stage 4 suspension-line-load-ratio data

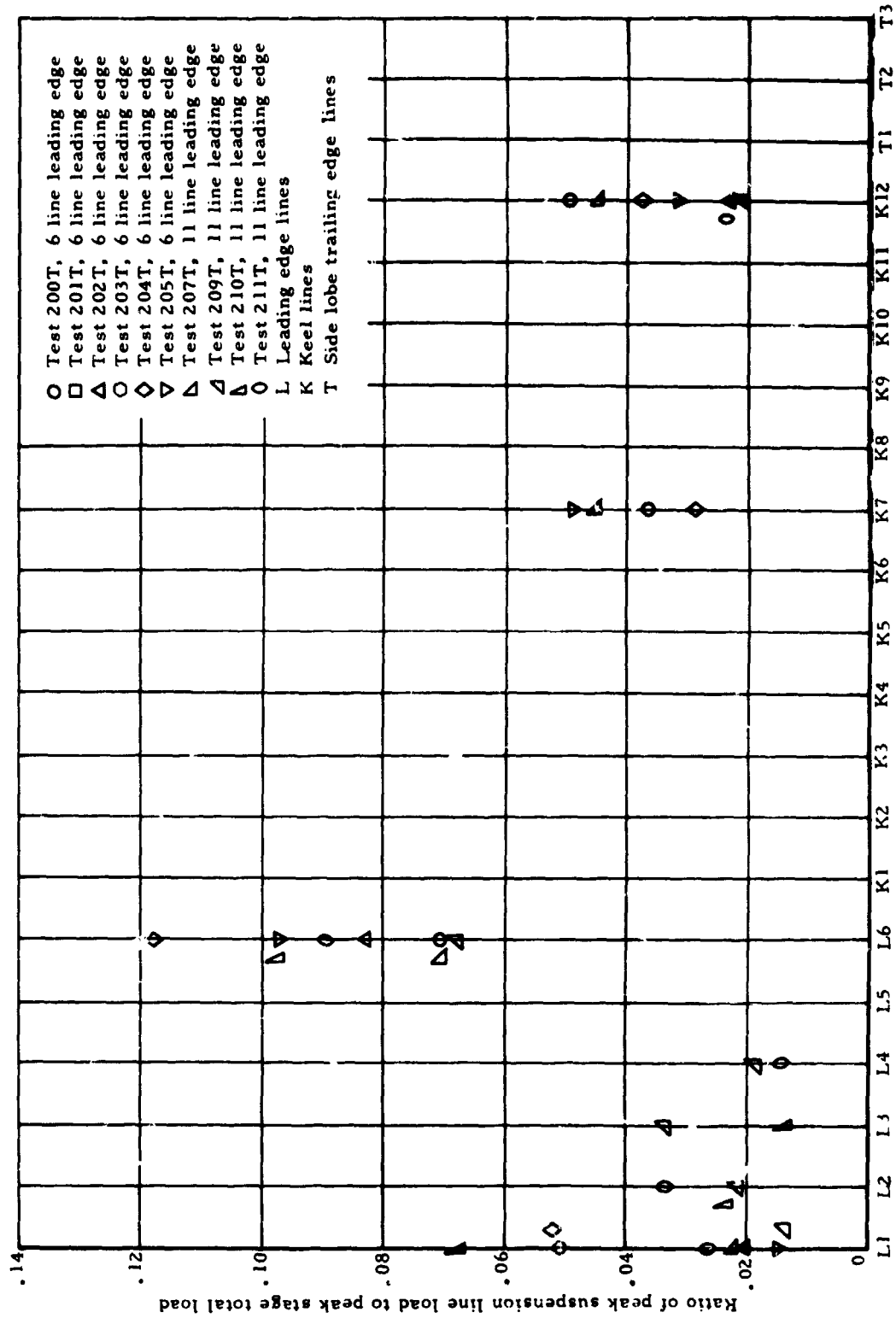

Figure 90. Twin keel parawing, full open suspension-line-load-ratio data

b. The parawing sustained heavy structural damage, e.g., Tests 201S, 206T and 208T.

All line load measurements were made in the left side suspension lines.

Test 200S utilized a reefing system with 11.6 percent first stage reefing. The twin keel tests utilized reefing systems A, B and C with 8, 10 and 14 percent first and second stage reefing. Reefing systems B and C included a 25-inch line that gathered the center section nose during the first three stages. Tests which utilized this nose reefing were 206T, 207T, 209T, 210T and 211T. These same tests also utilized an eleven-suspension-line-leading-edge parawing version, rather than the six-line version.

Figures 86 and 87 indicate that the first and second stage reefing percentages had no effect on the measured line load ratios. The effect, if any, of reefing Version A (Figure 26) in comparison with Versions B (Figure 27) and C (Figure 28) cannot be determined, since these versions utilized 6- and 11-suspension-line-leading-edge parawings, respectively.

Figures 91 and 92 present suspension-line-load-ratio envelopes for all deployment stages for both the 6- and 11-suspension-line-leading-edge parawings. Values for the 6-line leading edge parawing were taken from maximum values measured during the intermediate-scale test program, as well as from values measured during the small-scale free flight and wind tunnel programs. Values for the 11-line leading edge parawing were taken from the intermediate-scale test program. In cases where data were scarce (forward keel and trailing edge lines) values were extrapolated from the 6-line parawing configuration. Comparison of Figures 91 and 92 shows that the suspension-line-load-ratios for the 11-suspension-line-leading-edge parawings are substantially less than those for the 6-line configuration.

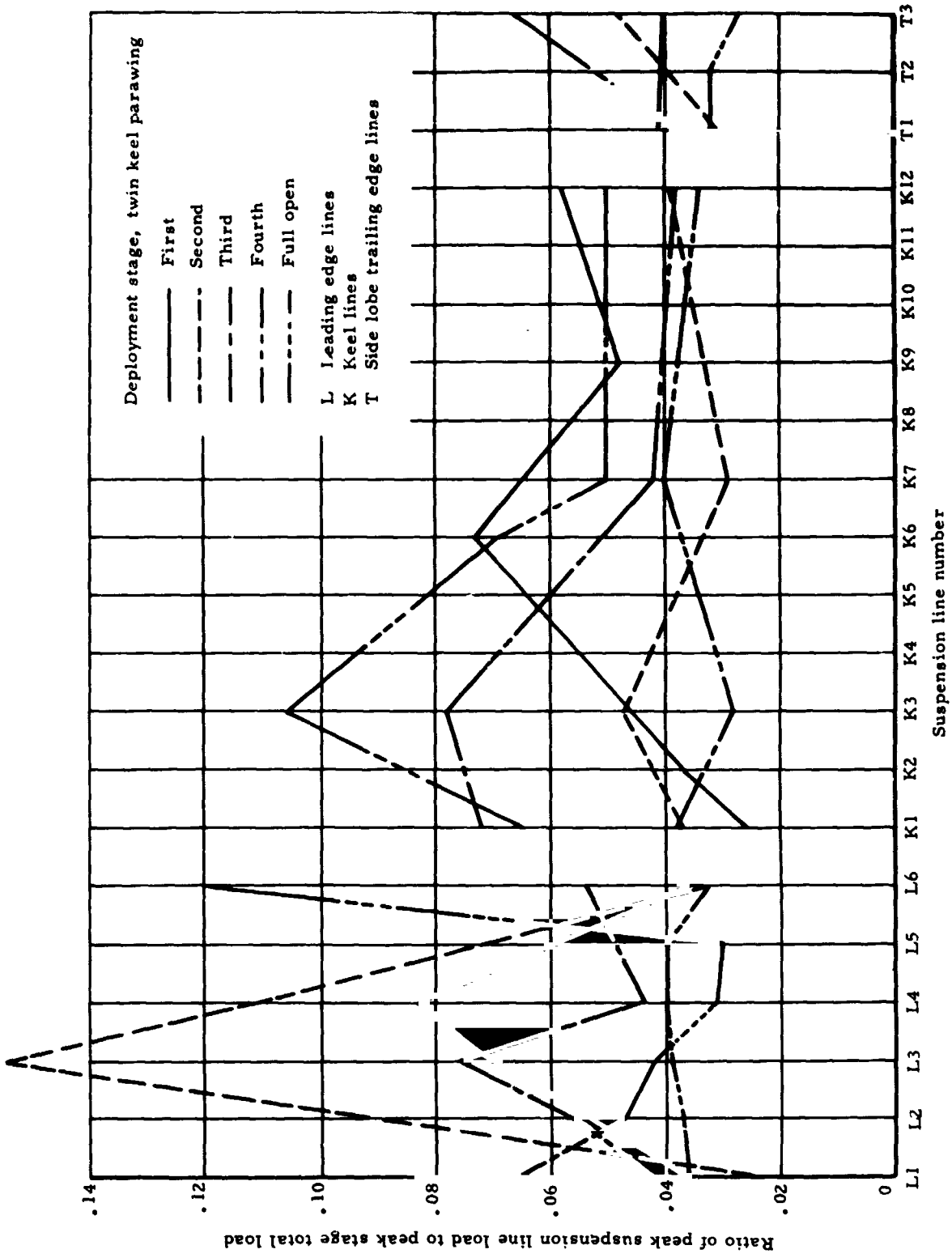

Figure 91. Ratio of peak-suspension-line load to peak-stage-total load vs suspension-line location, 6-line-leading-edge parawing configuration

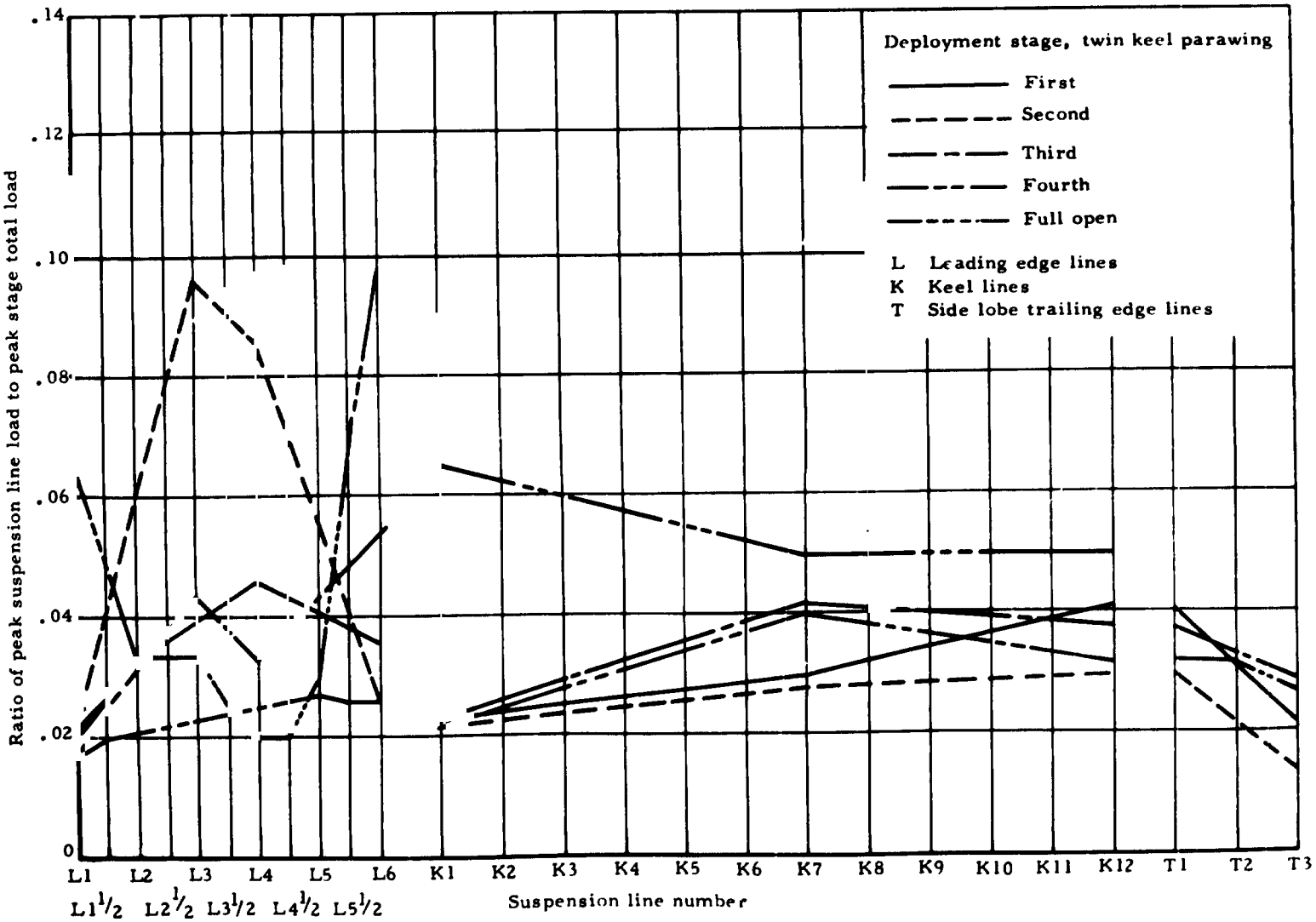

Figure 92. Ratio of peak suspension-line load to peak stage total load vs suspension-line location, 11-line-leading-edge parawing configuration

Suspension-line-load ratios for all deployment stages for the 11-line leading edge, twin keel parawing are summarized in Table 11. The values listed in this table are considered to be the "best estimate" maximum values for the 11-line parawing configuration, based on all applicable test data. It may be noted that the second stage produces the highest load ratios for all leading edge lines, except for lines 1, 1-1/2, 5-1/2 and 6. For these lines plus all the keel lines, the full open stage produces the highest load ratios. First stage provides the peak load ratio for side-lobe-trailing-edge line 1, while third stage causes the peak load ratio for trailing edge lines 2 and 3.

Line load ratios measured in Test 200S (Table 10) show that the peak leading-edge-line-load ratios for the single keel parawing are less than those for the comparable leading edge lines on the twin keel parawing. However, the single keel parawing peak rear-keel-line-load ratios are higher than the peak rear-keel-line-load ratios for the twin keel parawing.

In general, the reefing systems utilized in the parawing test program resulted in nonuniform suspension line loading. This non-uniformity of line loading is both intrastage (i.e., unequal loading of individual suspension lines in a given reefing stage), and stage-to-stage (i.e., unequal loading of a given line from stage to stage). Table 10 and Figures 91 and 92 identify both of these types of line load nonuniformity. The degree of line load non-uniformity is evidenced by the fact that for the intermediate-scale parawings, the ratio of total available suspension line strength to maximum design load was 3.5 on the single keel specimens, 4.3 on the 6-line-leading-edge, twin keel specimens (Versions I and II) and 4.9 on the 11-line-leading-edge, twin keel specimens (Versions III through VII).

TABLE 11. - RATIO OF PEAK-SUSPENSION-LINE LOAD TO PEAK-STAGE-TOTAL LOAD FOR 11-LINE-LEADING-EDGE, TWIN KEEL PARAWING CONFIGURATION[1]

Line No.	Deployment stage				
	1	2	3	4	Full Open
L1	.023	.022	.018	.017	.065
L1½	.028	.040	.025	.020	.050
L2	.033	.060	.032	.021	.034
L2½	.036	.078	.038	.022	.034
L3	.040	.096	.044	.023	.034
L3½	.043	.090	.039	.024	.025
L4	.046	.086	.033	.025	.020
L4½	.043	.071	.037	.026	.020
L5	.041	.055	.043	.027	.030
L5½	.039	.040	.049	.026	.065
L6	.036	.026	.054	.026	.097
K1	.023	.022	.023	.022	.065
K2	.024	.023	.026	.025	.062
K3	.025	.024	.029	.028	.060
K4	.026	.025	.033	.031	.057
K5	.028	.026	.036	.034	.055
K6	.029	.027	.039	.037	.052
K7	.030	.028	.042	.040	.050
K8	.032	.028	.041	.038	.050
K9	.034	.029	.040	.037	.050
K10	.037	.029	.039	.035	.050
K11	.039	.030	.038	.034	.050
K12	.041	.030	.038	.032	.050
T1	.041	.030	.038	.032	0
T2	.031	.022	.033	.032	0
T3	.022	.014	.029	.027	0

[1] Best estimate of maximum values.

L - Leading edge line

K - Keel line

T - Side-lobe-trailing-edge line

Parawing Canopy Failures and Failure Analyses

General. - In the course of the intermediate-scale parawing flight test program, a number of tests resulted in significant parawing canopy structural failures. Analysis of these canopy failures indicated that the failures could be grouped by failure mode, with probable causes identified for each failure mode. The following pages identify the significant canopy structural failures which occurred, establish the failure modes, cite the corrective actions taken and discuss the efficacy of the corrective actions.

It is significant that despite the major canopy damage incurred during the deployment process in several of the flight tests, all of the damaged wings did open and achieve a steady gliding configuration. This fact clearly demonstrates the positive opening characteristics and inherent opening reliability of the parawing device. Also, all damaged wings achieved a low vertical rate-of-descent prior to touchdown of the test vehicle. In fact, no test in the entire parawing program of seventy-five aerial drop tests resulted in loss of a test vehicle or even in major damage to a test vehicle -- a record seldom equalled in aerodynamic decelerator development programs.

Significant parawing canopy failures and failure modes. - Significant canopy structural failures occurred in seven intermediate-scale parawing aerial tests. These tests were single keel Test 201S and twin keel Tests 202T, 205T, 203T, 208T, 211T and 206T. Figures 93 through 99 show the major parawing canopy damage incurred in these tests. Figure 100 shows a photograph of the Test 206T parawing in steady gliding flight, with some of the canopy damage in evidence.

From analyses of the canopy failures which occurred in these tests a total of four failure modes were identified. All the significant canopy damage in the seven tests cited above could be

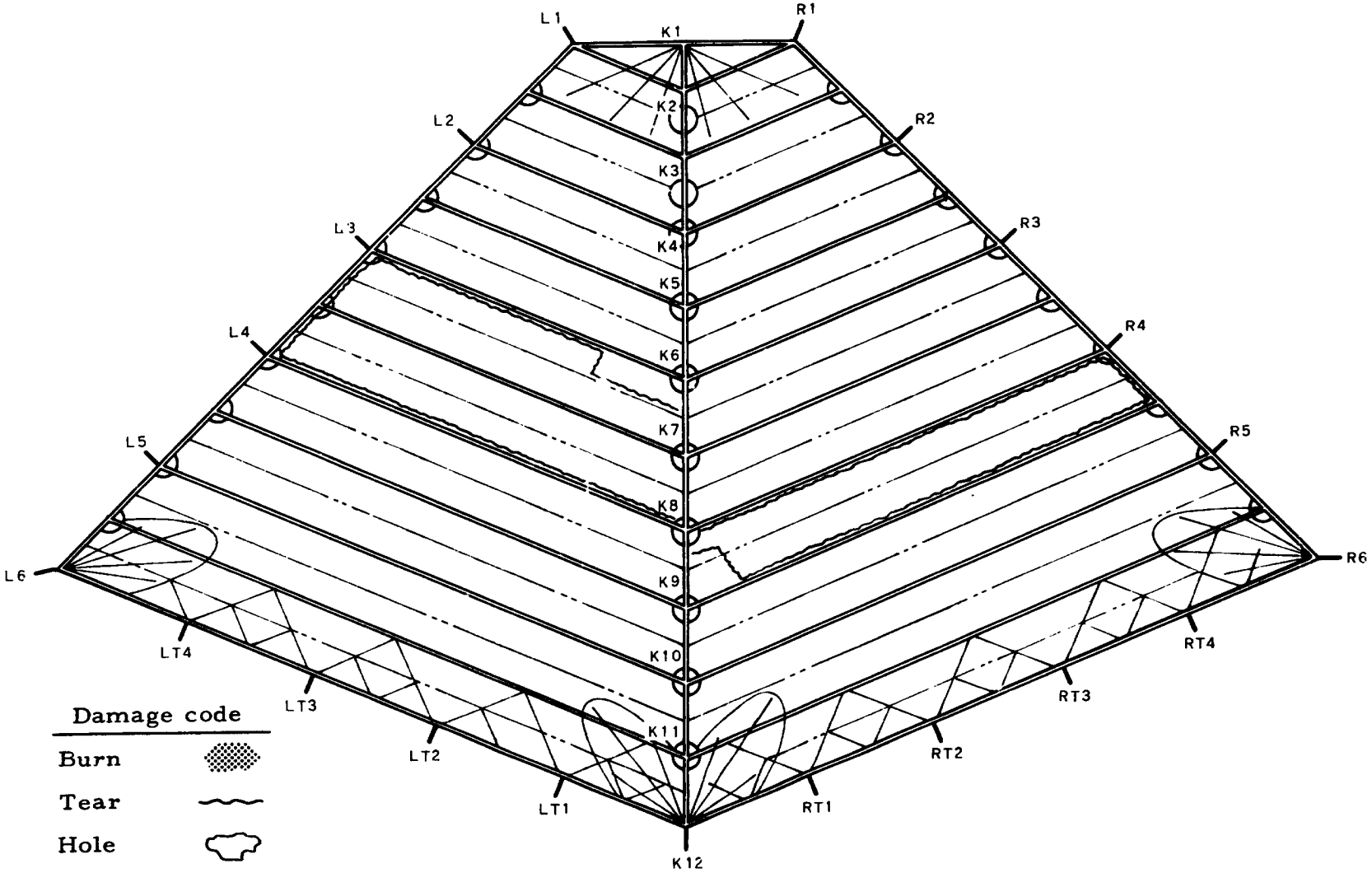

Figure 93. Major canopy damage, Test 201S

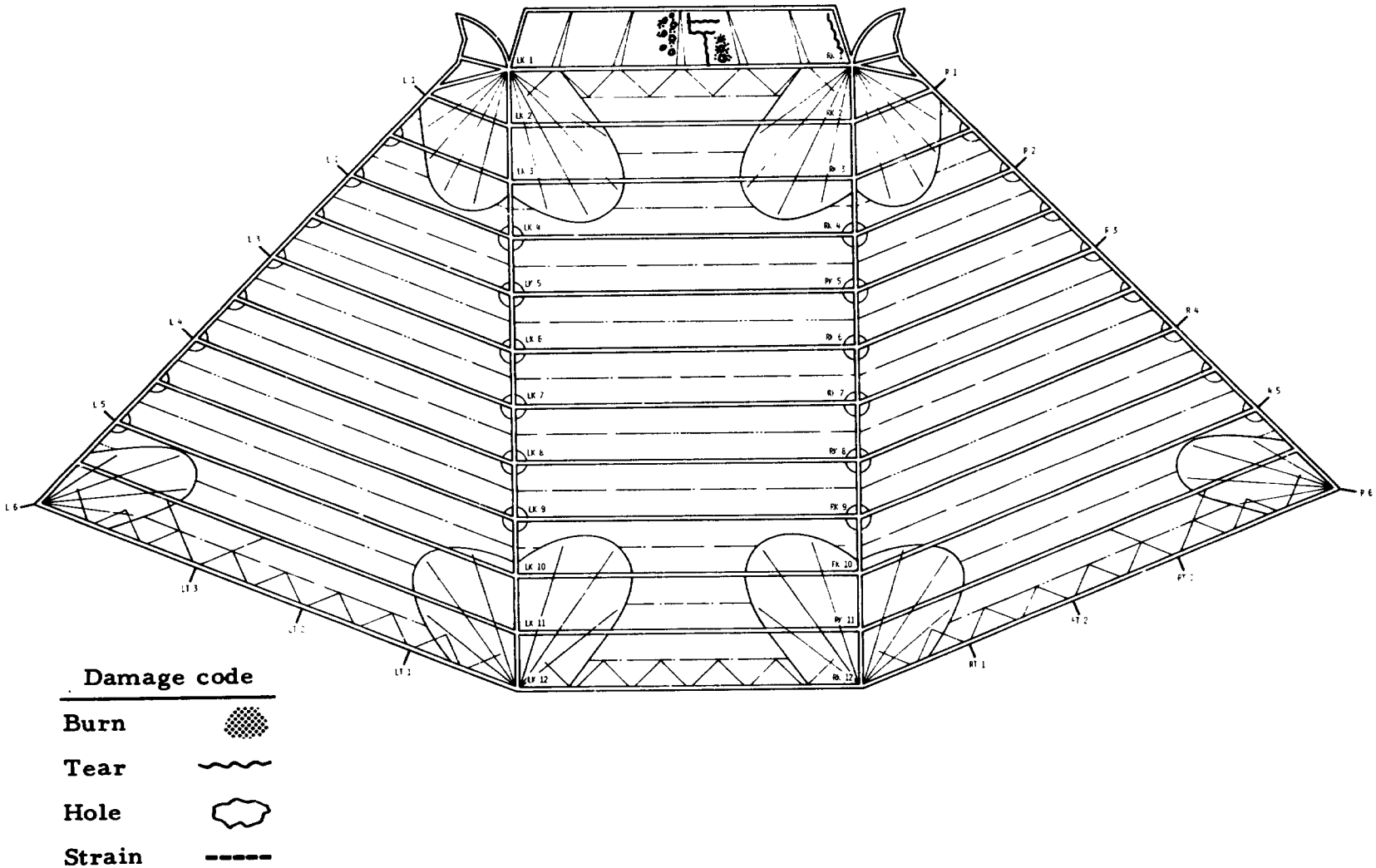

Figure 94. Major canopy damage, Test 202T

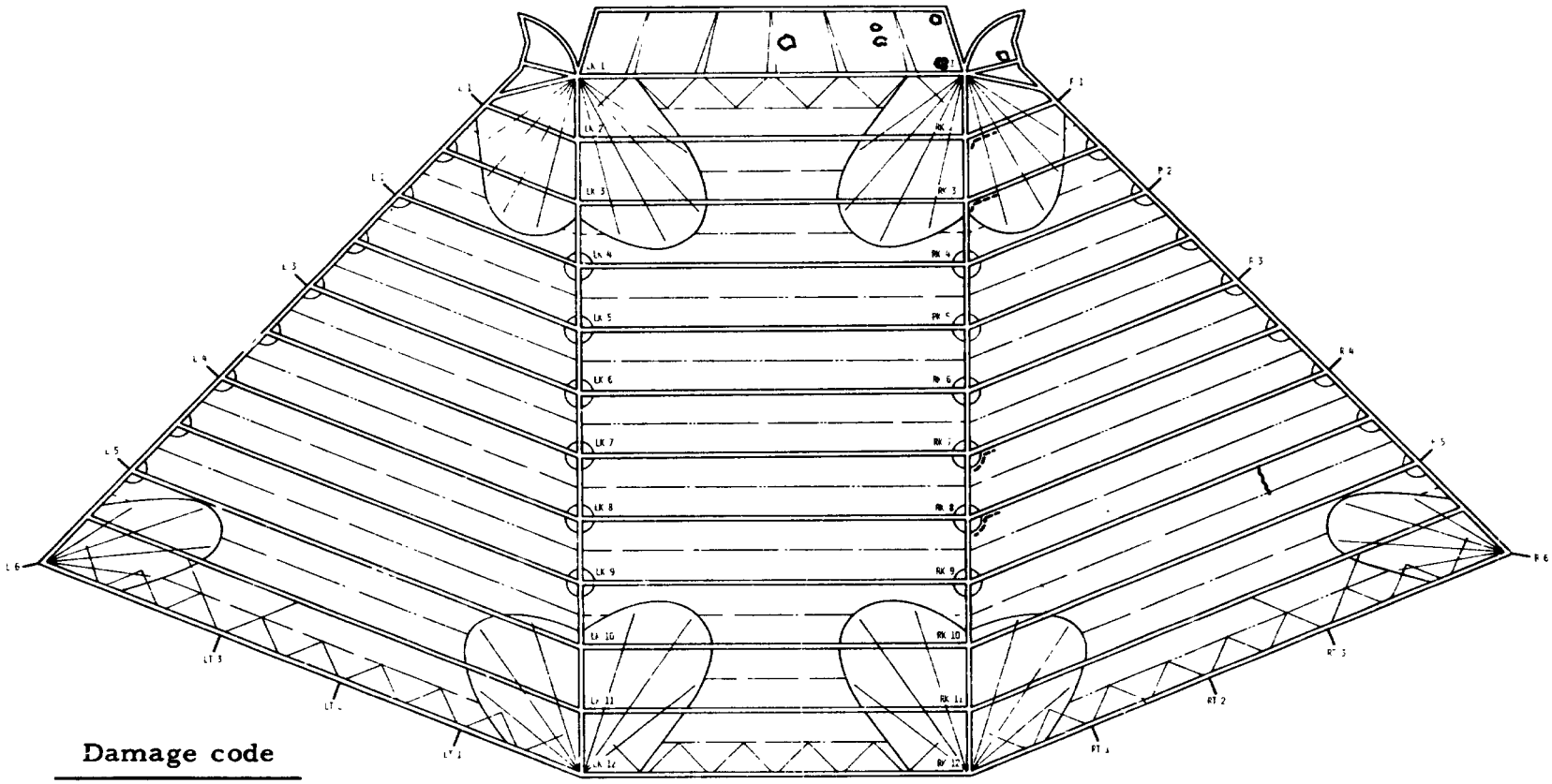

Figure 95. Major canopy damage, Test 205T

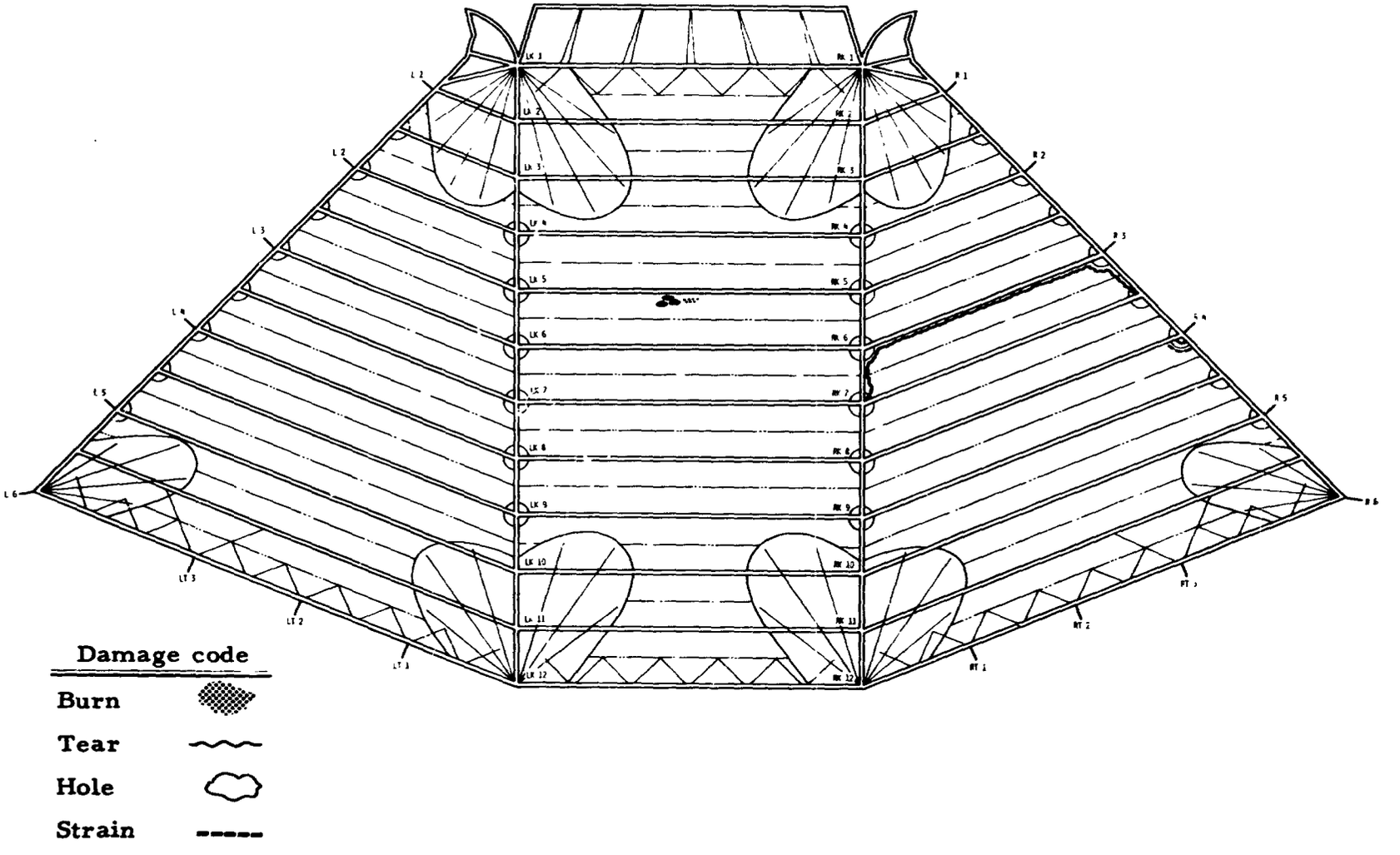

Figure 96. Major canopy damage, Test 203T

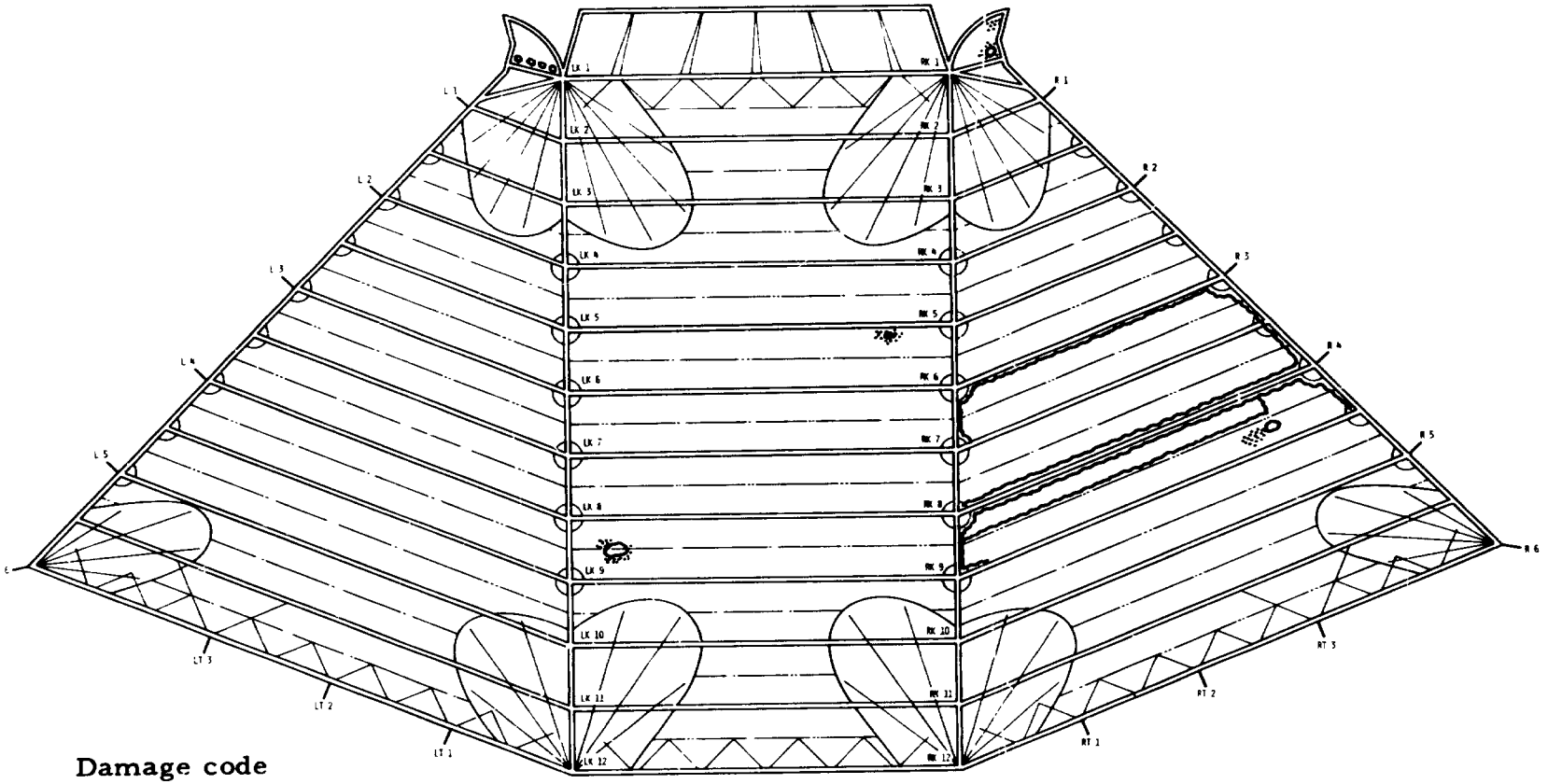

Figure 97. Major canopy damage, Test 208T

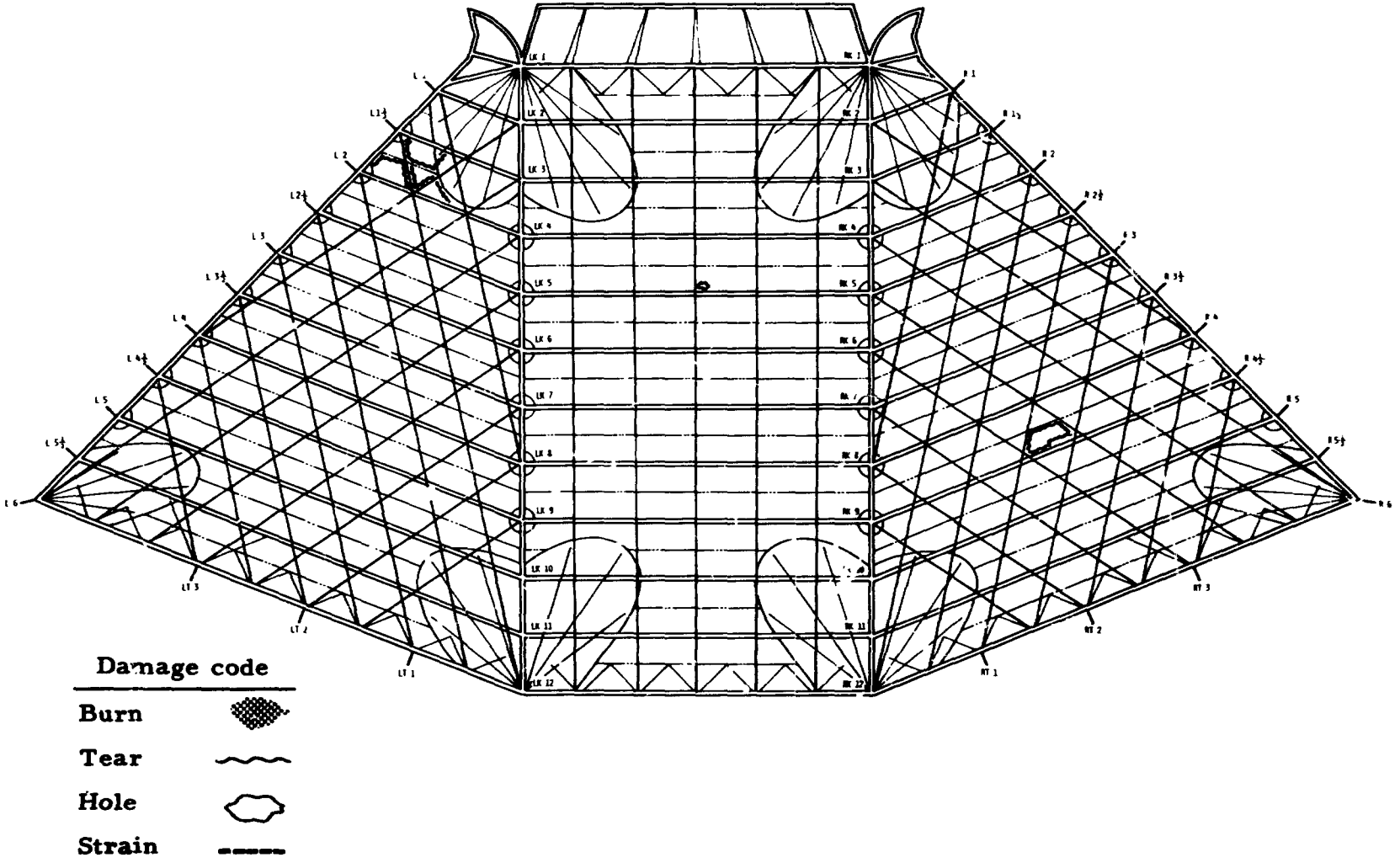

Figure 98. Major canopy damage, Test 211T

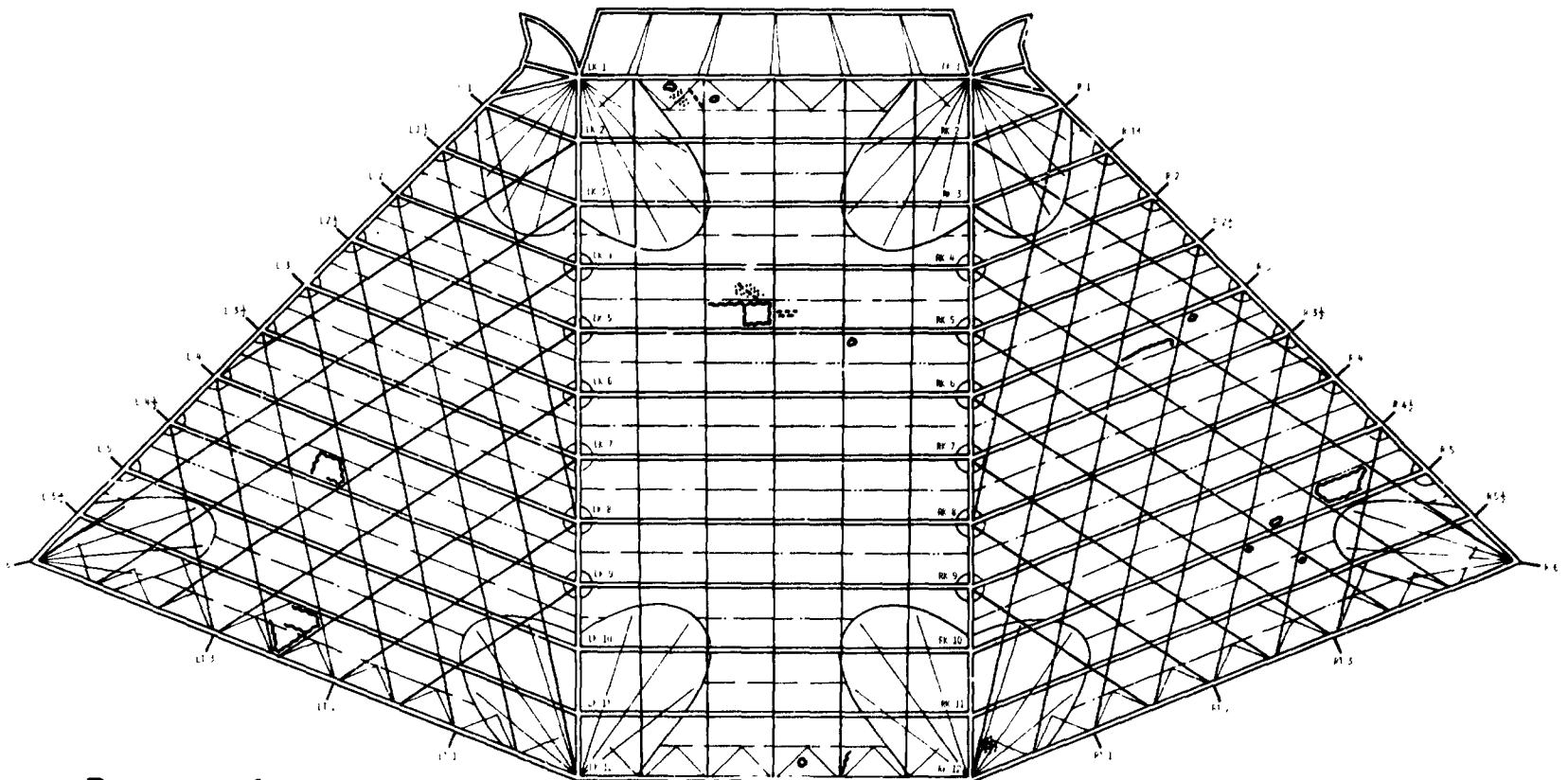

Figure 99. Major canopy damage, Test 206T

Figure 100. Test 206T parawing in gliding flight, showing some of the canopy damage.

related to these four failure modes. Table 12 presents the four failure modes, the time of their occurrence in the deployment process, the apparent cause(s) of the failure mode, the test occurrence and damage identification for each failure mode, and lastly, the corrective actions taken.

Efficacy of the corrective actions. - For three of the four failure modes shown in Table 12, namely, modes 2, 3 and 4, the corrective actions taken were completely successful. For failure mode 1, the corrective action was only partially successful.

In the instance of failure mode 2, 11 flights were flown after the corrective actions had been implemented on the test wings, with no reoccurrence of this failure mode. (Of the 11 rlights the first 3 flights -- 207T, 250T and 251T -- were flown with added lines and larger patches only; the last 8 tests were flown with added lines, larger patches and the ripstop tape matrix.) For failure mode 3, 11 flights were flown after the corrective actions had been implemented, with little if any significant damage in the contoured nose area of the wing. For failure mode 4, 5 tests were flown after the corrective action had been implemented, with no further tear damage in the forward area of the side lobes.

In the case of failure mode 1, the corrective action, consisting of addition of a ripstop tape matrix, was designed to prevent extensive tear propagation of the cloth damage, but not necessarily to eliminate the occurrence of localized cloth damage. The corrective action did perform its design purpose, as demonstrated in 11 tests, beginning with Test 207T. However, localized damage to canopy cloth continued to occur in these 11 tests, with the amount of such damage increasing at the higher deployment dynamic pressures. In 2 tests, notably 211T and 206T, canopy cloth tears occurred with tear propagation confined by the ripstop tapes. These tears, although confined, resulted in holes of significant size in the wing canopies which degraded both the deployment and gliding flight performance of the wings.

TABLE 12.- PARAWING CANOPY FAILURE MODES, TEST OCCURRENCES AND CORRECTIVE ACTION

Failure mode	Time of occurrence in the deployment process	Apparent cause of failure	Test occurrence - damage identification	Corrective action (1)
1. Localized canopy cloth damage, often followed by propagating tears in the cloth until stopped by heavier canopy structure	Initial parawing deployment and 1st stage reefed inflation	Localized cloth abrasion damage during initial canopy stretchout and first stage reefed inflation, and/or localized cloth overload during first stage reefed inflation	201S - panel tearout in right hand lobe 205T - longitudinal tear in right hand lobe 208T - holes in center and right lobe 211T - large hole in right hand lobe 206T - large holes in left, center and right hand lobes	Matrix of ripstop tapes sewn on canopy to limit tear propagation
2. Structural failure in the central areas of the wing leading edges, often followed by propagating tears in the cloth until stopped by heavier canopy structure	2nd stage reefed inflation	High concentrated loads at the number 3 and 4 leading-edge-line-attachment locations, with inadequate canopy structure in the direction of the loads	201S - two-panel tearout in left hand lobe 203T - panel tearout in right hand lobe, torn gusset at R4 208T - three-panel tearout in right hand lobe	a) ten leading edge lines (five on each leading edge) added between existing lines 3 and 6 b) larger semicircular bad distribution patches added in the central, leading-edge-line-attachment locations c) alignment of ripstop tapes to provide structure in the direction of load during 2nd stage inflation
3. Holes, burns and tears in the contoured nose section of the wing	Holes and burns-probably during initial parawing deployment, tears probably during 3rd stage reefed inflation	Cloth burn/abrasion damage from contact with leading edge skirt band and/or nose snubber lines, tears due to dynamic loading condition following 2nd stage disreef	202T - 2 large tears and numerous burn holes and burn areas in contoured nose panel 205T - numerous small holes in contoured nose panel	a) encasement of the five nylon-nose-snubber lines in cotton sateen sleeves b) separate reefing added for the nose section of the wing
4. Tears in the forward areas of the side lobes, between the leading edge skirt band and the edge of the forward keel line fan patch	2nd or 3rd stage reefed inflation	Marginal canopy structural strength in the direction of load during 2nd or 3rd stage reefed inflation	211T - tears in forward portion of left hand lobe, between the leading edge skirt band and the forward keel line fan patch	Four fan-patch tapes extended to the intersection of existing ripstop tapes

(1) accomplished on the two keel parawing only

Thus, in the case of failure mode 1, the corrective action can only be considered as partially successful. Possible avenues toward minimizing or eliminating localized canopy cloth damage during the initial phases of parawing deployment include improved canopy cloth materials, a protective covering for the damage-susceptible canopy cloth areas, selective canopy porosity to minimize canopy buffeting following initial canopy stretchout, or alternative reefing schemes which provide better control of the canopy cloth following initial canopy deployment.

GLIDING FLIGHT PHASE

Straight Flight Aerodynamic Test Data

General. - The following paragraphs, figures, and table present the straight-gliding-flight data obtained during the controllable vehicle flights and bomb vehicle tests. The data are presented in groups, with each group containing the data obtained during one test flight. The type of data obtained during the test, plus any items of special interest concerning the data are discussed. Generally, the data plots show L/D, lift coefficient, drag coefficient, and resultant force coefficient as a function of tip-suspension-line-length and/or rear-keel-suspension-line length.

As discussed in APPENDIX B, the instrumentation which measured angle-of-attack, velocity and angle-of-sideslip in these tests was calibrated in a wind tunnel. However, data processed using the corrections indicated by the wind tunnel tests showed large deviations, compared with gliding flight performance data obtained by phototheodolite tracking (ASKANIA). When the uncorrected L/D data determined by the on-board test instrumentation were compared with ASKANIA determined L/D data, excellent correlation between the two sets of data was obtained. Consequently, all of the flight test data from the controllable test vehicle flights presented in this

report are based directly on the flight angles indicated by the test instrumentation. No corrections were made to the flight data for interference effects on the test instrumentation due to the upwash from the wing, or for flow field deviations due to the proximity of the test instruments to the test vehicle. Also, no corrections were made to the data to account for the drag and lift of the test vehicle. Wind tunnel data and small-scale free flight data used in this report were taken from Reference 1. Detailed descriptions of the small-scale models and more complete data are available in Reference 1.

Test 250T. - This was the first test with a 4000-square foot, twin keel parawing utilizing a controllable test vehicle. Twin keel parawing Version III was used for this test at a wing loading of 0.86 psf. During this test, a wide range of tip-suspension-line lengths was tested. Only two rear-keel-suspension-line lengths were tested. The flight path data obtained during this flight indicated maximum L/D values of approximately 2.0 which were much lower than had been obtained during previous bomb vehicle tests. The flight maneuver pattern during this test was such that valid flight path angle data could not be obtained from ASKANIA. Thus, the validity of the data obtained from the on-board flight path measuring instrumentation could not be checked. Figures 101 through 104 present data from this test.

Test 251T. - Twin keel parawing Version III was used for this test at a wing loading of 0.99 psf. Variations in both the tip-suspension-line lengths and the rear-keel-suspension-line lengths were tested. L/D performance (approximately 3.0) measured by the on-board instrumentation was in the range of values previously obtained during wind tunnel and free flight tests. As with Test 250T, an ASKANIA check on L/D performance could not be obtained in this test. Figures 105 through 108 present data from this test.

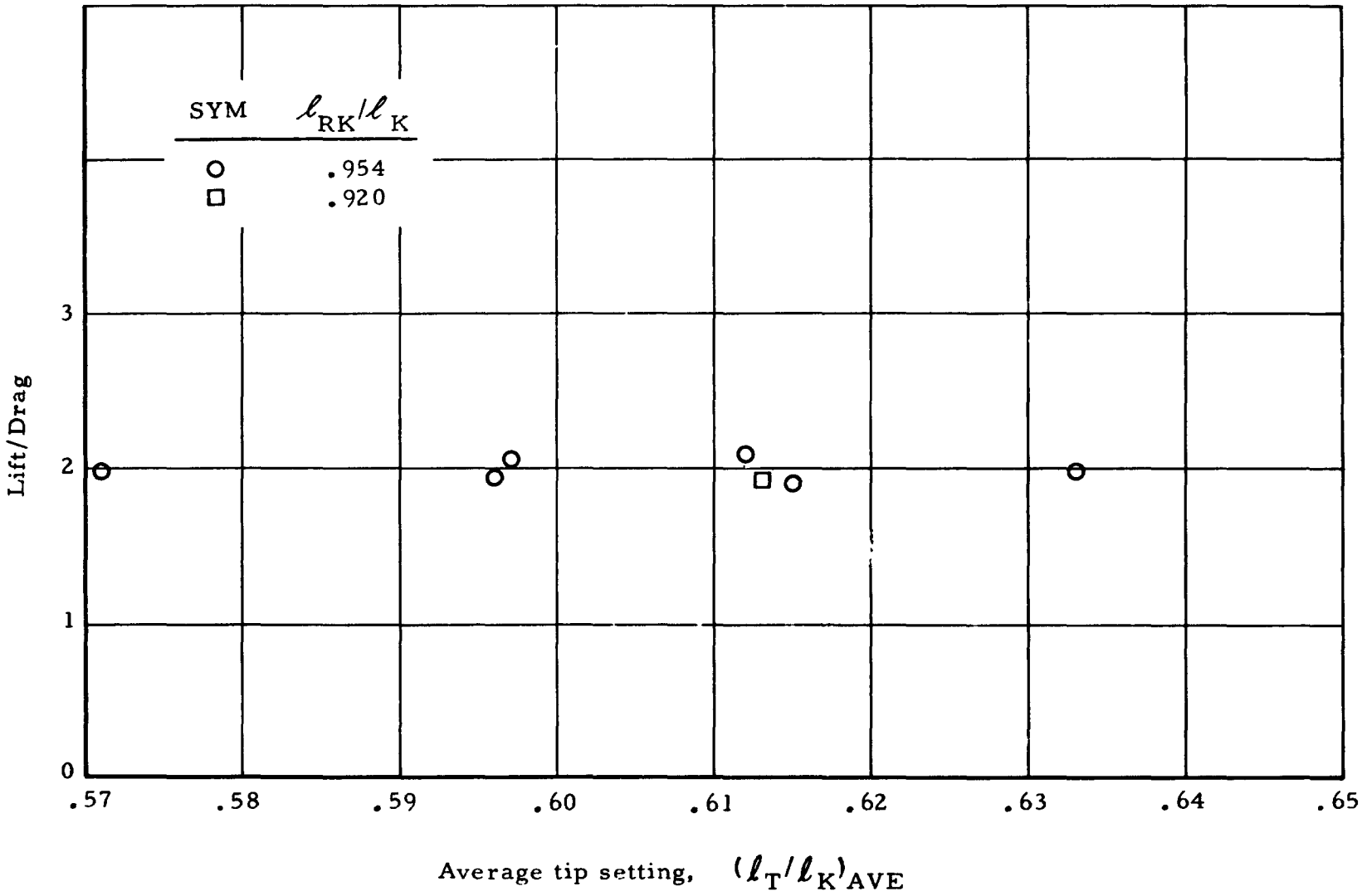

Figure 101. Lift-to-drag ratio versus average tip setting, Test 250T

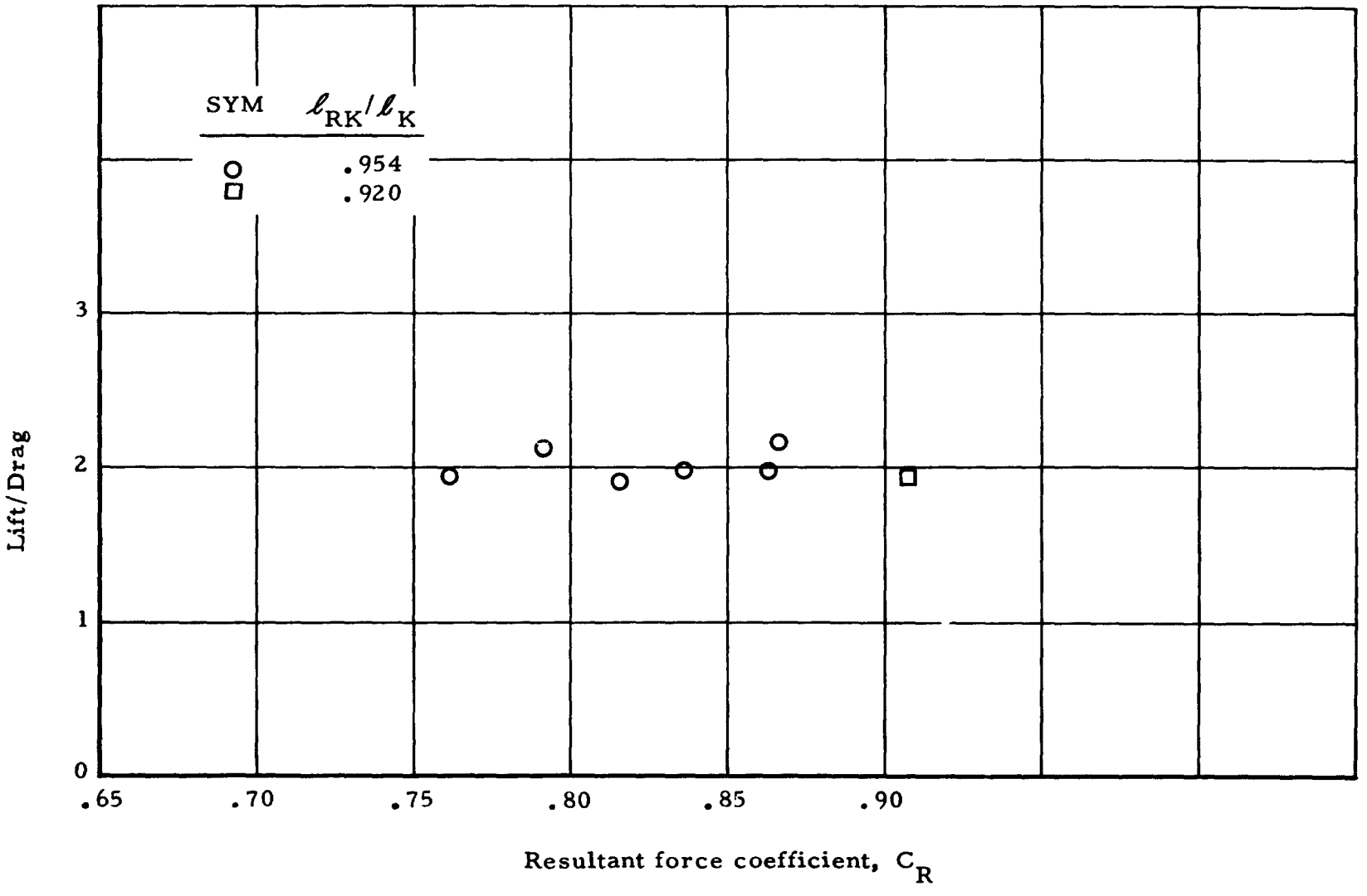

Figure 102. Lift-to-drag ratio versus resultant force coefficient, Test 250T

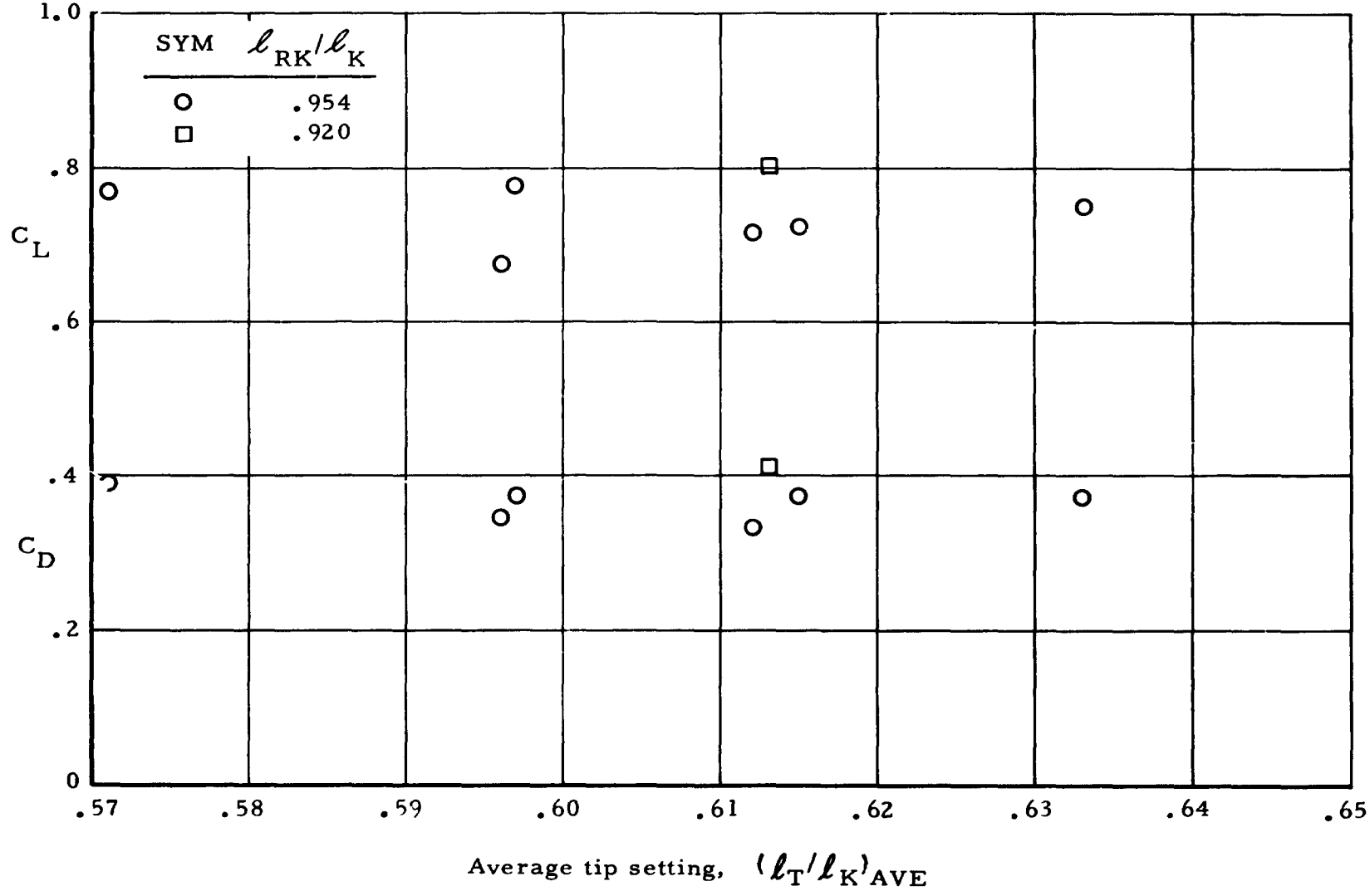

Figure 103. Lift coefficient and drag coefficient versus average tip setting, Test 250T

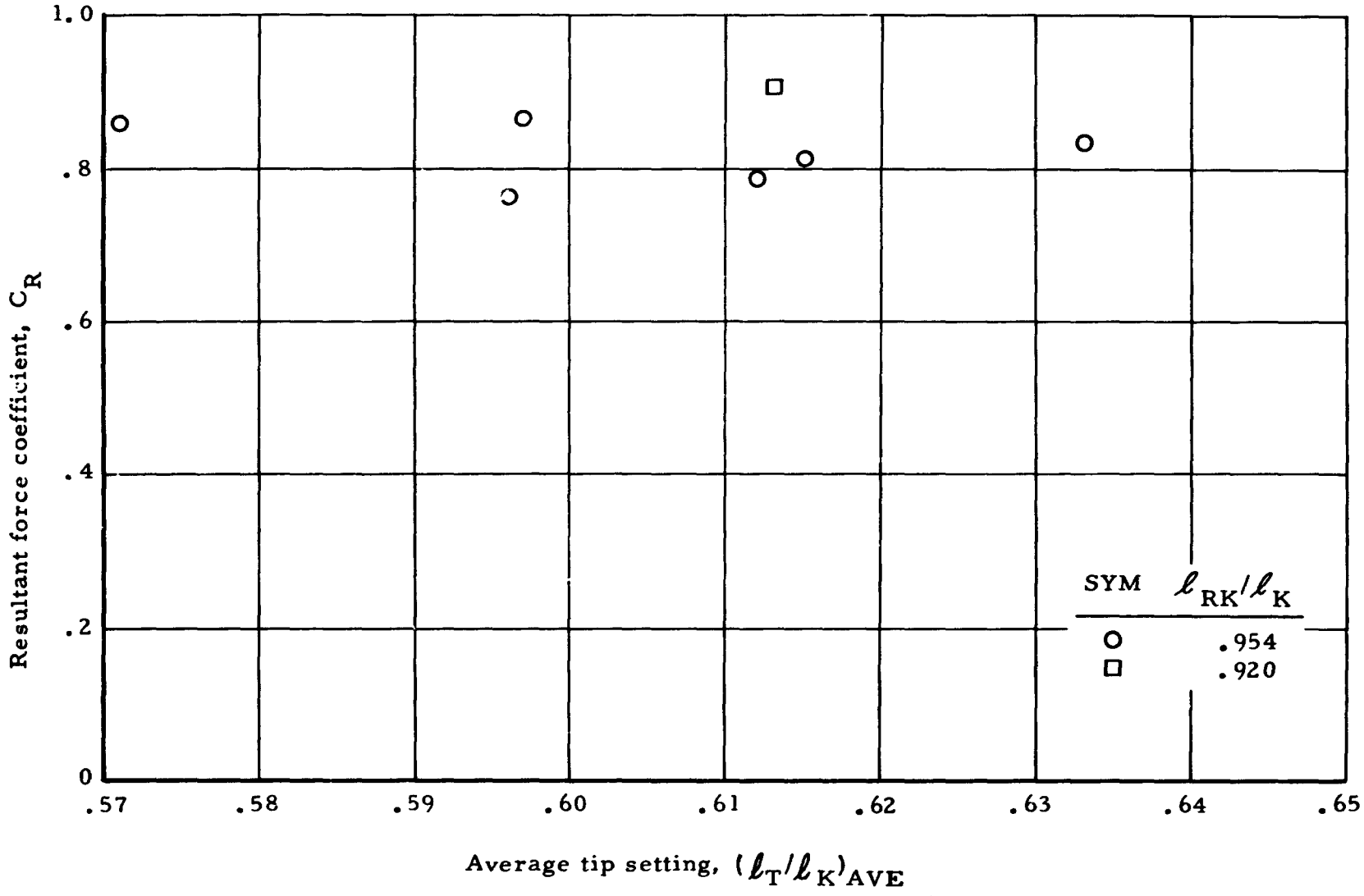

Figure 104. Resultant force coefficient versus average tip setting, Test 250T

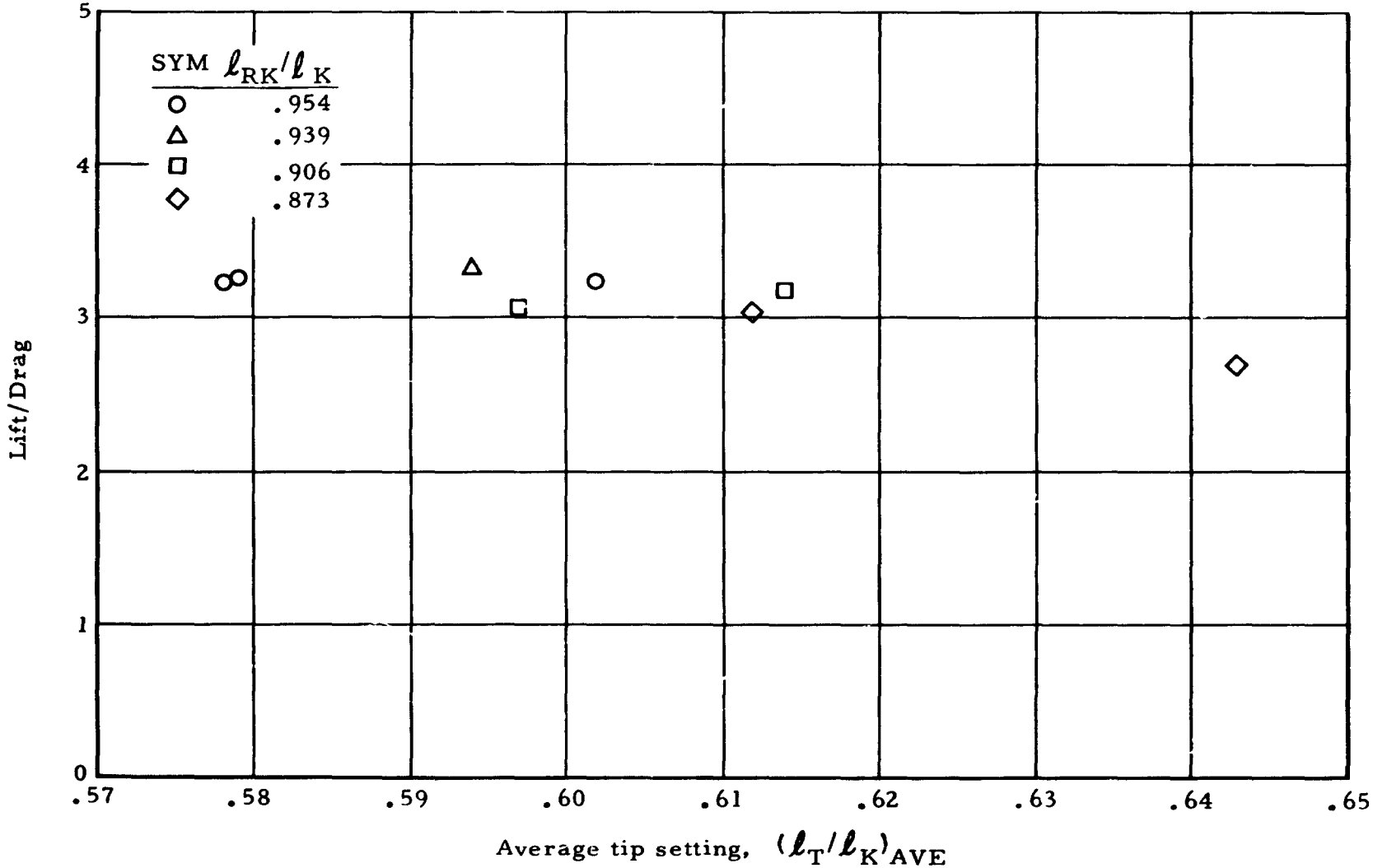

Figure 105. Lift-to-drag ratio versus average tip setting, Test 251T

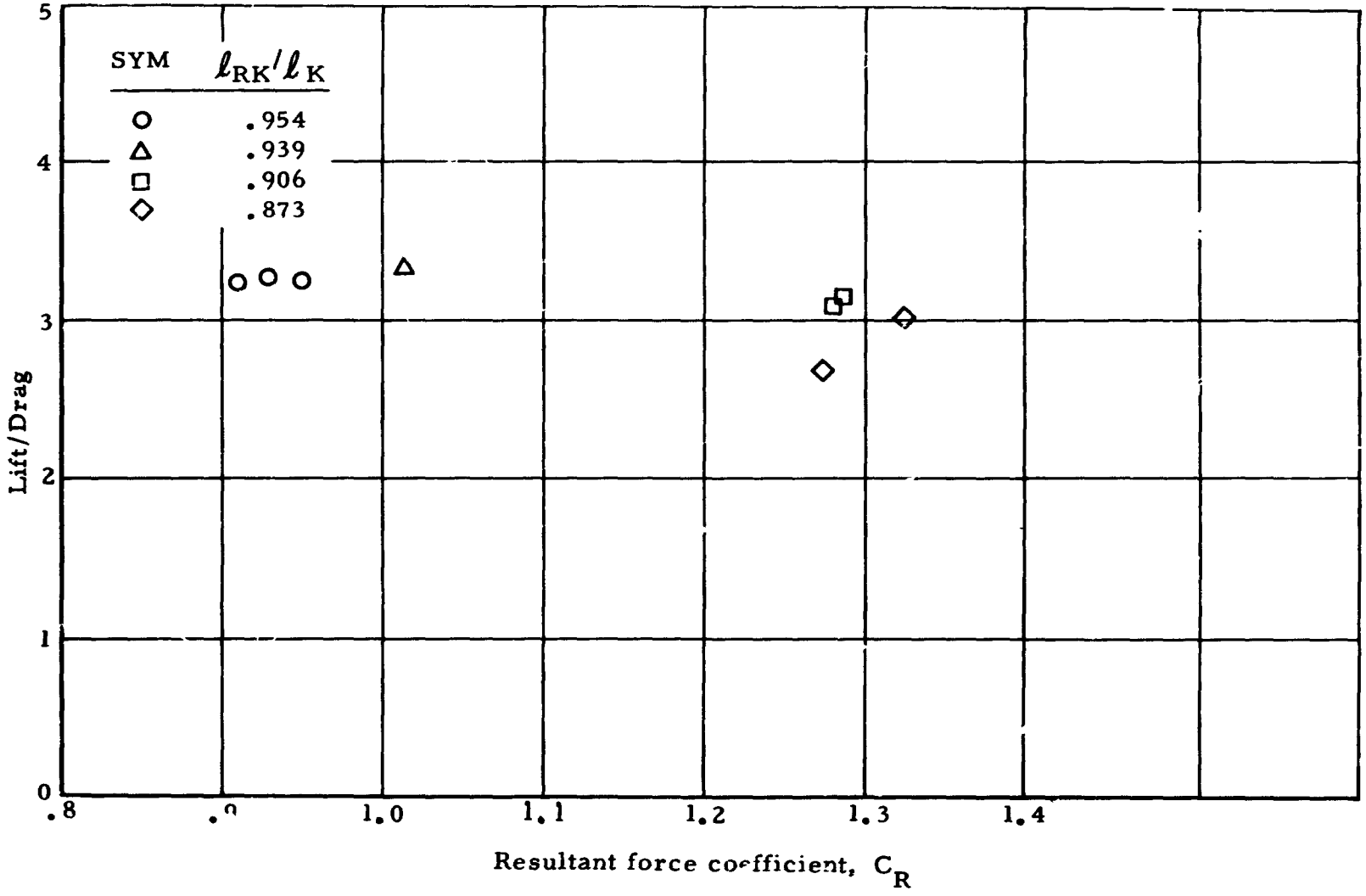

Figure 106. Lift-to-drag ratio versus resultant force coefficient, Test 251T

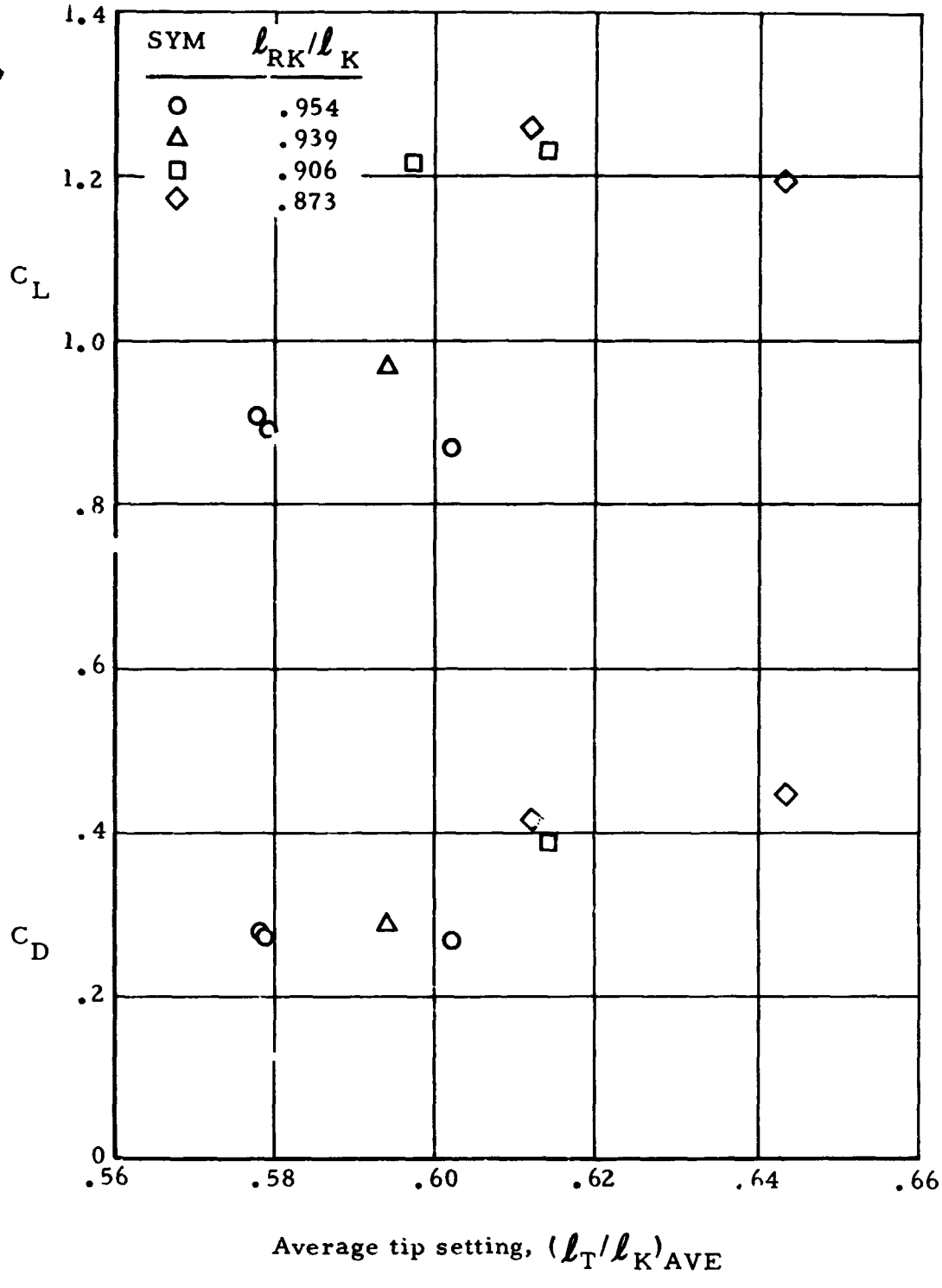

Figure 107. Lift coefficient and drag coefficient versus average tip setting, Test 251T

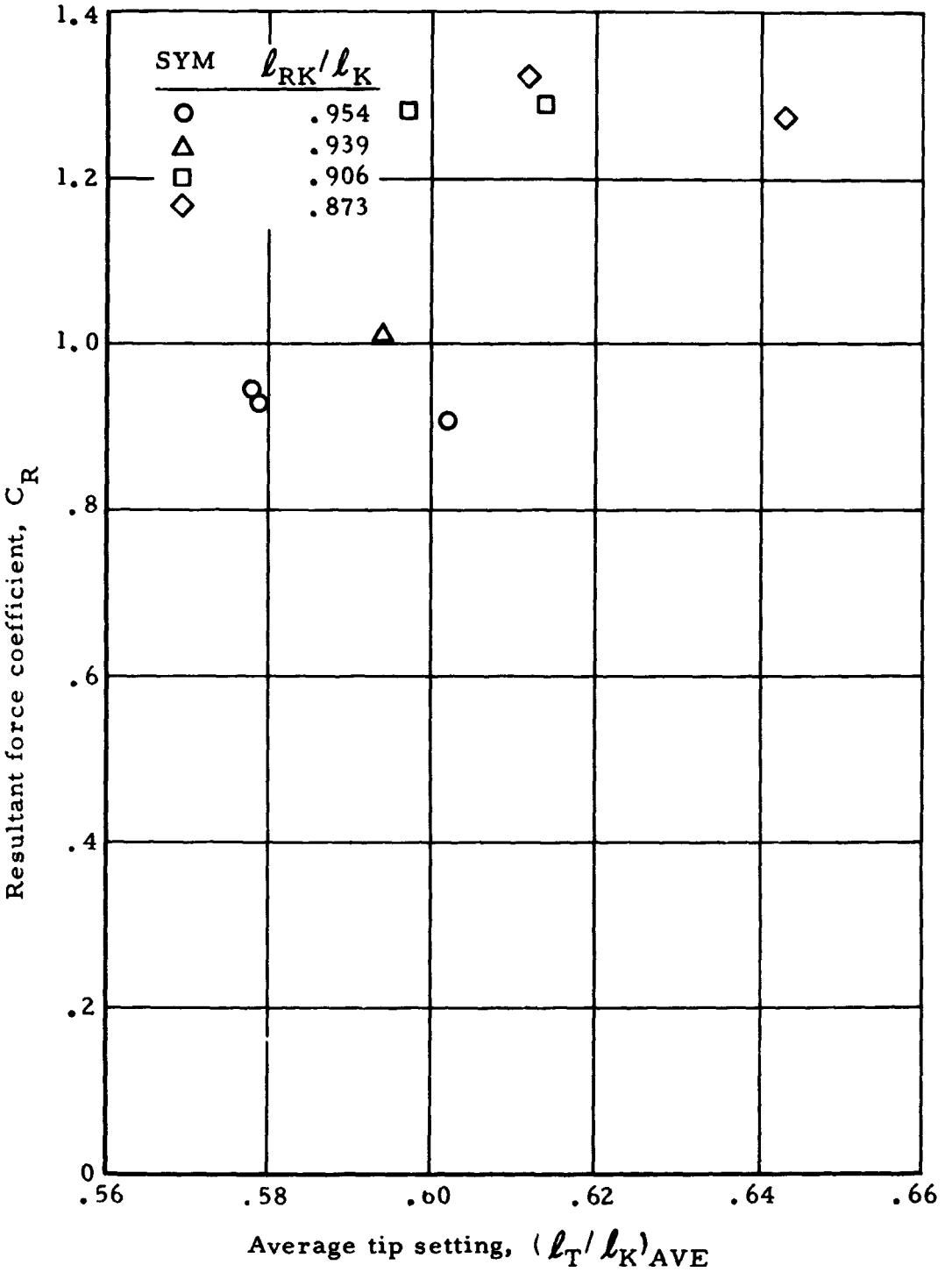

Figure 108. Resultant force coefficient versus average tip setting, Test 251T

Test 252T. - Twin keel parawing Version IV was used for this test at a wing loading of 1.0 psf. During this test, the on-board airspeed indicator was damaged; as a result, no airspeed data were obtained. The lack of airspeed data precluded calculation of the lift, drag, and resultant force coefficients. The flight path angle data obtained from the on-board instrumentation during this flight agreed quite well with flight path angle data obtained from ASKANIA. Figures 109 and 110 present data from this test.

Test 253T. - Twin keel parawing Version VI was used for this test at a wing loading of 1.25 psf. During this test a range of lengths was tested for both the tip suspension lines and the rear keel suspension lines. The airspeeds measured by the on-board airspeed indicator during this test appear low, relative to values measured on other tests. The possibility exists that the airspeed indicator was damaged prior to the gliding portion of the flight, although positive evidence of damage was not obtained. Because of the relatively low airspeed values measured, the values computed for lift, drag, and resultant force coefficients were appreciably higher than those obtained during the other 4000-square foot parawing flight tests. For this flight, the flight path angle data from ASKANIA agreed quite well with the flight path angle data obtained from the on-board instrumentation. The gliding flight data from Test 253T are presented in Figures 111 through 115.

Test 254T. - Twin keel parawing Version VI was used for this test at a wing loading of 1.50 psf. During this test, a range of lengths was tested for both the tip suspension lines and the rear keel suspension lines. No unusual occurrences were noted during this flight. The gliding flight data from this test are presented in Figures 116 through 120. The maneuvers performed during this test precluded any attempt to compare flight path angle data from ASKANIA with comparable data measured by on-board instrumentation.

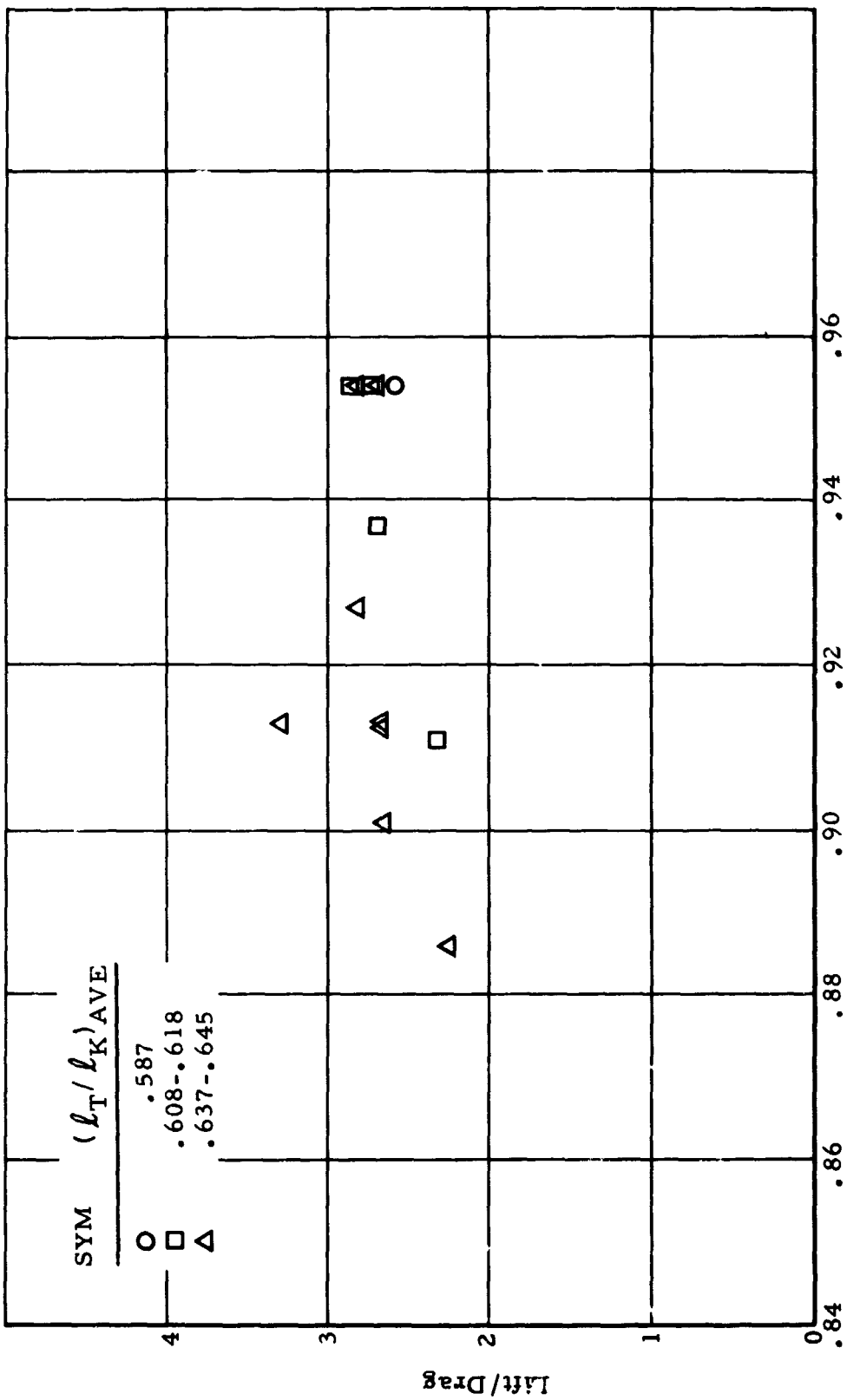

Figure 109. Lift-to-drag ratio versus rear keel setting, Test 252T

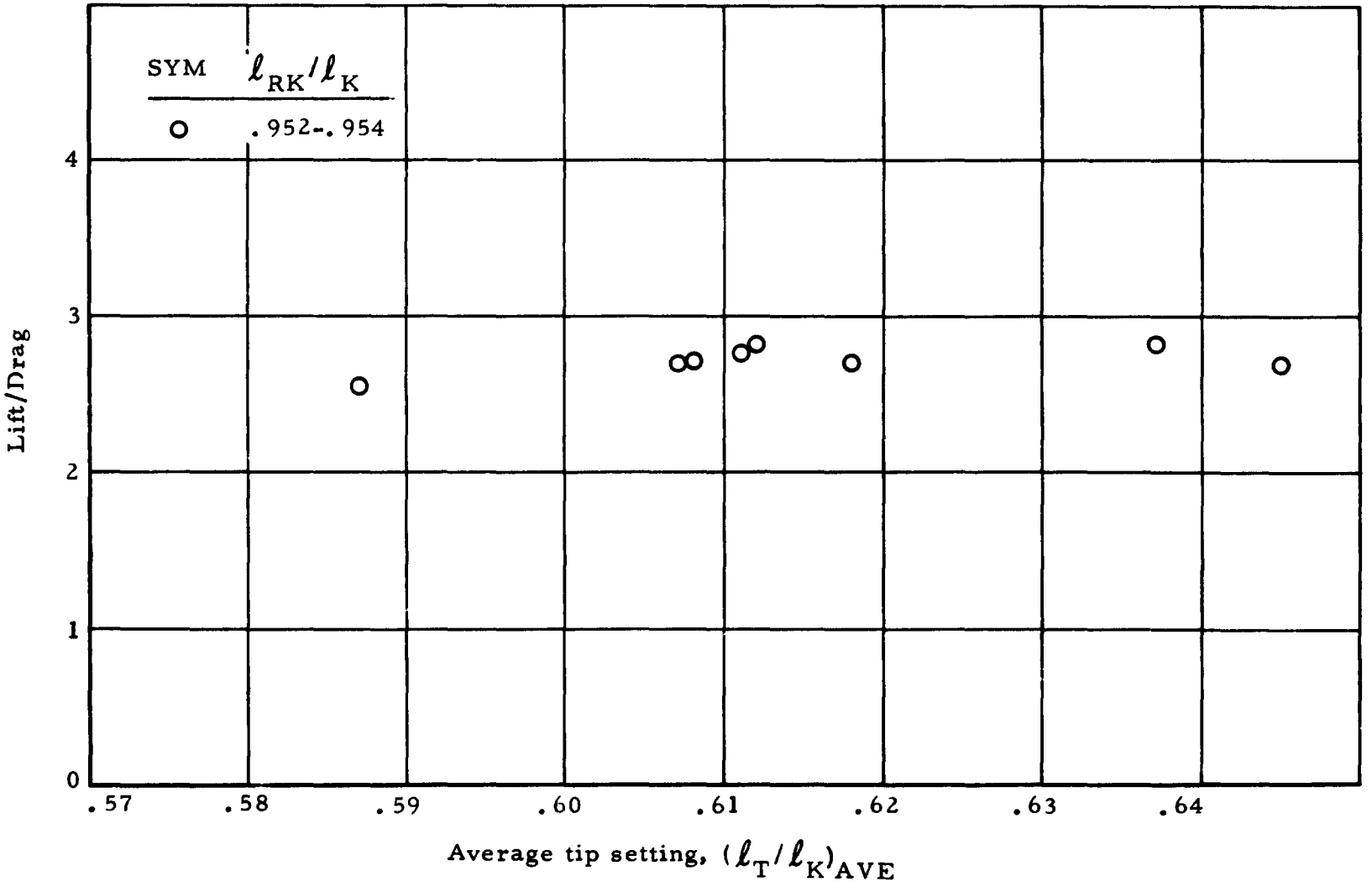

Figure 110. Lift-to-drag ratio versus average tip setting, Test 252T

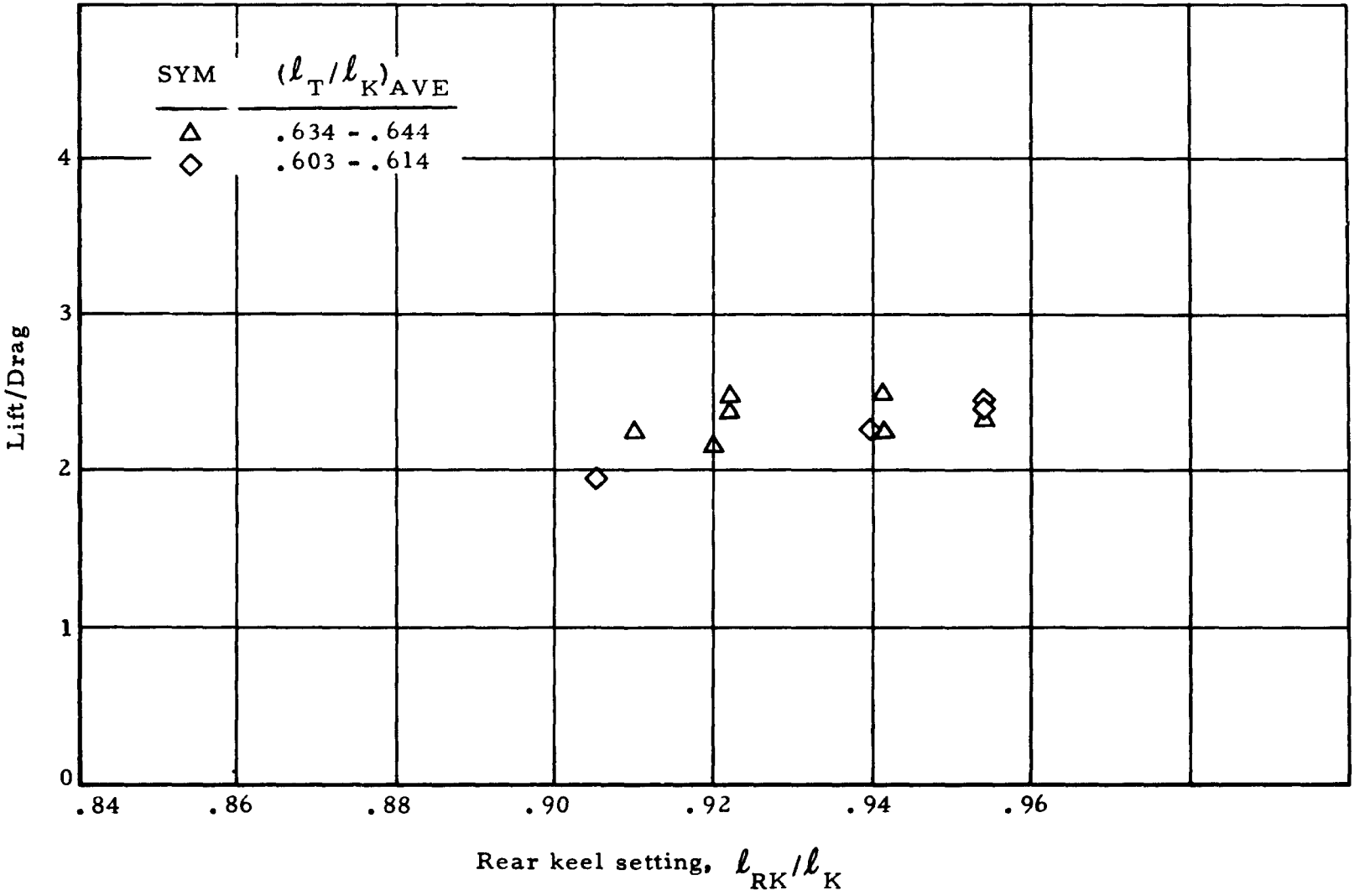

Figure 111. Lift-to-drag ratio versus rear keel setting, Test 253T

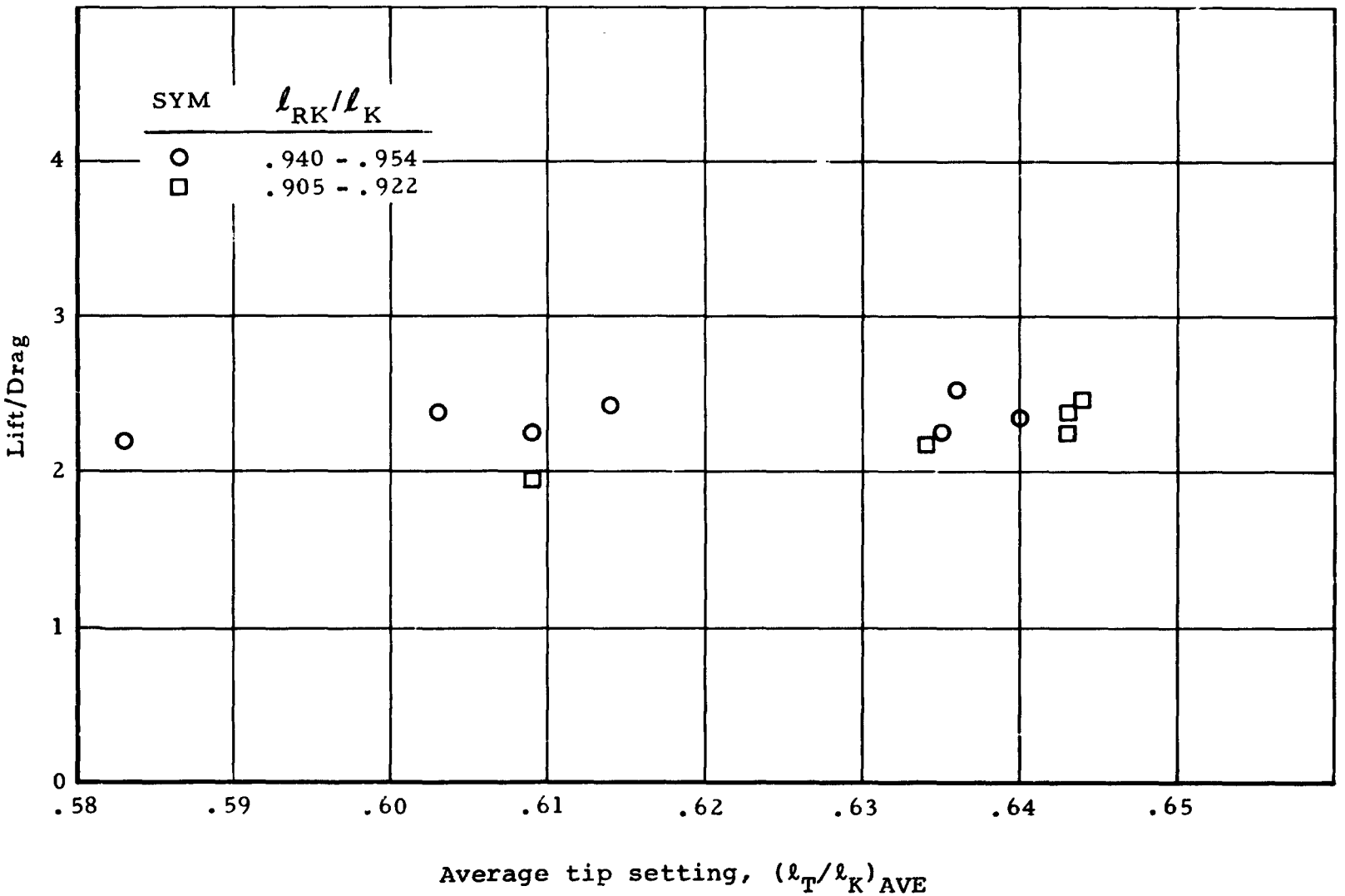

Figure 112. Lift-to-drag ratio versus average tip setting, Test 253T

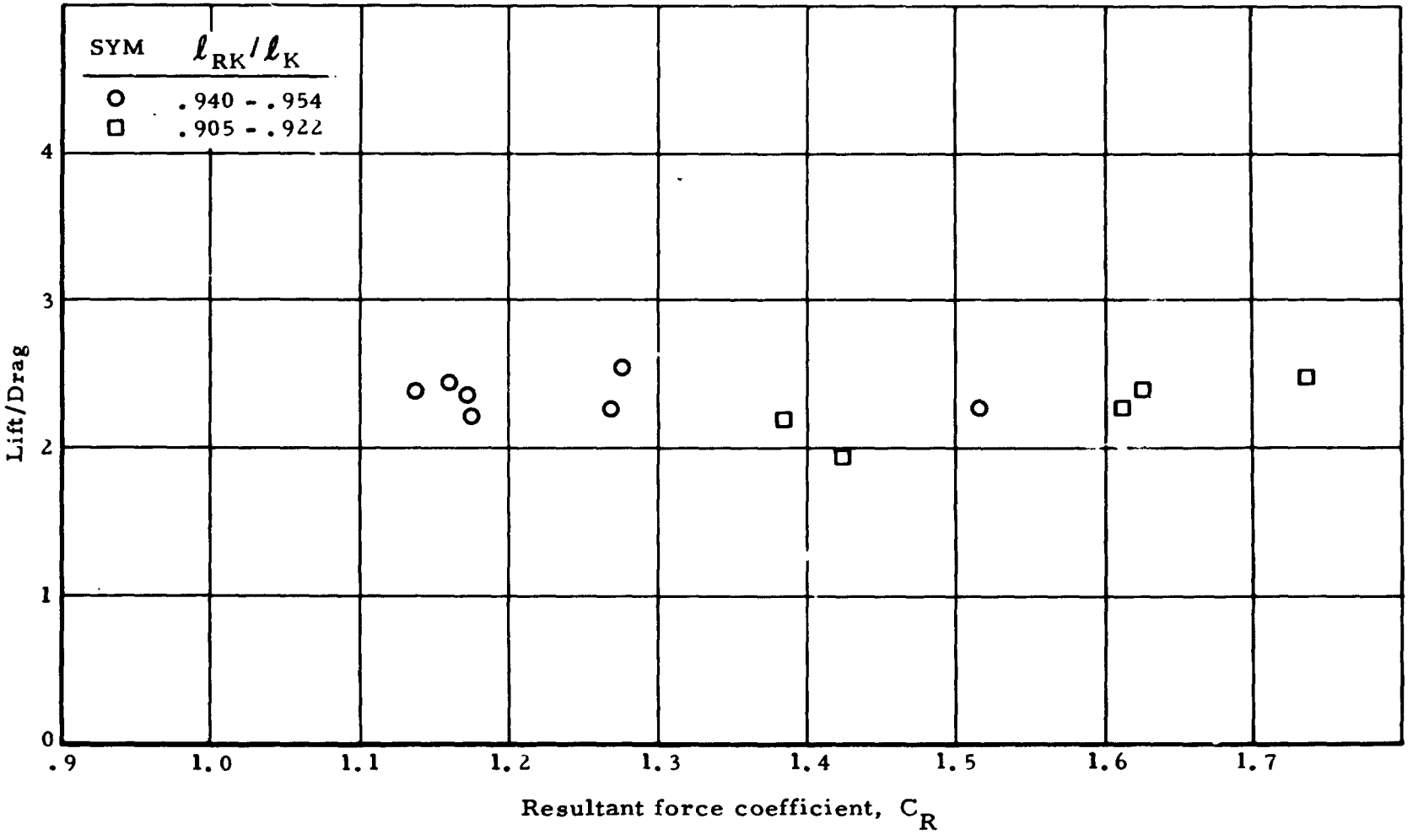

Figure 113. Lift-to-drag ratio versus resultant force coefficient, Test 253T

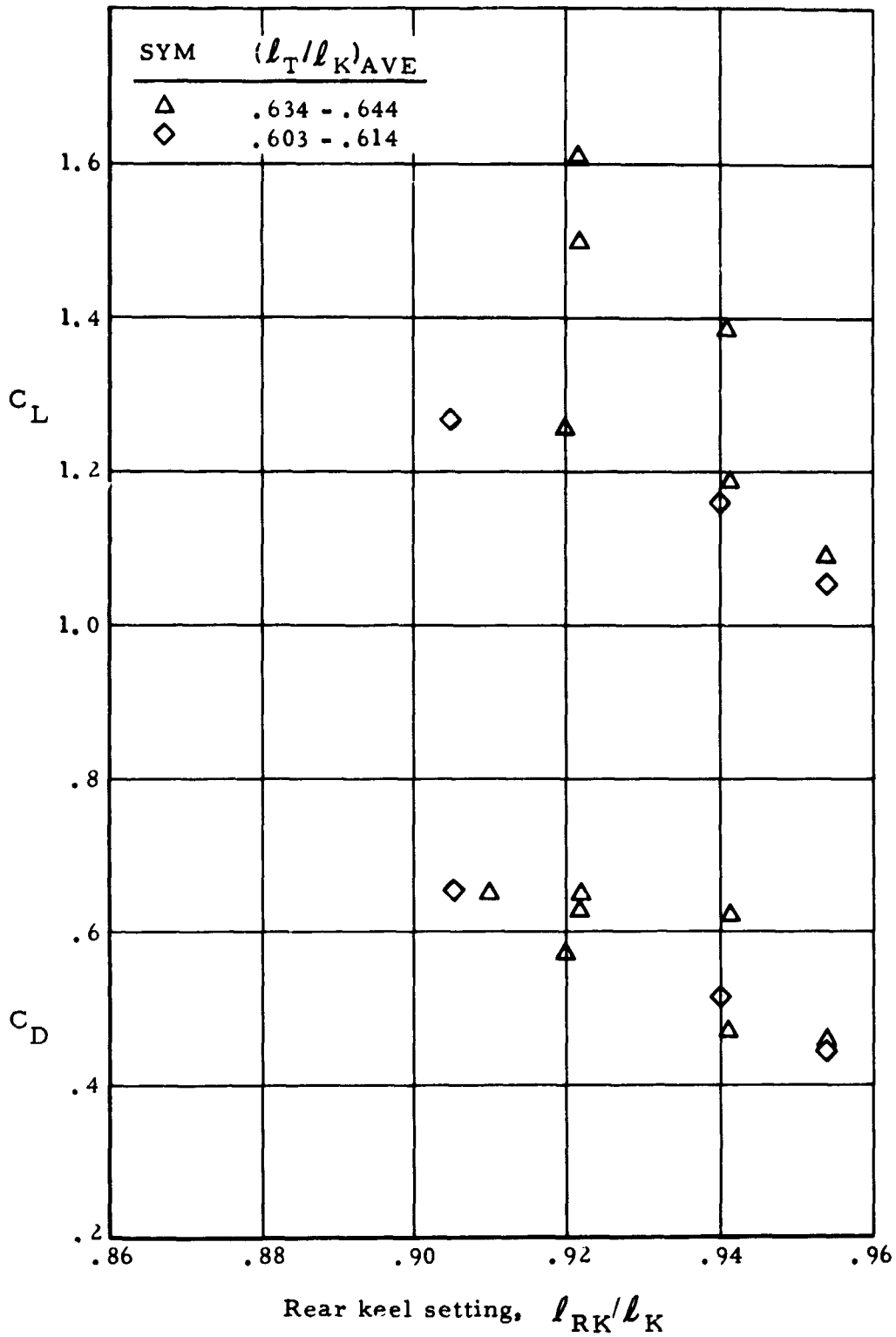

Figure 114. Lift coefficient and drag coefficient versus rear keel setting, Test 253T

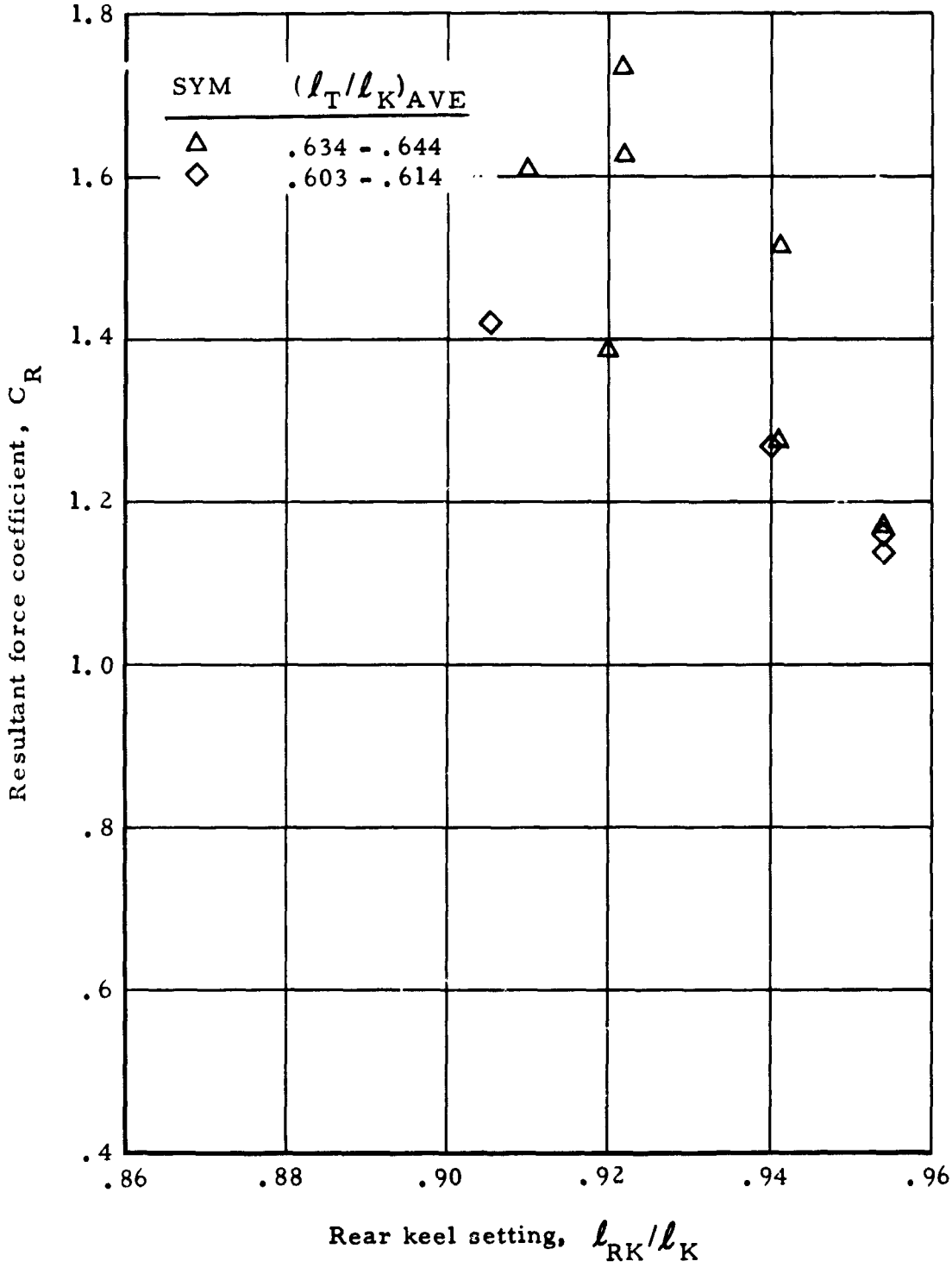

Figure 115. Resultant force coefficient versus rear keel setting, Test 253T

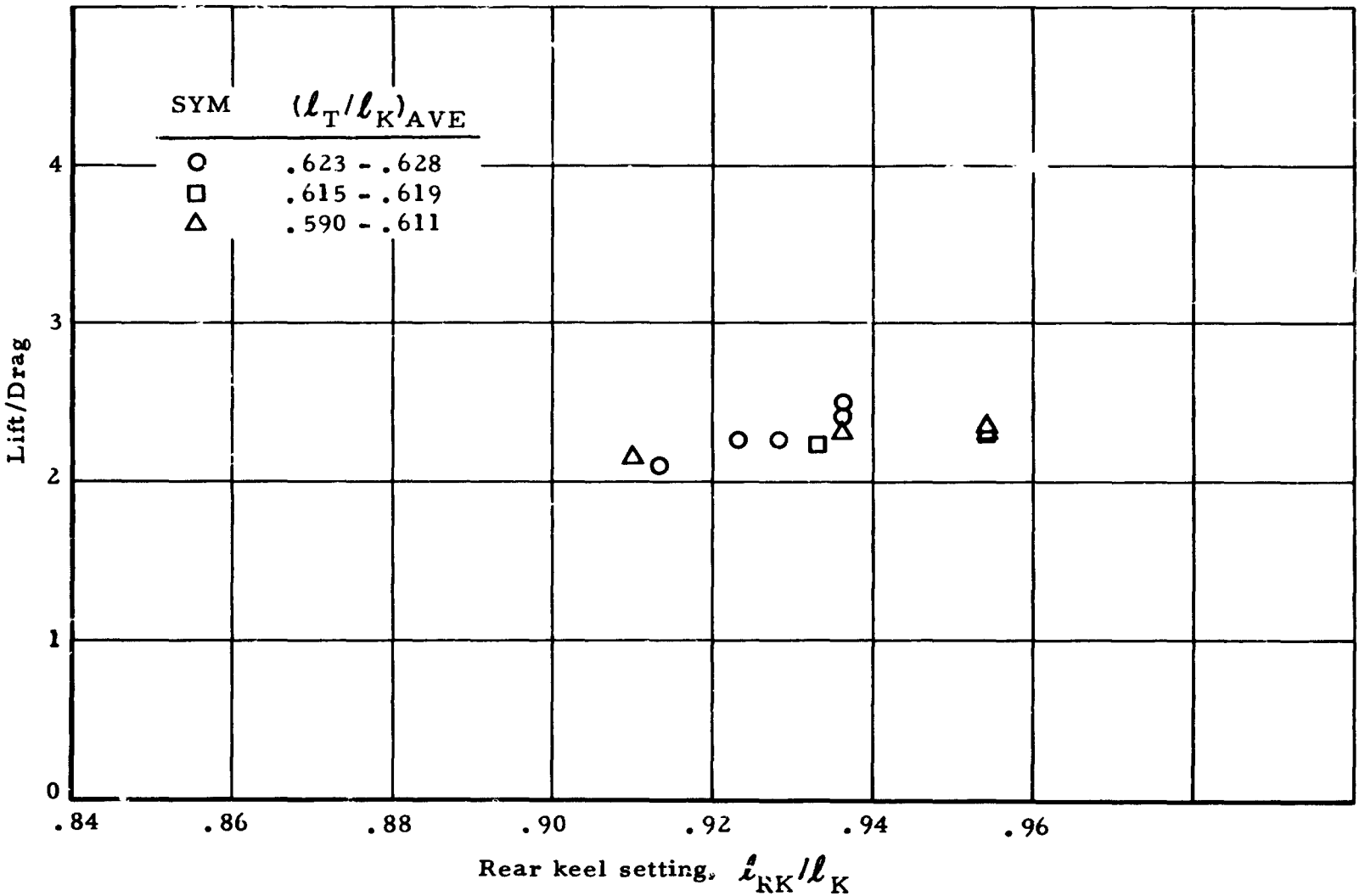

Figure 116. Lift-to-drag ratio versus rear keel setting, Test 254T

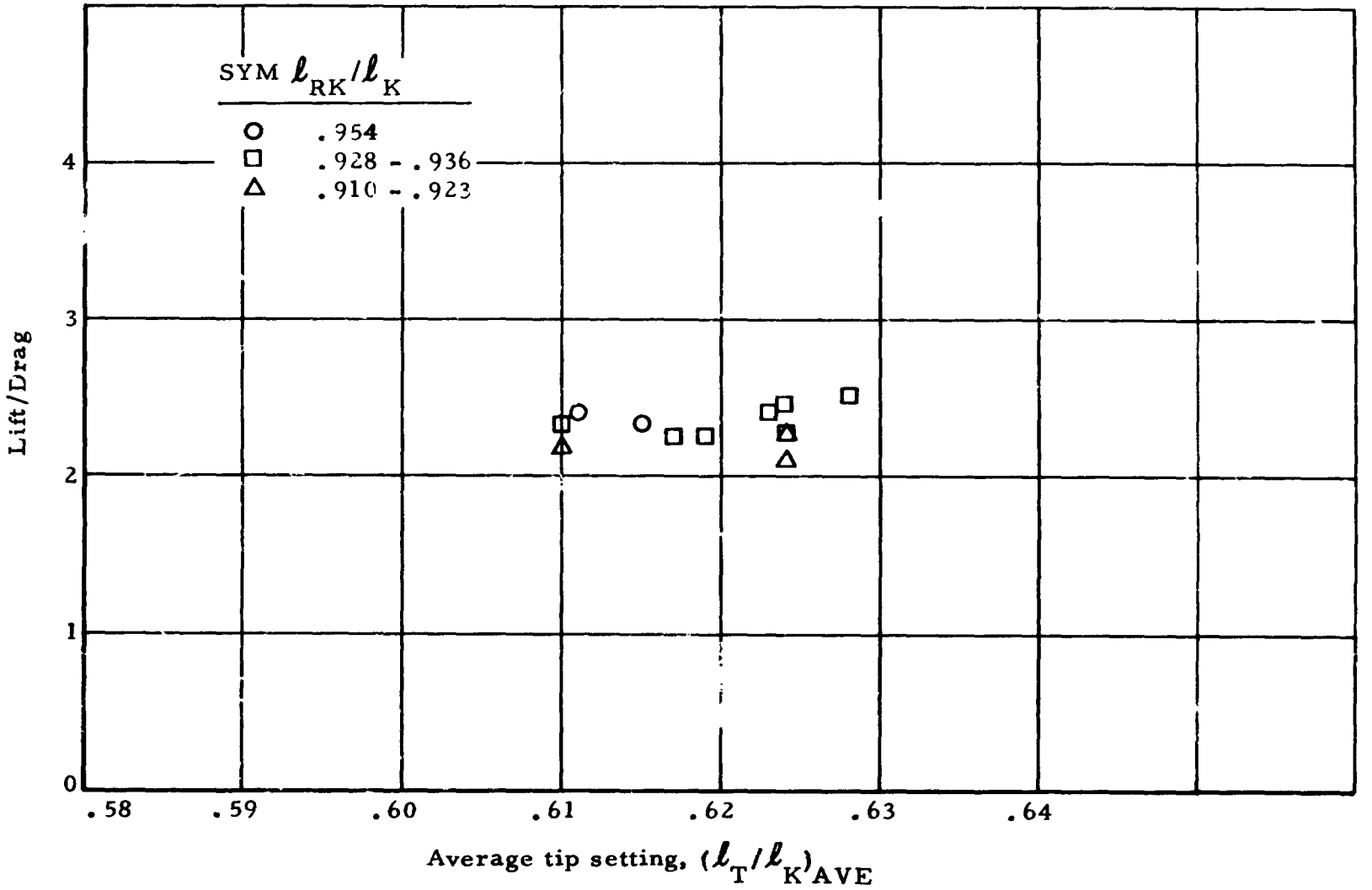

Figure 117. Lift-to-drag ratio versus average tip setting, Test 254T

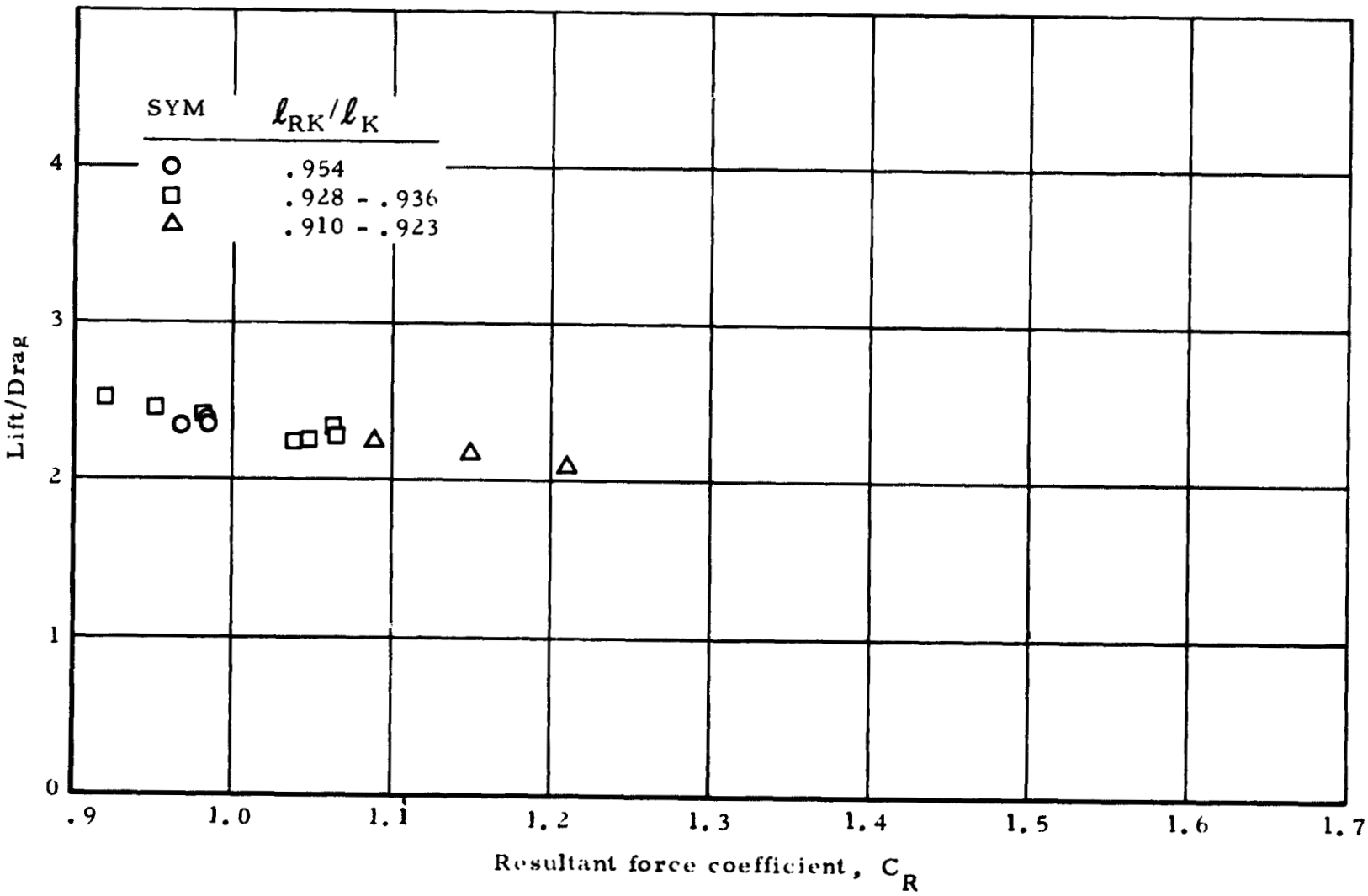

Figure 118. Lift-to-drag ratio versus resultant force coefficient, Test 254T

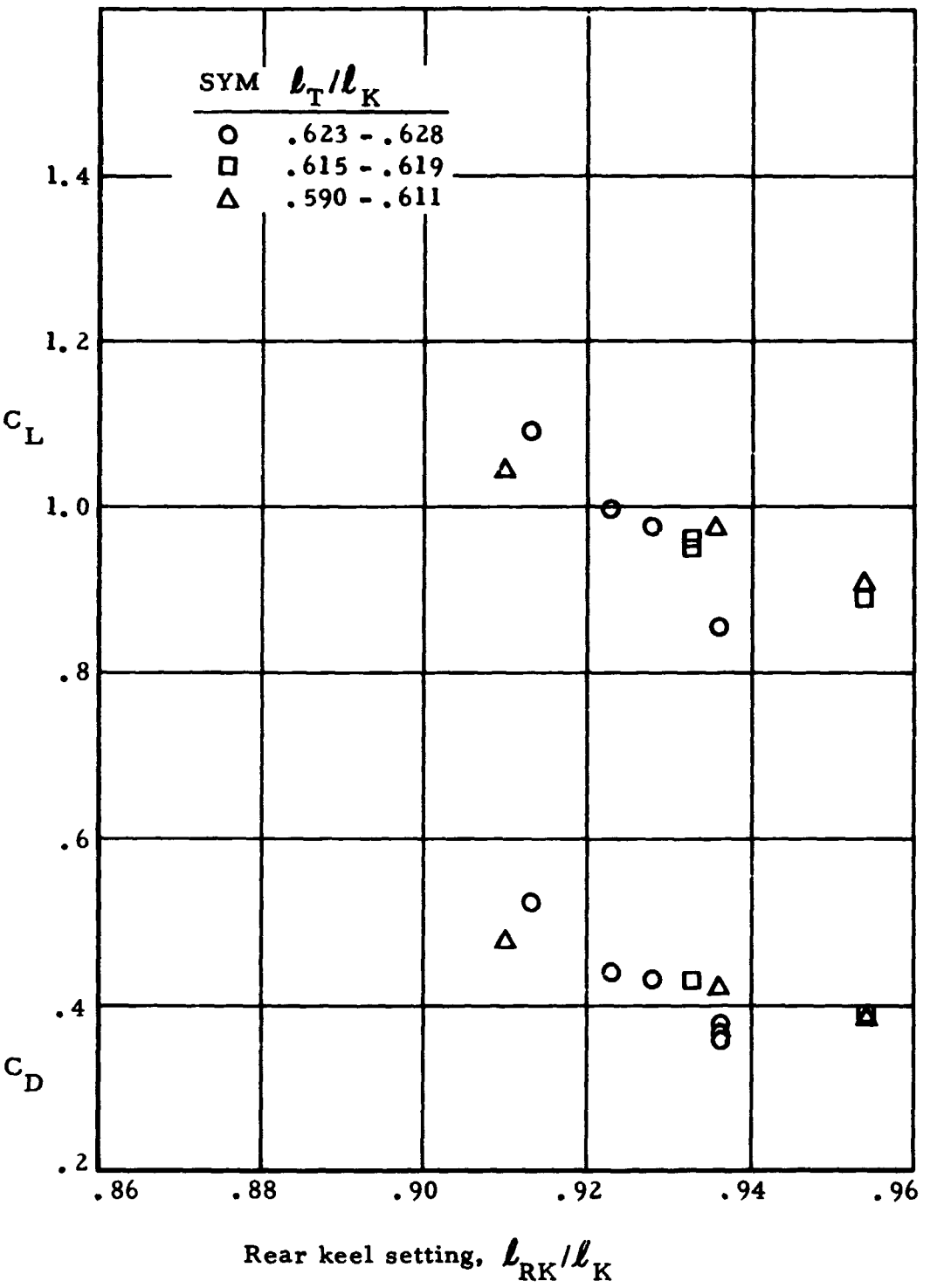

Figure 119. Lift coefficient and drag coefficient versus rear keel setting, Test 254T

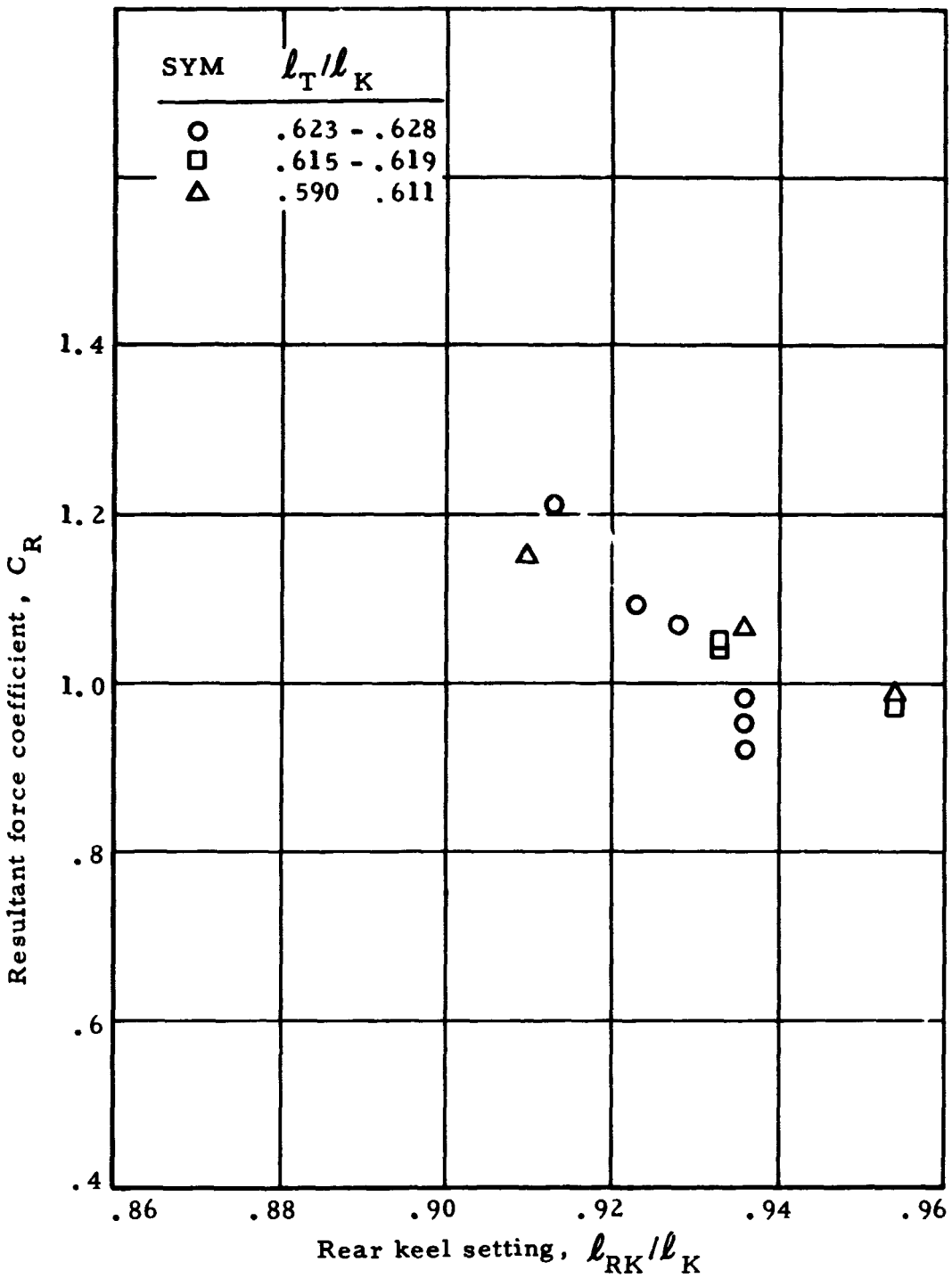

Figure 120. Resultant force coefficient versus rear keel setting, Test 254T

Test 255T. - Twin keel parawing Version VI was used for this test at a wing loading of 1.50 psf. During this test, only a range of tip-suspension-line lengths was tested. No unusual occurrences were noted during this flight. The gliding flight data from this test are presented in Figures 121 through 124. The maneuvers performed during this test precluded an attempt to compare flight path angle data from ASKANIA with comparable data measured by on-board instrumentation.

Bomb test data. - Table 13 gives gliding performance data from three bomb vehicle tests. These data were obtained from ASKANIA and represent averages of flight path angle and velocity over the entire portion of the flight after steady-state gliding conditions were achieved. The data from only three tests (205T, 209T and 210T) are shown in Table 13. These were the only tests during which the parawing test specimen was in a normal operating condition during the gliding portion of the flight, and during which sufficient ASKANIA data were obtained to give reliable averages. In order to obtain reliable ASKANIA data for gliding flight it was necessary that the parawing fly in a relatively slow spiral maneuver. With this flight pattern ASKANIA data from several complete 360-degree turns could be utilized, in order to average out the effects of wind and vertical air mass movements on the data.

TABLE 13. - GLIDING FLIGHT TEST RESULTS FROM BOMB VEHICLE TESTS

Test	W/S, psf	ℓ_{RK}/ℓ_K	$(\ell_T/\ell_K)_{AVE}$	L/D	C_L	C_D	C_R
205T	1.25	.954	.603	2.75	.618	.225	.658
209T	.953	.954	.603	2.93	.577	.197	.610
210T	.953	.954	.603	2.69	.606	.224	.646

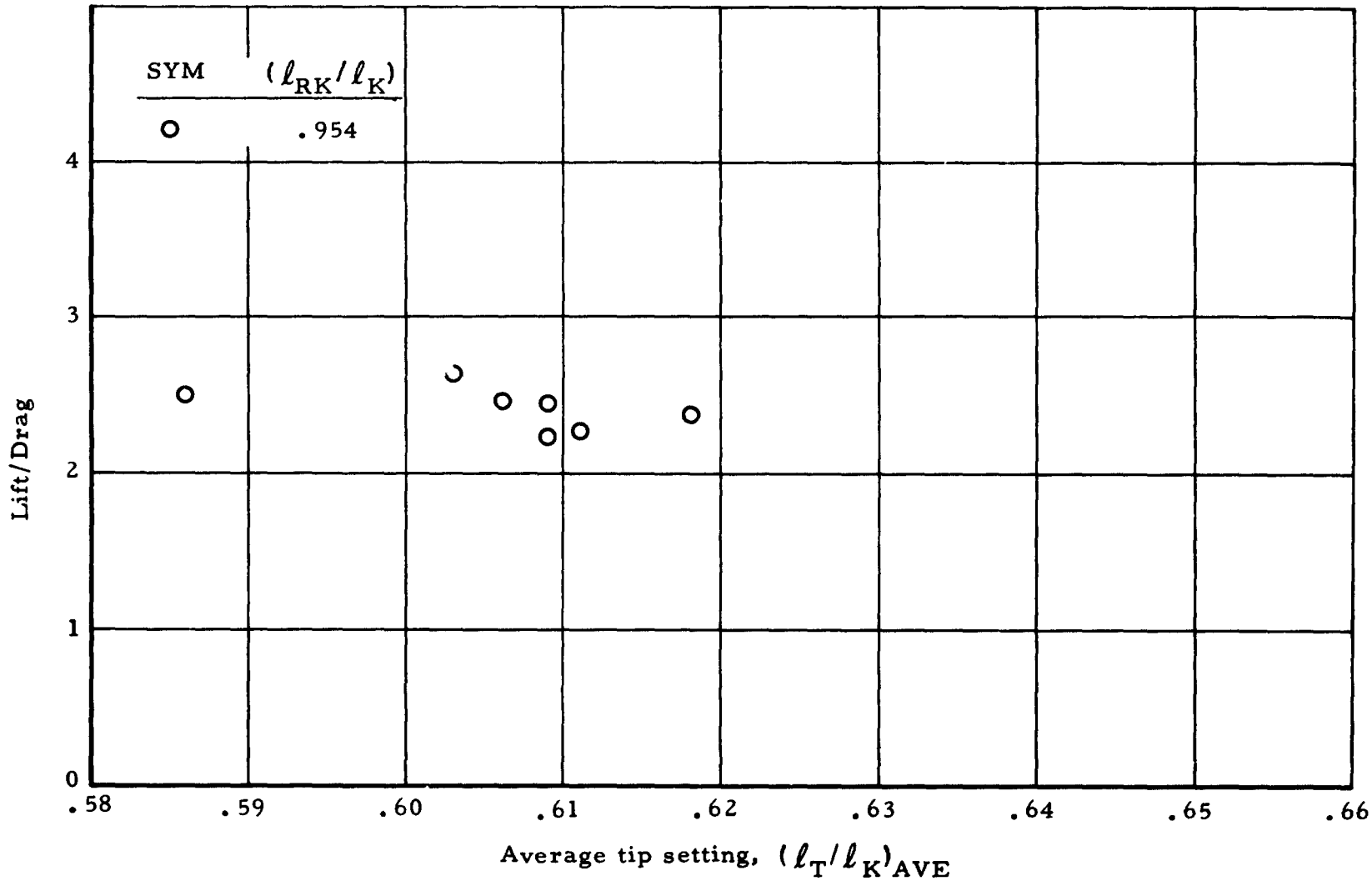

Figure 121. Lift-to-drag ratio versus average tip setting, Test 255T

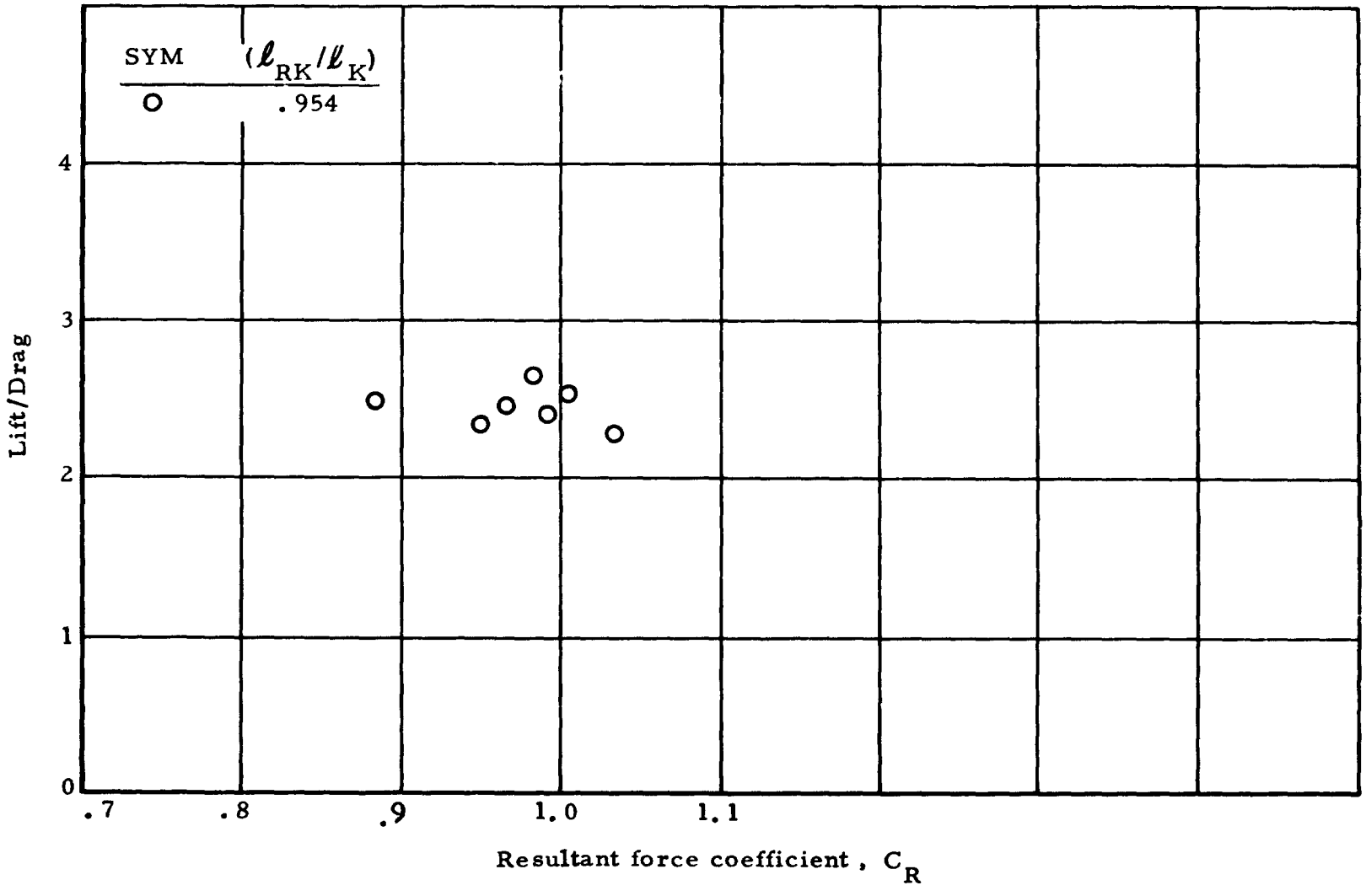

Figure 122. Lift-to-drag ratio versus resultant force coefficient, Test 255T

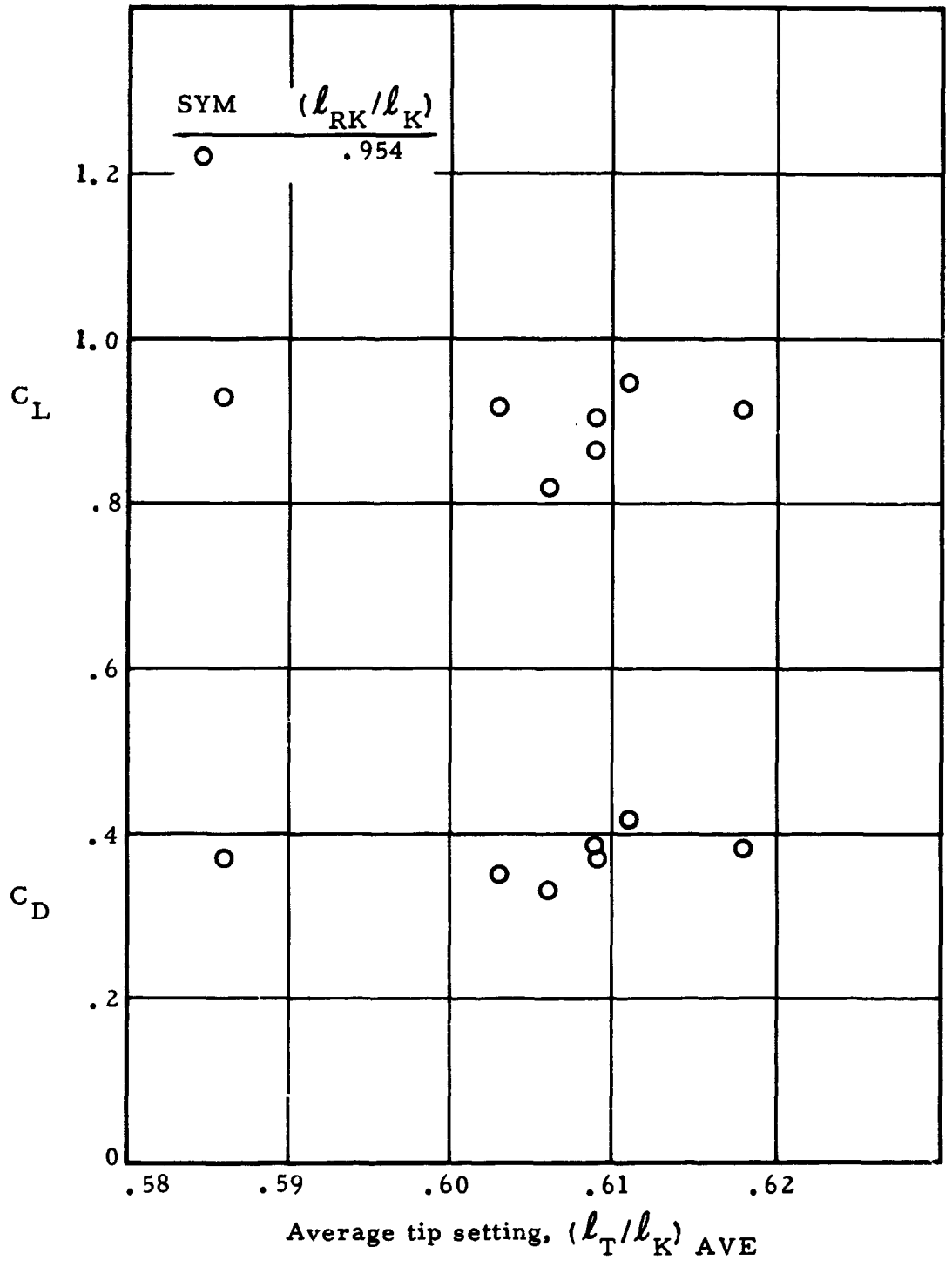

Figure 123. Lift coefficient and drag coefficient versus average tip setting, Test 255T

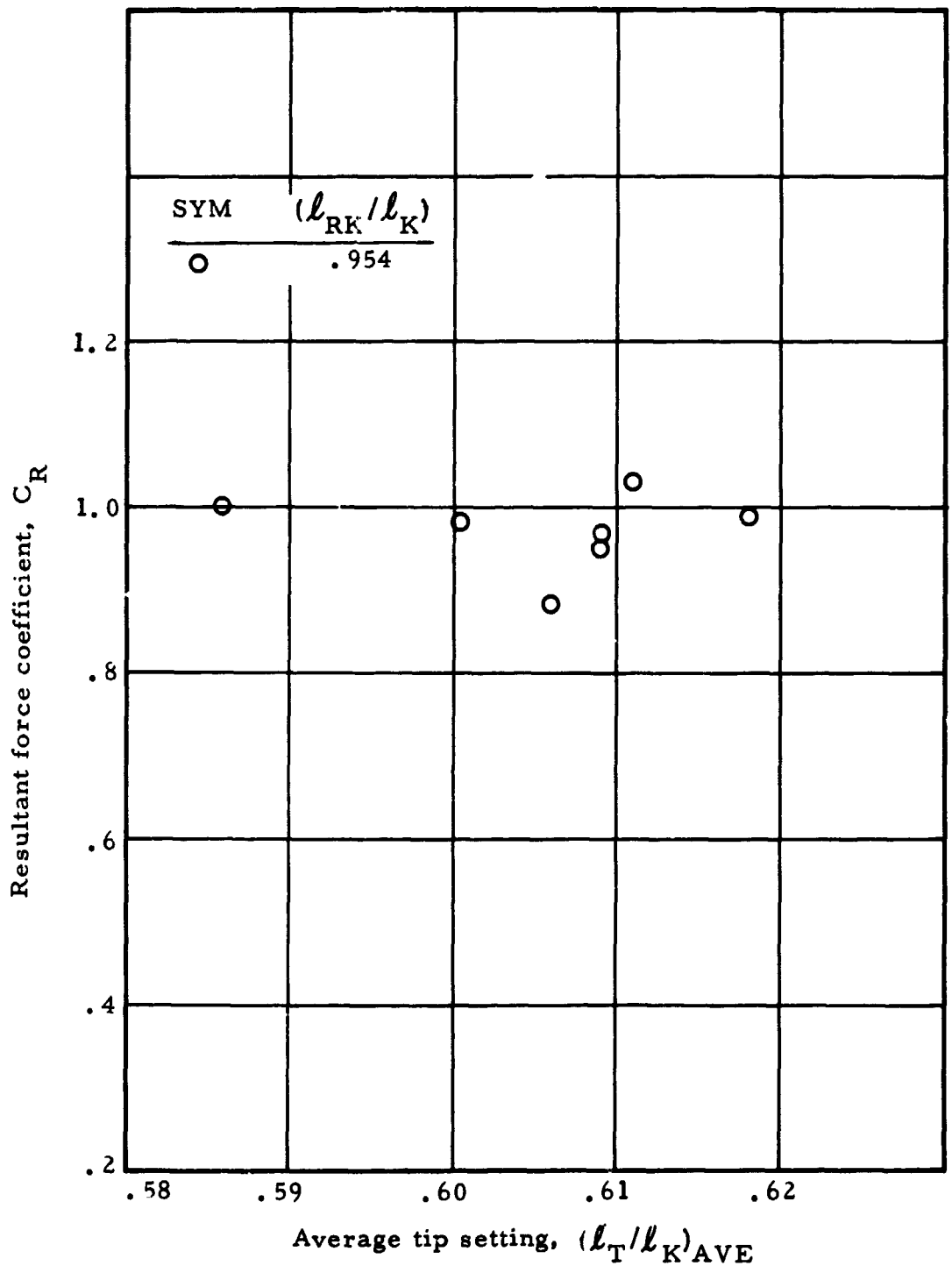

Figure 124. Resultant force coefficient versus average tip setting, Test 255T

Straight Flight Aerodynamic Test Data Analysis

Effect of wing construction on L/D performance. - Figure 125 is a composite plot of data, showing the L/D performance obtained during the 4000-square foot parawing free-flight tests, compared with typical L/D performance obtained with a 400-square foot model during wind tunnel tests. The wind tunnel data were taken from Reference 1. The L/D data are presented as a function of the average tip setting (where tip setting refers to the ratio of the tip-suspension-line length to keel length). All the free flight data are for the wings at approximately the same rear keel setting (ℓ_{RK}/ℓ_K = .954). The free flight data in Figure 125 are for three different wing constructions. The wing in Test 205T (Version I) had six lines per leading edge and no ripstop tapes on the canopy. The wings in Tests 250T and 251T (Version III) had eleven lines per leading edge and a minimum ripstop network, consisting of four longitudinal tapes on each of the outboard sections of the wing. The wings in Tests 252T, 253T, 254T, 255T, 209T and 210T (Versions IV, V, VI and VII) had eleven lines per leading edge and a full ripstop tape matrix on the wing canopy. The data in Figure 125 show no distinguishable effect of the various wing constructions on L/D performance. The datum point for the wing with six lines per leading edge and no ripstop tapes (Test 205T) falls in the upper center of the data band. The data points for the wing with eleven lines per leading edge and a minimum ripstop tape network (Tests 251T and 250T) provide the boundaries of the measured L/D performance, with the highest and the lowest L/D values. L/D values for the wings with eleven lines per leading edge and a full ripstop tape matrix generally fall in the central portion of the data band. This result is somewhat in contrast with wind tunnel tests of 400 sq ft wings reported in Reference 1, wherein the addition of a ripstop tape matrix to the wing canopy resulted in a significant (10 percent) decrease in L/D performance.

SYM	Test No	W_{D/S_W}	ℓ_{RK}/ℓ_K	Wing Version
○	250T	.86	.954	III
□	251T	.99	.939 - .954	III
◇	252T	1.00	.952 - .954	IV
△	253T	1.25	.940 - .954	VI
⬡	254T	1.50	.954	VI
▽	255T	1.50	.954	VI
◺	205T	1.25	.954	I
◇	209T	.95	.954	V
⬠	210T	.95	.954	VII
– – –	Wind Tunnel	≃1.0	.900	Typical 400 ft^2

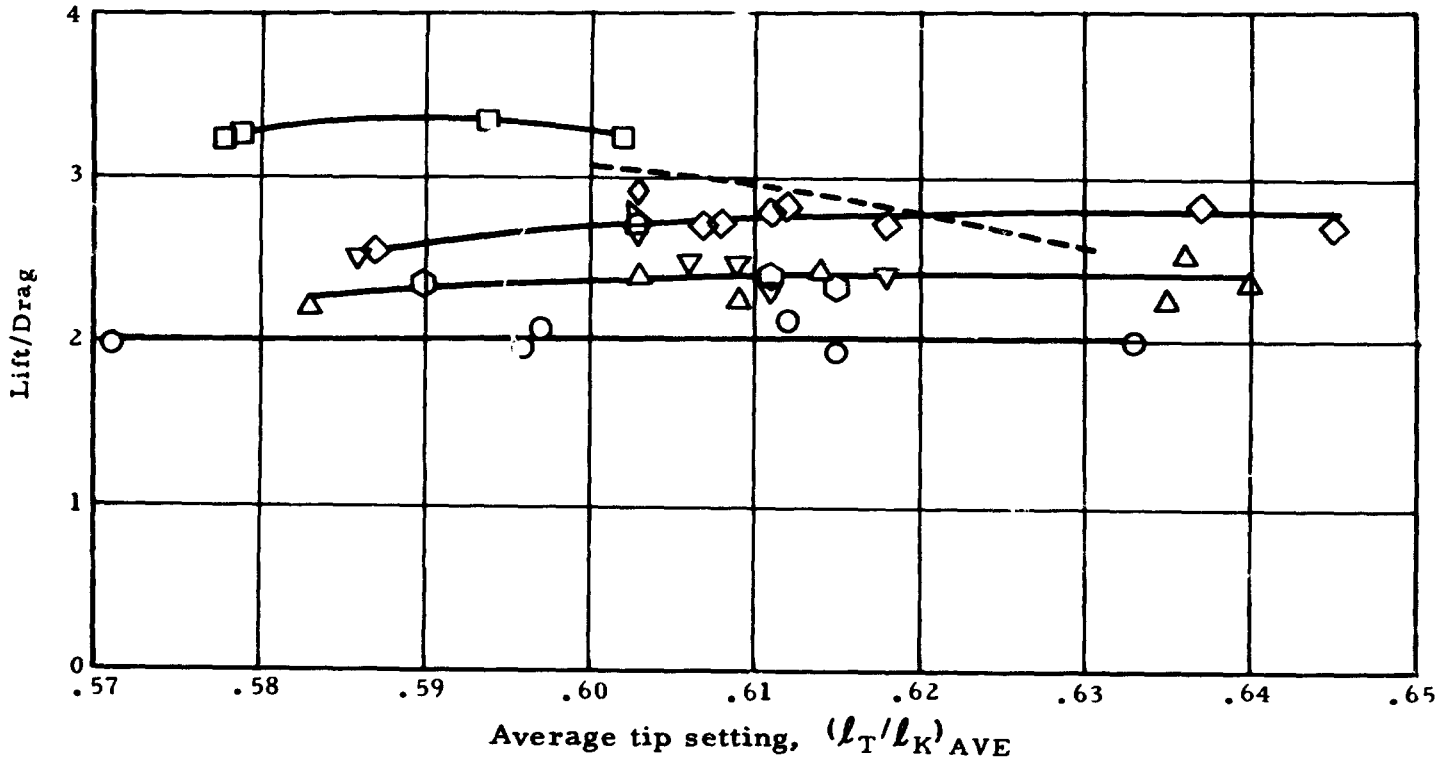

Figure 125. Lift-to-drag ratio versus average tip setting

Effect of tip-suspension-line length on L/D performance. - Although there is considerable variation in L/D performance from test to test, Figure 125 shows very little variation in L/D with tip-suspension-line length over the range of lengths tested during the intermediate-scale tests. The wind tunnel tests showed a pronounced variation of L/D with variation in the tip-suspension-line lengths. The data in Figure 125 show that L/D decreased as the tip setting was increased from 0.60 to 0.63.

During the intermediate-scale tests, the longest tip setting that could be used was about 0.64. Tip lengths longer than this caused improper wing inflation, with the leading edges of the wing collapsing and with resulting tip flutter. The shortest tip settings tested did not result in a stall. Consequently, the shortest allowable tip setting was not determined for straight flight.

As shown by Figure 125, considerable variation in L/D performance was measured from test to test for controllable vehicle flights. The L/D data on Figure 125 were obtained from the on-board instrumentation. During Tests 252T and 253T verification of the on-board instrumentation accuracy was obtained by comparing L/D data from it with L/D data determined from ASKANIA data under controlled conditions. The flight path angles measured during Tests 250T and 251T differ considerably from those measured in the other tests. As a result little confidence is held for the accuracy of these measurements. L/D data obtained during Tests 252T, 253T, 254T, 255T, 205T, 209T and 210T are considered representative of the L/D performance actually achieved during the flight test program.

Effects of rear-keel-suspension-line length on gliding-flight characteristics. - Figures 126 and 127 show L/D, C_L and C_D as functions of the rear keel setting. These data show the same variation of performance from test to test as previously identified

SYM	Test No	W_{D/S_W}	$(\ell_T/\ell_K)_{AVE}$	Parawing Version
○	250T	.86	.596 - .605	III
□	251T	.99	.594 - .602	III
◇	252T	1.00	.607 - .618	IV
△	253T	1.25	.603 - .614	VI
⬡	254T	1.50	.590 - .619	VI
▽	255T	1.50	.603 - .611	VI
◣ (1)	205T	1.25	.603	I
◆ (1)	209T	.95	.603	V
⬢ (1)	210T	.95	.603	VII

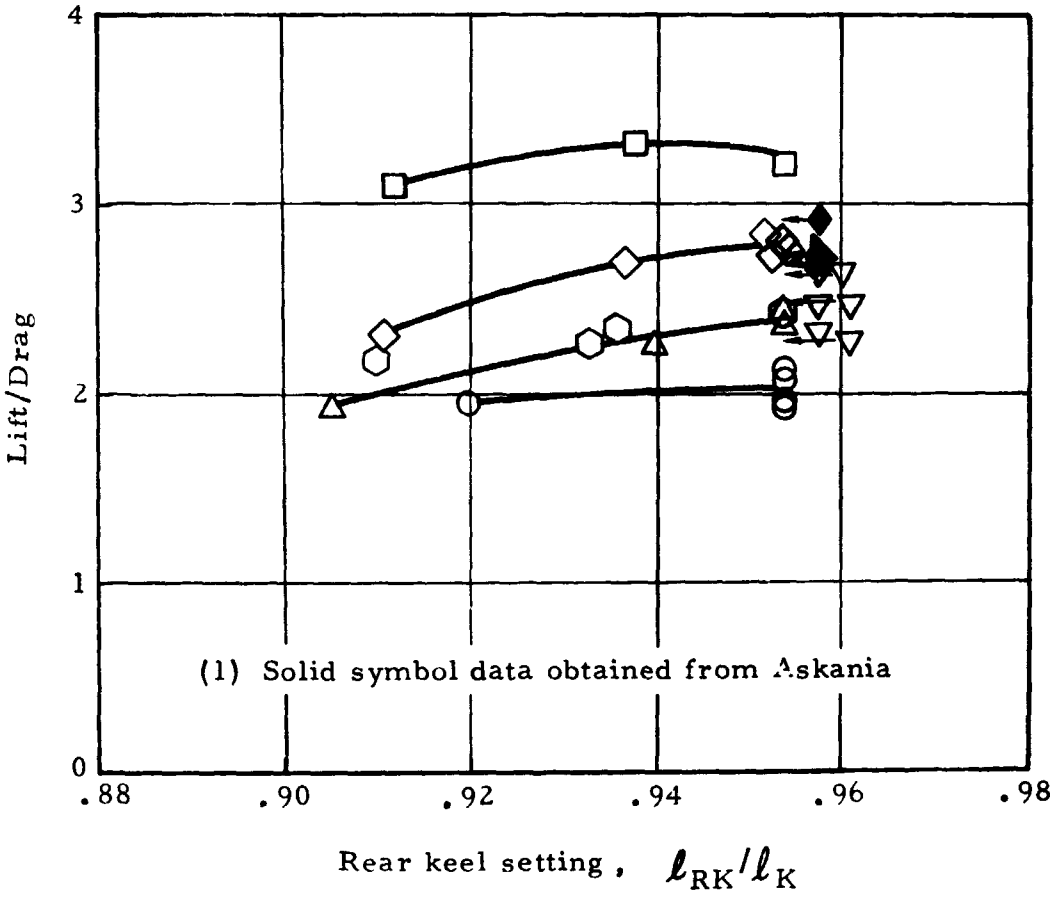

Figure 126. Lift-to-drag ratio versus rear keel setting

SYM	Test No	W_{D/S_W}	$(\ell_T/\ell_K)_{AVE}$	Paravwing Version
○	250T	.86	.596 - .605	III
□	251T	.99	.594 - .602	III
⬡	254T	1.50	.590 - .619	VI
▽	255T	1.50	.603 - .611	VI
◣ (1)	205T	1.25	.603	I
◆ (1)	209T	.953	.603	V
● (1)	210T	.953	.603	VII

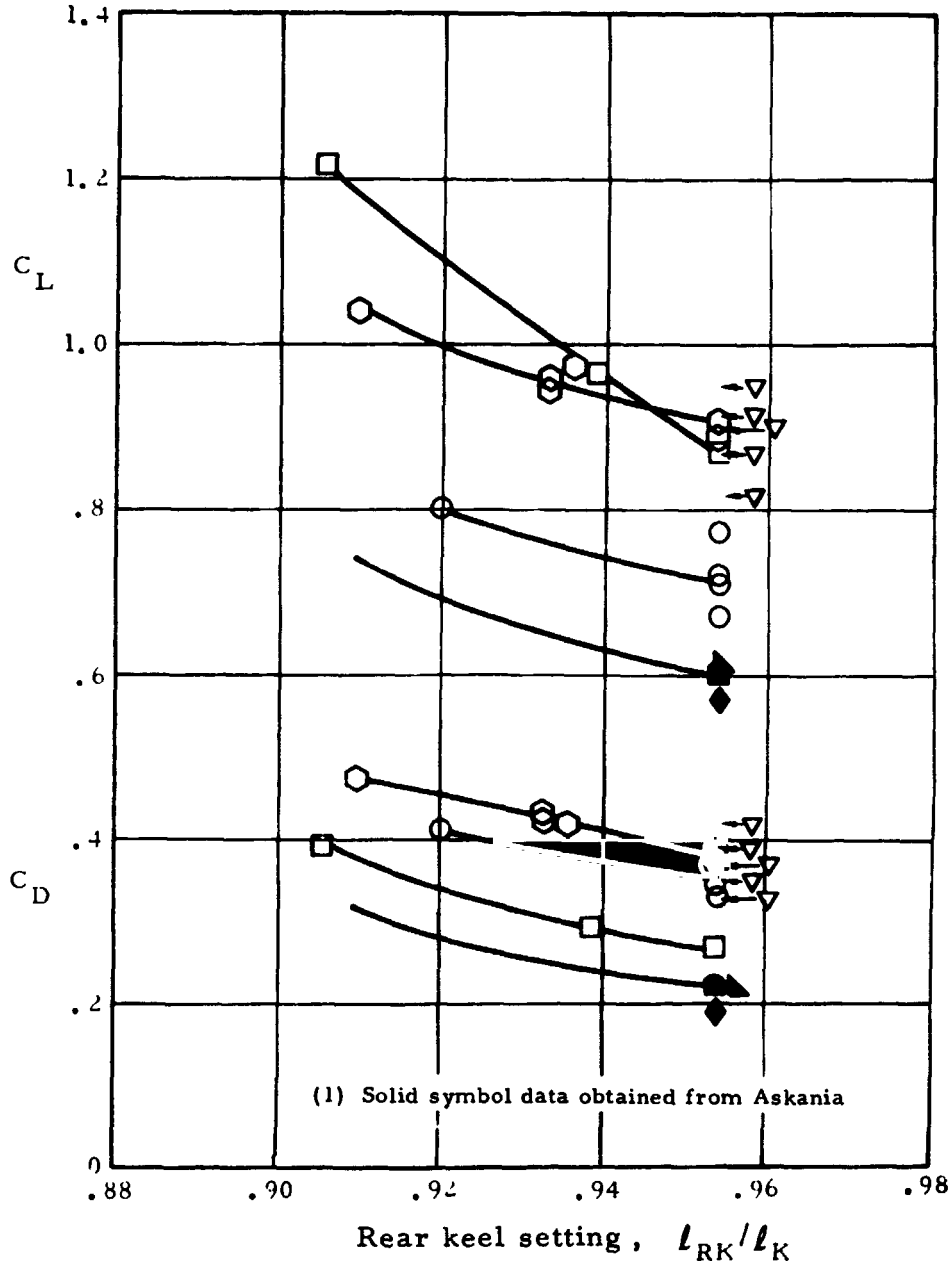

Figure 127. Lift coefficient and drag coefficient versus rear keel setting

in the section on the effects of tip setting. As before, the flight path angle measurements obtained during Tests 250T and 251T are not considered accurate. The remainder of the data shown on Figure 126 defines the range of L/D performance achieved during the free-flight tests. As shown by Figure 126, L/D could be reduced approximately 0.5 below the maximum attainable L/D by retracting the rear-keel-suspension lines.

Figure 127 presents the C_L and C_D data obtained during the controllable vehicle tests and the bomb vehicle tests. As with the L/D data, there were appreciable differences in the data from test to test. In particular, large differences exist in the values of C_L and C_D determined from ASKANIA in the bomb vehicle tests, compared with those determined from the on-board instrumentation in the controllable vehicle tests. These differences were felt to be due to airspeed measurements as provided by the on-board instrumentation, compared with the airspeed measurements provided from ASKANIA. To verify this, an analysis was performed of the rate-of-descent data, both from ASKANIA and from the on-board instrumentation. Results of this analysis are presented in Table 14.

Table 14 shows average rate-of-descent values converted to mean-sea-level conditions for several tests, both from ASKANIA measurements and from on-board measurements. Table 14 also presents the ratio of ASKANIA MSL rate-of-descent for Test 250T to the MSL rate-of-descent for each test. (Use of Test 250T as a baseline was arbitrary.) Finally, since rate-of-descent is proportional to the square root of wing loading, the ratio of the square root of wing loading for Test 250T to the square root of wing loading for each test is presented. A study of Table 14 shows that on-board measured rate-of-descent for each test was consistently and significantly lower than ASKANIA measured rate-of-descent. Also, the ASKANIA rate-of-descent ratio compared closely with the square-root-of-wing loading ratio for each test. From

TABLE 14. - INTERMEDIATE-SCALE TEST RATE-OF-DESCENT DATA

Test no.	ASKANIA MSL rate-of-descent, fps	On-board MSL rate-of-descent, fps	Ratio of ASKANIA MSL rate-of-descent for Test 250T to ASKANIA MSL rate-of-descent for test	Square root of ratio of W_D/S_W for Test 250T to W_D/S_W for test
250T	11.5	12.2	1.00	1.00
251T	12.2	9.0	.94	.93
252T	12.5	----	.92	.93
253T	14.5	11.5	.79	.83
254T	15.3	14.0	.75	.76
255T	15.5	13.0	.74	.76
205T	13.67	----	.84	.83
209T	11.71	----	.98	.95
210T	12.23	----	.94	.95

this analysis it was concluded that the on-board airspeed measurements were consistently low, resulting in high values for the aerodynamic coefficients based on these airspeed data. The C_L and C_D values determined using ASKANIA airspeed data appeared to be correct for the 72 ft ℓ_K twin keel parawings. For this reason the C_L and C_D curves based on ASKANIA data are used in subsequent performance discussions and presentations for this wing.

Figures 128 and 129 present L/D, C_L and C_D data obtained during wind tunnel tests with 15 ft ℓ_K and 22.7 ft ℓ_K models, respectively. Figures 130 and 131 compare representative data from these tests with the results of the small-scale, free flight tests and the intermediate-scale, free flight tests. These data show that the L/D performance obtained during the intermediate-scale, free flight tests compares favorably with L/D performance measured during the small-scale, free flight tests. Neither the small-scale nor the intermediate-scale free flight tests produced L/D values as high as those obtained during the wind tunnel tests. During the wind tunnel tests, the model mounting system separated by a significant amount, the tip suspension lines and rear keel suspension lines from the main group of suspension lines (see Reference 1). This attachment arrangement resulted in undetermined differences in inflated shapes between the free flight and the wind tunnel parawing configurations. These differences may have been the cause of the mismatch between the free flight and wind tunnel data.

Effect of wing loading on L/D performance. - Figure 132 is a plot of L/D versus wing loading for the intermediate-scale free flight tests. These data show that for the wing loading range tested (0.95 psf to 1.50 psf), L/D decreased as wing loading increased. It should be recognized that these data are from tests where the parawing was either at a fixed rigging (200 Series tests) or with parawing trim capability limited to the tip lines and rear

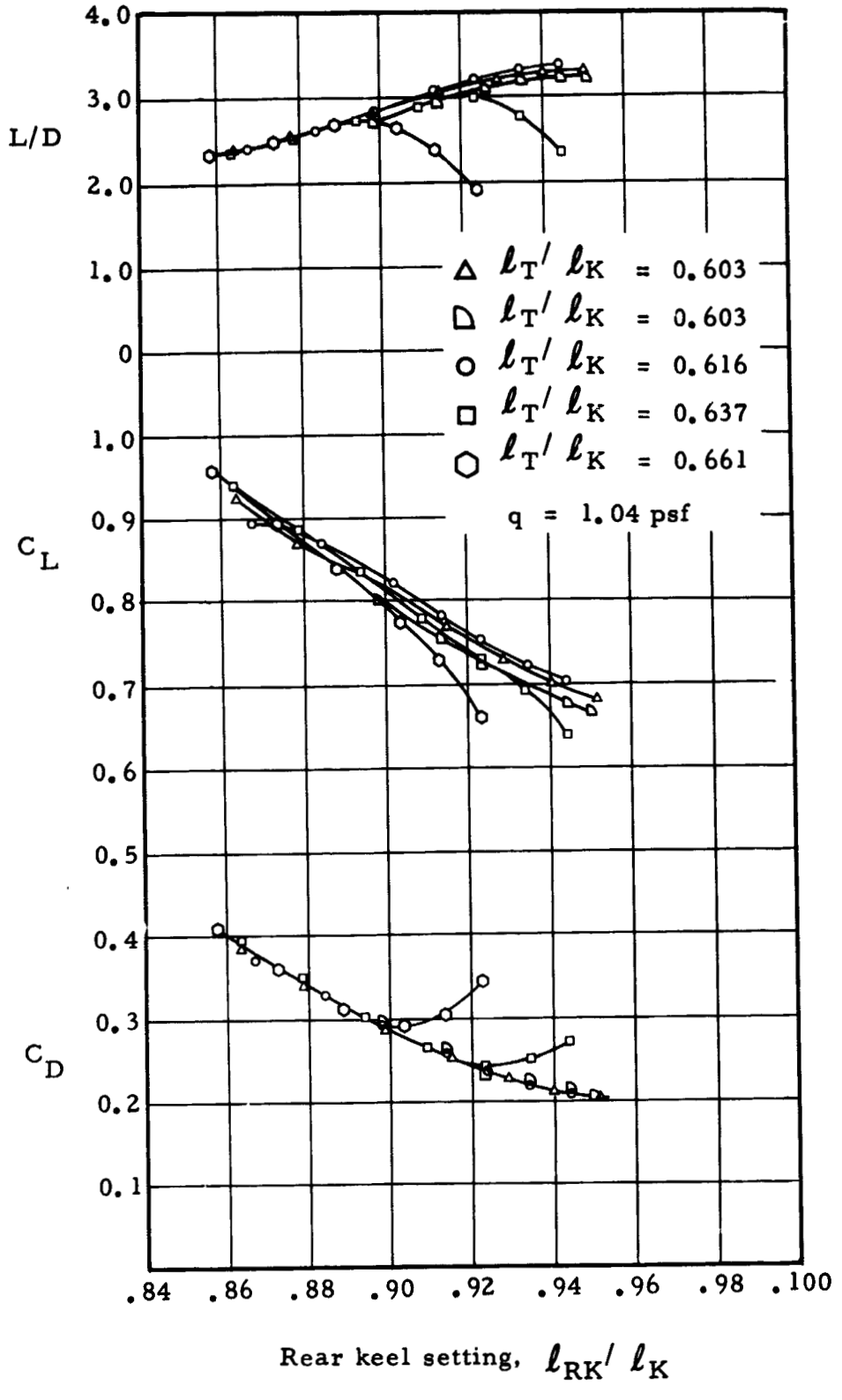

Figure 128. Performance data for 15 ft ℓ_K twin-keel parawing

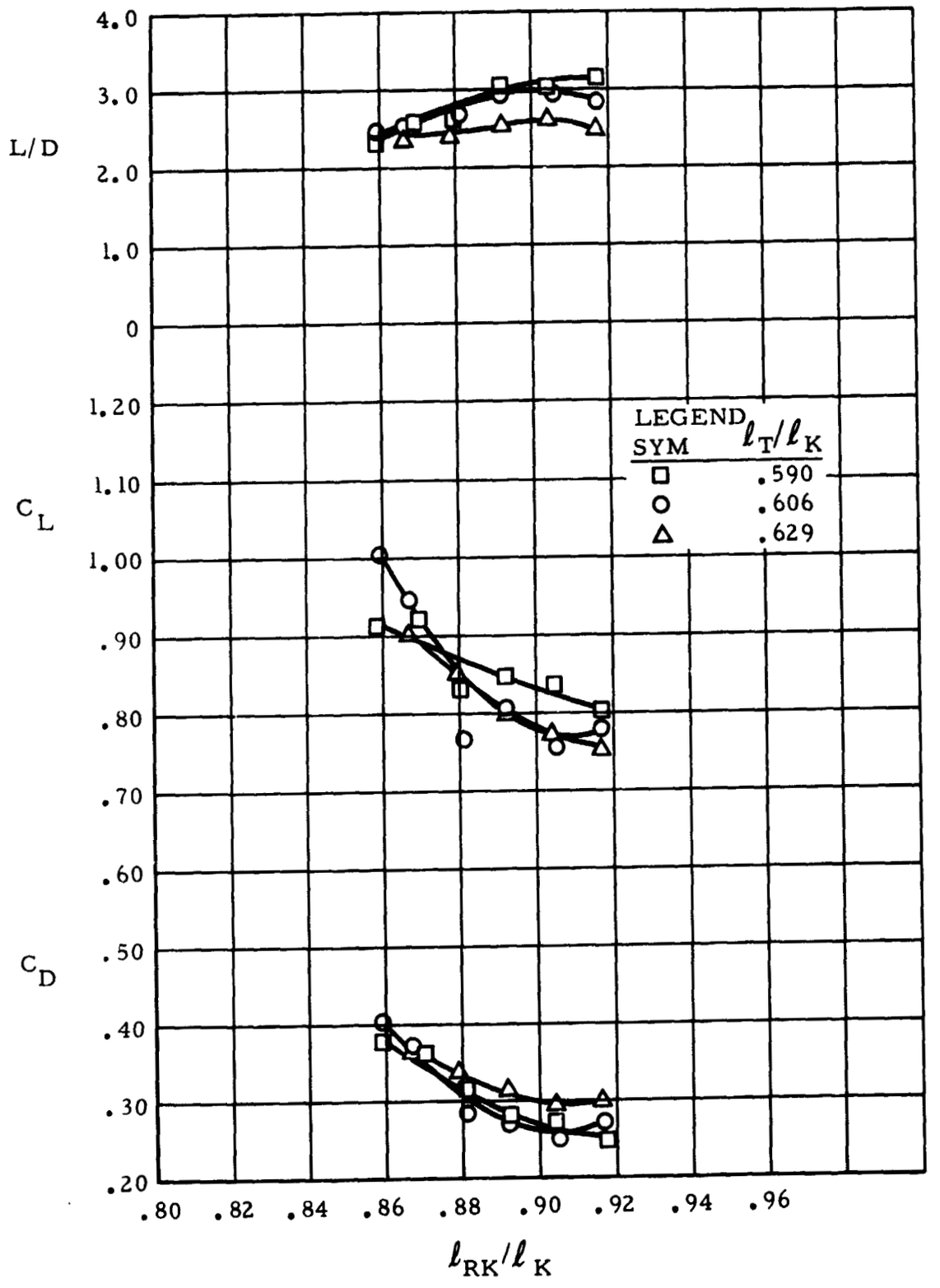

Figure 129. Performance data for 22.7 ft ℓ_K twin keel parawing

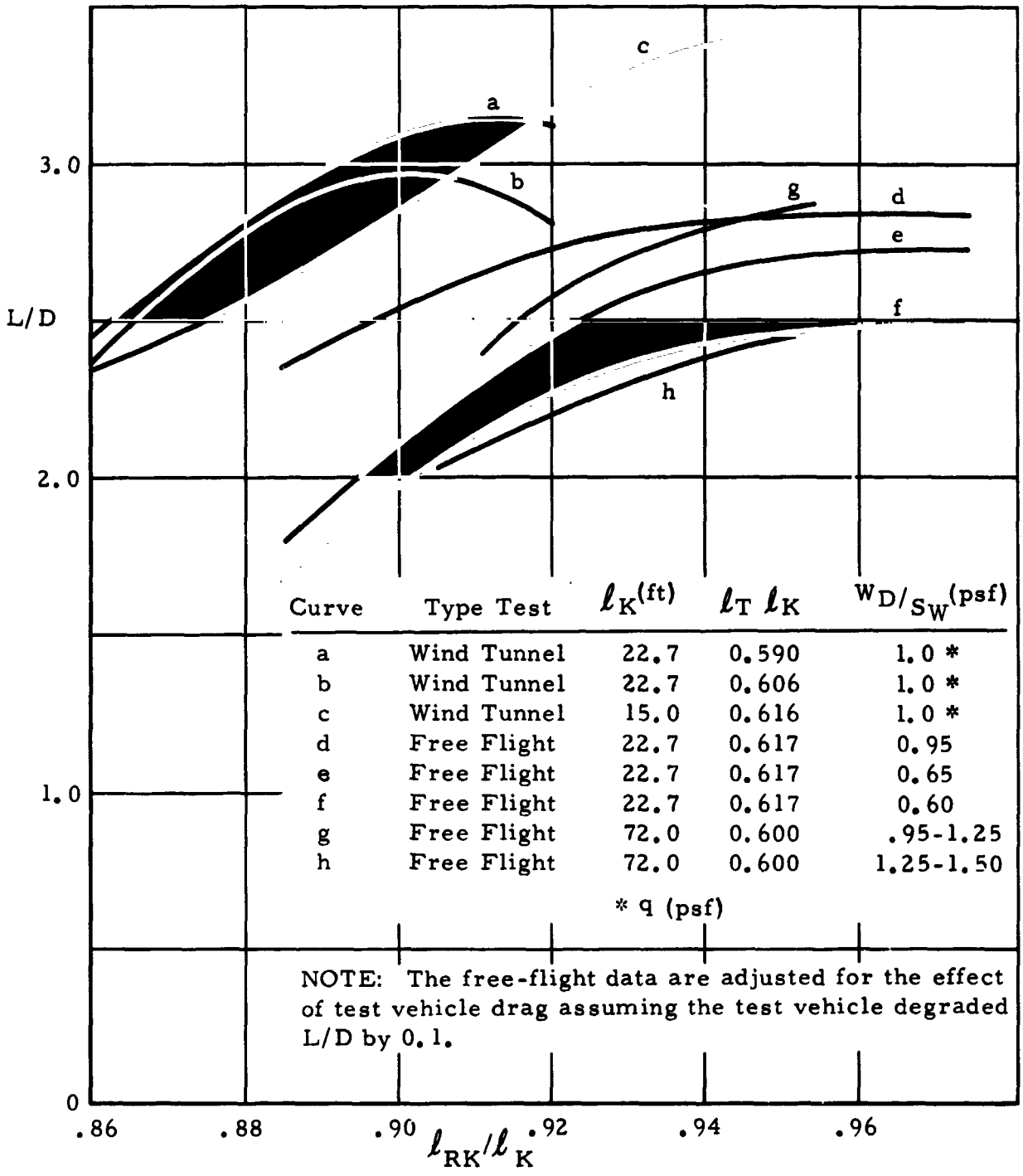

Curve	Type Test	ℓ_K(ft)	$\ell_T\ \ell_K$	W_D/S_W(psf)
a	Wind Tunnel	22.7	0.590	1.0 *
b	Wind Tunnel	22.7	0.606	1.0 *
c	Wind Tunnel	15.0	0.616	1.0 *
d	Free Flight	22.7	0.617	0.95
e	Free Flight	22.7	0.617	0.65
f	Free Flight	22.7	0.617	0.60
g	Free Flight	72.0	0.600	.95-1.25
h	Free Flight	72.0	0.600	1.25-1.50

* q (psf)

NOTE: The free-flight data are adjusted for the effect of test vehicle drag assuming the test vehicle degraded L/D by 0.1.

Figure 130. Free-flight and wind tunnel L/D performance for twin-keel parawing

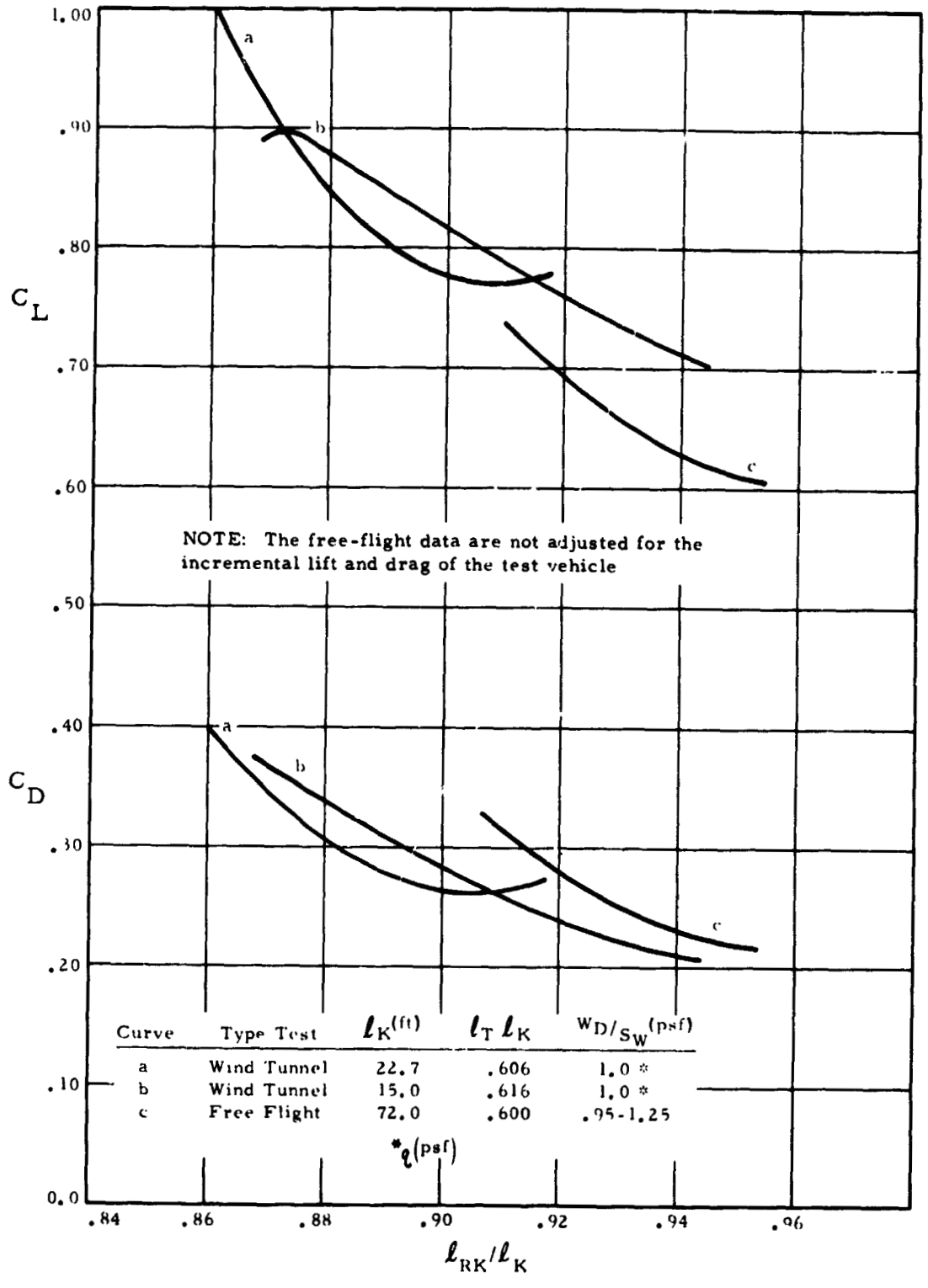

Figure 131. Free-flight and wind tunnel lift and drag coefficient data

SYM	Test no	$(\ell_T/\ell_K)_{AVE}$	ℓ_{RK}/ℓ_K	Parawing version
◇	252T	.607-.618	.954	IV
△	253T	.603-.614	.954	VI
○	254T	.590-.619	.954	VI
▽	255T	.603-.611	.954	VI
◺	205T	.603	.954	I
◇	209T	.603	.954	V
∩	210T	.603	.954	VII

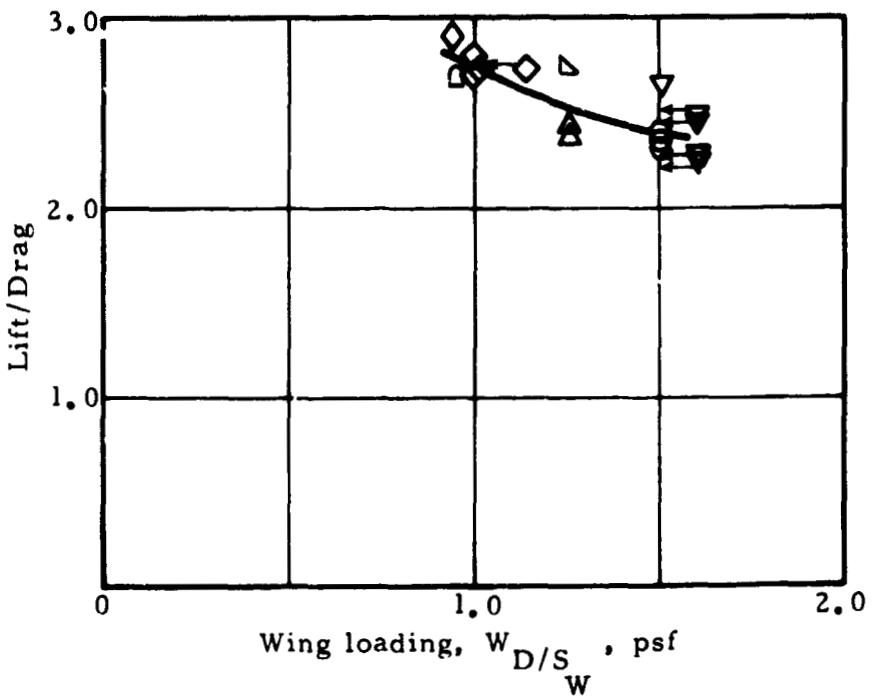

Figure 132. L/D versus wing loading

keel lines (250 Series tests). Therefore, the complete parawing suspension line rigging may not have been optimum in these tests, because of deployment-load-induced suspension line elongation. Because of apparent inaccuracies in the measurement of velocity, insufficient data were obtained to determine how the lift and drag coefficients varied with wing loading.

Figures 133, 134 and 135 show previously obtained free flight and wind tunnel data for 22.7 ft ℓ_K parawing models. These data, particularly the wind tunnel data, show significant variations of L/D with changes in wing loading and dynamic pressure. Figure 134 shows L/D plotted versus dynamic pressure and also versus an approximate equivalent wing loading, where an assumed C_R value of 0.6 was used to convert from dynamic pressure to wing loading by the relation

$$\frac{W_D}{S_W} = C_R\, q \approx 0.6\, q$$

Figure 136 is a composite plot of small-scale, free flight and wind tunnel data, and intermediate-scale free flight data. The wind tunnel data in this figure are plotted versus the approximate equivalent wing loading, based on as assumed C_R value of 0.6 as described above. The data in Figure 136 show a similarity between the wind tunnel tests and the 72 ft ℓ_K pa awing free flight tests, relative to the variation of L/D with wing loading.

Figure 135 shows the C_L and C_D variation of two models, one with and one without chordwise reinforcing tapes. The plots in Figure 135 indicate that as dynamic pressure was increased in the wind tunnel, C_D also increased. This behavior of increasing C_D with increasing dynamic pressure occurred for both models tests. The variation of the C_L data with dynamic pressure in Figure 135 was not as consistent as that shown for the C_D data. The model without the reinforcing tape network showed a reduction in C_L as

SYM	Model	$(\ell_T/\ell_K)_{AVE}$	ℓ_{RK}/ℓ_K
O	36 suspension line	.617	.954
□	44 suspension line	.630	.954

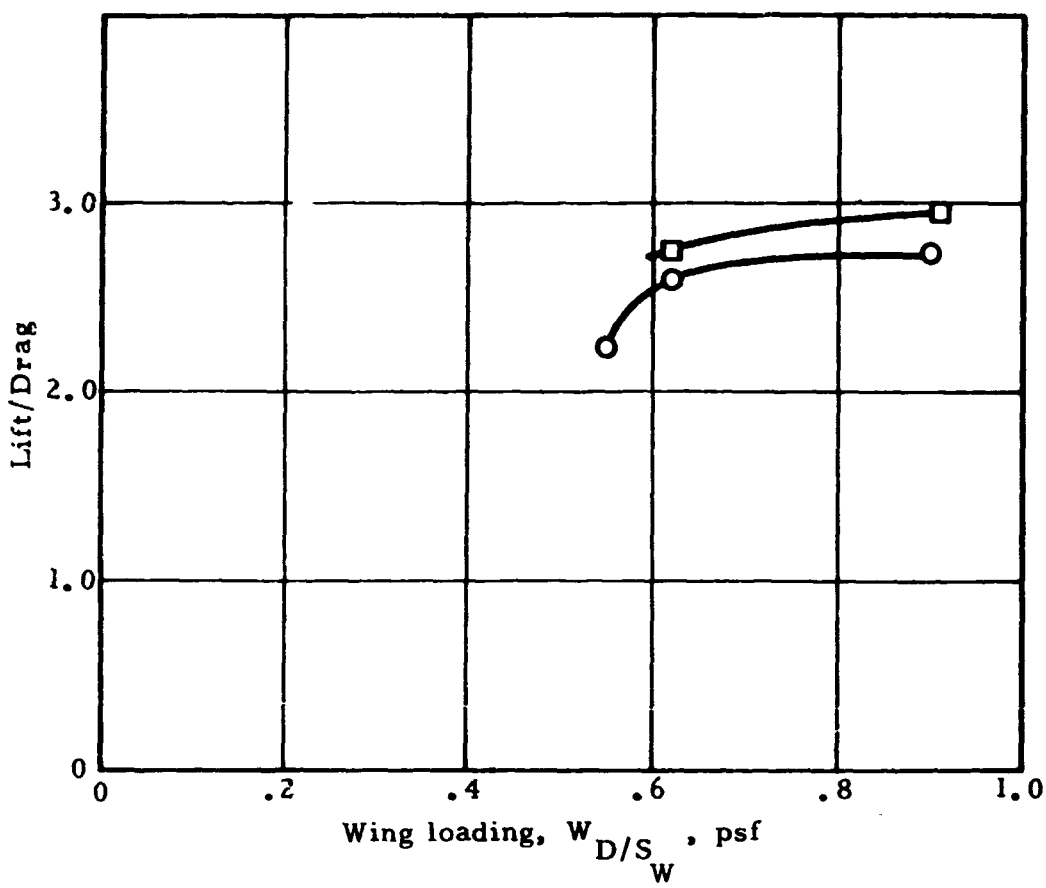

Figure 133. L/D vs. wing loading for 22.7 ft ℓ K twin-keel parawing models during free-flight tests

SYM	Model	ℓ_{RK}/ℓ_K	$\left(\ell_T/\ell_K\right)_{AVE}$
◇	22.7 ft ℓ_K (without tapes)	.914	.590
△	22.7 ft ℓ_K (with tapes)	.892	.607

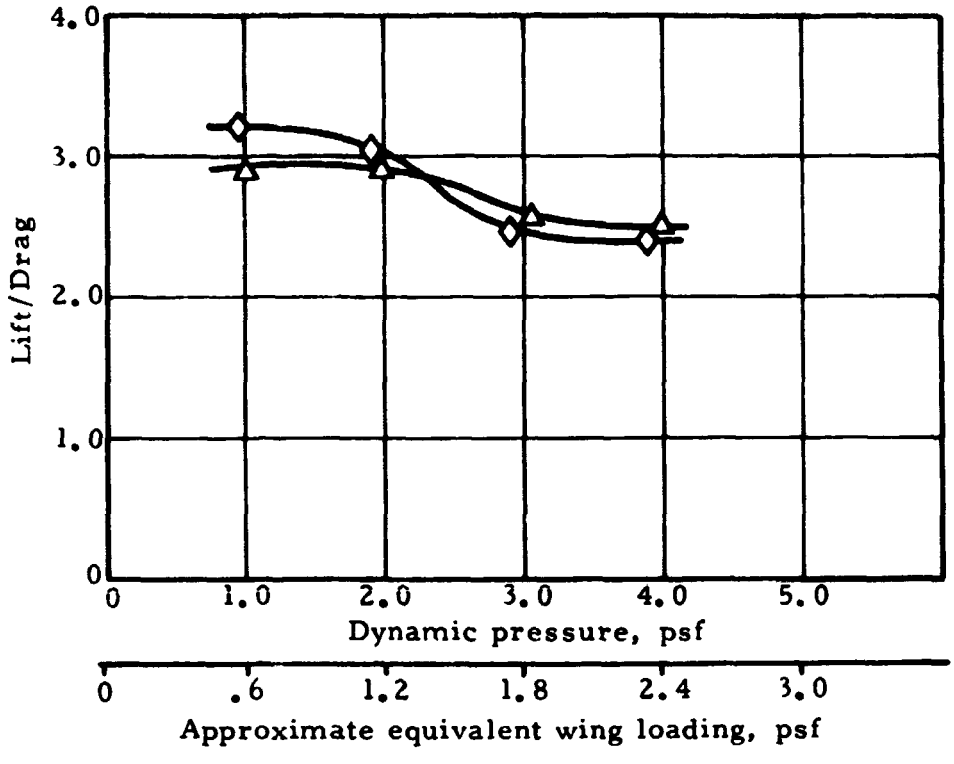

Figure 134. L/D vs. dynamic pressure and wing loading for 22.7 ft ℓ_K twin-keel parawings during wind tunnel tests

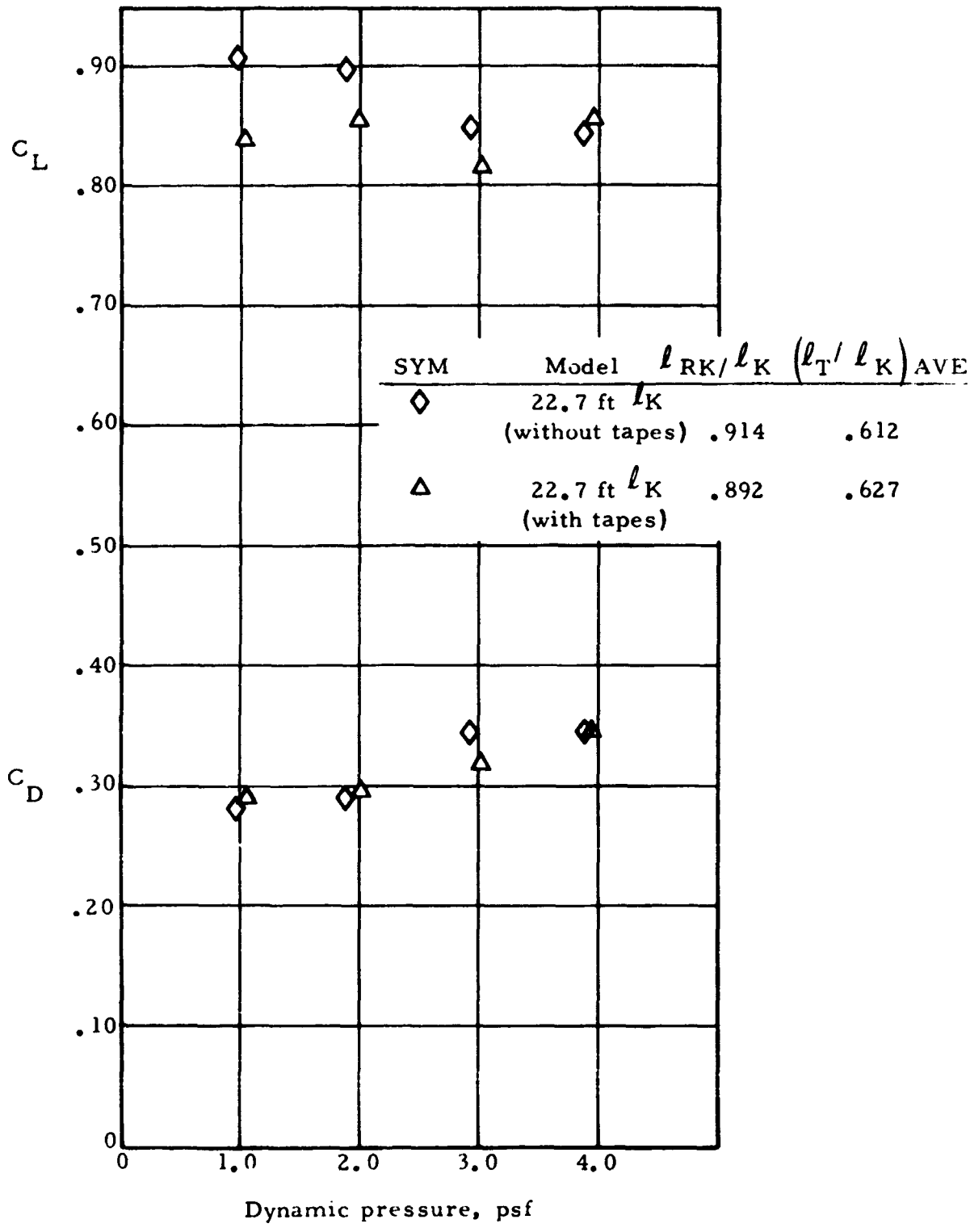

Figure 135. C_L & C_D versus dynamic pressure for 22.7 ft ℓ_K twin-keel parawings during wind tunnel tests

Curve	Data source	ℓ_K
a	wind tunnel	22.7 ft
b	wind tunnel	22.7 ft
c	free flight	22.7 ft
d	free flight	22.7 ft.
e	free flight	72 ft

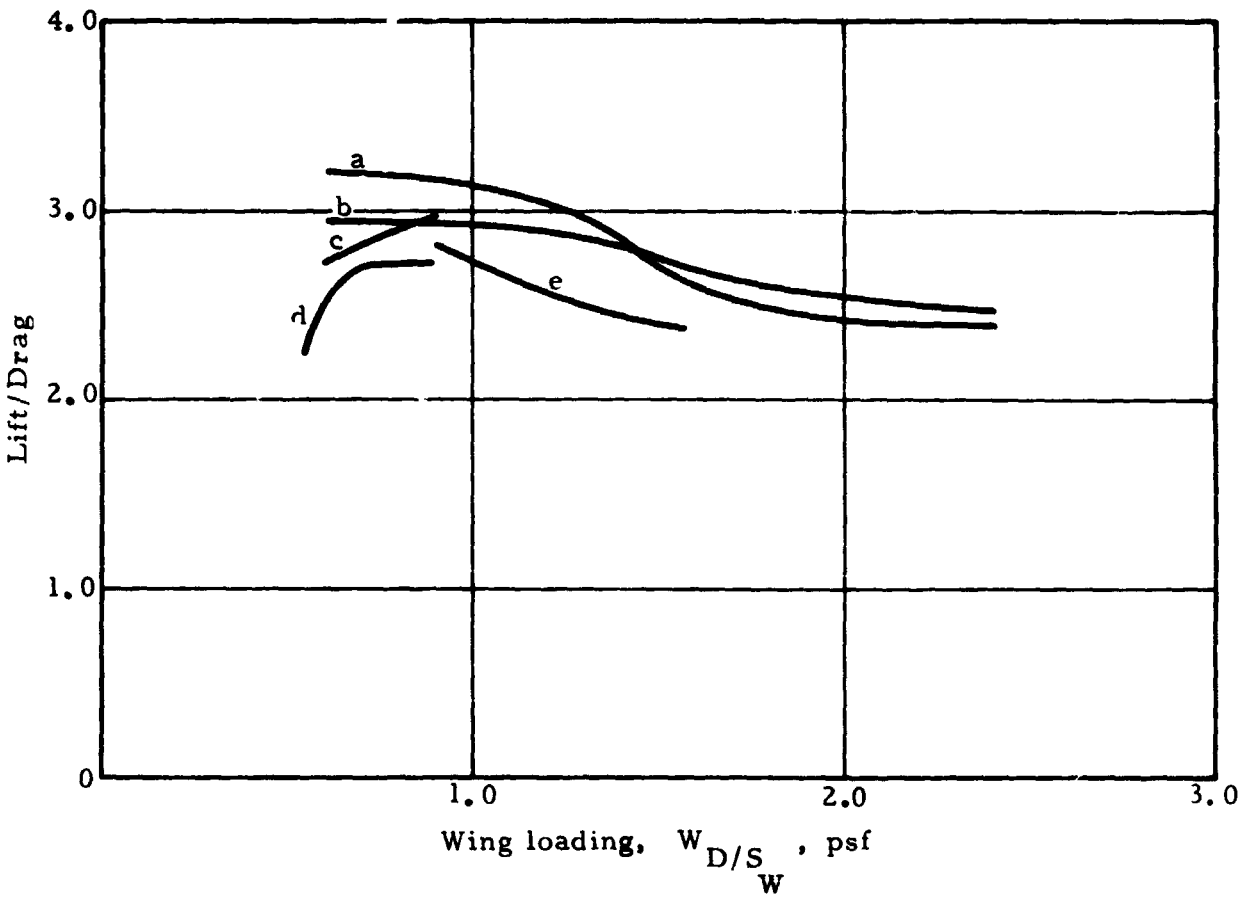

Figure 136. Composite of L/D performance as a function of wing loading

dynamic pressure increased. The model with the reinforcing network showed no appreciable change in C_L as dynamic pressure increased. The canopy structure of the model with the tape reinforcing network approximated the canopy structure of the 72 ft ℓ_K models flown on the controllable vehicle. On the basis of the wind tunnel test data the probable reason for the decrease in L/D with increasing wing loading for the 72 ft ℓ_K model tests, was an increase in drag coefficient. Cause of this increase in drag coefficient was not determined.

Turn Rate Test Data and Analysis

Figures 137 through 142 present the turn rate data obtained during the intermediate-scale parawing tests. The data are shown as plots of turn rate versus differential tip setting. Turn rate is defined as the angular rate of change of heading. Differential tip setting is defined as the difference in length between the two tip suspension lines divided by the reference keel length, ℓ_K. Any combination of tip suspension line lengths that resulted in the right tip suspension line being shorter than the left tip suspension line was considered a right turn input. The reverse is true for combinations which resulted in the left tip suspension line being shorter than the right tip suspension line.

During the various tests, numerous combinations of tip suspension line lengths were tested. For purposes of data presentation, the turn rate data are plotted and identified in groups defined by the length of one tip suspension line. The length of this tip suspension line varied over only a small range, while the length of the other tip suspension line varied over a large range. The differential produced between the two tip suspension lines was the turn control input. Also listed in the figures is the range of rear keel settings corresponding to the given set of data defined by the reference tip setting range.

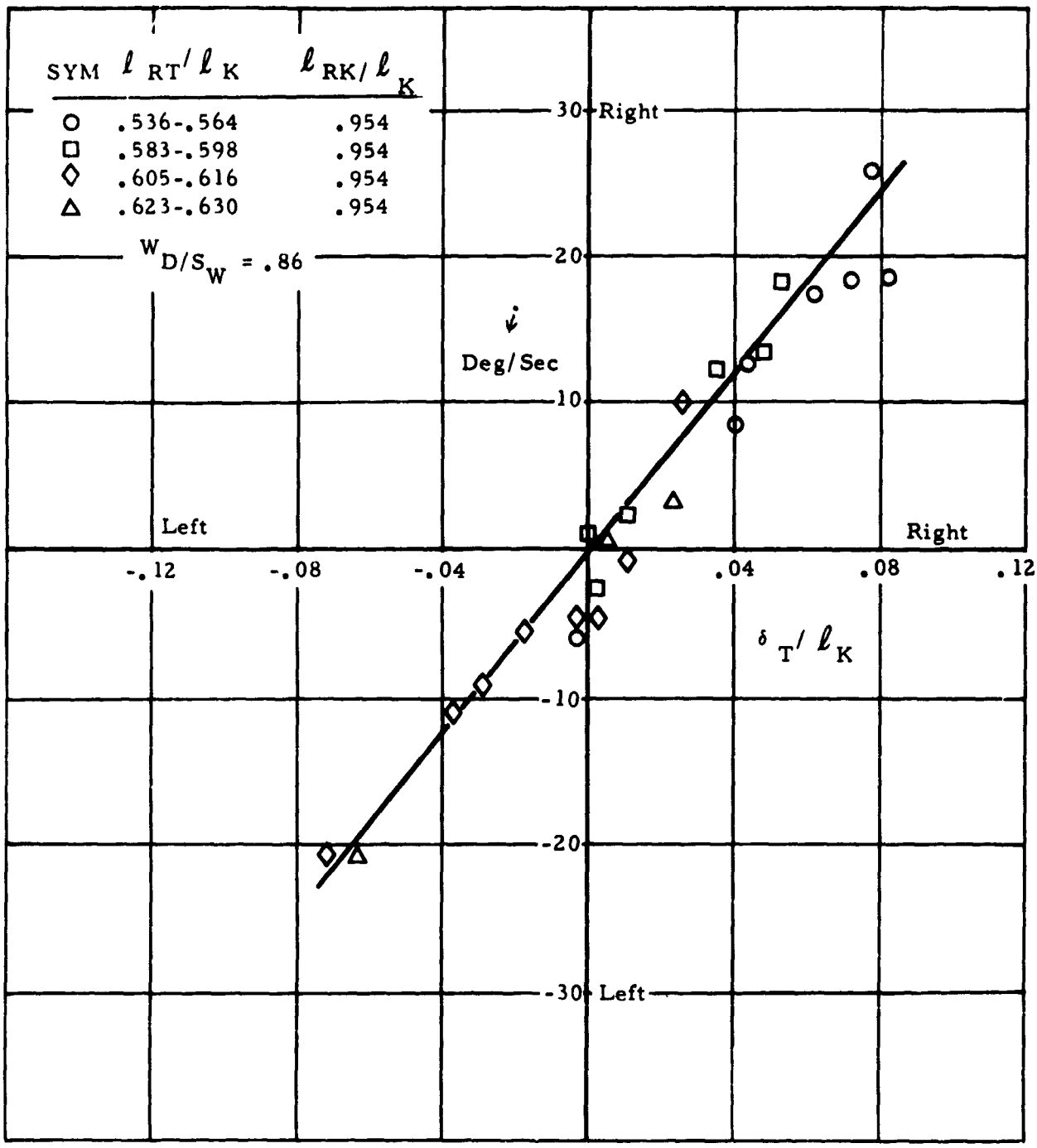

Figure 137. Turn rate versus differential tip setting, Test 250T

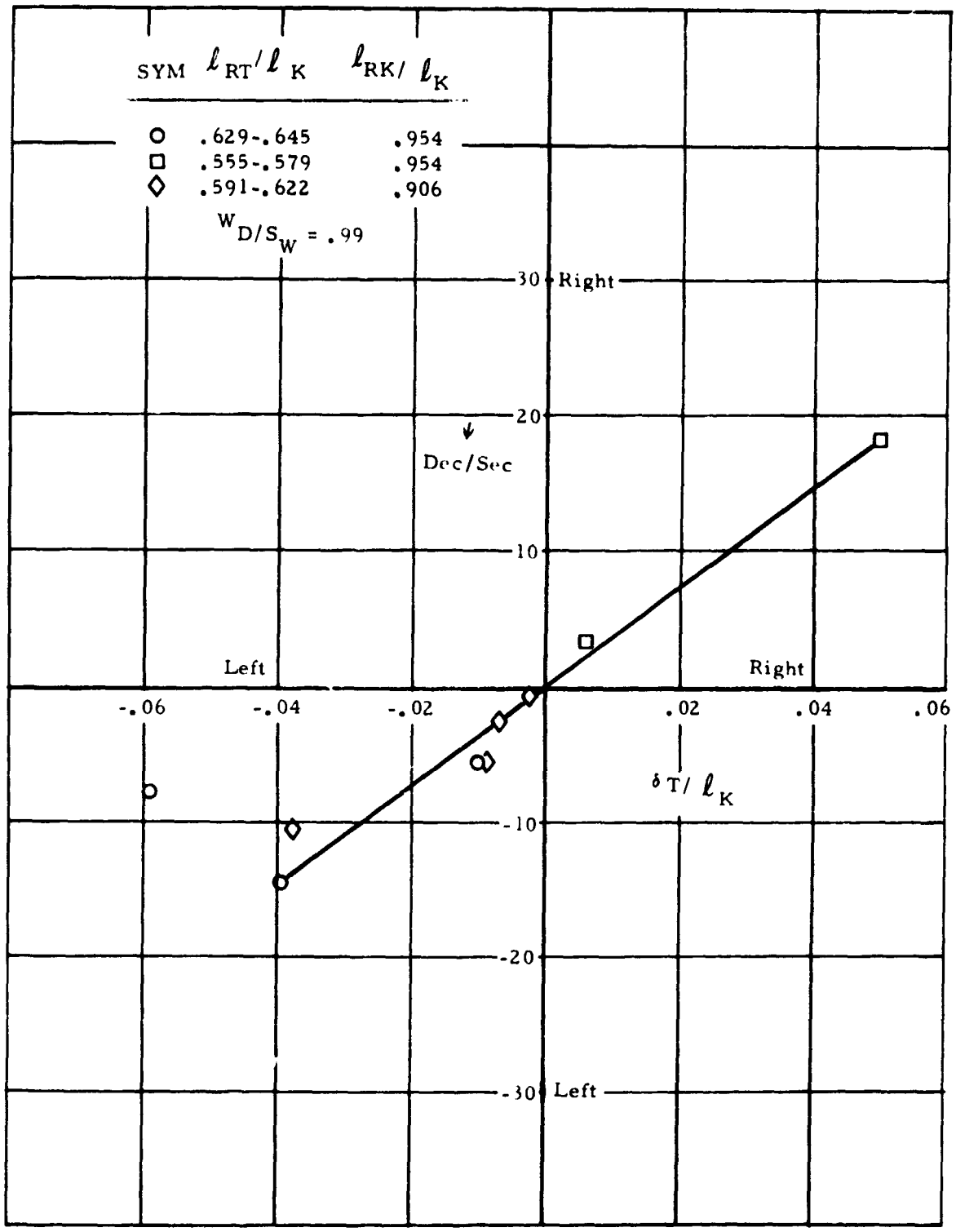

Figure 138. Turn rate versus differential tip setting, Test 251T

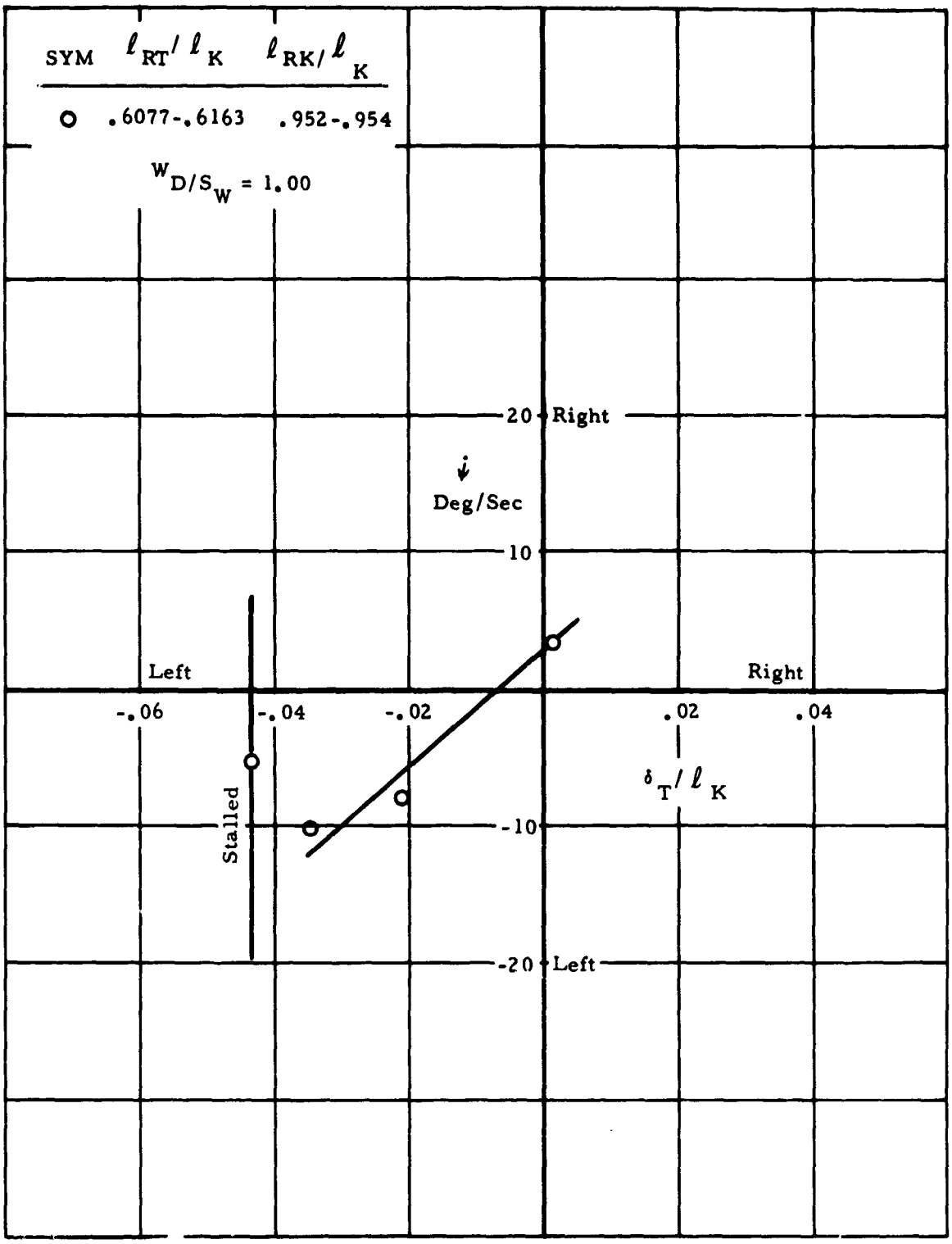

Figure 139. Turn rate versus differential tip setting, Test 252T

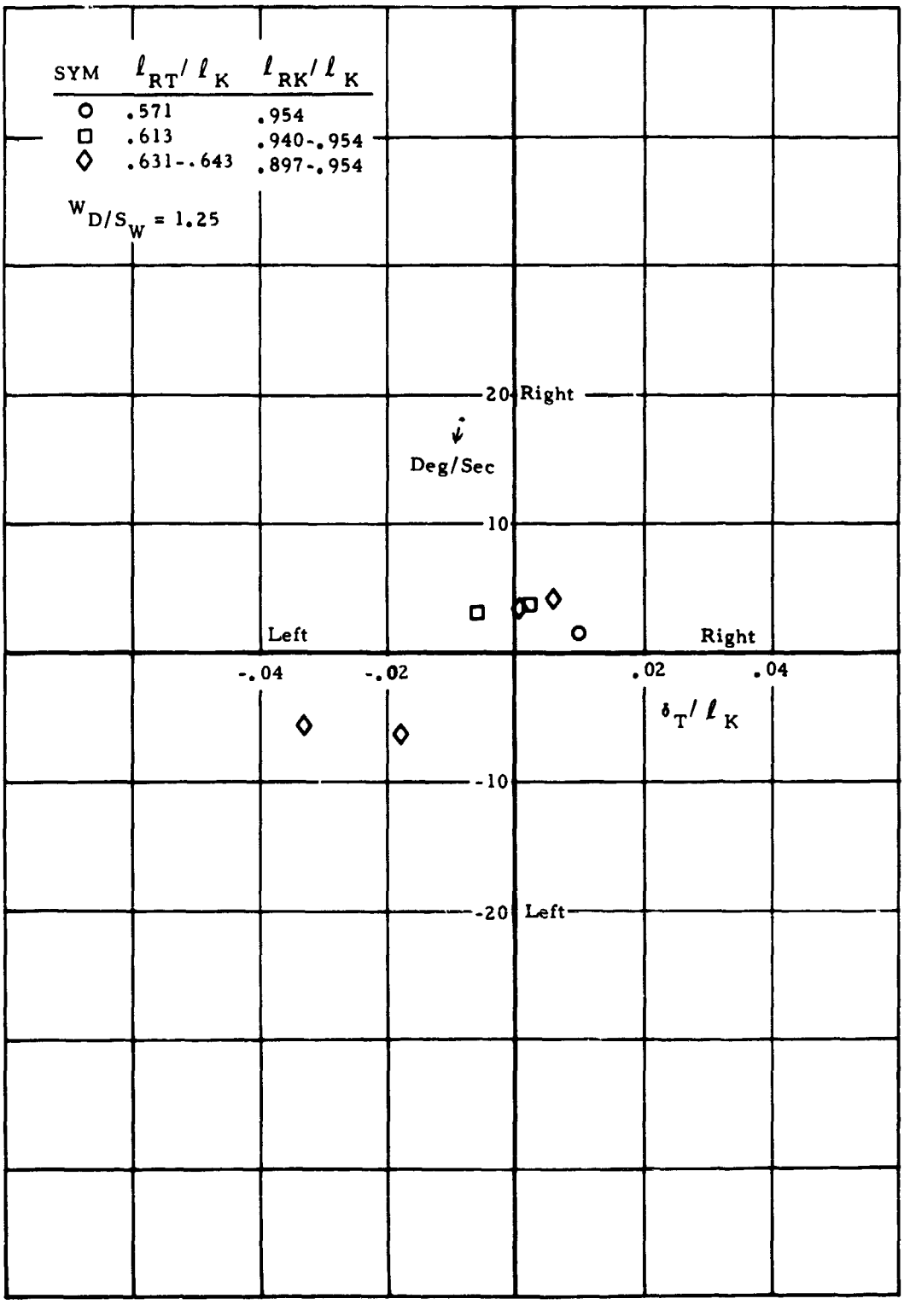

Figure 140. Turn rate versus differential tip setting, Test 253T

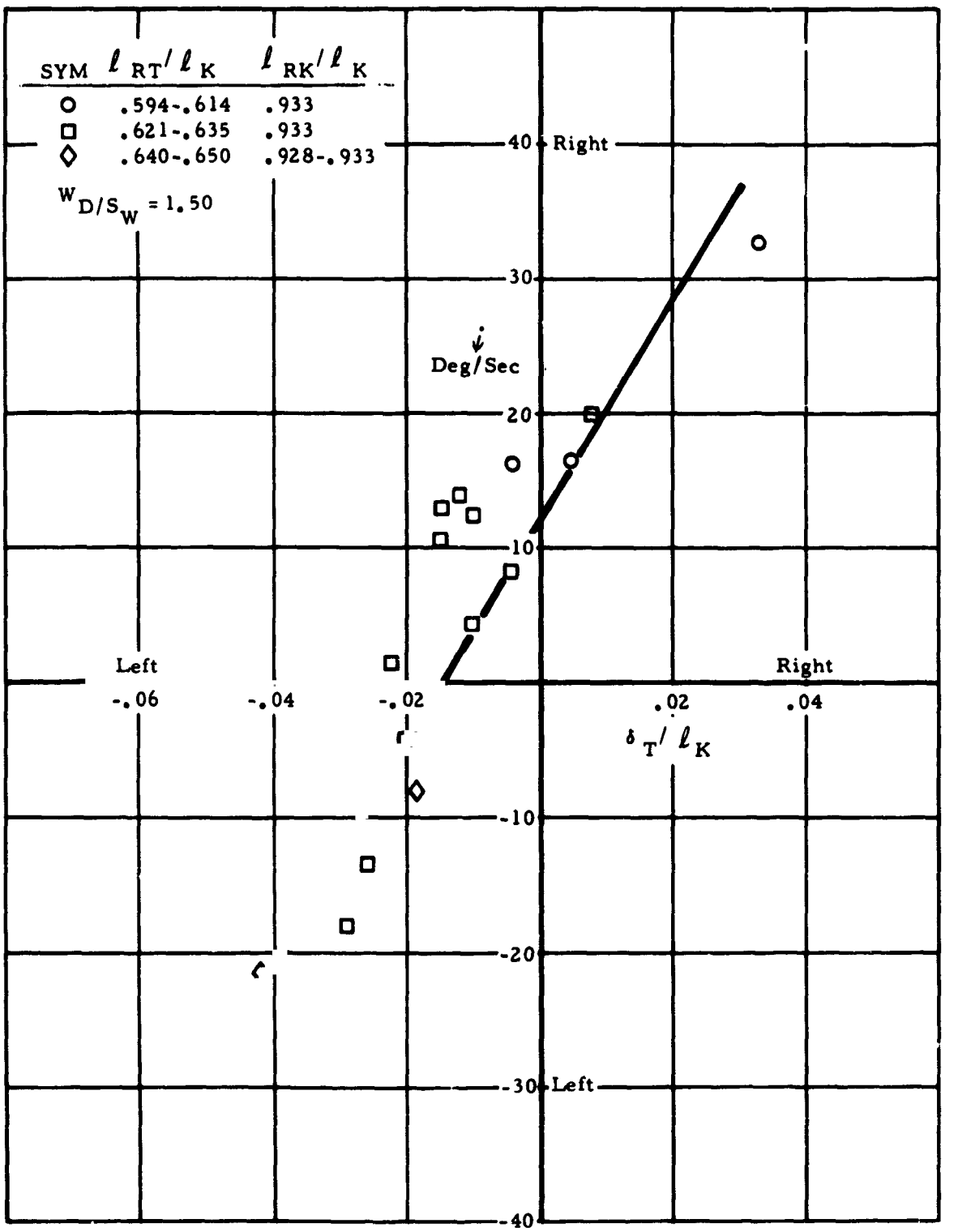

Figure 141. Turn rate versus differential tip setting, Test 254T

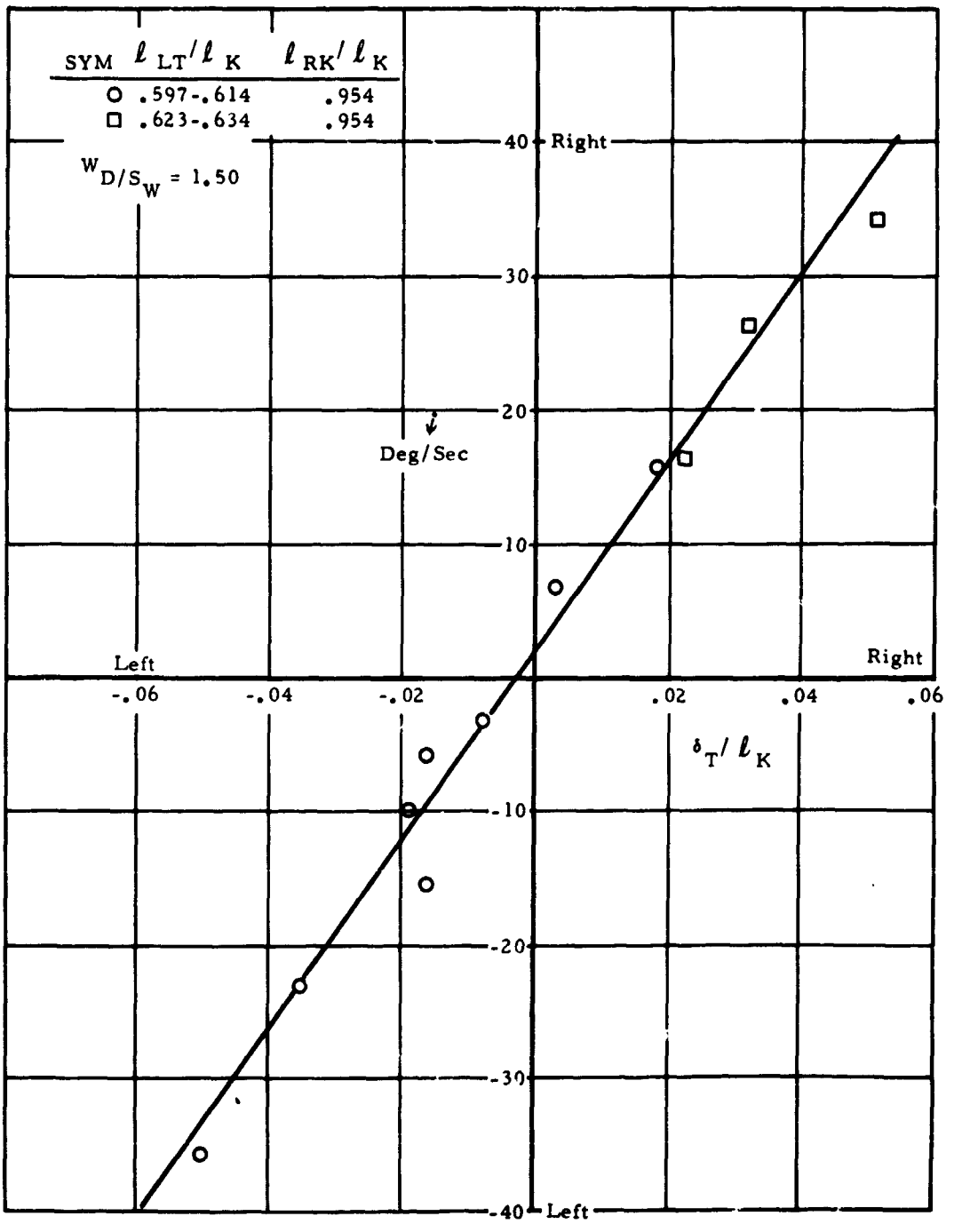

Figure 142. Turn rate versus differential tip setting, Test 255T

Examination of the data in Figures 137 through 142 shows that in general, turn rate was a linear function of differential tip setting for a given wing loading. There were limits, however, on the maximum differential tip setting that could be used to generate a turn. Two separate effects determined the maximum allowable differential tip setting, as follows: (1) The maximum tip setting allowable for either tip suspension line was approximately 0.64. Extending the tip suspension line beyond this setting resulted in improper inflation of the wing and erratic flight. (2) Minimum tip setting allowable for either tip suspension line was approximately 0.57. Retraction of a tip suspension line to a setting less than 0.57 resulted in erratic flight behavior, due apparently to a partially stalled condition. The data from Tests 251T and 253T demonstrate condition (1). As shown by the data on Figures 138 and 140, turn response was limited for the case where the reference tip setting was in the range of 0.631 to 0.645. The data from Test 252T demonstrate condition (2). During Test 252T, turn rate was limited, due to a stall which occurred when one tip suspension line was retracted to a setting of approximately 0.56.

The data obtained during this test program indicate that for a given wing loading, turn rate is a linear function of the differential tip setting, provided the setting of the longer tip suspension line does not exceed approximately 0.64, and the setting of the shorter tip suspension line is not less than 0.57. Based on these limits the maximum differential tip setting is 0.07.

During the small-scale parawing test program, turn rate data were obtained. These data also showed turn rate as a linear function of control input. Figure 143 shows the slopes of turn rate versus control input plotted as a function of wing loading divided by the reference length, ℓ_K. These data plotted on a logarithmic scale approximate a straight line and indicate that the ratio of $\dot{\psi}/\delta_T/\ell_K$ is an exponential function of $\frac{W/S}{\ell_K}$. Figure 143 shows data

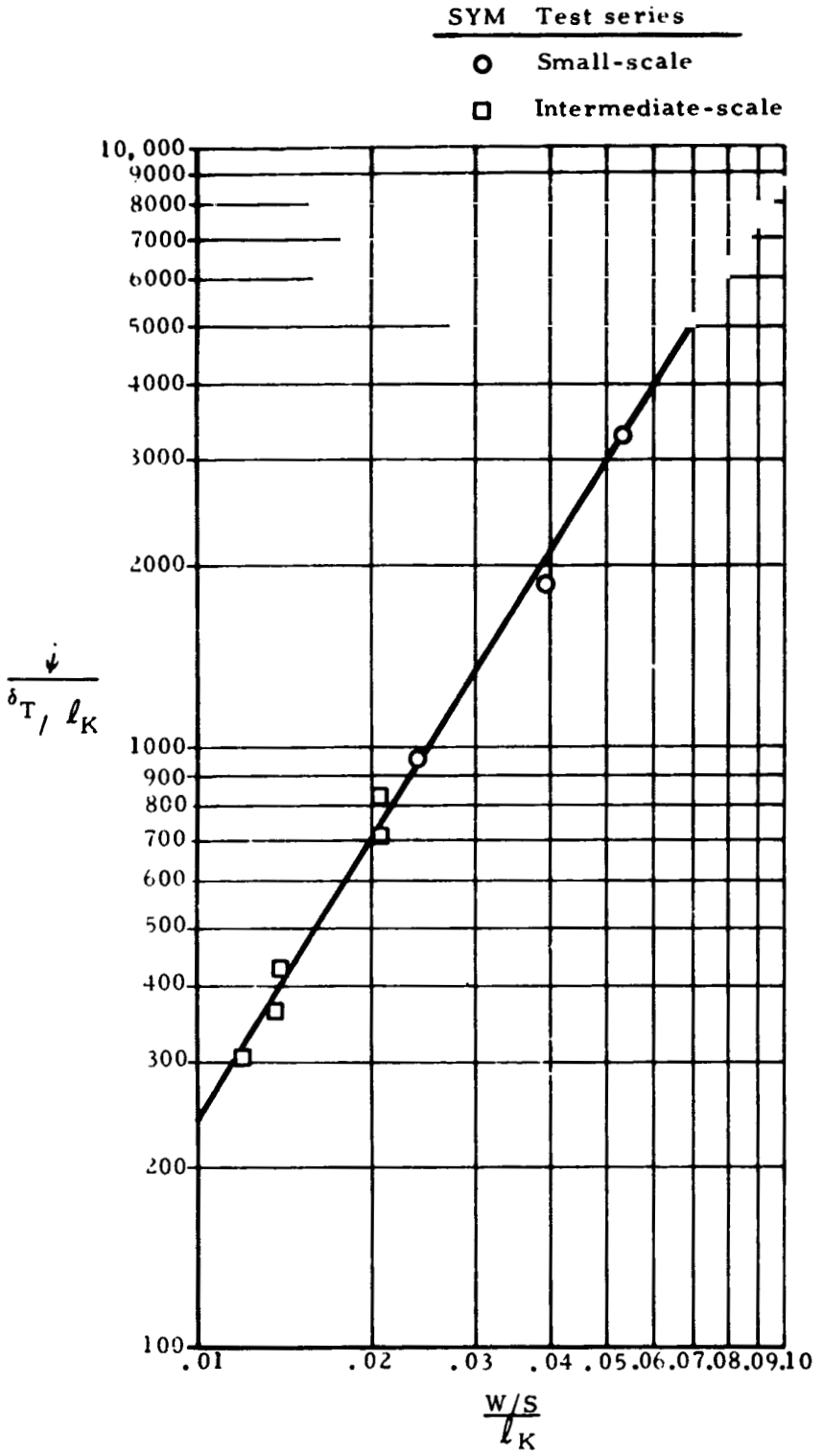

Figure 143. Turn rate response as a function of wing loading and reference keel length, based on 400 and 4000 square foot wing area parawing tests

from both the 400 square foot and 4000 square foot parawing tests. An empirical equation which relates turn rate response to the ratio of wing loading over reference length is:

$$\frac{\dot{\psi}}{\delta_{T/\ell_K}} = 3.248\left(\frac{W_D/S_W}{\ell_K}\right)^{1.564} \times 10^5$$

Based on the above equation, the indicated turn rate capability of the 4000 sq ft twin keel parawing with a maximum differential tip setting of 0.07 is 53 degrees per second at a wing loading of 1.5 psf and 40 degrees per second at a wing loading of 1.25 psf.

Control Force Test Data and Analysis

Figures 144 and 145 present the force measurements obtained for the tip suspension lines. The data are presented in the form of ratios. For straight gliding flight, Figure 144 gives the ratio of the average of the force in the left and the right tip suspension lines, to the suspended weight. The data in Figure 144 are plotted as a function of the average tip setting. Figure 145 gives the tip suspension line force data obtained during the turn tests. These data are presented as the ratio of the individual-tip-suspension-line load to $C_R S_W q$. The data are plotted as a function of the individual tip setting. $C_R S_W q$ is, by definition, the total resultant force experienced by the parawing during flight. The data on both Figures 144 and 145 show appreciable scatter. The probable cause of the scatter in these data was the method used to measure the forces. The control line winch was instrumented in such a manner that eccentricities in the winch shaft rotation resulted in application of an incremental force to the load cell. The force applied to the load cell due to shaft rotation was a function of shaft position. Consequently, the measured load was high or low, depending on the position at which the winch stopped. An average line through the data presented in both figures is probably a good approximation of the actual force in the tip suspension line, as a function of its length. Both sets of load data appear to vary linearly with tip setting.

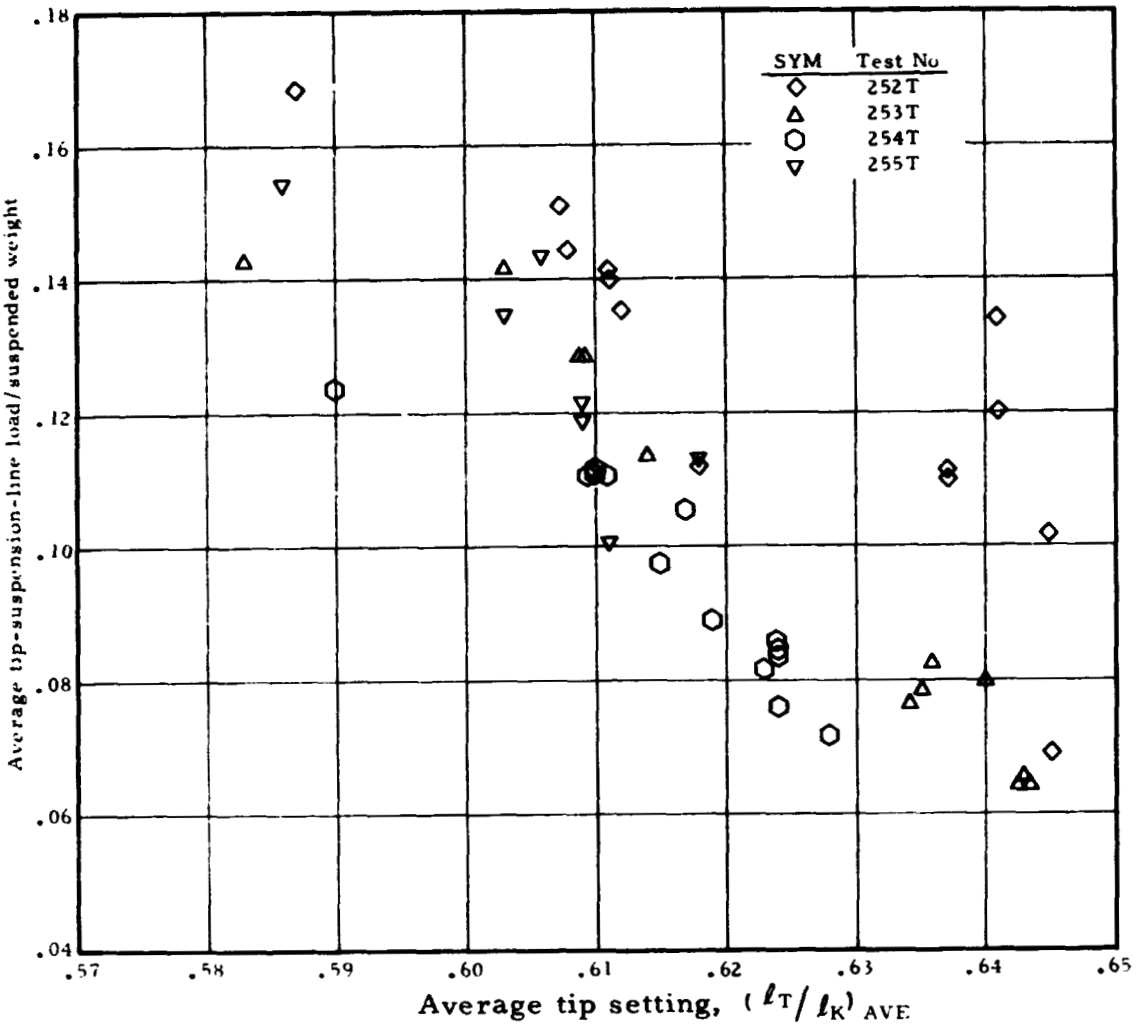

Figure 144. Average tip-suspension-line-load ratio during straight flight as a function of average tip setting

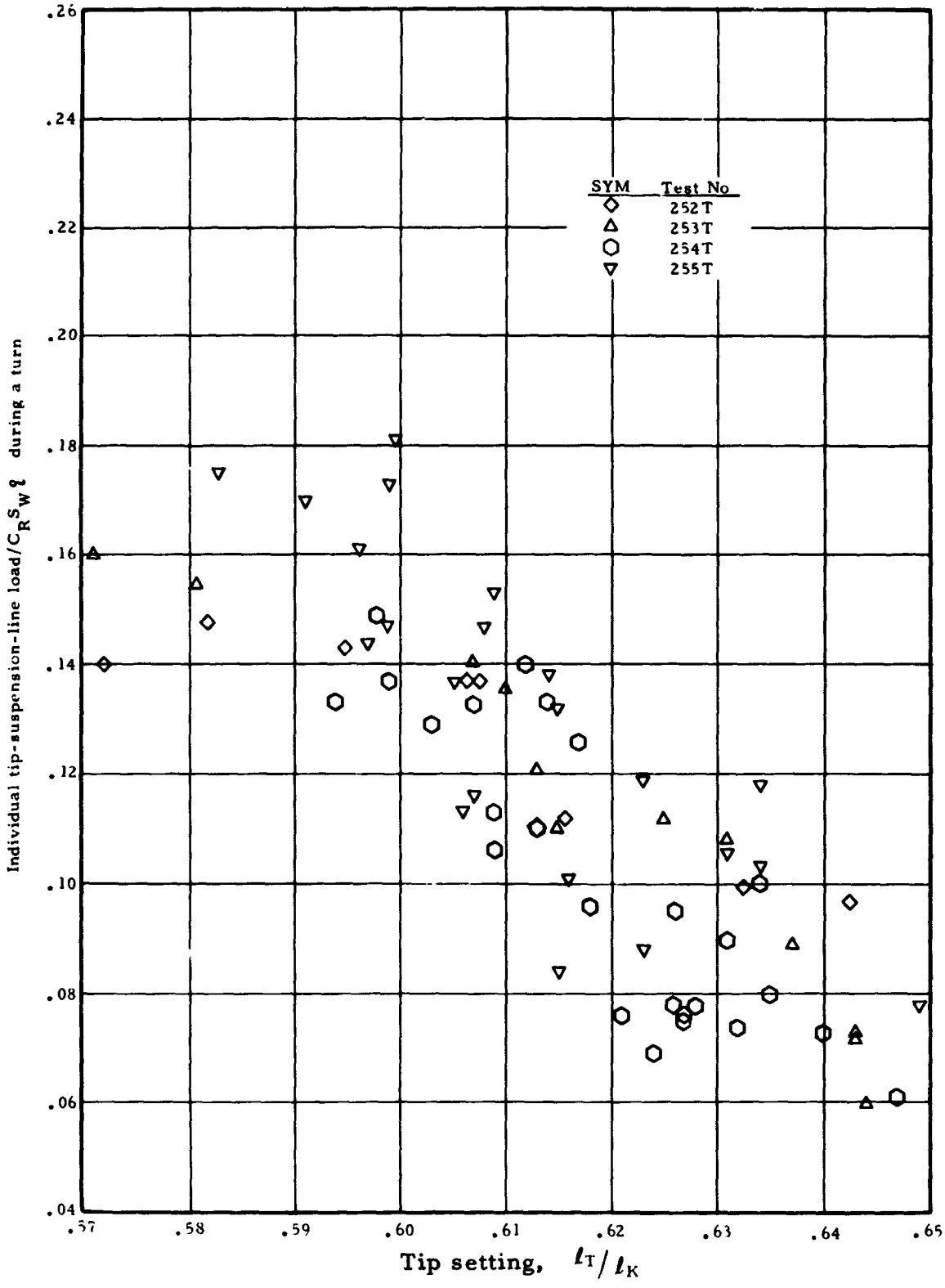

Figure 145. Tip-suspension-line-load ratio during a turning maneuver as a function of tip setting

Summary of Gliding Flight Performance

Both the bomb-vehicle tests and controllable vehicle tests showed that the twin keel parawing configuration flown had stable flight characteristics when the tip setting was about 0.605, and the rear keel setting was in the range of 0.940 to 0.956. For these control line settings, the wing maintained a solidly inflated condition with no tendency to stall during turning maneuvers or when encountering turbulent-air flight conditions. Also, when trimmed for straight flight, the wing maintained straight flight without additional control inputs.

For system design purposes with the twin keel parawing configuration tested, an L/D of from 2.5 to 2.7 and a C_R of approximately 0.64 should be used. These numbers represent the performance that can be expected using the recommended tip and rear keel settings.

During the intermediate-scale test program it became apparent that for a given canopy and suspension line configuration, appreciable changes in L/D could not be accomplished by changing the lengths of either the tip suspension lines or the rear keel suspension lines. Extreme variations in the length of the tip suspension lines resulted in uncontrolled changes in flight characteristics. Too short tip lines resulted in wing stall. Too long tip lines resulted in wing-leading-edge collapse and erratic flight. Test results obtained during the intermediate-scale test program indicated that for the suspension line rigging used during this test program, the recommended tip setting and rear keel setting are approximately 0.605 and 0.95, respectively.

Modulation of L/D by shortening the rear-keel suspension lines was limited by wing stall. The maximum reduction of L/D that could be accomplished by shortening of the rear-keel suspension lines was approximately 0.5. Also, retraction of the rear-keel suspension lines to a setting of less than 0.94 apparently had the

effect of limiting the minimum length of tip suspension lines that could be used as a turn control input. This is logical, since decreasing the length of either the rear-keel or tip suspension lines had the effect of increasing the angle-of-attack of the wing. Thus, the combination of retracting the rear-keel suspension lines to modulate L/D and retracting a tip suspension line for a turn input was limited by the stall angle of the wing. It also follows that at the minimum L/D obtained by retracting the rear-keel suspension lines, any turn input would result in a wing stall. In general, it may be concluded that for a given configuration of wing and suspension line rigging, L/D cannot be modulated appreciably by changing the length of either the tip or rear-keel suspension lines.

Turn rate with the parawing attachment geometry used in this test program, was found to be a linear function of the difference in length between the tip suspension lines for a given wing loading. The maximum allowable differential between the tip lines was found to be 0.07 ℓ_K, with the additional limitation that the shorter tip line was no shorter than 0.57 ℓ_K and the longer tip line was no longer than 0.64 ℓ_K. Retracting a tip line to a length less than 0.57 ℓ_K resulted in the wing stalling on the retracted-tip side. Extending a tip suspension line to a length greater than 0.64 resulted in collapse of the wing leading-edge on the extended-tip side. For a given size wing and control input, turn rate was found to be proportional to wing loading to the 1.564 power. This factor is important in that for systems with high wing loadings, only small control inputs would be required for relatively high turn rates. Such systems would be very sensitive to control inputs and require a precise control system.

CONCLUDING REMARKS

Based on the results of the parawing program, the following conclusions are drawn:

1. The parawing has very positive opening characteristics. In seventy-five aerial drop tests the parawing never failed to open, even in those tests where the parawing canopy sustained heavy damage in the deployment process. The tests confirmed the need for a five-stage deployment process to maintain deployment decelerations at or near a 3 G level.

2. Tests with the 4000 sq ft, twin keel parawing at conditions to simulate a full-scale (10,000 sq ft) parawing at a wing loading of 1.5 psf, showed that 8 percent reefing is required to maintain the deployment loads at or near a 3 G level. With 8 percent reefing and with nose reefing the full-scale parawing first, second, third, and fourth reefed stage and full open predicted loads are 3.4, 3.4, 3.3, 3.0 and 2.8 G's, respectively. However, the results of comparison of small- and intermediate-scale tests suggest that the scaling methods used in this program may not be wholly valid.

3. Suspension line loading for the parawing configuration tested was very nonuniform. Adding five lines on each leading edge of the twin keel parawing substantially reduced the load level of certain highly loaded, leading edge lines in the second reefed stage. Suspension line load ratios were found to be independent of reefing ratios.

4. First-reefed-stage filling time was found to be inversely proportional to the inlet area in tests with both 400 sq

ft and 4000 sq ft parawings. The 4000 sq ft parawing tests also indicated that first-reefed-stage filling time was inversely proportional to the velocity at parawing line stretch. Both 400 sq ft and 4000 sq ft parawing tests showed first-reefed-stage-drag-area growth was a two-step linear process.

5. The 4000 sq ft parawings, in the configurations tested, exhibited four modes of canopy structural failure. Corrective actions completely eliminated three of these four failure modes. The remaining failure mode -- localized canopy cloth damage in the early stages of deployment with propagating cloth tears -- was confined, but not eliminated. The corrective action, consisting of the addition of a ripstop tape matrix to the parawing canopy, limited the extent of tear propagation. However, localized canopy cloth damage continued to occur, with the frequency and extent of such damage increasing at the higher parawing deployment dynamic pressures.

6. Free flight values of maximum L/D were found to be in the range of 2.5 to 2.75 for the 4000 sq ft wing area twin keel models. Corresponding to this L/D performance range, the resultant force coefficient was found to be approximately 0.64. This performance was obtained with a nominal tip setting of 0.605 and a nominal rear setting of 0.940 to 0.954.

7. For the 4000 sq ft, twin keel configuration tested, L/D modulation by retracting either the rear-keel or tip suspension lines was not effective. L/D could be reduced approximately 0.5 by retraction of the rear-keel suspension lines. At this modulated L/D condition, the parawing was at the threshold of stall.

8. Twin keel parawing turn rate was found to be a linear function of the difference in length between the tip suspension lines, provided a tip setting (ℓ_T/ℓ_K) neither exceeded 0.640 nor was less than 0.570. Based on these limits, the maximum differential tip setting is 0.07. With a maximum differential tip setting of 0.07, the indicated turn rate capability of the 4000 sq ft twin keel parawing is 53 degrees per second at a wing loading of 1.5 psf and 40 degrees per second at a wing loading of 1.25 psf.

9. Twin keel parawing turn rate was found to be proportional to (wing loading/keel length)$^{1.564}$.

10. The 4000 sq ft twin keel parawings flown during this test program were aerodynamically stable and controllable. With tip and rear keel settings of 0.605 and 0.950, respectively, the canopy maintained a stable inflation and showed no tendency to stall during turning maneuvers or in turbulent-air flight conditions. The twin keel parawing was directionally stable and responded quickly and precisely to turn control inputs, both entering and leaving a turn.

11. The parawings could be stalled by retracting the rear keel control line or the tip lines. The wings were easily recovered from the stall by returning to the gliding-trim control line settings.

APPENDIX A

TEST VEHICLES AND INSTRUMENTATION

The test vehicles used in the intermediate-scale parawing flight test program, together with their associated instrumentation, are described in this appendix. Two different types of test vehicles were used in the intermediate-scale program. The first was a bomb-type test vehicle, designed and built by Northrop, for use in parawing aerial deployment tests. The second was a sled-type, controllable test vehicle, designed and built by the NASA, Manned Spacecraft Center, for use in parawing controlled aerial gliding-flight tests. Both of these vehicle types and their associated instrumentation are described in the following pages.

Intermediate-Scale Bomb-Type Test Vehicle

General description. - The intermediate-scale bomb-type vehicle, of which two identical vehicles were built, was cylindrical in shape, with a hemispherical nose and a flared, cone-cylinder aft section. The vehicle had an overall length of 11 feet, 8 inches, a forebody diameter of 37 inches, and an aft section maximum diameter of 59 inches. The aft deck was sized to permit a parawing attachment arrangement scaled to the parachute deck of the Apollo command module. The vehicle was capable of being ballasted from a minimum weight of approximately 2600 pounds to a maximum weight of approximately 6000 pounds.

The vehicle was equipped with a pair of skids for landing and for support and attachment to Air Force extraction sleds used with either a C-119- or a C-130-type launch aircraft. The vehicle was also equipped with a single top mounted attach lug for launch from the bomb bay of a B-66 aircraft. Figure 146 shows a sketch of this vehicle.

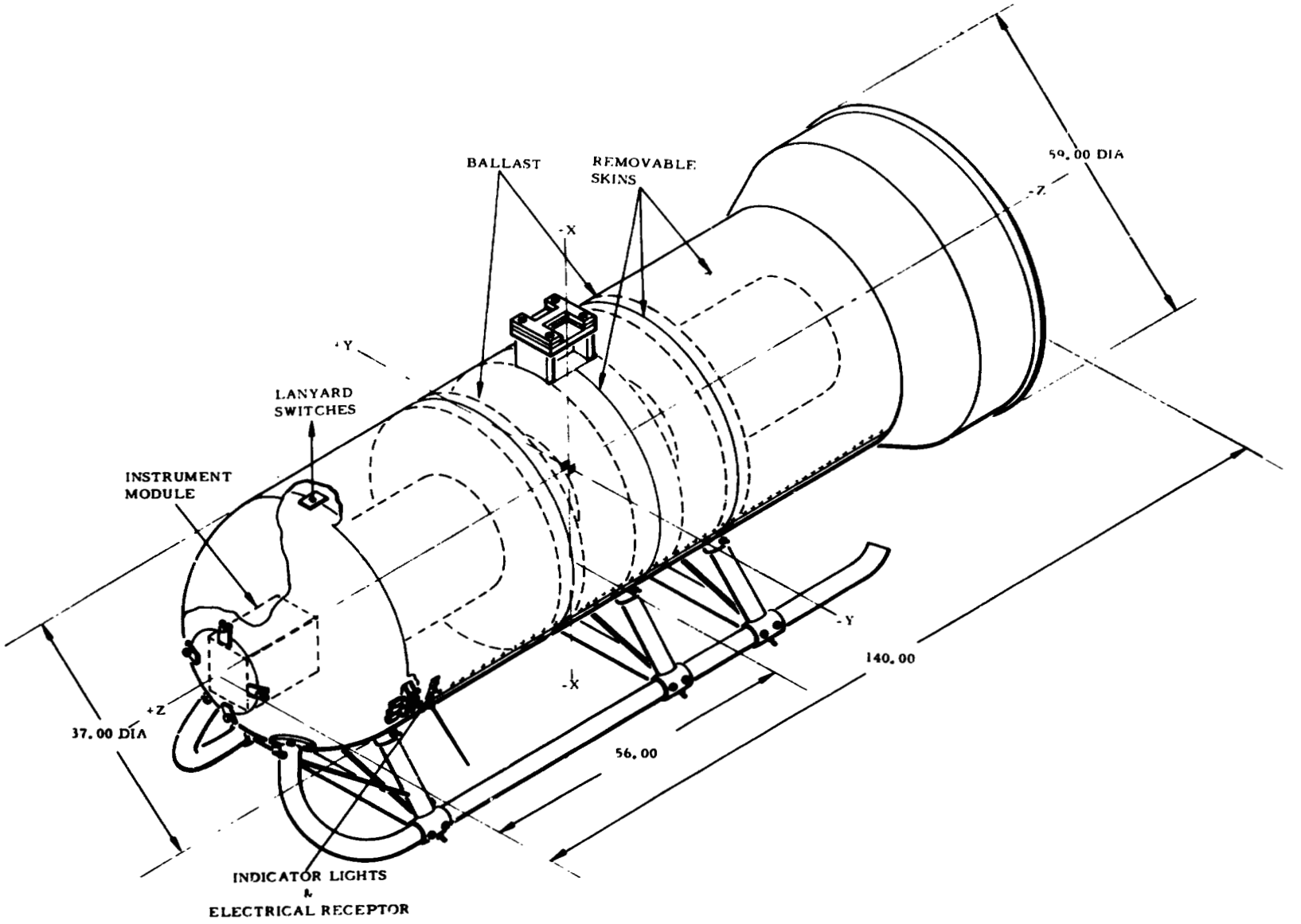

Figure 146. Intermediate-scale, bomb-type test vehicle

The basic bomb test vehicle structure consisted of a heavy steel pipe central core, to which were mounted a hemispherical nose, forward, center and aft bulkhead assemblies, and an aft deck assembly. These sections were designed to be slipped onto the central pipe core and then securely fastened to the core. The major subassemblies to the bomb structure are illustrated in Figure 147.

Gross weight changes to the vehicle were accomplished by adding (or removing) semicircular steel discs to the center bulkhead assembly. These ballast discs were normally added in pairs, one on each side of the bulkhead, in order to maintain the vehicle center-of-gravity position at the center bulkhead station. Small weight adjustments to the vehicle were made by adding (or removing) lead shot in four compartments located in the hemispherical nose section.

The aft deck assembly served several functions. First, it provided an enclosure for the packed parawing system and the deployment system, including the programmer parachute(s) and the parawing pilot chute(s). Second, it provided a structural deck for attachment of the parawing and programmer parachute(s) to the vehicle and for retention of the parawing, programmer parachute, and pilot chute packs. Third, the flared shape of this assembly provided aerodynamic stability to the test vehicle following vehicle separation from the launch aircraft and after programmer parachute disconnect. Figure 148 shows a photograph of one of the intermediate-scale bomb test vehicles.

Instrumentation. - The instrumentation module, containing the battery power supply, the sequencing unit, the telemetry unit, and the 3-axes accelerometer package, was mounted in the nose section of the vehicle. This module, the same as that used in the small-scale bomb vehicle, was installed in the vehicle by removal of a cover plate in the forward end of the nose. Aft mounted instrumentation and pyrotechnics, such as the total load transducers, the individual-suspension-line-load transducers, and the cartridges

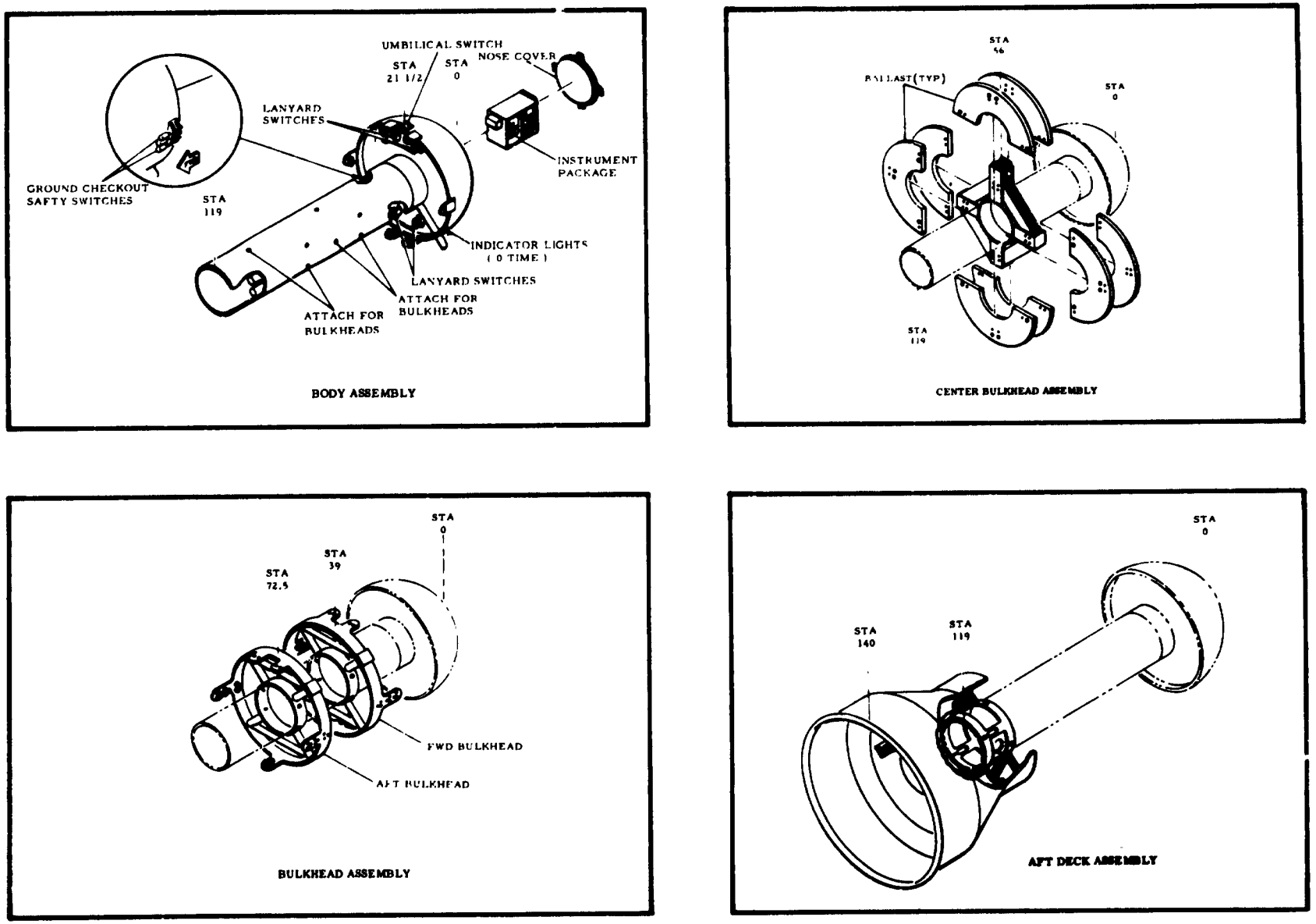

Figure 147. Major structural subassemblies of bomb-type test vehicle

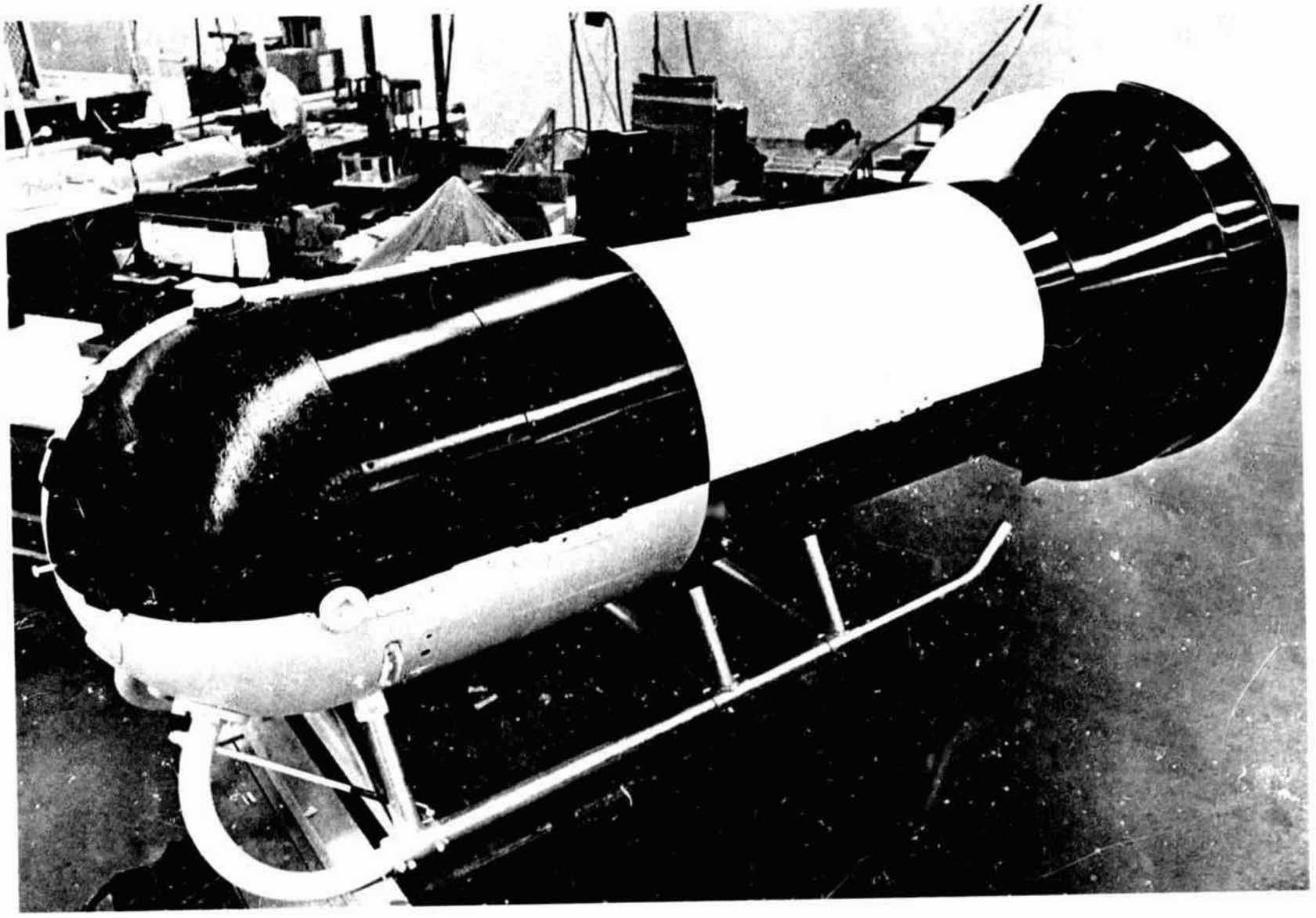

Figure 148. Photograph of intermediate-scale, bomb-type test vehicle

for initiating programmer parachute disconnect and parawing line transfer, were connected to the instrumentation module through electrical cabling between the aft structural deck and the module. An aft looking 16mm camera, located just forward of the structural deck, was also electrically connected to the instrumentation module. A block diagram of the instrumentation module is shown in Figure 149. Table 15 lists the instrumentation used for a typical bomb vehicle test.

In addition to the aforementioned instrumentation, the bomb vehicle was equipped with two sets of lanyard actuated sequencer switches, ground checkout switches and test indicator lights, all mounted in the vehicle nose section. The set of sequencer switches mounted on the top of the vehicle nose section was designed for use with the vehicle launched from the bomb bay of a B-66 aircraft. The lower set of sequencer switches was designed for use with the vehicle launched on an extraction sled from either the C-119 or the C-130 aircraft.

Intermediate-Scale, Controllable, Sled-Type Test Vehicle

General description. - The intermediate-scale, controllable, sled-type test vehicle was developed by the NASA, Manned Spacecraft Center, Houston, Texas, for controllable parachute testing in the 5000 pound payload range. Two basically identical vehicles were designed and fabricated for use. The two vehicles differed only in their weight range capability. The serial no. 1 vehicle had a weight range from 3106 pounds to 3646 pounds, while the serial no. 2 vehicle had a weight range from 3711 pounds to 5646 pounds.

The controllable test vehicle structure had a rectangular planform base, consisting of two large skids, fabricated from 15-inch steel channel. To the base was mounted a load bearing structure, consisting of four, 47-inch long sections of 5-inch diameter steel pipe, coupled with stabilization braces, as shown in Figure 150. Atop the load bearing structure was mounted an upper deck.

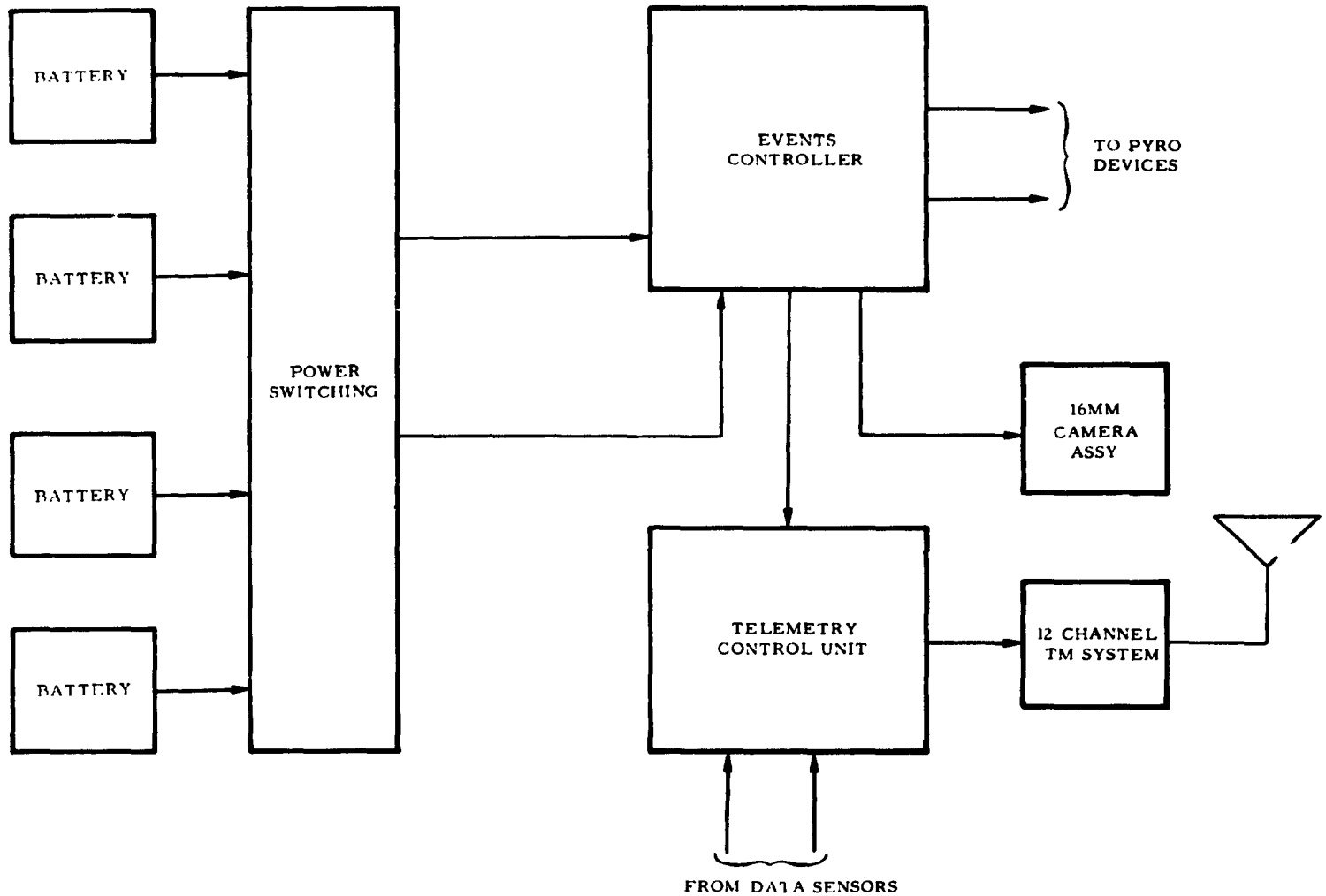

Figure 149. Block diagram of instrumentation module for intermediate-scale bomb vehicle

TABLE 15. - INSTRUMENTATION FOR A TYPICAL BOMB-VEHICLE TEST (200T)

IRIG TM channel	Parameter measured	Sensor range
18	Outboard riser load (left)	0 to 5000 lbs
17	Suspension-line load (LK12)	0 to 5000 lbs
16	Suspension-line load (L7)	0 to 5000 lbs
13	Main load (aft)	0 to 15,000 lbs
12	Suspension-line load (16)	0 to 5000 lbs
11	Suspension-line load (L1)	0 to 5000 lbs
10	Outboard riser load (right)	0 to 5000 lbs
9	Main load (forward)	0 to 15,000 lbs
8	Z-axis acceleration	-1 to +4.5 G
7	Y-axis acceleration	-2.30 to +3.50 G
6	X-axis acceleration	-2.31 to +3.89 G
5	Events	- - - -

NOTE: Suspension-line loads were measured in place of accelerations (channels 8, 7, 6) on some tests.

The upper deck was circular in planform, 52 inches in diameter and constructed of 1/4-inch steel plate. The deck was supported by a square framwork of 4-inch H beams, through which parawing loads were transmitted to the vehicle structure. The upper deck was sized to permit a parawing attachment arrangement scaled to the parachute deck of the Apollo command module.

Between the upper deck and the base was a large instrumentation pallet, to which was mounted all load sensitive equipment. The pallet rested on two blocks of aluminum honeycomb. The pallet was free to move vertically, guided by the four main structural steel pipes, with the blocks of honeycomb serving as an impact attenuation subsystem. The basic vehicle structure measured 122 inches in overall length, 55 inches in width and 47.7 inches in height.

Vehicle weight changes were accomplished by adding steel plates and lead weights at four locations on the heavy steel skids, as indicated in Figure 150. The ballast was arranged to provide vehicle inertias and flight characteristics dynamically similar to a 15,000 pound Apollo command module.

The vehicle was equipped with a control system, consisting of three independent motor-winch devices which were located on the instrumentation pallet and were activated by ground radio command. Control cables for each of the three motor-winch devices were routed through fairings in the vehicle upper deck to the parawing tip suspension lines (2) and the rear keel suspension line(s) (1).

When rigged for flight, the parawing risers were connected to attachment hardware on the upper deck. This attachment hardware was similar to that used with the bomb test vehicle, except for the additional feature of parawing disconnect. The disconnect system, which included cable cutters to sever the three control cables, served to completely separate the parawing specimen at impact to prevent vehicle dragging, or to jettison a failed parawing prior to deployment of the emergency recovery system.

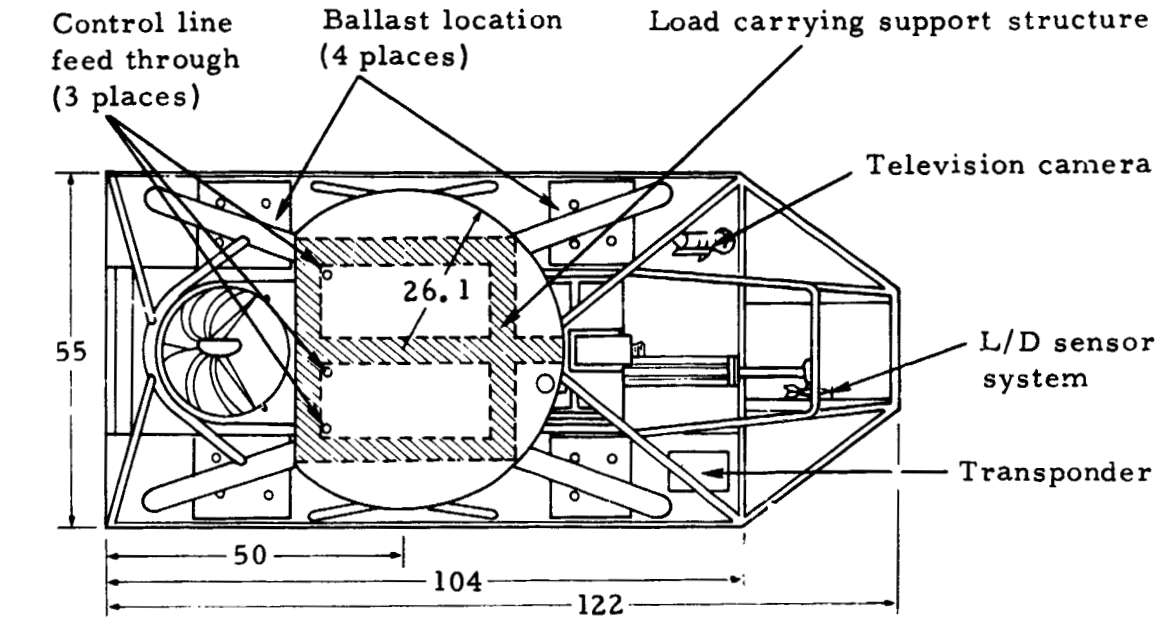

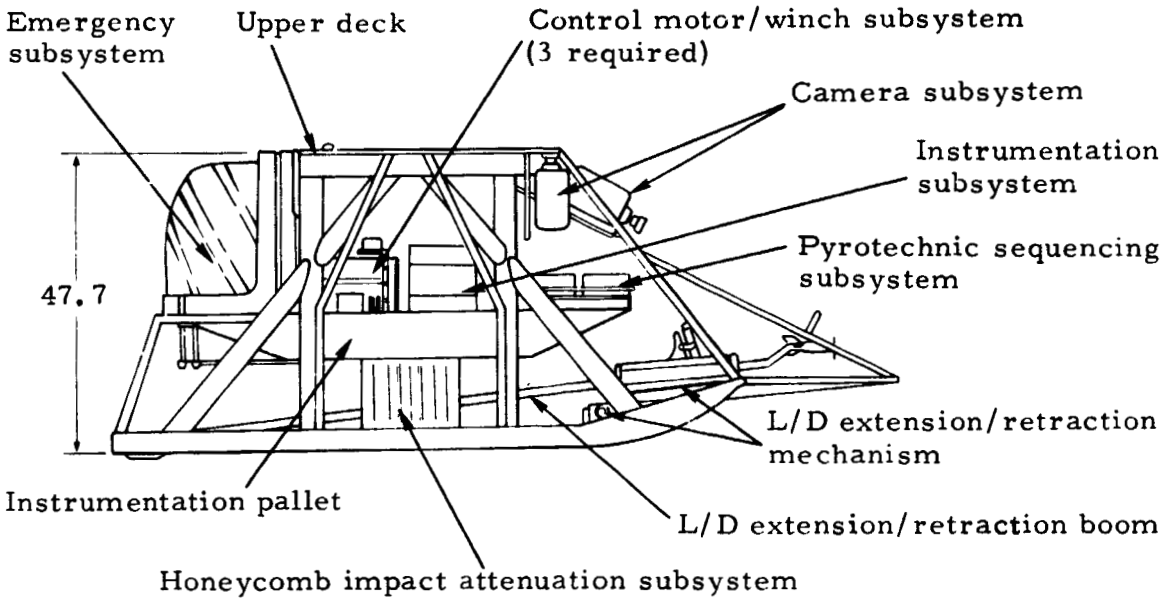

Note: 1. Not to scale
2. Dimensions given in inches are approximate

Figure 150. Intermediate-scale, controllable, sled-type test vehicle, showing location of principal subsystems

The parawing pack itself was mounted on top of the upper deck and held in place with a suitable retention system. The programmer parachute pack was mounted to the support structure forward of the upper deck, with harness attachment to disconnect fittings on the upper deck. Figure 151 shows a photograph of the serial no. 1 controllable test vehicle rigged for flight prior to Test 250T.

The controllable test vehicle was equipped with a radio-command activated, emergency recovery system. This system was designed to recover the test vehicle in the event of failure of the parawing test specimen. The emergency system consisted of a drogue gun, a pilot parachute and an 84-ft D_o ringsail parachute. This system was located on the aft end of the test vehicle, below the upper deck.

To provide suitable positioning of an L/D sensor and airspeed indicator in relatively undisturbed air, the vehicle was configured with an extending boom system. The boom itself consisted of a cantilever-mounted, square aluminum tube which could be radio commanded to extend or retract. The boom and sensor assembly were normally retracted at launch and extended only after parawing gliding flight was established. Also, the boom was normally retracted prior to vehicle impact to protect the sensor.

Instrumentation. - The instrumentation system for the vehicle was designed to measure onboard parameters and events and telemeter this information to a ground receiving station. The onboard telemetry consisted of a 15-channel unit. Fourteen channels were used for real time monitoring and one channel was commutated for sampling data from 16 parameters, for a total telemetry output of 30 channels of information. Table 16 lists the instrumentation used for the controllable-vehicle tests.

The data collection devices included: (a) three accelerometers for measuring vehicle vertical, lateral, and longitudinal accelerations; (b) load cells for measuring total parawing loads, control

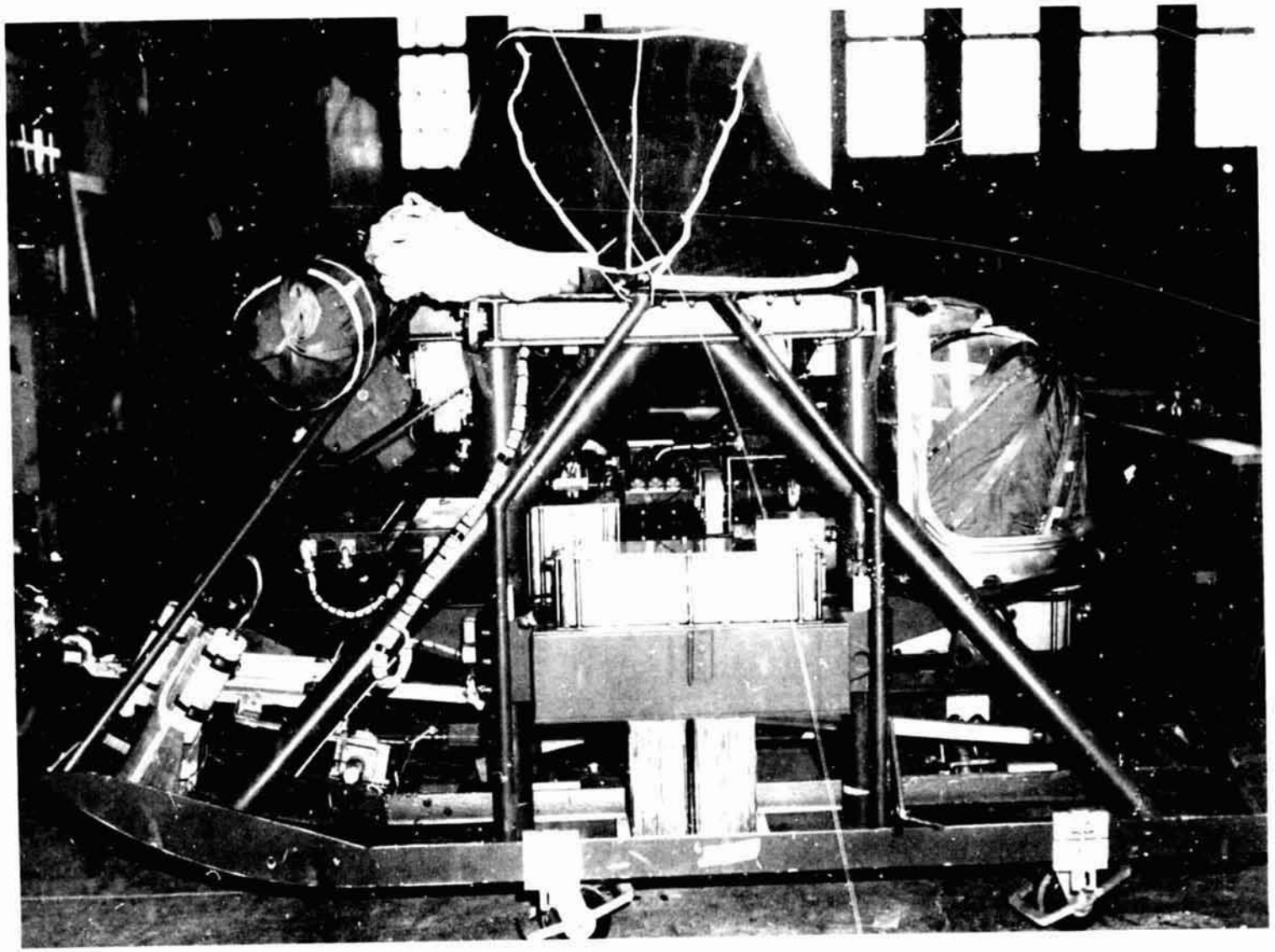

Figure 151. Photograph of the intermediate-scale, controllable sled-type test vehicle rigged for Test 250T

TABLE 16

INSTRUMENTATION FOR CONTROLLABLE-VEHICLE TESTS
Continuous Data

IRIG TM channel	Parameter measured	Sensor range
15	Left tip-line load	0 to 1000 lbs
14	Z-axis acceleration	±10 G
13	Aft main load	0 to 15,000 lbs
12	Forward main load	0 to 15,000 lbs
11	Airspeed indicator	0 to 60 fps
10	Nose load	0 to 750 lbs
9	Keel control-line load	0 to 2000 lbs
8	Right tip-line load	0 to 1000 lbs
7	Angle of attack	0° to 90°
6	Directional heading	$\pm 180^{\circ}$
5	Vertical reference (θ)	$\pm 45^{\circ}$
4	Keel-control-line position	0 to -68 in
3	Right-tip-line position	0 to -68 in
2	Left-tip-line position	0 to -68 in

TABLE 16. - CONTINUED

Commutated Data (IRIG E Channel)

Commutator switch position	Parameter measured	Sensor range
3,18,33,48,63,78	Left riser load	0 to 5000 lbs
4,19,34,49,64,79	Right riser load	0 to 5000 lbs
5,20,35,50,65,80	X-axis acceleration	±2.5 G
6,21,36,51,66,81	Ambient pressure	0 to 15 psia
7,22,37,52,67,82	Y-axis acceleration	±2.5 G
8,23,38,53,68,83	Roll rate (p)	±150 deg/sec
9,24.39,54,69,84	Pitch rate (q)	±150 deg/sec
10,25,40,55,70,85	Yaw rate (r)	±150 deg/sec
11,41,71	Sideslip angle	±45°
13,43,73	Suspension-line transfer - event	- - - -
14,44,74	Parachute disconnect - event	- - - -
15,45,75	Emergency parachute armed - event	- - - -
16,46,76	Boom extended - event	- - - -
26,56,86	Program parachute - event	- - - -
27,57,87	Zero time - event	- - - -
28,58,88	Battery voltage	- - - -

NOTE: The data were commutated using a 90 by 10 commutator. The first eight sensors were attached to six switches each, and thus, were commutated at 60 samples/sec; the remaining eight were attached to three switches each, and thus, were commutated at 30 samples/sec. On tests 250T and 251T, ambient pressure and sideslip angle were interchanged from what is shown above.

line loads, and parawing nose line (L1 and R1) load; (c) three linear potentiometers for measuring control line positions; (d) a three-axis rate gyro unit for measuring vehicle roll, pitch, and yaw rates; (e) a directional gyro for vehicle azimuth readout; (g) a special sensor for measuring vehicle angle-of-attack, yaw angle and airspeed; (h) a vertical reference sensor; (i) wiring for indicating key test events; and (j) a resistive voltage divider for measuring the instrumentation battery voltage. Items (g) and (h) were mounted on the forward end of the extensible boom device previously identified.

In addition to the aforementioned instrumentation, the vehicle was equipped with two 16mm cameras. One camera was vertically mounted to record the parawing deployment process. The other camera was forward facing to view the extensible boom sensors and ground ahead of the vehicle. Finally, the vehicle was equipped with a forward-and-down viewing television camera which provided a TV monitor picture at the ground controller station, of the view ahead of the vehicle.

APPENDIX B

DATA PROCESSING AND CORRECTION PROCEDURES

This appendix summarizes the data processing and data correction procedures used in the intermediate-scale parawing test program.

Bomb-Type Test Vehicle

Test system dynamic pressure versus time. - Phototheodolite tracking data provides velocity of the test system relative to the ground. To compute test system dynamic pressure, the velocity must be referenced to the ambient air. Thus, ground based velocity measurements must be corrected for movements of the ambient air relative to the ground. The normal method for making these corrections is through use of RAWIN wind data obtained by tracking a sounding balloon. This method has the disadvantage that the RAWIN balloon measurements are not made at the same time or in the same location as the actual drop test. For these reasons, significant errors can occur in making wind corrections using RAWIN data. To overcome this difficulty, a different method of wind correction was used in the intermediate-scale parawing aerial drop tests. During the initial phase of the parawing deployment sequence, the test system was essentially moving vertically, relative to the ambient air. Using the time of parawing first-stage disreef as the reference point, the horizontal velocity component as measured by phototheodolite at this instant was used as the wind correction during the parawing deployment process. This correction method assumes that the wind velocity and direction over the altitude range of parawing deployment is constant and equal to the measured horizontal velocity component at parawing first-stage disreef. The phototheodolite velocity measurements during the deployment process were corrected by subtracting vectorially the reference

point, horizontal velocity component. Using the corrected velocity measurements and the atmospheric density obtained by RAWIN sounding balloon, corrected dynamic pressure was computed for the duration of the parawing deployment process.

Total force applied to the parawing during the deployment process. - On-board instrumentation provided force measurements which, when telemetered to the ground receiving station, were recorded as force-time histories of the flight. The force measurements were those forces applied to the bomb vehicle by the parawing through the four risers. To obtain a total measured force-time history, the individual riser forces were summed at discrete time intervals in the deployment process. These total-riser-force measurements were then corrected for the mass of the parawing test specimen itself. Normally, this correction is not made for cloth-type decelerators, since the mass of the decelerator is a very small percentage of the mass of the test system. However, in the case of the intermediate-scale parawing test systems, the mass of the parawing was as much as 11 percent of the system mass. The total parawing force was obtained by multiplying the measured total riser force by the ratio of the total system mass to the mass of the system below the force measuring links.

Drag area growth and full inflation time for parawing first-reefed-stage. - The parawing drag area growth characteristics during the first-reefed-stage inflation were obtained from analysis of on-board photographic coverage of the parawing deployment. The technique was to measure the length and width of the projected parawing planform during the inflation process, under the assumption that the drag area was proportional to the product of the measured length and width. The point of full reefed inflation was determined by plotting the length-width products versus time from line stretch and approximating the resulting curve with straight-line segments. The time and value of length-width ratio where the

plot indicated that full reefed open had been reached were used to non-dimensionalize the data. Finally, plots of drag area over drag area at full reefed inflation versus percent of time to full reefed inflation were prepared.

Lift-to-drag ratio and rate-of-descent during parawing gliding flight on the bomb-type vehicle. - All the bomb-type vehicle tests that resulted in a properly inflated, gliding parawing configuration resulted in a spiral gliding descent of the parawing. The average L/D was determined by a numerical averaging of the ratio of horizontal-to-vertical velocity during the gliding portion of flight. Due to the spiral nature of the system flight path, the effects of wind were thus cancelled out by the averaging process. Phototheodolite measured rate-of-descent during the gliding portion of flight, converted to mean-sea-level conditions, was also averaged and used as the reference velocity in computing lift, drag, and resultant force coefficients.

Lift, drag, and resultant force coefficients. - The lift, drag, and resultant force coefficients were computed, based on the average L/D and the average mean-sea-level rate-of-descent during the gliding portion of the parawing flight. Atmospheric data for these calculations were obtained by RAWIN sounding balloon. Figure 152 presents the axis system and the equations used to compute these coefficients.

First stage filling time. - Filling times were determined by analysis of on-board photographic coverage. For these analyses, filling time was defined as the time from line stretch to that time when the projected area of the first stage became relatively constant at the steady-state, fully inflated condition.

Resultant force area ($C_R S_W$) versus time during deployment. - Resultant force area versus time was obtained by dividing the total corrected force by the corrected dynamic pressure.

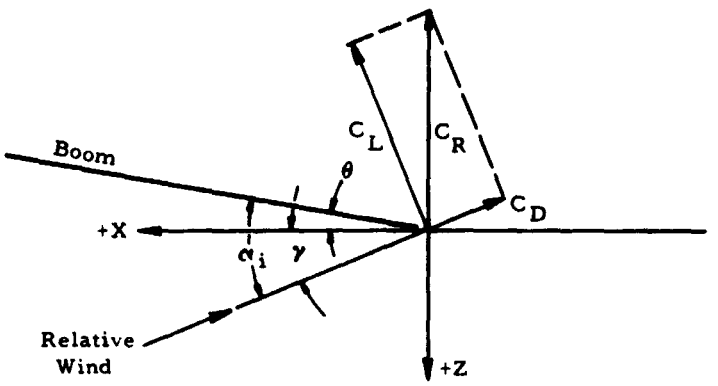

Bomb-type test vehicle

$$\gamma = \tan^{-1}\left(\frac{1}{L/D}\right)$$

$$V_{MSL} = \frac{V_{v(MSL)}}{\text{Sin } \gamma}$$

$$q = \frac{1}{2} \rho_o \, (V_{MSL})^2$$

Controllable test vehicle

$$\gamma = \theta - \alpha_i$$

$$\frac{L}{D} = \frac{1}{|\tan \gamma|}$$

$$\rho = \frac{p}{32.174 \, RT}$$

$$q = \frac{1}{2} \rho \, V_i^2$$

Bomb-type and controllable test vehicles

$$C_R = \frac{W_D}{q \, S_W}$$

$$C_D = \frac{C_R}{\sqrt{\left(\frac{L}{D}\right)^2 + 1}}$$

$$C_L = C_D \left(\frac{L}{D}\right)$$

γ	Flight path angle, measured negative down from horizontal, degrees
θ	Angle of boom relative to earth axis system horizontal, degrees
α_i	Angle of attack indicated by the boom sensor, degrees
V_i	Velocity indicated by the sensor, ft/sec
$V_{v(MSL)}$	Rate of descent, average, corrected to mean-sea-level, ft/sec.
V_{MSL}	Velocity, average, corrected to mean-sea-level, ft/sec.
ρ_o	Mass density of air at sea-level, slugs/ft^3
p	Pressure of air, lbs/ft^2
R	Specific gas constant
T	Temperature of air, degrees Rankine

Figure 152. Axis system and equations used in determining C_L, C_D and C_R

Controllable Vehicle Tests

Dynamic pressure, total force, and resultant force area during the deployment phase of the flight. - For the deployment phase of the flight, data processing was handled in the same manner as described for the bomb-type vehicle tests.

L/D during the gliding portion of the flight. - Lift-to-drag ratio during the gliding portion of the controllable vehicle tests was determined by measuring the flight path angle of the test system relative to the ambient air. Measurements were made with a vane-type indicator which measured angle-of-attack and angle-of-sideslip of the instrument mounting boom, relative to the ambient air, and a pendulum-type instrument which measured the altitude of the test-instrument-mounting boom relative to an earth-horizontal-reference plane. The combination of these measurements provided flight path angle of the test system relative to the ambient air. The test instrumentation was mounted on a boom which projected forward of the test vehicle. In order to account for the effects of the flow field around the test vehicle on the indicated flight path angle, the test instrumentation/test vehicle combination was calibrated in a wind tunnel. The results of the wind tunnel tests showed that the flight path angle was defined as follows:

γ Flight path angle, measured negative down from horizontal (degrees) $= \theta - \alpha_1$

θ Angle of boom relative to earth axes system horizontal, degrees

α_1 Boom angle-of-attack in degrees as derived from the boom sensor reading (corrected for payload interference effects)

$$= \alpha_i + 1.8300 - 0.3157\,\beta' - 0.1290\,V_i + .00387\,V_i\beta'$$

α_i Angle of attack indicated by the boom sensor, in degrees

β' Angle of sideslip at the moment reference center in degrees

$$= \sin^{-1}\left(\frac{V_i \sin \beta_1 - rx + pz}{V_i}\right)$$

β_1 Sideslip angle indicated by the boom sensor, in degrees

V_i Velocity indicated by the sensor in feet per second

r, p Angular velocities about the Z- and X-axes, respectively, in radians per second

x X-axis displacement of the sensor from the moment reference center in feet

z Z-axis displacement of the sensor from the moment reference center in feet

During the flight test program, comparisons of the corrected values of L/D with phototheodolite-derived L/D data showed poor correlation. On the other hand, values of L/D based on the uncorrected, measured angles gave excellent correlation with phototheodolite-derived L/D data. Consequently, all intermediate-scale controllable-vehicle-flight-test L/D data in this report are based directly on instrumentation-measured flight path angles. No corrections were made for the effects of test vehicle or parawing on the flow field in which the L/D sensor system operated. The L/D values presented in this report are numerical averages over time intervals of approximately ten to fifteen seconds, with the data being sampled at the rate of one point per second. All values of L/D are for straight flight or very slow rates of turn.

Lift, drag, and resultant force coefficients. - Lift, drag, and resultant force coefficient values presented in this report for the controllable-test-vehicle flights were based on uncorrected flight-path-angle measurements, indicated airspeed as measured by on-board instrumentation, on-board instrumentation atmospheric pressure measurements and sounding balloon atmospheric temperature data. The time intervals for which coefficient data were analyzed corresponded with those over which L/D data were computed. Figure 152 presents the axis system and the equations used to compute these equations.

Turn rate. - Turn rate was measured from recordings of headings indicated by an on-board directional gyro. The turn rate data presented in this report were obtained graphically by measuring the slope of the directional-heading-versus-time plots. The graphic measurements were always made during time intervals when the system was in steady-state turn.

APPENDIX C

CHRONOLOGICALLY ORDERED RESUMES OF TESTS

Test 200T

The objective of Test 200T was to check twin keel parawing test vehicle system operation under minimum load conditions and to verify the parawing reefing system performance. A Version No. I twin keel parawing was used in this test.

Launch of the 2879 pound (W_D) bomb test vehicle from the C-130 aircraft and deployment of the programmer parachute were as planned. Following programmer parachute disconnect, two pilot parachutes were deployed, which in turn deployed the parawing. Extraction and stretchout of the parawing from its deployment bag were normal. Dynamic pressure at the time of parawing line stretch was 28 psf, compared with 20 psf planned. Altitude at line stretch was 4754 ft, compared with 5000 ft planned.

All parawing reefed stages were normal. However, the line transfer event occurred approximately 1.1 seconds after third stage disreef, rather than the 3.0 seconds planned. Cause of the abbreviated fourth reefed stage interval was twofold. First, the time from programmer disconnect to parawing line stretch actually required about one second longer than planned. Since the line transfer event was controlled by an electric time delay initiated at programmer parachute disconnect, while the third stage disreef was controlled by a reefing-cutter-pyrotechnic time delay initiated at parawing line stretch, the longer time to line stretch reduced the fourth reefed stage interval by one second. Secondly, the third stage reefing cutters fired approximately 0.9 second long. The short fourth reefed stage prevented the wing from opening fully, prior to the line transfer event. Thus, these two events were

somewhat merged, rather than separate and distinct. This anomaly caused no particular problem, either in the deployment sequence or in the subsequent gliding phase of the flight.

The gliding portion of the flight was normal, with the system stable throughout the flight. The system made a very slow turn to the left at a rate of approximately 1.4 degrees per second. Average MSL rate-of-descent measured was 9.35 fps, and the average lift-to-drag ratio was 3.21, as determined from ASKANIA data.

Post test inspection revealed no significant damage to either the parawing or the test vehicle. All instrumentation for the test functioned as planned, except for the load link on line L6, which registered a no-load signal until the line transfer event.

As a result of the abbreviated fourth reefed stage in this test, the nominal time between third stage disreef and the line transfer event was increased from 3.0 seconds to 5.0 seconds on all subsequent bomb vehicle tests.

Test 204T

The objective of Test 204T was to obtain design and scaling data for a full-scale parawing system by means of scaled test conditions simulating a 15,000 pound system weight deployed at 18,000 ft altitude, at a dynamic pressure of 70 psf. A Version No. I wing was flown in this test.

Launch of the 3786 pound (W_D) test vehicle from the C-130 aircraft and deployment of the programmer parachute were as planned. Following programmer parachute disconnect, a pilot parachute was deployed, which in turn deployed the parawing. Extraction and stretchout of the parawing were normal. Dynamic pressure at the time of parawing line stretch was 49.2 psf, compared with 44.3 psf planned. Altitude at line stretch was 18,784 ft, compared with 18,000 ft planned.

All parawing reefed stages were normal. However, the bomb vehicle developed a spinning and coning type of oscillation after first reefed stage inflation. These vehicle motions damped out during subsequent stages of the deployment.

The gliding portion of the flight was normal, with the parawing-vehicle system stable throughout the flight. The system made a slow turn to the left at a rate of approximately 3 degrees per second. At 102 seconds into the flight the ASKANIA cameras were, for reasons unknown, shut down; these cameras were not restarted until 1360 seconds into the flight, some 21 seconds prior to impact. For those portions of the flight where data were collected, the average MSL rate-of-descent was 10.43 fps, and the average lift-to-drag ratio was 3.08, as determined from ASKANIA data.

Post test inspection revealed no significant damage to either the parawing or the test vehicle. Two minor discrepancies were noted. One was the loss of the two, second stage reefing cutters located at line RK2, due to broken reefing cutter pocket tack ties which permitted the cutters to fall out of their pockets after functioning. The other was shearing of a roll pin on one of the vehicle mounted, line transfer assemblies. The function of the roll pin was to prevent rotation of the assembly beyond a fixed angular displacement.

Test 200S

The objective of Test 200S was to check single keel parawing-test vehicle system operation under minimum load conditions and to verify the parawing reefing system performance. A Version No. I single keel parawing was flown in this test.

Launch of the 2868 pound (W_D) bomb test vehicle from the C-119 aircraft and deployment of the programmer parachute were normal, except for a momentary hangup of the programmer pack against the inside of the vehicle aft can, due to initial pitchover of the

vehicle at launch. Following programmer parachute disconnect, two pilot parachutes were deployed, which in turn deployed the parawing. Extraction of the parawing from its deployment bag was normal. Dynamic pressure at the time of parawing line stretch was 29.4 psf, compared with 25.0 psf planned. Altitude at line stretch was 4882 ft, compared with 5000 ft planned.

All parawing reefed stages were normal. Following the line transfer event the nose of the parawing tucked under and remained in that position throughout the gliding flight. The suspension line rigging for this test had been used previously in small-scale Tests 105S and 107S. The tendency for nose tuck with this rigging was evident in Test 107S, when shortly after line transfer in that test, the nose tucked under and remained so tucked until touchdown. Average MSL rate-of-descent for Test 200S was 14.46 fps, and the average lift-to-drag ratio was 1.69, as determined from ASKANIA data.

Post test inspection revealed no damage to the parawing, other than two small burn holes, 1/4-inch and 1/2-inch long, in the left-hand lobe in the panel bounded by L3-1/2, K7, L4 and K8, plus numerous scuff marks and discolorations distributed over the canopy. The bomb vehicle was undamaged in the test.

Test 201S

The objective of Test 201S was to demonstrate the capability of a 5000 pound system to be successfully deployed at the minimum required altitude and dynamic pressure, namely 3000 ft and 30 psf, respectively. A Version No. I single keel wing was flown in this test.

Launch of the 4997 pound (W_D) bomb test vehicle from the C-130 aircraft, deployment of the programmer parachute and system operation until programmer parachute disconnect were as planned. Following programmer parachute disconnect two pilot parachutes were

deployed, which in turn deployed the parawing. Extraction and stretchout of the parawing from its deployment bag were normal. Dynamic pressure at the time of parawing line stretch was 32.6 psf, compared with 30 psf planned. Altitude at line stretch was 2627 ft, compared with 3000 ft planned.

At 1.35 seconds after parawing line stretch, as the wing neared or reached first stage reefed inflation, the right lobe split and collapsed. The tear appeared to start at a point near the center of the right lobe, just forward of the lateral tape between K9 and R4-1/2. The tear propagated parallel to this lateral tape in both directions, stopping at the keel just forward of line K9 on the inboard side. On the outboard side the tear propagated to the leading edge tape, then forward along the leading edge tape to the lateral tape from R4 to K8 and continued inboard, parallel to and just aft of this tape, from R4 to the K8 keel line reinforcing patch. Thus, the right lobe damage was a complete tearing out of the panel bounded by K8, R4, R4-1/2 and K9, except for the space between K8 and K9, where the torn panel remained attached to the wing.

At the time of first stage disreef, the dynamic pressure was 27.5 psf, compared with 12 psf planned, due to failure and subsequent collapse of the right lobe. At 0.18 second after first stage disreef the left lobe split. The left lobe failure was a tear in the canopy cloth extending from the edge of the K8 keel line reinforcing patch outboard, parallel to and just forward of the lateral tape from K8 to L4, to the L4 reinforcing patch. The tear continued forward along the leading edge to L3, then inboard, parallel to and just aft of the L3 to K6 lateral tape to a point approximately 75 percent of the distance from L3 to K6. At this point the tear took a 90 degree jog to a midpanel location and then continued its path parallel to the lateral tape, until it reached the keel at a point approximately midway between keel lines K6 and K7.

Despite the major damage to both lobes, the system decelerated to a dynamic pressure of 10.7 psf at the time of second stage disreef, compared with 5.6 psf planned. The remaining stages were abnormal, due to the extensive damage to the wing. Following the line transfer event the wing inflated in two sections, with the forward and aft sections held together only by the leading edges and keel structure. Rate-of-descent at touchdown was 35 fps. Minor damage to the vehicle aft parawing compartment was incurred at impact.

A post test inspection of the parawing identified the following canopy damage, in addition to the extensive canopy cloth tears in both the right and left lobes of the wing previously described: (1) numerous burns on the underside of the reinforcing patch at L3, (2) broken stitching along the leading edge for approximately 12 inches at the reefing ring located at L3-1/2, (3) broken keel stitching at K8, (4) a 1-inch long cloth tear in the right lobe near the keel, between K10 and K11, (5) a burn hole, 2-1/2-inches in diameter, between K5 and K6, and (6) a curved scuff or abrasion mark near the center of the right lobe, extending from aft of the lateral reinforcing tape between K9 and R4-1/2 to a point forward of the reinforcing tape where it merged with the tear in the right lobe panel. Figure 93 identifies the major canopy damage incurred in this test.

An extensive failure analysis of this test was conducted. The conclusion of this analysis was that the parawing failure in Test 20IS most probably was caused by damage to the canopy cloth prior to or during initial deployment. Laboratory tests of the canopy cloth material showed that with the cloth under load, a small hole or cut introduced in the cloth would immediately propagate, if the load were 18 to 24 percent of the rated cloth strength or greater.

As a part of the failure analysis a number of alternative corrective measures were considered. Of the several alternatives, the recommended corrective action was the addition to the single keel canopy of a cloth cap made of nylon parachute material. This cap was to provide protection to the low porosity canopy cloth from friction/abrasion damage, plus a redundant secondary load path in the event of canopy cloth failure. Design of such a cloth cap was completed. However, no single keel parawings were so modified, and no further single keel parawing aerial tests were conducted, subsequent to Test 201S.

Test 201T

The objective of Test 201T was to demonstrate the capability of the parawing to be successfully deployed on a 5000 pound payload at the minimum required altitude and dynamic pressure, namely 3000 ft and 30 psf, respectively. A Version No. I wing was used in this test.

Launch of the 5034 pound (W_D) bomb test vehicle from the C-119 aircraft, deployment of the programmer parachute and system operation through programmer parachute disconnect were as planned. Following programmer parachute disconnect, two pilot parachutes were deployed which in turn deployed the parawing. Extraction of the parawing from its deployment bag was normal. Dynamic pressure at the time of parawing line stretch was 32.9 psf, compared with 30 psf planned. Altitude at line stretch was 3740 ft, compared with 4000 ft planned (Note: the altitude for parawing deployment was increased from the originally planned 3000 ft to 4000 ft, as a safety measure following the parawing structural failure in Test 201S).

All parawing reefed stages up through the third stage were normal. At third stage disreef the left trailing edge of the wing failed to disreef. The wing left trailing edge remained gathered

throughout the flight. After line transfer the wing performed erratically until impact. Average rate-of-descent in this period was 41.6 fps. However, only minor damage to the vehicle aft parawing compartment was incurred at impact.

Post test inspection of the wing revealed that the trailing-edge-gathering-line loop on the left side at L6 had, prior to third stage disreef, been pulled partially into the outboard reefing cutter at LK12. This in effect introduced two thicknesses of 10,000 pound nylon line into a reefing cutter rated to cut a maximum 12,000 pounds of nylon line. When the outboard reefing cutter at LK12 fired, the guillotine knife blade partially severed the two thicknesses of the gathering-line loop and then stopped, effectively jamming the loop in the cutter. This prevented the free end of the gathering line severed by the inboard (redundant) third stage cutter at RK12 from threading through the outboard LK12 cutter to free the left trailing edge of the wing.

Corrective action to prevent possible occurrence of this problem in subsequent flights was a reduction in the strength of the trailing-edge gathering line from 10,000 pounds to 6000 pounds. This fix was utilized on all subsequent flights until Test 206T, when a modified third-stage-trailing-edge reefing system was introduced.

The post test inspection also identified some minor damage to the parawing canopy. This damage included: (1) three burns, from 1/4-inch to 1/2-inch in size, located in the left hand section of the wing, approximately 10 ft inboard from the leading edge in the panel bounded by L4-1/2, LK9, L5 and LK10, (2) two holes, 1/2-inch and 1-inch in diameter, on the reinforcing patch at L3-1/2, (3) two burn holes 3-inches aft of the nose leading edge and 30 inches inboard from RK1, plus approximately a dozen superficial burns in the same area, (4) a 1/8-inch diameter hole in the right section of the wing between RK10 and RK11, approximately 10 ft outboard from the keel, and (5) a 1-1/4-inch hole and 3-inch long burned area just forward of the trailing edge at RT2.

Test 202T

The objective of Test 202T was to obtain design and scaling data for a full-scale parawing system by means of scaled test conditions simulating a 15,000 pound parawing-vehicle system deployed at a dynamic pressure of 100 psf and an altitude of 14,000 ft. (The originally planned deployment altitude was 18,000 ft. However, maximum launch altitude for the C-119 used in this test was 20,000 ft. To obtain a near-vertical flight path at parawing deployment, it was necessary to lower the deployment altitude from 18,000 ft to 14,000 ft.) A Version No. I wing was flown in this test.

Launch of the 3792 pound (W_D) bomb test vehicle from the C-119 aircraft and deployment of the programmer parachute were as planned, except for a momentary hangup of the programmer pack against the inside of the vehicle aft can, due to initial pitchover of the vehicle at launch. Following programmer parachute disconnect a pilot parachute was deployed, which in turn deployed the parawing. At the time of parawing line stretch the dynamic pressure was 69.6 psf, compared with 63.3 psf planned. Altitude at line stretch was 14,107 ft, compared with 14,000 ft planned.

All parawing reefed stages were normal. However, there was an estimated 180 degree twist in the parawing suspension lines during the first reefed stage. At third reefed stage inflation some minor damage was observable in the center section nose area of the wing.

The gliding portion of flight was normal, with the system making a slow turn to the left at the rate of approximately 2 degrees per second. Average MSL rate-of-descent for the gliding portion of flight was 14.4 fps, and average lift-to-drag ratio was 2.07, as determined from ASKANIA data. The relatively low L/D ratio in this test suggests that the parawing damage in the nose area of wing, although relatively minor, may have had a significant effect on gliding performance.

Post test inspection of the wing disclosed that the significant damage incurred by the wing in this test consisted of the following:

a. An inverted, L-shaped tear in two panels in the contoured nose section of the wing, to the right of center. Each leg of the tear was approximately 54 inches in length, one leg being along the leading edge reinforcing tape and the second leg extending aft to the heavy lateral reinforcing webbing connecting keel lines LK1 and RK1. In the area of the tear were twelve burn/abrasion holes and several small scuffed areas.

b. Broken stitching at the forward end of the right keel, which joined the center section and the right hand section skirt bands. Failure of this stitching permitted the right lobe and the center nose section to be pulled apart, causing a 36-inch tear in the canopy cloth in the center section contoured nose area, adjacent to and inboard of the keel skirt band. Approximately 30 percent of the stitching in the corresponding left keel-nose location also failed; however, the remaining stitching prevented a tear in the cloth.

c. Friction burns on the skirt band in the nose area and on two of the nose snubber lines which attach the nose skirt band to the reinforcing webbing between LK1 and RK1.

d. Broken stitching in the webbing loops which hold six of the reefing rings at the nose.

Figure 94 identifies the major canopy damage incurred in this test.

A post test failure analysis determined from a study of both motion pictures of the test and the parawing test specimen itself, that most, if not all, of the nose damage described above occurred as the nose section of the parawing reached full inflation following second stage disreef. The analysis cited the rapid forward

acceleration of the nose area following disreef to third stage, the resulting rapid drag area growth, and the subsequent sudden arrest of the rapidly moving skirt band and reefing ring mass, as causing a dynamic loading condition, similar in nature to the "snap stress" identified by Asfour in Reference 3.

The recommended corrective actions from the Test 202T failure analysis (which, incidentally, was still in progress at the time of Test 205T, and thus, had the benefit of Test 205T results) were: (1) encasement of the five nylon nose snubber lines in cotton sateen sleeves, (2) separate reefing for the nose section of the wing, and (3) reinforcement of the skirt corner joints at LK1 and RK1. The corrective actions cited above were implemented on a phase-in basis during the remainder of the test program. Reinforcement of the skirt corner joints at LK1 and RK1 was accomplished on the wing for Test 209T and on the wings for all subsequent tests (i.e., on wing Versions IV through VII). Implementation of the other two changes is identified in the description of Test 205T.

Test 205T

The objective of Test 205T was to provide a parawing system test at a test weight of 5000 pounds, with parawing deployment at an intermediate range dynamic pressure of 70 psf, at the maximum required altitude of 18,000 ft. This test was also to serve as a comparison test point for the small-scale parawing scaled Test 102T. Due to altitude limitations with the C-119 launch aircraft, the planned parawing deployment altitude for this test had to be lowered from 18,000 ft to 14,000 ft, thus compromising to a degree the match of this test with small-scale Test 102T. A Version No. I wing was flown in this test.

Launch of the 5031 pound (W_D) bomb test vehicle from the C-119 aircraft and deployment of the programmer were as planned, except for a momentary hangup of the programmer pack. Following programmer parachute disconnect, a pilot parachute was deployed which in

turn deployed the parawing. At the time of parawing line stretch the dynamic pressure was 76.3 psf, compared with 70 psf planned. Line stretch altitude was 14,326 ft, compared with 14,000 ft planned.

All parawing reefed stages were normal. However, after first stage reefed inflation the bomb vehicle developed a spinning and coning type of oscillation. These vehicle motions damped out after second stage inflation. After fourth stage inflation a longitudinal tear in the righthand section of the wing was observed.

The gliding portion of the flight was normal, with the parawing-vehicle system stable throughout the flight. The system made a constant turn to the left at a rate of approximately 6.7 degrees per second. Average MSL rate-of-descent measured was 13.67 fps, and average lift-to-drag ratio was 2.75 during the gliding portion of the flight, as determined from ASKANIA data. At touchdown the vehicle impacted on a small hill. The vehicle tipped over, landing on its back rather than on the landing skids, causing some minor damage to the vehicle aft can assembly.

Post test inspection of the parawing revealed that the significant canopy damage incurred by the wing in this test consisted of the following:

a. Seven small burn or abrasion holes in the right hand side of the contoured nose of the wing, ranging in size from 1/8-inch to 1-1/4-inches in diameter. Also present was a small scuffed spot in the vicinity of two of the holes.

b. A 20-inch long tear in the canopy fabric in the right section of the wing. The tear was located inboard approximately one-third the distance from the leading edge to the keel, and extended rearward from the R4-1/2 to RK9 lateral tape to within 3/8-inch of the next lateral seam (untaped).

c. Severe seam strain damage in the right section of the wing adjacent to the reinforcement gussets at keel line attachment locations RK2 and RK3, and minor seam strain damage to the wing adjacent to the reinforcement gussets at keel-line-attachment locations RK7 and RK8.

Figure 95 shows the major parawing canopy damage which occurred in this test.

A post test failure analysis concluded that the burn/abrasion damage in the nose area occurred during deployment and was caused by friction resulting from contact of the nose area canopy fabric with the nose snubber lines or the leading edge skirt band. Similar, but more extensive, damage of this type had been incurred by the wing in Test 202T. It is perhaps significant to note that the canopy damage in the nose area of the wing apparently had a small or even negligible effect on L/D during steady glide in this test, but appeared to have had a significant effect on L/D performance of the wing in Test 202T.

Recommended corrective action to minimize or eliminate the nose area canopy damage was: (1) encasement of the five nylon nose snubber lines in cotton sateen sleeves, and (2) separate reefing of the nose area of the wing, with disreef occurring at third stage disreef, 12 seconds after line stretch and simultaneous with disreef of the trailing edges of the wing.

The failure analysis concluded that the 20-inch long tear was the result of initial, localized abrasion damage. A small scuff mark adjacent to the tear supported this conclusion. Finally, the failure analysis concluded that the seam strains adjacent to the four keel line attachments were the result of marginal canopy strength in the direction of the load path during third-stage-reefing-inflation peak loading. From the locations of the seam strains one could surmise that the lateral tapes in these locations are oriented at an angle forward of the load paths during peak reefed loading. No separate corrective action was recommended for

this problem, since the addition of the separate nose reefing was expected to reduce the magnitude of the third stage reefed load.

The corrective actions cited were implemented on a phase-in basis during the remainder of the test program. Encasement of the nylon snubber lines in cotton sateen sleeves was first accomplished on the wing for Test 208T and was thereafter incorporated on the wings used in all subsequent drop tests. The separate nose reefing was accomplished on the wing for Test 207T, and thereafter incorporated on the wings used in all subsequent drop tests.

Test 203T

The objective of Test 203T was to obtain design and scaling data for a full-scale parawing system by means of scaled test conditions simulating a 15,000 pound parawing-vehicle system deployed at a dynamic pressure of 100 psf and an altitude of 14,000 ft. (The originally planned deployment altitude was 18,000 ft. However, maximum launch altitude for the C-119 used in this test was 20,000 ft. To obtain a near vertical flight path at parawing deployment, it was necessary to lower the deployment altitude from 18,000 ft to 14,000 ft.) Planned parawing deployment conditions for this test were identical with those for Test 202T. A Version No. I wing was used in this test.

Launch of the 3805 pound (W_D) bomb test vehicle from the C-119 aircraft, deployment of the programmer parachute and system operation through programmer parachute disconnect were normal. Following programmer parachute disconnect a pilot parachute was deployed, which in turn deployed the parawing. At the time of parawing line stretch the dynamic pressure was 64 psf, compared with 63.3 psf planned. Altitude at line stretch was 14,568 ft, compared with 14,000 ft planned.

First stage reefed inflation was rapid and positive. After first stage reefed inflation the bomb vehicle developed a spinning and coning type of oscillation. Following disreef to the second

reefed stage, the canopy cloth in the right lobe of the wing failed adjacent to the semi-circular reinforcing gusset at the R3 suspension-line-attachment location. The tear progressed from its inception point near the leading edge at R3, in a line parallel to and approximately 6 inches aft of the lateral tape between R3 and RK6, to the keel at the circular reinforcing gusset at the RK6 line location. The tear then progressed around the gusset at RK6 and aft to the gusset at RK7, partially tearing through the RK7 gusset before stopping. Also, the tear progressed from its inception point at L3, aft along the leading edge to the semi-circular-reinforcing gusset at the R3-1/2 reefing ring position, partially tearing the gusset before stopping. Following this panel failure, the righthand lobe collapsed. At disreef to third stage the dynamic pressure was 6.9 psf, compared with 4.3 psf planned, due to the reduced drag area as a result of the damage to the right lobe. Subsequent deployment stages were nearly normal, with the damaged right hand lobe reinflating in third stage and remaining inflated in the transition to gliding flight.

The gliding portion of flight appeared normal, with the parawing-vehicle system stable throughout the flight. The system made a constant turn to the left at the rate of 4.2 degrees per second. During this portion of the flight the average MSL rate-of-descent was 14.95 fps, and the average lift-to-drag ratio was 1.83, as determined from ASKANIA data.

Post test inspection of the parawing test specimen identified the following additional canopy damage, above and beyond the torn panel previously described:

a. A tear in the semi-circular reinforcing gusset at the R3 line attachment location, approximately 8 inches from the leading edge, along one of the gusset reinforcing tapes.

b. The semi-circular reinforcing gusset at the R4 line attachment location torn from the leading edge skirt band for a distance of approximately 8 inches and torn from the lateral reinforcement tape approximately 8 inches, plus approximately 6 inches of seam strain in the peripheral stitch pattern of the gusset.

c. Five small tears, ranging in length from 1/4 inch to 1-1/2 inches and an adjacent 9 inch long burn area in the center section of the wing, just aft of the lateral tape between the LK5 and RK5 and approximately midway between the two keel line locations.

Figure 96 shows the major canopy damage sustained by the wing in this test.

A post test failure analysis indicated that the cause of the failure was inadequate strength at leading edge number 3 line attachments and at the reefing ring attachments between leading edge lines 3 and 4. The strength inadequacy was due to load paths in the first and second stage reefed stages that are directed rearward of the existing lateral tapes between the leading edge and the keel, toward the center of pressure of each outer lobe.

Recommended corrective action was further reinforcement of all leading edge gusset reinforcements, except those at leading edge line number 1 and those aft of leading edge line number 4. The further reinforcement suggested was larger diameter gussets of stronger cloth, or the addition of diagonal tapes radiating rearward from the intersection of the lateral tapes with the leading edge skirt band.

Test 208T

The objective of Test 208T was to qualify the Version No. II wing design for flights with a 4000 pound descent weight controllable test vehicle.

Launch of the 5024 pound (W_D) bomb test vehicle and deployment of the two programmer parachutes were as planned, except for a momentary hangup of the programmer parachute packs against the inside of the vehicle aft can. Following disconnect of the programmer parachute, two pilot parachutes were deployed. The pilot chutes in turn deployed the parawing from its deployment bag. Dynamic pressure at the time of parawing line stretch was 27.5 psf, compared with 36 psf planned. Altitude at line stretch was 18,882 ft, compared with 18,000 ft planned. In the first stage inflation the right lobe inflated more fully than normal, while the center and left lobes failed to fill to their normal size. Due to this anomaly, the dynamic pressure at the time of disreef to second stage was 21.2 psf, compared with 15.8 psf planned. Upon disreef to second stage only the right lobe disreefed, taking the major portion of the second stage load. Disreef of the left lobe was delayed until disreef to third stage. As the right lobe approached second stage full inflation the canopy cloth in the lobe failed. The tear originated near the R3 line attachment location and quickly propagated inboard to the keel and aft along both the keel and the leading edge to the R4-1/2 to RK9 lateral tape, resulting in the loss of three panels in the right lobe of the wing.

At second stage disreef the dynamic pressure was 12 psf, compared with 8.4 psf planned. This higher than planned dynamic pressure was due both to the damage in the right lobe and the failure of the left lobe to disreef. At second stage disreef the center lobe disreefed, followed immediately by disreefing of the left lobe. All subsequent stages of the deployment were normal.

In the gliding portion of the flight the wing descended in a tight spiral turn at the rate of 58 degrees per second and at an average rate-of-descent of 45 fps. At an altitude of 1300 ft the turn and descent rates of the system decreased to 17 degrees per second and 25 fps, respectively. The average lift-to-drag ratio

of the wing for the final 1300 ft of descent was approximately 1.2, as determined from ASKANIA data. No damage was incurred by the test vehicle at impact.

A post test inspection of the parawing revealed the following damage to the canopy:

a. A tear in the right lobe beginning at the leading edge at the R3 line attachment location, propagating along and just aft of the R3 to RK6 lateral tape to the keel, along the keel from RK6 to RK7, stopping at the R3-1/2 to RK7 lateral tape near its juncture with the RK7 line attachment circular gusset. The tear also propagated from its inception point at R3, aft along the leading edge to R4, then inboard along and just forward of the R4-RK8 lateral tape to the keel, stopping at the RK8 line attachment circular gusset.

b. A tear in the right lobe beginning at the R4 line attachment location, propagating inboard along and just aft of the R4 to RK8 lateral tape, and then along the keel and the leading edge to the R4-1/2 to RK9 lateral tape.

c. Several burn holes and burned or abraded areas in the nose area, center and right sections of the wing.

d. The cotton sateen sleeve covering one end loop on the first stage reefing line was missing entirely, and the tack ties on the sleeve covering the other end loop were broken, with the sleeve itself jammed together at the end of the loop. This condition strongly suggested that the cotton sateen sleeve on the left lobe first-stage-reefing-line end loop had been the cause of the first-stage-reefing-line hangup, and the resulting failure of the left lobe to disreef at the proper time in the deployment sequence.

e. A 6-inch tear on the third-stage-reefing-cutter pocket located at RK12, extending from the cutter flap downward along the side of the pocket. The reefing cutter had been lost from the pocket in test.

Figure 97 identifies the major canopy damage incurred by the wing in this test.

A post test failure analysis attributed failure of the parawing to the following contributory factors:

a. Excessive dynamic pressure at first stage disreef, due to incomplete inflation of the left and center lobes of the wing.

b. Excessive rate of first stage disreef of the right lobe, due to higher-than-normal vehicle velocity and high skirt tension caused by right lobe overinflation.

c. Overloading of the right lobe in second stage inflation, due to delay of the left lobe disreef function and resultant loss of load sharing between left and right lobes.

Based on the findings of the failure analysis, the following corrective actions were proposed:

a. Reduction to minimum size of the first stage reefing line connector loop, with the loop threaded through the R6 and L6 reefing rings. This arrangement would prevent lateral shifting of the loop, thus insuring an equal mouth circumference for each of the outer lobes.

b. Removal of the cotton sateen sleeves on the first-stage-reefing-line end loops, and replacement with a teflon material applied to the end loops by dipping. This change would reduce the possibility of a lockup of the end loops in the reefing rings.

c. Addition of five leading edge lines at the five locations where lateral seams terminate at reefing rings only, with the opposite ends terminating at existing keel lines. The added lines would redistribute the loading along the skirt and reduce the unit load at L3 and R3 following disreef to second stage.

d. Reinforcement of the local failure inception points at L3 and R3.

As a result of the twin keel parawing structural and operational failures encountered in Tests 203T and 208T, all remaining planned parawing tests were stopped, pending a thorough review and analysis of the problems encountered in these tests, and implementation of selected modifications to the parawing test specimens. As a result of this review and analysis a decision was made to incorporate the following modifications on the twin keel parawing specimens:

a. Improved first stage reefing system to eliminate nonsymmetrical inflation of the individual lobes and to eliminate possible first stage reefing line hangups.

b. Addition of ten leading edge lines (five on each leading edge) at the midpositions between the existing lines from L1 to L6 and R1 to R6.

c. Reinforcement of the leading-edge-line attachment structure for certain highly loaded leading edge lines.

d. Addition of separate nose reefing as a part of the third stage reefing system, with disreef of the nose reefing concurrent with disreef of the trailing edges of the wing.

e. Addition of a network of ripstop tapes on the wing canopy to limit propagation of tears in the canopy cloth.

In order to resume testing of the parawings at the earliest possible time, the above modifications were implemented in two steps. One wing, the Serial No. 1 twin keel parawing, was provided with modifications (a) through (d) above, plus a minimum ripstop tape network, consisting of four longitudinal tapes on each of the two outer lobes. This wing, the Version No. III twin keel wing, was flown in Tests 207T, 250T and 251T. Two wings, the Serial Nos. 2 and 4 twin keel parawings, were provided with modifications (a) through (e) above, where the ripstop tape modification consisted of a complete matrix of tapes over the entire wing canopy. The Serial No. 4 wing in the Version No. V was flown in Tests 209T and 211T. The Serial No. 2 wing in the Version No. IV was flown in Test 252T.

Test 207T

The objective of Test 207T was to qualify the Version No. III wing design for flights with a 4000 pound descent weight controllable vehicle. Test 207T was a repeat of Test 208T, with a Version No. III wing in place of the Version No. II wing which had sustained major canopy structural damage in Test 208T.

Launch of the 4994 pound (W_D) bomb test vehicle and deployment of the programmer parachute were as planned. Following disconnect of the programmer parachute, two pilot parachutes were deployed which in turn deployed the parawing. Extraction and stretchout of the parawing from its deployment bag were normal. At the time of parawing line stretch the dynamic pressure was 37.1 psf, compared with 36 psf planned. Altitude at line stretch was 14,840 ft, compared with 18,000 ft planned. (Weather conditions at the test site, in the form of high altitude cloud cover, necessitated a last minute reduction in the launch altitude from the planned 22,500 ft, to 20,000 ft, with the consequent reduction in parawing deployment altitude.)

All stages of parawing deployment were normal. This was the first test of the parawing with separate nose reefing, and it performed as planned. Following the line transfer event the wing did not proceed to a steady-state glide. The gliding portion of the flight was characterized by a cyclic folding in of the wing tips, together with a tucking back and to one side of the parawing nose, followed by reinflation of the tips and nose. Subsequent investigation, plus a small-scale parawing aerial test conducted at LRC, confirmed that this abnormal gliding behavior was due to the longer-than-normal tip line lengths that had been rigged for this test. The average MSL rate-of-descent during the gliding portion of flight was 19.44 fps, and the average lift-to-drag ratio for the flight was 2.32, as determined from ASKANIA data.

Post test inspection of the parawing identified only minor damage, consisting of two 1-inch long tears in the righthand nose section of the wing, adjacent to the RK1 line attachment reinforcement gusset.

One anomaly in this test was a loose connection in one of the six, individual-suspension-line load links. The loose connection fed noise into the TM signals for all the loads-instrumented suspension lines. Because of this noise some peak line loads were lost, and the validity of the others is suspect.

Test 250T

The objective of Test 250T was to obtain gliding flight data with a minimum weight, controllable test vehicle. The Version No. III twin keel parawing was flown in this test.

Launch of the 3444 pound (W_D) controllable test vehicle and deployment of the programmer parachute were normal. Following disconnect of the programmer parachute, two pilot parachutes depolyed the parawing in a normal manner. At the time of parawing line stretch the dynamic pressure was 23.9 psf, compared with 21 psf planned. Altitude at line stretch was 19,010 ft, compared

with 18,000 ft planned. The vehicle was launched at an altitude 1000 ft higher than originally planned to extend the duration of parawing gliding flight. In general, all of the 250 series parawing tests with the controllable vehicle were launched at higher altitudes than originally planned, with resulting higher-than-planned parawing deployment altitudes, in order to extend the duration of gliding flight and accomplish more maneuvers with the controllable test system.

All the reefed stages in the parawing deployment sequence were normal. Following the line transfer event, ground control of the system was achieved and a prescribed maneuver plan flown. The L/D measured in this test varied from a maximum of 2.12 to a minimum of 1.92. Maximum turn rate achieved in this test was 25.9 degrees per second.

Touchdown of the vehicle was normal, with the vehicle coming to rest on its skids. Total time of the flight fror launch was 20 minutes, 14 seconds.

Post test inspection of the parawing revealed no significant damage to the canopy, other than a number of scuff marks on the canopy and one 3/8-inch long cloth tear in the left lobe nose area, adjacent to LK1.

Test 251T

The objective of Test 251T was to obtain gliding flight data and to determine the effect of wing loading on gliding flight performance. The Version No. III twin keel parawing was flown in this test.

The 3977 pound (W_D) controllable vehicle was launched from the C-119 aircraft at an altitude of 22,160 ft, compared with 19,350 ft originally planned. The higher launch altitude was requested in order to obtain the maximum amount of gliding flight time possible. Deployment of the programmer parachute and operation to disconnect were normal. Following programmer disconnect,

10.61 seconds after launch, two pilot parachutes were deployed. However, the pilot parachutes did not immediately deploy the parawing. For a period of approximately 22 seconds the test vehicle with the two inflated pilot parachutes continued to descend in a near vertical trajectory. In this time period the controllable test vehicle rotated beneath the pilot parachutes.

At 32.23 seconds after launch the parawing pack was finally pulled free of its retention system and deployed. At parawing line stretch, 32.97 seconds after launch, the dynamic pressure was 43.3 psf, compared with 24 psf planned. Altitude at line stretch was 15,970 ft, compared with 18,000 ft planned.

At 33.75 seconds after launch or 0.78 second after parawing line stretch, line transfer occurred. This event, initiated by an electric timer onboard the test vehicle, was scheduled to occur 30 seconds after launch, or 20 seconds after programmer parachute disconnect. Thus, due to the 22-second hangup of the parawing pack, line transfer occurred entirely out of sequence, during parawing first stage reefed inflation. However, due to the severe suspension line twistup, the line transfer event did not immediately manifest itself, since the twistup tended to hold the lines at the pre line-transfer length, relative to the parawing skirt. Also, the line twistup apparently prevented arming of the reefing cutters at parawing line stretch. First stage disreef occurred approximately 9 seconds after line stretch, compared with the nominal 6 seconds planned. At first stage disreef, the dynamic pressure was 25.8 psf, compared with 10.8 psf predicted. The extremely high dynamic pressure at first stage disreef was due to the twisted suspension lines which prevented a normal first stage parawing reefed inflation.

Second stage disreef occurred 46.07 seconds after launch. This event took place about 4 seconds later than planned, relative to line stretch, again indicating a late reefing-cutter-time-delay

initiation. Based on the dynamic pressure at second stage disreef, the parawing drag area in the second reefed stage was about normal.

Third stage disreef was not distinguishable, due to the previously cited anomalies of line twistup and early line transfer.

At approximately 86 seconds after launch the suspension lines had untwisted, but due to rotational inertia of the payload, the lines then commenced to wrap up in the opposite direction. At 120 seconds after launch the suspension lines had achieved a normal condition, and at approximately 130 seconds after launch the wing was in steady glide.

At the start of the parawing deployment sequence the forward riser, left lateral riser and nose load transducers all failed. Thus, the deployment total loads data were not obtained for this test.

From approximately 165 seconds after launch until vehicle touchdown at 853 seconds, the system was flown in a prescribed maneuver plan by the ground controller. The wing was very stable and controllable in gliding flight and achieved a maximum L/D of 3.32. The maximum turn rate measured in this test was 18.2 degrees per second. This was not necessarily the maximum possible turn rate of the system, since less than the full tip-control-line travel was used to achieve this turn rate.

Post test inspection of the parawing revealed only superficial damage to the canopy. However, some of the suspension lines had evidence of burn damage, and many of the suspension-line-stowage flutes were badly torn, due to the severe line twistup during deployment.

The post test inspection identified that failure of a cutter knife was responsible for the delay in deployment of the parawing. One of two mechanical cutter knives used to free the parawing pack from its retention system had broken in test usage, with the knife

portion of the assembly having dropped away during the test. Subsequent laboratory tests revealed that the knife assembly as designed was marginally adequate for its application; however, knife assemblies from the lot in use were found to have been heat treated to an excessive hardness, a condition which contributed to this failure. Corrective action consisted of replacing these mechanical knife assemblies in the system with heavier, stronger mechanical cutter knife assemblies.

Test 209T

The objective of Test 209T was to obtain design and scaling data for a full-scale parawing system by means of scaled test conditions simulating a 15,000 pound parawing-vehicle system deployed at a dynamic pressure of 100 psf and an altitude of 14,000 ft. As such, this test was a repeat of Test 203T, with a Version No. V parawing in place of the Version No. I parawing that had incurred major canopy structural damage in Test 203T.

Launch of the 3811 pound (descent weight) bomb test vehicle from the C-119 aircraft and deployment of the programmer parachute were as planned. Following programmer parachute disconnect, a pilot parachute was deployed which extracted the parawing from its deployment bag. At parawing line stretch the dynamic pressure was 62.5 psf, compared with 63.3 psf planned; altitude was 14,175 ft, compared with 14,000 ft planned.

Parawing operation through first stage disreef was normal. At 0.36 second after first stage disreef, near the time of second stage peak load, the third-stage, trailing-edge reefing line failed. The aft portions of the wing quickly inflated, forming an unstable reefed configuration. Subsequent reefed performance was erratic, with the wing tending to collapse and reinflate several times. Second stage disreef and subsequent disreef of the nose section occurred during this period of erratic behavior. The line transfer event occurred as planned, and the wing achieved a normal, stable gliding configuration.

The steady-glide portion of the flight was normal, with the wing making a steady turn to the right at the rate of 5.3 degrees per second. Average MSL rate-of-descent during the gliding portion of the flight was 11.7 fps, and the average L/D measured was 2.9, as determined from ASKANIA data.

Post test inspection of the parawing revealed no significant damage to the wing in this test. A failure analysis conducted as a result of failure of the trailing edge reefing line determined that the cause of this failure was a sharp edge on the third-stage reefing cutter anvil. Corrective action was to provide a generous chamfer on the anvils of reefing cutters used in all subsequent tests.

Test 211T

The objective of Test 211T was to qualify the parawing design for use with a 6000 pound controllable vehicle and to establish parawing flight performance at a wing loading of 1.5 psf. A Version No. V wing was used in this test.

Launch of the 6009 pound (W_D) bomb test vehicle, deployment of the programmer parachute and operation until programmer parachute disconnect were as planned. Following programmer parachute disconnect a pilot parachute deployed the parawing in a normal manner. Parawing line stretch occurred at a dynamic pressure of 49.3 psf, compared with 50 psf planned; altitude at line stretch was 18,320 ft, compared with 18,000 ft planned. During first stage reefed inflation a hole developed in the right lobe canopy cloth. The hole, measuring approximately 51 inches by 24 inches, was roughly centered in the lobe between RK9 and RK4-1/2, just forward of the lateral reinforcing tape connecting the aforementioned line attachment positions. The hole caused the right lobe to partially collapse, reducing the first stage drag area to about 300 sq ft from the normal 350 to 400 sq ft expected with 10 percent ℓ_K first stage reefing. The dynamic pressure at the time of first stage disreef was 25 psf, compared with 17.2 psf planned.

The second reefed stage was normal, although the peak second stage load was higher than pl ined, due to the high dynamic pressure at first stage disreef. Following second stage disreef and during third stage inflation, several tears appeared in the nose area of the left lobe, in the panel bounded by L1-1/2, L2, LK3 and LK4. The tears extended from the leading edge to about the center of the aforementioned panel. The remainder of the deployment process was normal, except that the duration of the fourth reefed stage was somewhat abbreviated at 3.67 seconds, compared with 5.0 seconds planned, due to cumulative reefing cutter and line transfer time delay tolerances.

The gliding portion of the flight was normal, with the wing making a steady right turn at approximately 10 degrees per second. Average MSL ate-of-descent during the gliding portion of the flight was 18.1 fps, and the average L/D measured was 1.9, as determined from ASKANIA data. At touchdown the vehicle impacted in rocky terrain and fell over on its back. The vehicle received some damage at landing; the aft can was bent in on one side, and a metal skin panel just aft of the hemispherical nose was ruptured.

Post test inspection of the parawing identified that in addition to the previously described canopy damage, there were several small holes, ranging in size from 1/4-inch to 1-1/2-inches in diameter, in the wing canopy cloth. These holes were mainly in the central (or high pressure) areas of all three lobes of the wing. Figure 98 identifies the major canopy damage sustained by the wing in this test.

A failure analysis was carried out of the canopy damage incurred by the parawing in this test. It was concluded from the analysis that the large hole in the right hand lobe of the wing (and also the several small holes in the central portions of each lobe) were the result of tape-on-cloth or cloth-on-cloth abrasion which occurred during initial deployment of the parawing. It was

further concluded from the analysis that the tear damage in the nose area of the left lobe was caused by the high loads in the second and third reefed stages, as a result of the damaged canopy in the first reefed stage. Recommended corrective action was to extend the four fan patch tapes emanating from LK1 and RK1 for distances ranging from 6 to 13 ft to points where each tape joined an intersection of a pair of existing ripstop tapes. Implementation of this change resulted in the creation of Version Nos. VI and VII of the twin keel parawing, which were flown in all tests subsequent to Test 206T.

Test 252T

The objective of Test 252T was to obtain gliding flight data and to determine the effect of wing loading on gliding flight performance. The Version No. IV twin keel parawing was flown in this test.

The 4007 pound (W_D) controllable test vehicle was launched from the C-119 aircraft at an altitude of 23,670 ft. Deployment of the programmer parachute and system operation until programmer parachute disconnect were normal. Following programmer parachute disconnect, two pilot parachutes were deployed. The two pilot parachutes in turn deployed the parawing. At the time of parawing line stretch the dynamic pressure was 23.5 psf, compared with 27 psf planned. Altitude at line stretch was 22,345 ft.

All stages of parawing deployment were normal. Following the line transfer event at 32.5 seconds after launch, control of the system was taken by the ground controller. The tip lines were retracted and a stable, gliding configuration was established at approximately 60 seconds after launch. Approximately 80 seconds after launch the vehicle instrumented boom was extended and the system flown to a prescribed maneuver plan by the ground controller. The wing was very stable and controllable in flight. Measured L/D performance during steady gliding flight varied from a

minimum of 2.26 to a maximum of 2.82. The maximum turn rate measured in this test was 10.1 degrees per second; however, this was not necessarily the maximum possible turn rate for the system, since less than half the total available tip line travel was used to achieve this turn rate.

Two anomalies occurred during the gliding-flight-portion of this test. One was loss of on-board measured total velocity, due to loss of the propeller on the boom-mounted airspeed indicator. The other anomaly was an apparent mechanical binding in the rear-keel-line-control-cable drive system, which invalidated the measured rear-keel-control-line loads.

Touchdown of the test vehicle was normal, with the vehicle remaining upright following ground impact. Total time of the flight from launch was 21 minutes, 43.8 seconds.

Post test inspection of the parawing revealed no significant damage to the canopy or lines.

Test 206T

The objective of Test 206T was to demonstrate the capability of the parawing to be successfully deployed with a 5000 pound payload at the maximum required altitude and dynamic pressure, namely 18,000 ft and 100 psf, respectively. Also, this test was to provide test data for comparison with data from small-scale parawing tests conducted at conditions scaled to match the 206T test conditions.

Launch of the 5001 pound (W_D) bomb test vehicle from the C-119 aircraft and deployment of the programmer parachute were as planned. Following programmer parachute disconnect, a pilot parachute was deployed, which in turn deployed the parawing. At the time of parawing line stretch the dynamic pressure was 94.7 psf, compared with 100 psf planned; altitude at line stretch was 18,115 ft, compared with 18,000 ft planned.

During first stage reefed inflation, tears and holes developed in the canopy, as evidenced by loose and flapping material, and by a piece of material separating from the center lobe of the canopy. At first stage disreef the dynamic pressure was 38.5 psf, compared with 21.5 psf planned. This higher than planned dynamic pressure was due to canopy damage sustained during initial parawing deployment and first stage inflation. At first stage disreef the left lobe disreefed 0.25 second later than the right lobe.

Following first stage disreef, several holes and tears became visible in the parawing canopy. These included a 50-inch wide by 16-inch long hole in the right lobe on the outboard side of the panel between R4-1/2 and R5, a 55-inch wide lateral tear in the right lobe near the center of the panel bounded by R3, RK6, R3-1/2 and RK7, and a 24-inch square hole in the left hand lobe near the center of the panel bounded by L4, LK8, L4-1/2 and LK9. At second stage disreef the dynamic pressure was 8.5 psf, essentially as planned.

During third stage reefed inflation another hole, located in the canopy center lobe, became visible. This hole, roughly rectangular in shape and measuring approximately 40 inches wide by 24 inches long, was located in the left center of the panel bounded by LK4, RK4, LK5 and RK5.

Immediately following third stage disreef, one additional hole of significant size was observed. This irregular shaped hole was located in the left lobe just forward of the trailing edge and centered between LT2 and LT3. Figure 99 shows the major canopy damage incurred by the wing in this test.

Following line transfer, the wing established a stable gliding configuration and flew in a steady right turn at a rate of 11.5 degrees per second. Figure 100 provides a photograph of the damaged wing in steady gliding flight. The average MSL rate-of-descent during the gliding portion of the flight was 16.7 fps,

and the average L/D for the gliding portion of flight was 2.13, as determined from ASKANIA data.

Post test inspection of the parawing revealed that in addition to the large holes and tears described above, there were 22 additional small holes, ranging in size from 1/16-inch to 2-inches in diameter, distributed somewhat randomly throughout the wing canopy. Also, several burned and abraded areas were identified, particularly in the center section nose area and in an area just forward of the center lobe rectangular hole. In general, the large holes and tears had in each case been confined by the ripstop tape matrix that surrounded each of the cloth failure locations.

In addition to the canopy damage cited above, the post test inspection identified that the second stage reefing cutters located at the RK2 line attachment location had been lost in test. The tack ties which held the top of the pocket to the heavy keel webbing had been torn loose, allowing the reefing cutters to flip out of the cutter pocket, once the cutters had fired and severed the second stage reefing line.

A failure analysis of this test concluded that most, if not all, of the canopy damage had been initiated during initial parawing deployment and first stage reefed inflation. The rather extensive evidence of burn and abrasion damage to the canopy supported the conclusion that the canopy cloth failures had been initiated by localized damage to the cloth, caused by cloth-to-cloth or tape-to-cloth contact in the time interval between initial canopy stretchout and first stage reefed inflation. It is in this period of time when much of the canopy cloth is uncontrolled and subjected to aerodynamic buffeting. The duration of this time interval is a function of the first stage reefing ratio used, with the interval increasing with decreasing reefing ratio (longer filling time). The severity of the canopy buffeting is a function of dynamic pressure at the time of initial parawing deployment. In this test

the first stage reefing ratio was 0.08 ℓ_K, the lowest ratio used in any of the intermediate-scale parawing tests. The dyanmic pressure of 95 psf at parawing line stretch was the highest value of all of the intermediate-scale parawing tests. Thus, these two factors tended to provide both a relatively long and severe period of canopy buffeting with the resulting damage to the parawing canopy.

Recommended corrective action, within the constraints of the existing reefing system and the specified parawing deployment environment, was to cover selected portions of the parawing canopy, particularly the high pressure crown areas of each lobe, with a layer of parachute type nylon cloth, to protect the canopy cloth from buffeting damage. This corrective action was not implemented on the parawing specimens used in the remaining intermediate-scale tests; however, this concept was subsequently integrated into the preliminary design for a full-scale parawing.

Test 253T

The objective of Test 253T was to obtain gliding flight data at a specified wing loading of 1.25 psf. The Version No. VI twin keel parawing was flown in this test.

The 5011 pound (W_D) controllable test vehicle was launched from the C-119 aircraft at an altitude of 24,050 ft. Deployment of the programmer parachute and system operation until programmer parachute disconnect were normal. Following programmer parachute disconnect, two pilot parachutes were deployed which in turn deployed the parawing. At the parawing line stretch event dynamic pressure was 27.8 psf, compared with 32 psf planned. Altitude at line stretch was 22,640 ft.

All stages of parawing deployment were normal. Following the line transfer event at 32.72 seconds after launch, control of the system was taken by the ground controller. The tip lines were

retracted, and a stable, gliding configuration was established. At 91.5 seconds after launch the vehicle instrumented boom was extended, and the system was flown by the ground controller according to a prescribed maneuver plan. The measured L/D performance during steady, gliding flight varied from a minimum of 1.93 to a maximum of 2.5. The maximum turn rate flown in this test was approximately 6 degrees per second. However, this was not necessarily the maximum turn rate capability of the system, since only approximately 20 percent of the available tip line retraction was used to achieve this turn rate.

Two anomalies occurred relative to the gliding portion of this flight. The first was relatively low onboard velocities measured in this test. These apparently low readings resulted in computed coefficients of lift, drag and resultant force (C_L, C_D, and C_R) that were quite high, relative to previous test data. The second anomaly was an apparent drift in the zero reference of the data acquisition system for rear-keel-control-line load, which invalidated these data.

Touchdown of the test vehicle was normal, with the vehicle coming to rest on its skids. Total time of the flight from launch to touchdown was 21 minutes, 53.5 seconds.

Post test inspection of the parawing revealed only superficial damage to the canopy. This damage consisted of a 3-inch long tear in the center nose section of the wing, just aft of and parallel to the lateral reinforcing tape between LK1 and RK1; a 1-1/2-inch long tear in the right section of the wing in the central area of the panel bounded by RK10, R5, R5-1/2 and RK11, and a few scuff marks in the aft areas of the right and left sections of the wing.

Test 210T

The objective of Test 210T was to obtain design and scaling data for a full-scale parawing system, by means of scaled test conditions simulating a 15,000 pound parawing-vehicle system deployed at a dynamic pressure of 100 psf and an altitude of 18,000

ft. As such, this test was a repeat of Test 209T, except for a parawing deployment altitude of 18,000 ft instead of the 14,000 ft altitude in Test 209T. A Version No. VII wing was flown in this test.

Launch of the 3813 pound (W_D) bomb test vehicle from the C-119 aircraft and deployment of the programmer parachute were normal. Following programmer parachute disconnect, a pilot parachute was deployed, which in turn deployed the parawing. At the time of parawing line stretch the dynamic pressure was 62.1 psf, compared with 63.3 psf planned; altitude at line stretch was 18,600 ft, compared with 18,000 ft planned.

All phases of the deployment sequence were as planned. Some vehicle oscillation was noticeable until the line transfer event. Following line transfer the wing established a steady glide, with a slow turn to the left at a rate of approximately 3.9 degrees per second. Average MSL rate-of-descent during the gliding portion of the flight was 12.2 fps, and the average L/D in steady glide was 2.69, as determined from ASKANIA data. Vehicle touchdown was normal with the vehicle coming to rest on its landing skids, with no damage.

Post test inspection of the parawing revealed only minor damage of a superficial nature. This damage consisted of the following: two small burn holes, measuring 1-inch and 1/2-inch in length, in the center section of the wing, located just forward of the lateral tape between LK6 and RK6; three small holes, varying in size from 1/16 to 3/8-inch in diameter in the top layer of cloth in the reinforcing patches at LK12 and RK12; and a 1/4-inch hole in the left section of the wing, just aft of the reinforcing tape between L4 and LK8 and approximately midway between those two line positions.

One anomaly in this test was the loss of loads data for the LK12 suspension line. Post test inspection identified that a connecting wire from the load link to the vehicle had broken following disconnect of the programmer parachute.

Test 254T

The objective of Test 254T was to obtain gliding flight data and to determine the effect of wing loading on gliding flight performance. The Version No. VI wing was flown in this test.

The 6011 pound (W_D) controllable test vehicle was launched from the C-119 aircraft at an altitude of 23,540 ft. Vehicle launch, deployment of the programmer parachute and system operation through programmer parachute disconnect were normal. Following programmer parachute disconnect, two pilot parachutes were deployed; the pilot chutes in turn deployed the parawing. At the time of parawing line stretch the dynamic pressure was 31.4 psf, compared with 36 psf planned; the altitude at line stretch was 22,075 ft.

All stages of parawing deployment were as planned. Following the line transfer event at 32.3 seconds after launch, control of the system was taken by the ground controller. The tip lines were retracted and a stable, gliding configuration was established at approximately 70 seconds after launch. At 118 seconds after launch the vehicle instrumented boom was extended and the system flown by the ground controller to a prescribed maneuver plan. Measured L/D performance during steady gliding flight in this test varied from a maximum of 2.51 to a minimum of 2.10. The maximum turn rate measured in this test was 32.7 degrees per second; however, this was not necessarily the maximum possible turn rate capability of the system, since less than full tip-control-line retraction was used to achieve this turn rate.

Touchdown of the test vehicle was normal, with the vehicle coming to rest on its landing skids. Total time of the flight was 16 minutes, 22.2 seconds.

Post test inspection of the parawing revealed only minor damage of a superficial nature. This damage consisted of two 1/16-inch diameter holes in the left section of the wing, just forward

of the LT2 line attachment location, a 3-inch long tear in the center nose section of the wing, just aft of the reinforcing tape between LK1 and RK1, a 12-inch long scuff mark in the center lobe aft of the reinforcing tape between LK2 and RK2, and an 8-inch long burned area in the left section of the wing on the inside layer of the LK12 reinforcing patch. Also, the two left side nose snubber lines were damaged near the nose reefing rings.

Only anomaly in this test was a telemetry calibration signal that was initiated approximately six seconds after parawing line stretch, for a duration of about two seconds. This signal obscured the loads readings during a significant portion of parawing second-stage reefed inflation, making the apparent second-stage peak load questionable.

Test 255T

The objective of Test 255T was to obtain gliding flight data and to determine the effect of wing loading on gliding flight performance. Also, this test was conducted to determine the degree of repeatability of parawing flight performance. To this end the test conditions were the same as those for Test 254T. The Version No. VI wing was flown in this test.

The 6014 pound (W_D) controllable test vehicle was launched from the C-119 aircraft at an altitude of 24,700 ft. Vehicle launch, deployment of the programmer parachute and system operation through programmer parachute disconnect were normal. Following programmer parachute disconnect, two pilot parachutes were deployed; the pilot parachutes in turn deployed the parawing. At the time of parawing line stretch the dynamic pressure was 31 psf, compared with 36 psf planned; the altitude at line stretch was 23,260 ft.

All stages of deployment were normal. Following the line transfer event at 32.03 seconds after launch, control of the system was taken by the ground controller. The tip lines were retracted and a stable, gliding configuration was established approximately 80 seconds after launch. At 91.8 seconds after launch the vehicle instrumented boom was extended and the system flown by the ground controller to a prescribed maneuver plan. Measured L/D performance during steady gliding flight in this test varied from a maximum of 2.64 to a minimum of 2.24. The maximum turn rate measured in this test was 35.8 degrees per second. This turn rate is considered a near-maximum turn rate for single-tip-line turn control, based on previous test data.

Touchdown of the test vehicle was normal, with the vehicle coming to rest on its landing skids. Total time of the flight was 15 minutes, 25.4 seconds.

Post test inspection of the parawing revealed no significant damage to the wing, other than two burned areas and a scuff mark in the nose area of the center section, adjacent to RK1, two scuff marks in the righthand section, and some damage to one nose snubber line, second line inboard from LK1.

One anomaly of the test was the loss of both second stage reefing cutters after they had performed their function. The reefing cutter pocket had been torn free of the keel at RK2, similar to that which had occurred in Tests 204T and 206T, allowing the cutters to fall out. This anomaly had no effect on the test.

REFERENCES

1. Linhart, Eugene M., and Buhler, W. Carey: Wind Tunnel and Free Flight Investigation of All-Flexible Parawings at Small Scale. NASA CR 66879, June 1969.

2. Moeller, John H.: A Method of Load Prediction for Parachutes in Cluster; J. Aircraft, July-August 1967, pp. 339-342.

3. Asfour, K. J.: Analysis of Dynamic Stress in an Inflating Parachute; Proceedings of the AIAA Aerodynamic Deceleration Systems Conference, Houston, Texas, September 7-9, 1966.